

AWARD NUMBER: W81XWH-14-1-0500  
MR130240

**TITLE: Toward a Molecular Understanding of Noise-Induced Hearing Loss**

PRINCIPAL INVESTIGATOR: Ronna Hertzano, MD PhD

CONTRACTING ORGANIZATION: University of Maryland School of Medicine  
Baltimore, MD 21201

REPORT DATE: October 2018

TYPE OF REPORT: Annual Report

PREPARED FOR: U.S. Army Medical Research and Materiel Command  
Fort Detrick, Maryland 21702-5012

DISTRIBUTION STATEMENT: Approved for Public Release;  
Distribution Unlimited

The views, opinions and/or findings contained in this report are those of the author(s) and should not be construed as an official Department of the Army position, policy or decision unless so designated by other documentation.

# REPORT DOCUMENTATION PAGE

*Form Approved*  
*OMB No. 0704-0188*

Public reporting burden for this collection of information is estimated to average 1 hour per response, including the time for reviewing instructions, searching existing data sources, gathering and maintaining the data needed, and completing and reviewing this collection of information. Send comments regarding this burden estimate or any other aspect of this collection of information, including suggestions for reducing this burden to Department of Defense, Washington Headquarters Services, Directorate for Information Operations and Reports (0704-0188), 1215 Jefferson Davis Highway, Suite 1204, Arlington, VA 22202-4302. Respondents should be aware that notwithstanding any other provision of law, no person shall be subject to any penalty for failing to comply with a collection of information if it does not display a currently valid OMB control number. **PLEASE DO NOT RETURN YOUR FORM TO THE ABOVE ADDRESS.**

<b>1. REPORT DATE</b> October 2018		<b>2. REPORT TYPE</b> Annual Report		<b>3. DATES COVERED</b> 30SEP2017 - 29SEP2018	
<b>4. TITLE AND SUBTITLE</b>  Toward a Molecular Understanding of Noise-Induced Hearing Loss				<b>5a. CONTRACT NUMBER</b>	
				<b>5b. GRANT NUMBER</b> W81XWH-14-1-0500	
				<b>5c. PROGRAM ELEMENT NUMBER</b>	
<b>6. AUTHOR(S)</b>  Ronna Hertzano, MD, PhD  E-Mail: rhertzano@smail.umaryland.edu				<b>5d. PROJECT NUMBER</b>	
				<b>5e. TASK NUMBER</b>	
				<b>5f. WORK UNIT NUMBER</b>	
<b>7. PERFORMING ORGANIZATION NAME(S) AND ADDRESS(ES)</b> University of Maryland School of Medicine Baltimore, MD 21201				<b>8. PERFORMING ORGANIZATION REPORT NUMBER</b>	
<b>9. SPONSORING / MONITORING AGENCY NAME(S) AND ADDRESS(ES)</b>  U.S. Army Medical Research and Materiel Command Fort Detrick, Maryland 21702-5012				<b>10. SPONSOR/MONITOR'S ACRONYM(S)</b>	
				<b>11. SPONSOR/MONITOR'S REPORT NUMBER(S)</b>	
<b>12. DISTRIBUTION / AVAILABILITY STATEMENT</b>  Approved for Public Release; Distribution Unlimited					
<b>13. SUPPLEMENTARY NOTES</b>					
<b>14. ABSTRACT</b> The purpose of this project is to generate the cell type-specific molecular blueprint of changes in gene expression following different types of noise exposure and their treatments, in the inner ear. To this end, we have (a) Established the hair cell (HC) and supporting (SC) cell-specific translatoe of adult mouse inner ears; (b) Established the molecular changes induced by PTS-resulting noise exposure in HC, SC and whole inner ears, 6 and 24 hours after noise exposure and began the TTS analysis; (c) We identified critical differences in the response of male and female mice to noise, and obtained approval to modify Specific Aim 3 to focus on the response to Heat Shock profiling male and female mice, separately.					
<b>15. SUBJECT TERMS</b> Permanent threshold shift, Temporary threshold shift, Noise induced hearing loss, Ribotag, RNA-seq, hair cell, supporting cell, SAHA, Heat shock, sex differences					
<b>16. SECURITY CLASSIFICATION OF:</b>			<b>17. LIMITATION OF ABSTRACT</b>	<b>18. NUMBER OF PAGES</b>	<b>19a. NAME OF RESPONSIBLE PERSON</b>
<b>a. REPORT</b>	<b>b. ABSTRACT</b>	<b>c. THIS PAGE</b>			<b>USAMRMC</b>
Unclassified	Unclassified	Unclassified	Unclassified	130	<b>19b. TELEPHONE NUMBER</b> (include area code)

**Page**

**Table of Contents**

<b>1. Introduction</b>	<b>4</b>
<b>2. Keywords</b>	<b>4</b>
<b>3. Accomplishments</b>	<b>4</b>
<b>4. Impact</b>	<b>4</b>
<b>5. Changes/problems</b>	<b>8</b>
<b>6. Products, Inventions, Patent Applications, and/or Licenses</b>	<b>8</b>
<b>7. Participants and other collaborating organizations</b>	<b>9</b>
<b>8. Special reporting requirements</b>	<b>11</b>
<b>9. Appendices</b>	<b>11</b>

## 1. INTRODUCTION

Noise induced hearing loss (NIHL) is a major health concern for the Department of Defense. Noise exposure often is inevitable, and may result in a permanent loss of hearing. Unfortunately, there are no treatments to prevent or reverse NIHL. As a first step towards designing targeted therapeutics, we suggested to generate mouse models which allow cell type-specific transcriptome analysis in the ear. These, in turn, will be used to analyze the genes expressed in the hair cells (HC) and supporting cells (SC) of adult mice before and after different types of noise exposure as well as pre-conditioning treatments, which in mice, can ameliorate NIHL. Here we report our progress over the fourth year of the project, in which we (a) followed the plan obtained in the in-person review to extend the cell type-specific blueprint following noise to be sex-specific and (b) consolidated our findings from the first three years of the project and published three peer reviewed manuscripts;

## 2. KEYWORDS

Permanent threshold shift, Temporary threshold shift, Noise induced hearing loss, Ribotag, RNA-seq, Hair cell, Supporting cell, SAHA, Heat shock, Sex differences, Estrogen

## 3. ACCOMPLISHMENTS

**Specific Aim 1: To determine the OHC- and SC-specific transcriptional and signaling cascades activated in vivo in response to PTS-inducing noise exposure**

- **Major Task 1:** To establish the OHC- and SC-specific transcriptome of adult mouse inner ears. Progress by subtasks:
  - i. Obtain ACURO approval following UMSOM IACUC approval – complete.
  - ii. Mouse crosses and tissue harvesting – complete.
  - iii. Tissue processing – complete, polysome IP – complete, submission of samples for RiboTag-seq – complete; RiboTag-seq – complete.

Major task 1 is complete and the results were reported in the annual report for 2017.

**New this year – through the baseline expression pattern of OHC we identified and validated a key regulator of OHC functional maturation, described our findings in a peer-reviewed manuscript that is now accepted for publication in *Nature*. The significance of this original finding has far-exceeded our original expectations, and through a broad collaboration we were able to show that mutations in it underlie age related hearing loss in mice, and that it is necessary for OHC electromotility. Furthermore, we were able to**

**show that ectopic expression of this transcription factor can induce OHC-specific gene expression in inner hair cells and confer electromotility to inner hair cells. The full manuscript is attached as appendix 1.**

- **Major Task 2:** To determine the OHC- and SC-specific transcriptional and signaling cascades activated in response to PTS-inducing noise injury. Progress by subtasks:
  - i. Mouse crosses, noise exposure, tissue harvesting, histological analysis, ABR and DPOAE measurements. Complete.
  - ii. Tissue processing – complete.
  - iii. Data analysis – largely reported last year.
  - iv. Validation experiments – polysome IP to be used for RT-qPCR – complete. Tissue harvesting for immunohistochemistry and in situ hybridization - complete.

Major task 2 is complete. Based on our results showing a difference in response to noise between male and female mice (see new Specific Aim 3), the validation with nanoString will be performed on the new tissue obtained from male and female separated.

**Specific Aim 2: To determine the OHC- and SC-specific signaling cascades activated in vivo in response to otoprotective interventions.**

This Aim was designed to define the cell type-specific molecular blueprint of interventions that may ameliorate NIHL. In our previous annual reports we discussed the rationale for maintaining the TTS and Heat Shock. The heat shock goal was transferred to a modified Specific Aim 3 that is also sex-specific.

**TTS-inducing noise exposure:** Complete and reported last year. **Figure 1** shows part of the validation of this dataset including the experimental parameters indicating that the TTS noise exposure used in the study is of a type that induced Hidden Hearing Loss (i.e., hearing thresholds remain stable however inner hair cell afferent synapses are lost). As discussed in the in-person review a second dataset has now been generated that is sex-specific (see Specific Aim 3). **Figure 2** shows some of the gene clusters that are uniquely changed after either PTS or TTS-inducing noise exposures. A particularly interesting cluster is cluster 3 which consists of genes uniquely upregulated only following TTS noise exposure.

Within this cluster – a striking novel example is DFNA5, which in its absence mice and human suffer from genetic hearing loss. Here our data suggest that overexpression of this gene may have a role in otoprotection. These data are being summarized and prepared for publication.

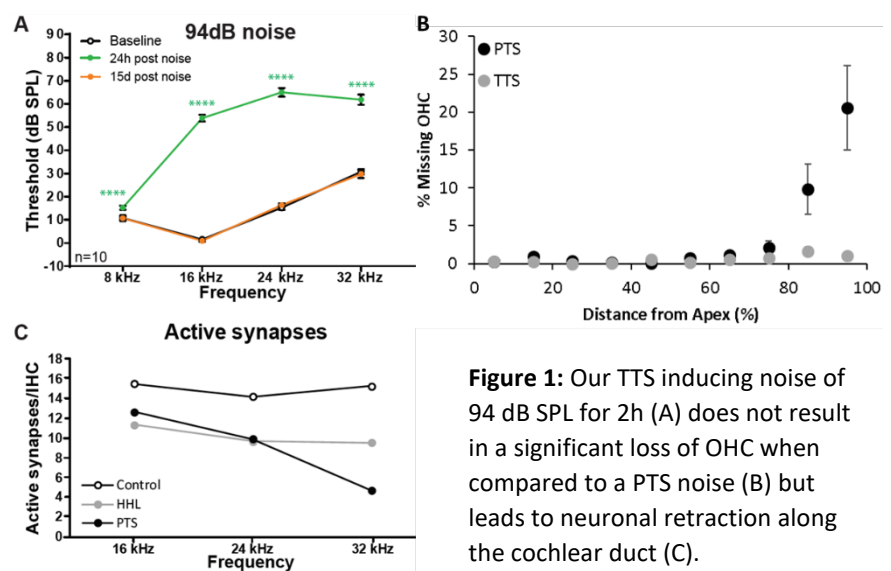


**Figure 1:** Our TTS inducing noise of 94 dB SPL for 2h (A) does not result in a significant loss of OHC when compared to a PTS noise (B) but leads to neuronal retraction along the cochlear duct (C).

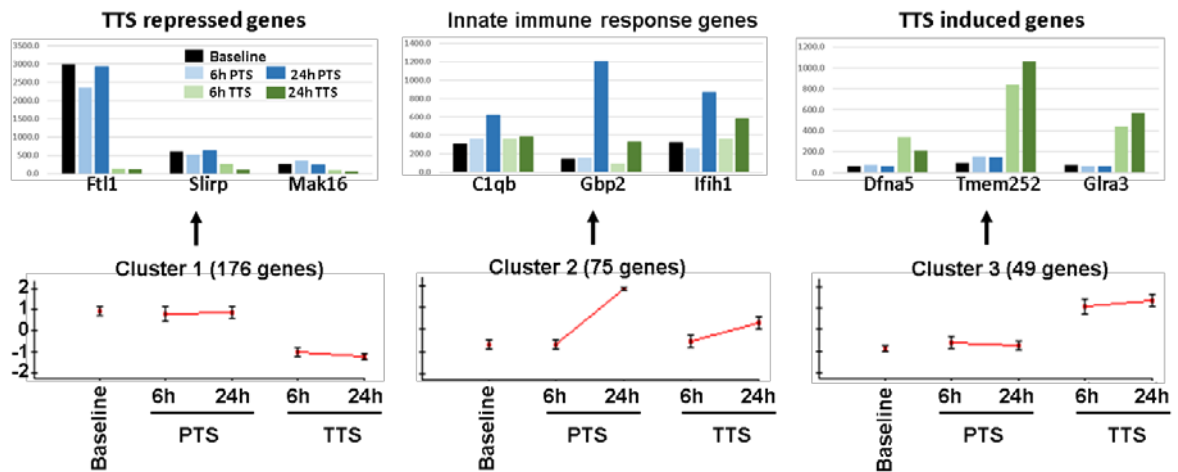


**Figure 2:** Examples of gene expression clusters with a different pattern in response to PTS and TTS. Cluster 1 contains genes repressed after a TTS noise when compared to baseline and PTS. Cluster 2 contains genes highly induced 24h following a PTS noise only and is enriched for the GO 0045087 (innate immune response, FDR=0.009). Cluster 3 contains genes induced only after a TTS noise. The latter is particularly interesting as it is likely to contain genes with a protective effect on hearing.

**Specific Aim 3:** Following the in-person review of the award in the summer 2017, specific aim 3 was redesigned to allow us to both study the response to Heat Shock with and without noise exposure as originally planned as well as obtain all tissue separately from male and female mice.

**New this year:**

- **Major Task 1:** male and female tissue collected separately for baseline, PTS and TTS  
 New baseline - Tissue collection, tissue processing and library preparation for sequencing are complete for OHC and SC  
 PTS (105dB) – Tissue collection and tissue processing is complete for OHC and SC. Library preparation is 85% complete for OHC and 50% complete for SC.  
 TTS (94db) – Tissue collection and processing is complete for OHC and 75% complete for SC. Library preparation is pending.
- **Major Task 2:** male and female tissue collected separately for heat shock with/without noise  
 Heat shock only - Tissue collection and tissue processing is complete for OHC and ongoing for SC.  
 Heat shock and noise - pending

### Key research accomplishments

- Publication of three peer-reviewed manuscripts describing key findings from the project in the following journals: *Biology of Sex Differences*, *BMC Genomics* and *Nature*.
- Identification of OHC and SC unique genes and their regulators.
- Molecular description of the response to PTS in OHC, SC and whole inner ear.
- Molecular description of the response to TTS.

- Key differences between the response to TTS and PTS.
- Critical differences in the response to noise between males and females.

#### **Future plans for next reporting period**

- Complete sequencing and analysis of the project data.
- Validation by nanoString.
- Preparation of the NIH blueprint for publication and data dissemination via the UMGEAR.org – a portal for sharing and analysis of gene expression that was generated by the project PI.

#### **Conclusion**

In this funding period we continued to work on generating a refined cell type-specific blueprint for the molecular changes that occur after NIHL – separated by sex. This change in plan is an outcome of the first three years of the project and the in-person review at the DoD. It was possible thanks to significant improvement in techniques, thanks to calibration work we performed as part of the project and also published this year in BMC Genomics. This is significant because it makes the RiboTag approach more accessible to additional researchers as less mice are needed per biological replicate. We also further characterized the initially identified sex-specific changes in the response to noise and published our findings in the peer reviewed literature. This was an unexpected outcome of the project. The project was designed to molecularly characterize previously published molecular interventions that ameliorate NIHL in mice. However, sex as a biological factor, had a stronger effect on the outcome of noise exposure than many of the tested interventions. This is significant, as our findings outline important guidelines in study design for NIHL and are also a basis for development of therapeutics capitalizing on the estrogen signaling pathway (a project that is currently prepared for submission in response to W81XWH-18-HRRP-FARA). Finally, through the baseline analysis of OHC-specific translatomes, we identified *Ikzf2/helios* as a key regulator of OHC functional maturation. This exciting finding resulted in a team collaboration which culminated in a recently accepted manuscript to Nature. We are very excited about the work that originated from this project and see the completion of the sequencing and nanoString validation of the generated blueprint our major task for this coming year. We plan to work diligently to make the data publication-ready as soon as possible so that this valuable molecular blueprint could be shared with the research community at large – from academics to pharma, to promote the discovery and testing of drugs to treat NIHL.

#### **Opportunities for training and professional development**

##### Training or fellowship awards:

Benjamin Shuster, BS: participated in the Association for Research in Otolaryngology as well as in the Gordon Research Conference (July 2018) where he presented data on sex differences in hearing and the response to noise.

Beatrice Milon, PhD, participated in the Association for Research in Otolaryngology meeting as well as in the Gordon Research Conference (July 2018) where she expanded her knowledge both on hidden hearing loss as well as central pathways in auditory processing.

Ryan Casserly, MD (worked in the Hertzano laboratory for 5-month full time research rotation in 2017): presented his findings in the Association for Research in Otolaryngology 2018

Laboratory meetings - since obtaining funding from the DoD the entire Hertzano laboratory engages in in-depth study of current literature and techniques to study NIHL and has been increasing their knowledge and experience through laboratory meetings and journal clubs. The team has also trained two additional laboratories in the department (laboratories of Drs. Ahmed and Riazuddin) who now focus some of their work on NIHL. In addition, two years ago, we developed a new series of laboratory meetings named H&H (Hearing and Hormones) attended by Dr. Jessica A. Mong (a neuroendocrinologist with a focus on sex differences in the brain) and our group. Finally, the PI organized a translational auditory and vestibular research day focused on NIHL in the fall of 2018. This day was a tremendous success with over 100 participants from universities in the region was used to educate and disseminate knowledge on NIHL (agenda attached in appendix 2).

#### Professional development

All members working on the DoD project participate in laboratory meetings, the translational Auditory and Vestibular research day, the Association for Research in Otolaryngology mid-winter meeting.

#### **4. IMPACT**

The impact of the work on the project in this funding period was accomplished primarily via publications and presentations in professional meetings. Our findings on sex differences in NIHL and hearing are already changing study design in the field.

#### **5. CHANGES/PROBLEMS**

We had a delay in the breeding efficiency this year and therefore the baseline heat shock experiments are done on C57BL/6 and not the mixed background. However, with improvements to the sequencing protocol, we can now catch up over the year thanks to requiring less mice per biological replicate.

All changes in structure and expenditures have been reported in the in-person review (within the presentation) and are within the limits of the budget of the project.

No significant changes were made to biohazards.

Our IACUC animal protocol #0915006 linked to this project expired on September 16<sup>th</sup> 2018. A new animal protocol to complete the experiments was submitted and approved by the IACUC. The new protocol #0818004 and the approval letter are attached as appendices 3 and 4.

#### **6. PRODUCTS**

##### **Publications, abstracts, and presentations**

##### Publications

Three manuscripts were accepted for publication during this reporting period.

The manuscript describing differences in response to noise between male and female mice has been published in *Biology of Sex Differences*: Milon B, Mitra S, Song Y, Margulies Z, Casserly R, Drake V, Mong JA, Depireux DA, Hertzano R. **The impact of biological sex on the response to noise and otoprotective therapies against acoustic injury in mice.** *Biol Sex Differ.* 2018 Mar 12;9(1):12.

The kit comparison manuscript has been published in BMC Genomics: Song Y, Milon B, Ott S, Zhao X, Sadzewicz L, Shetty A, Boger ET, Tallon LJ, Morell RJ, Mahurkar A, Hertzano R. **Comparative analysis of library prep approaches for sequencing low input translome samples.** BMC Genomics. 2018 Sep 21;19(1):696.

The manuscript describing the identification of *Ikzf2* as a key regulator of the OHC translome was accepted for publication in Nature: Chessum L, Matern M, Kelly MC, Johnson SL, Ogawa Y, Milon B, McMurray M, Driver EC, Parker A, Song Y, Codner G, Esapa CT, Prescott J, Trent G, Wells S, Dragich AK, Frolenkov GI, Kelley MW, Marcotti W, Brown SDM, Elkon R, Bowl MR, Hertzano R. ***Ikzf2/helios* is a key transcriptional regulator of outer hair cell maturation.** Nature

### Abstracts and presentations

Our data about the PTS and TTS was presented at the ARO 2018 Mid-Winter Meeting (Symposium).

Hertzano H, Milon B, Mitra S, Ogawa Y, Shetty A, Zhang X, Depireux D, Elkon R. A cell-type specific blueprint of the molecular changes following noise exposure.

The findings about the role of estrogen in the differences in response to noise between male and female was presented at the ARO 2018 Mid-Winter Meeting (podium presentation) and the 2018 Auditory Systems Gordon Research Conference (poster).

Casserly R, Mitra S, Viechweg S, Shuster B, Myers A, Song Y, Milon B, Depireux D, Mong J, Hertzano H. Estrogenic protection from noise-induced hearing loss in females but not in males. ARO Mid-Winter Meeting.

Shuster B, Casserly R, Viechweg S, Myers A, Milon B, Depireux D, Mong J, Hertzano H. Probing the Role of Estrogen in Hearing. GRC 2018.

## 7. PARTICIPANTS AND OTHER COLLABORATING ORGANIZATIONS

### Individuals who work on the project

<b>Name</b>	<b>Ronna Hertzano</b>
<b>Project Role</b>	<b>PI</b>
<b>Researcher identifier</b>	
<b>Nearest person month worked:</b>	<b>2</b>
<b>Contribution to the project</b>	<b>Overall responsibility for the proposal and all aspects of the research program including: hiring and training personnel, ensuring quality of data, interpretation of data, oversight of methods, administrative responsibility and reporting to the DoD.</b>
<b>Funding support</b>	<b>NIH R01, DC013817 (PI); NIH R01, DC003544 (Co-I); Hearing Health Foundation – HRP support for gEAR (PI); MPower The State Grant – Center for Excellence in Cochlear Implants (Co-PI); R01 DC016595 (Co-I); NIMH, R24MH114815 (PI)</b>

<b>Name</b>	<b>Didier Depireux</b>
<b>Project Role</b>	<b>Co-I</b>
<b>Researcher identifier</b>	
<b>Nearest person month worked:</b>	<b>1.2</b>
<b>Contribution to the project</b>	<b>Oversight of the noise exposure protocols, ABR and DPOAE setup and measurements; Discussion and analysis of Male/Female data.</b>
<b>Funding support</b>	<b>MII, Translational Research in Hearing Foundation, Capita foundation, NIH/NIDCR</b>

<b>Name</b>	<b>Ran Elkon</b>
<b>Project Role</b>	<b>Co-I</b>
<b>Researcher identifier</b>	
<b>Nearest person month worked:</b>	<b>1.2</b>
<b>Contribution to the project</b>	<b>Data analysis and study design</b>
<b>Funding support</b>	

<b>Name</b>	<b>Yang Song</b>
<b>Project Role</b>	<b>Analyst</b>
<b>Researcher identifier</b>	
<b>Nearest person month worked:</b>	<b>1.2</b>
<b>Contribution to the project</b>	<b>Data analysis</b>
<b>Funding support</b>	

<b>Name</b>	<b>Beatrice Milon</b>
<b>Project Role</b>	<b>Research Supervisor</b>
<b>Researcher identifier</b>	
<b>Nearest person month worked:</b>	<b>6 months</b>
<b>Contribution to the project</b>	<b>Study design, tissue collection, schedule oversight, training Benjamin Shuster, RiboTag IP, RNA analysis, cytochrome c oxidase</b>
<b>Funding support</b>	

<b>Name</b>	<b>Benjamin Shuster</b>
<b>Project Role</b>	<b>Research Assistant</b>
<b>Researcher identifier</b>	
<b>Nearest person month worked:</b>	<b>12</b>
<b>Contribution to the project</b>	<b>Tissue collection, noise exposures, male/female analysis, preparation of review on sex differences in hearing</b>

<b>Funding support</b>	
------------------------	--

**Changes in the other support of the PI/ other key personnel:**

- No significant changes.

**8. SPECIAL REPORTING – quad chart (original file submitted as appendix 5)**

**Towards a molecular understanding of noise induced hearing loss**  
 Log number: MR130240

PI: Ronna Hertzano      Org: University of Maryland School of Medicine      Award Amount: \$1,500,000



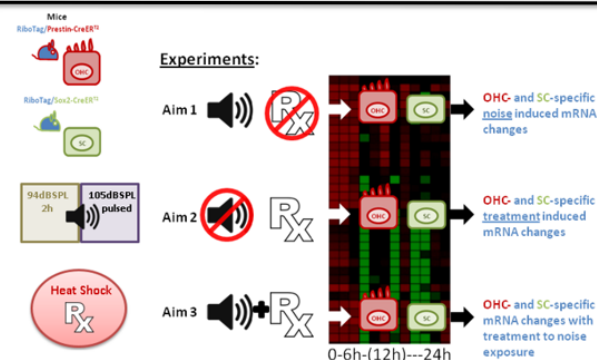
---

**Study/Product Aim(s)**

- Characterization of the translomes of adult outer hair cells (OHC) and supporting cells (SC) at baseline.
- Identification, characterization and validation of the cell type-specific translational changes secondary to noise trauma that induces a permanent in comparison to a temporary hearing loss.
- Identification of the cell type-specific signaling cascades activated during successful treatment of noise induced hearing loss in mice (e.g. Heat Shock).
- Define at least two key signaling cascades that could be targeted to develop new therapeutic interventions to prevent and treat noise induced hearing loss.
- Determine the sex-specific differences in the molecular response to noise exposure.

**Approach**

We established animal models that allow cell type-specific RNA extraction from adult mouse inner ears, to determine the cell type-specific translational changes at different time points following noise exposure with and without treatment, compared with the baseline translomes prior to exposure. Identified key regulatory pathways will be validated using real time RT-PCR.



**Experiments:**

Aim 1: Noise → OHC and SC-specific noise induced mRNA changes

Aim 2: Noise + Rx → OHC and SC-specific treatment induced mRNA changes

Aim 3: Noise + Rx + Heat Shock → OHC and SC-specific mRNA changes with treatment to noise exposure

0-6h-(12h)---24h

---

**Timeline and Cost**

Activities	CY	14-15	15-16	16-17	17-19
To establish the OHC- and SC-specific translome of adult mouse inner ears					
To determine the OHC- and SC-specific transcriptional and signaling cascades activated in response to PTS-inducing noise injury					
To determine the OHC- and SC-specific signaling cascades activated in vivo in response to otoprotective interventions					
To evaluate the OHC- and SC-specific signaling cascades affected in vivo in mice, in male s and females separately, to PTS and TTS noise, as well as Heat Shock, and PTS noise and Heat Shock combined					
<b>Estimated Budget (\$K)</b>		\$400	\$400	\$400	\$300

Updated: (October 26, 2018)

**Goals/Milestones**

**CY14-16 Goal – OHC- and SC- translomes at baseline**

- ☑ Identification and characterization of the OHC and SC-specific translomes

**CY15-16 Goal – Defining the inner ear translome in response to noise trauma**

- ☑ Identification of the key signaling cascades initiated by noise trauma
- ☑ Identification of differences in the response of male and female mice to noise

**CY16-17 Goal – In vivo dissection of cell type-specific changes in response to treatment and pre-treated noise exposure**

- ☑ Comparison of the cell type-specific molecular changes in response to PTS- and TTS- inducing noise exposure
- ☑ Improved approaches for Ribotag seq using fewer mice per experiment

**CY17-19 Goal – Defining the inner ear translome in response to noise trauma**

- ☐ Identification of at least two new pathways for generating new interventions to prevent and treat noise induced hearing loss
- ☐ Comparison of the cell type-specific molecular responses to PTS-inducing noise with and without protective interventions.
- ☐ Identify some of the sex-specific molecular changes in response to noise.

**Budget Expenditure to Date**  
 Projected Expenditure: 1,500,000  
 Actual Expenditure: 1,372,513

**9. APPENDICES**

Appendix 1a: Manuscript “Ikzf2/helios is a key transcriptional regulator of outer hair cell maturation” accepted for publication in *Nature*.

Appendix 1b: Manuscript “The impact of biological sex on the response to noise and otoprotective therapies against acoustic injury in mice”

Appendix 1c: Manuscript “A comparative analysis of library prep approaches for sequencing low input translome samples”

Appendix 2: Agenda for the 3<sup>rd</sup> Auditory and Vestibular Translational Research Day (2017)

Appendix 3: New Animal Protocol – no changes from the previous protocol – our animal protocol had to be renewed and therefore was re-submitted and approved

Appendix 4: Approval for new animal protocol

Appendix 5: Quad chart

# ***Ikzf2/helios* is a key transcriptional regulator of outer hair cell maturation**

Lauren Chessum<sup>1,11</sup>, Maggie S Matern<sup>2,11</sup>, Michael C Kelly<sup>3</sup>, Stuart L Johnson<sup>4</sup>, Yoko Ogawa<sup>2</sup>, Beatrice Milon<sup>2</sup>, Mark McMurray<sup>2</sup>, Elizabeth C Driver<sup>3</sup>, Andrew Parker<sup>1</sup>, Yang Song<sup>5</sup>, Gemma Codner<sup>1</sup>, Christopher T Esapa<sup>1</sup>, Jack Prescott<sup>1</sup>, Graham Trent<sup>2</sup>, Sara Wells<sup>6</sup>, Abigail K Dragich<sup>7</sup>, Gregory I. Frolenkov<sup>7</sup>, Matthew W Kelley<sup>3</sup>, Walter Marcotti<sup>4</sup>, Steve DM Brown<sup>1</sup>, Ran Elkon<sup>8,9</sup>, Michael R Bowl<sup>1,12,\*</sup>, Ronna Hertzano<sup>2,5,10,12,\*</sup>

<sup>1</sup>*Mammalian Genetics Unit, MRC Harwell Institute, Harwell Campus, Oxfordshire, OX11 0RD, UK*

<sup>2</sup>*Department of Otorhinolaryngology Head and Neck Surgery, University of Maryland School of Medicine, Baltimore, MD 21201, USA*

<sup>3</sup>*National Institute on Deafness and Other Communication Disorders, National Institutes of Health, Bethesda, MD 20892, USA*

<sup>4</sup>*Department of Biomedical Science, University of Sheffield, Sheffield, S10 2TN, UK*

<sup>5</sup>*Institute for Genome Sciences, University of Maryland School of Medicine, Baltimore, MD 21201, USA*

<sup>6</sup>*Mary Lyon Centre, MRC Harwell Institute, Harwell Campus, Oxfordshire, OX11 0RD, UK*

<sup>7</sup>*Department of Physiology, College of Medicine, University of Kentucky, Lexington, Kentucky 40536-0298, USA*

<sup>8</sup>*Department of Human Molecular Genetics and Biochemistry, Sackler School of Medicine, Tel Aviv University, Tel Aviv 69978, Israel*

<sup>9</sup>*Sagol School of Neuroscience, Tel Aviv University, Tel Aviv, Israel*

<sup>10</sup>*Department of Anatomy and Neurobiology, University of Maryland School of Medicine, Baltimore, MD 21201, USA*

<sup>11</sup>These authors contributed equally to this work

<sup>12</sup>These authors jointly supervised this work

\*Corresponding authors: Michael Bowl (m.bowl@har.mrc.ac.uk), Ronna Hertzano (rhertzano@som.umaryland.edu)

**The sensory cells responsible for hearing include the cochlear inner hair cells (IHCs) and outer hair cells (OHCs), with OHCs being necessary for sound sensitivity and tuning. Both cell types are thought to arise from common progenitors, however our understanding of the factors that control IHC and OHC fate remains limited. Here we identify *Ikzf2*/helios as an essential transcription factor required for OHC functional maturation and hearing. *Ikzf2*/helios is expressed in postnatal mouse OHCs, and a mutation in *Ikzf2* causes early-onset sensorineural hearing loss in the *cello* mouse model. *Ikzf2*<sup>cello/cello</sup> OHCs have greatly reduced prestin-dependent electromotile activity, a hallmark of OHC functional maturation, and show reduced levels of critical OHC-expressed genes such as *Slc26a5*/prestin and *Ocm*. Moreover, we show that ectopic expression of *Ikzf2*/helios in IHCs induces expression of OHC-specific genes, reduces canonical IHC genes, and confers electromotility to IHCs, demonstrating that *Ikzf2*/helios is capable of partially shifting the IHC transcriptome towards an OHC-like identity.**

The mature mammalian cochlea contains two distinct types of sensory cells, named inner and outer hair cells (HCs), each of which are highly specialized and, in humans, do not regenerate once damaged or lost<sup>1</sup>. Progressive loss of these cells, particularly the outer HCs (OHCs), underlies much of the aetiology of age-related hearing loss – a worldwide epidemic<sup>2,3</sup>. While these two cell types were first described by Retzius in the 1800's, the mechanisms underlying the specification of their common progenitor cells to functional inner versus outer HCs remain poorly understood. Additionally, attempts to direct stem cells towards HC fates have, to date, resulted only in the formation of immature HC-like cells that lack many of the markers of mature inner or outer HCs<sup>4</sup>. Given the vulnerability of the OHCs, identifying factors that specify OHC fate is crucial, not only for understanding the biology of this unique cell type, but ultimately for working towards regenerative therapies for hearing loss.

To define a set of high confidence OHC-expressed genes for downstream gene regulation analyses, we crossed the prestin-CreER<sup>T2</sup> mice, which can be induced to express Cre-recombinase specifically in OHCs, with the RiboTag mouse model, allowing for OHC-specific ribosome immunoprecipitation (IP)<sup>5,6</sup>. Cochlear ducts from *RiboTag*<sup>HA/+</sup>;*prestin*<sup>CreERT2/+</sup> mice were collected at five postnatal time points (postnatal day (P) 8, P14, P28, 6 weeks (wk), and 10 wk), and actively translated OHC transcripts were enriched for by ribosome IP, followed by RNA sequencing (RNA-seq) of all IP and paired input RNA (Extended Data Fig.1a-b, Supplementary Table 1). We calculated an OHC enrichment factor (EF) based on the IP/input log<sub>2</sub> fold change (LFC) for each gene at each time point (Supplementary Table 2). Reassuringly, known postnatal HC- and OHC-expressed genes such as *Pou4f3*, *Gfi1*, *Strc*, *Ocm* and *Slc26a5* generally had high EFs across time points (EF>1), while prominent IHC marker genes such as *Otof*, *Atp2a3* and *Slc17a8* were generally depleted from the IP samples (EF<-1). Additionally, marker genes for supporting cells, neurons and otic mesenchyme were also depleted (Extended Data Fig.1c). Further informatics analyses of our RiboTag OHC dataset demonstrated a systematic enrichment of OHC markers and depletion of IHC markers identified by a published adult mouse OHC and IHC transcriptomic dataset (Liu et al.)<sup>7</sup>, and overall classified the OHC-enriched transcripts into three clusters (Extended Data Fig.1d-f, Supplementary Table 3). Intersecting genes whose transcripts were enriched in OHCs in our most mature RiboTag OHC data point (10wk, EF>0.5) with the Liu et al. dataset resulted in a list of 100 highly confident postnatal OHC markers that are significantly and consistently enriched in postnatal OHCs (Fig.1a, Supplementary Table 4). We and others have previously shown that relevant transcriptional regulators can be discovered by analysing the promoters of cell-type specific genes to identify statistically over-represented transcription factor (TF) binding motifs<sup>8,9</sup>. A TF binding motif prediction analysis of the 100 OHC marker genes identified multiple enriched motifs in the 20 kb regions centered around the transcription

start site, the top five of which correspond to the TFs HNF4A, MZF1, POU3F2, IKZF2/helios and RFX3<sup>10</sup>. Of these TFs, only IKZF2/helios: was included in the list of 100 OHC marker genes; was found to be markedly enriched in OHCs at all time points (Fig.1b-c); and showed a ~4-fold enrichment in OHCs compared to IHCs in the Liu et al. dataset (Supplementary Table 4). Further characterization of helios protein expression in the inner ear confirmed that it is restricted to the OHC nuclei starting from P4, and persists in functionally mature OHCs (Fig.1d-f, Extended Data Fig.2a). Together, these data suggest an important role for *Ikzf2*/helios in regulating the OHC transcriptome from early postnatal to adult stages.

A recent phenotype-driven ENU-mutagenesis screen, undertaken at the MRC Harwell Institute, identified a C-to-A transversion at nucleotide 1551 of *Ikzf2* in the *cello* mouse mutant, causing a non-synonymous histidine-to-glutamine substitution (p.H517Q) in the encoded helios TF (Fig.1g, Extended Data Fig.2b-d)<sup>11</sup>. A combination of *in silico* mutation analyses, structural 3D modelling, immunolabeling of helios in the *cello* mutant mice, and *in vitro* assays predicted and validated a deleterious effect of the *cello* mutation on the ability of helios to dimerize without impairing its cellular localization (Fig.1g, Extended Data Fig.2e and 3). We further investigated the functional role of *Ikzf2* in hearing by assessing Auditory Brainstem Response (ABR) thresholds in wild-type and *cello* mice across several time points. Results show that *Ikzf2*<sup>*cello/cello*</sup> mice have progressive deterioration of hearing function starting as early as P16 (>60 dB SPL) with a threshold of  $\geq 85$  dB SPL by 9-months (Fig.2a-b, Extended Data Fig.4a-c). Using scanning electron microscopy, we show that the ultrastructure of the cochlear sensory epithelia and HC stereocilia bundles in the *cello* mice appear normal up to 1-month of age, after which the OHCs bundles, and later the IHCs bundles, begin to degenerate (Extended Data Fig.4d, 5a-d, Supplementary Tables 5-6). These data indicate that the hearing impairment in *cello* mice precedes the loss of HC bundles, and suggest that the helios mutation instead leads to a functional OHC deficit. Furthermore, by

utilizing a second *Ikzf2* mutant allele (*Ikzf2<sup>del1890</sup>*), which leads to an in-frame deletion of the 3<sup>rd</sup> coding exon, we confirm *Ikzf2* as the causative gene underlying the auditory dysfunction in the *cello* mutants. At 1-month of age, *Ikzf2<sup>cello/del1890</sup>* compound heterozygotes display elevated ABR thresholds (up to 40 dB SPL) compared to heterozygotes and wild-type mice (Extended Data Fig. 5e-f), confirming *Ikzf2<sup>cello</sup>* as the causative allele in the *cello* mutant.

To explore the effect of the *cello* mutation on OHC physiology we investigated the basolateral properties of OHCs. We found that the MET current (Extended Data Fig. 6a-c) and the adult-like potassium ( $K^+$ ) current  $I_{K,n}$  (Extended Data Fig. 6d-h) have normal biophysical characteristics in *Ikzf2<sup>cello/cello</sup>* OHCs. The resting membrane potential ( $V_m$ ) of OHCs is also similar between genotypes (*Ikzf2<sup>cello/+</sup>*:  $-68 \pm 2$  mV; *Ikzf2<sup>cello/cello</sup>*:  $-70 \pm 1$  mV). We then investigated whether helios regulates OHC electromotile activity. We found that stepping the membrane potential from  $-64$  mV to  $+56$  mV causes the OHCs from both genotypes to shorten (Fig.2c-d), as previously described<sup>12-14</sup>. However, *Ikzf2<sup>cello/cello</sup>* OHCs show significantly reduced movement compared to *Ikzf2<sup>cello/+</sup>* control OHCs (Fig.2e), even when the values are normalized to their reduced surface area (Fig.2f). We also found that young adult *Ikzf2<sup>cello/cello</sup>* mice have significantly reduced DPOAE responses ( $\leq -15$  dB SPL) compared to littermate controls (Fig.2g), further demonstrating impaired OHC function.

To identify genes regulated by helios in OHCs, we compared gene expression from cochleae of P8 *Ikzf2<sup>cello/cello</sup>* and their wild-type littermate controls by RNA-seq. We identified 105 upregulated and 36 downregulated genes in *Ikzf2<sup>cello/cello</sup>* cochleae (Supplementary Table 7), including downregulation of the canonical OHC markers *Slc26a5* and *Ocm*, which was confirmed by NanoString validation (Fig.2h). Furthermore, we did not observe modulation of other OHC-expressed TFs selected from Li et al., 2016 (Fig.2i)<sup>15</sup>, suggesting that the observed OHC gene dysregulation results from disruption of a specific transcriptional cascade. Interestingly, by P16 the transcript levels of *Car7*, *Ocm*, and *Slc26a5*, but not *Ppp1r17*, are

similar to wild-type littermate controls, suggesting the possibility that other factors may be compensating for the functional loss of *Ikzf2* by this time point (Extended Data Fig.6i).

To further characterize the transcriptional cascade downstream of *Ikzf2*/helios, we performed *in vivo* Anc80L65 adeno-associated virus (AAV) gene delivery of a myc-tagged *Ikzf2* or GFP (from hereon Anc80-*Ikzf2* and Anc80-*eGFP*) to neonatal inner ears of *Myo15<sup>Cre/+</sup>;ROSA26<sup>CAG-tdTomato</sup>* mice, sorted the cochlear HCs at P8, and measured resultant changes in gene expression using single cell RNA-seq (scRNA-seq) (Fig.3a, Extended Data Fig.7)<sup>16,17</sup>. The HCs from Anc80-*Ikzf2* injected inner ears separated into two distinct sets of clusters, containing both IHCs and OHCs. One set of IHCs and OHCs completely overlapped with the HCs from the Anc80-*eGFP* control injected ears (Fig.3b, bottom clusters), while the other set clustered separately (Fig.3b, top clusters). Separation of the two sets of clusters showed a clear correlation with Anc80-*Ikzf2* transgene expression (Fig.3b), where HCs in the bottom clusters had a lower expression of Anc80-*Ikzf2*, and the HCs in the top clusters had a higher expression of Anc80-*Ikzf2* (hereon defined as Anc80-*Ikzf2* low (-) and high (+), respectively). Because the HCs defined as Anc80-*Ikzf2* (-) clustered together with the HCs transduced with Anc80-*eGFP*, these two groups of HCs were merged and named Anc80-*Ikzf2* (-) IHCs and OHCs for all downstream analyses (Fig.3b-c).

While overexpression of *Ikzf2* in IHCs and OHCs did not change the expression of HC markers such as *Pou4f3* and *Calb1* (Fig.3d), it led to a significant downregulation of many genes whose transcripts were identified as IHC-enriched in the control HC populations, including *Otof*, *Rprm*, *Atp2a3*, and *Fgf8* (Fig. 3e, Extended Data Fig. 8, Supplementary Tables 8, 9, 10). Interestingly, some of the genes that are downregulated in both Anc80-*Ikzf2* transduced IHCs and OHCs are genes that are normally expressed in both cell types in early postnatal development, and that later become IHC-specific (e.g., *Pvalb* and *Otof*, Supplementary Table 10)<sup>18,19</sup>. This suggests that helios overexpression in OHCs results in an

accelerated downregulation of these genes. Additionally, helios overexpression in IHCs results in the upregulation of genes that are normally enriched in OHCs, such as *Ocm*, *Pde6d*, *Ldhb* and *Lbh* (Fig.3f, Extended Data Fig.8). Overall, these data suggest that during normal OHC development, helios likely functions to both decrease the expression of early pan-HC markers, such as *Otof*, in the maturing OHCs, as well as to upregulate OHC marker genes. A correlation analysis further validates the role of *Ikzf2* in regulating OHC-related gene expression (Extended Data Fig.8, 9, Supplementary Table 11). The effect of *Ikzf2* transduction on IHC gene expression was further validated by immunolabeling or *in situ* hybridization for OTOF, VGLUT3, OCM, prestin and *Fcrlb* (Fig.4, Extended Data Fig.10a-b). Further analysis of the surface characteristics of the transduced IHCs does not show a change from an IHC-like to an OHC-like stereociliary bundle, consistent with a partial role for helios in regulating OHC-fate (Extended Data Fig.10c). However, *Ikzf2* transduction resulted in the appearance of prominent voltage-dependent (non-linear) capacitance in IHCs (Extended Data Fig.10d-e), which is an electrical “signature” of prestin-dependent OHC electromotility<sup>20,21</sup>. These data indicate that Anc80-*Ikzf2* transduced IHCs start to acquire the major function of normal OHCs.

In conclusion, our study demonstrates that *Ikzf2*/helios is necessary for hearing and is a critical regulator of gene expression in the maturing postnatal OHC. In particular, our results suggest that *Ikzf2*/helios functions to suppress IHC and early pan-HC gene expression in OHCs, as well as upregulate canonical OHC marker genes. It further shows that *Ikzf2*/helios is sufficient to induce the essential functional characteristic of electromotility and many of the molecular characteristics of OHCs when expressed in early postnatal IHCs, albeit not all of them – supportive of the notion that additional OHC-expressed transcription factors are involved in postnatal OHC development. This is the first study to demonstrate functional shifts in postnatal HC molecular identities via viral gene delivery, and suggests that delivery of

combinations of TFs may lead to successful regeneration of functional OHCs in the deafened cochlea.

## References

1. Ehret, G. Development of absolute auditory thresholds in the house mouse (*Mus musculus*). *J. Am. Audiol. Soc.* **1**, 179–84 (1976).
2. Bielefeld, E. C., Tanaka, C., Chen, G. & Henderson, D. Age-related hearing loss: is it a preventable condition? *Hear. Res.* **264**, 98–107 (2010).
3. World Health Organization. Deafness and hearing loss fact sheet. *WHO Media centre* (2018). Available at: <http://www.who.int/mediacentre/factsheets/fs300/en/>.
4. Mittal, R. *et al.* Recent Advancements in the Regeneration of Auditory Hair Cells and Hearing Restoration. *Front. Mol. Neurosci.* **10**, 236 (2017).
5. Fang, J. *et al.* Outer hair cell-specific prestin-CreER T2 knockin mouse lines. *Genesis* **50**, 124–131 (2012).
6. Sanz, E. *et al.* Cell-type-specific isolation of ribosome-associated mRNA from complex tissues. *PNAS* **106**, 13939–13944 (2009).
7. Liu, H. *et al.* Characterization of Transcriptomes of Cochlear Inner and Outer Hair Cells. *J. Neurosci.* **34**, 11085–11095 (2014).
8. Elkon, R. *et al.* RFX transcription factors are essential for hearing in mice. *Nat. Commun.* **6**, 8549 (2015).
9. Hertzano, R. *et al.* Cell Type – Specific Transcriptome Analysis Reveals a Major Role for Zeb1 and miR-200b in Mouse Inner Ear Morphogenesis. *PLoS Genet.* **7**, e1002309 (2011).
10. Janky, R. *et al.* iRegulon : From a Gene List to a Gene Regulatory Network Using Large Motif and Track Collections. *PLOS Comput. Biol.* **10**, e1003731 (2014).
11. Potter, P. K. *et al.* Novel gene function revealed by mouse mutagenesis screens for models of age-related disease. *Nat. Commun.* **7**, 12444 (2016).
12. Ashmore, J. F. A fast motile response in guinea-pig outer hair cells: the cellular basis of the cochlear amplifier. *J. Physiol.* **388**, 323–47 (1987).
13. Brownell, W. E., Bader, C. R., Bertrand, D. & de Ribaupierre, Y. Evoked Mechanical Responses of Isolated Cochlear Outer Hair Cells. *Science (80- )*. **227**, 194–196 (1985).
14. Marcotti, W. & Kros, C. J. Developmental expression of the potassium current  $I_{K,n}$  contributes to maturation of mouse outer hair cells. *J. Physiol.* **520 Pt 3**, 653–60 (1999).
15. Li, Y. *et al.* Transcription Factors Expressed in Mouse Cochlear Inner and Outer Hair Cells. *PLoS One* **11**, e0151291 (2016).
16. Zinn, E. *et al.* In Silico Reconstruction of the Viral Evolutionary Lineage Yields a Potent Gene Therapy Vector. *CellReports* **12**, 1056–1068 (2015).
17. Landegger, L. D. *et al.* A synthetic AAV vector enables safe and efficient gene transfer to the mammalian inner ear. *Nat. Biotechnol.* **35**, 280–284 (2017).
18. Roux, I. *et al.* Otoferlin, Defective in a Human Deafness Form, Is Essential for Exocytosis at the Auditory Ribbon Synapse. *Cell* **127**, 277–289 (2006).
19. Simmons, D. D., Tong, B., Schrader, A. D. & Hawkes, A. J. Oncomodulin Identifies Different Hair Cell Types in the Mammalian Inner Ear. *J Comp Neurol* **518**, 3785–3802 (2010).
20. Santos-Sacchi, J. Reversible inhibition of voltage-dependent outer hair cell motility and capacitance. *J. Neurosci.* **11**, 3096–110 (1991).

21. Zheng, J. *et al.* Prestin is the motor protein of cochlear outer hair cells. *Nature* **405**, 149–155 (2000).

**Supplementary Information** is available in the online version of the paper.

**Acknowledgements** We thank L. Vizor, J. Sanderson and W. Chien for technical help and Z. Ahmed for helpful comments on the manuscript. This work was supported by Action on Hearing Loss (G65 to M.R.B., R.H., W.M. and S.D.M.B.), Medical Research Council (MC\_U142684175 to S.D.M.B.), Wellcome Trust (102892 to W.M.), NIDCD/NIH R01DC013817 and R01DC03544 (R.H.), DOD CDMRP MR130240 (R.H.), NIDCD/NIH T32DC00046 and F31DC016218 (M.S.M), the Intramural Program at NIDCD DC000059 (M.W.K), and NIDCD/NIH R01DC014658 (G.I.F.). S.L.J. is a Royal Society University Research Fellow. R.E. is a Faculty Fellow of the Edmond J. Safra Center for Bioinformatics at Tel Aviv University.

**Author Contributions** L.C., M.S.M., M.C.K., Y.O., B.M., M.M., G.C., C.T.E., G.I.F., M.W.K., W.M., S.D.M.B., M.R.B. and R.H. designed and interpreted the experiments. L.C., M.S.M., M.C.K., S.L.J., Y.O., B.M., M.M., A.P., J.P., R.H., E.C.D., G.T., A.K.D., G.I.F. and W.M. performed the experiments. Y.S. and R.E. analyzed the gene expression data. S.W. aided in the management of the *cello* colony. M.R.B. and R.H. conceived and coordinated the study. L.C., M.S.M., M.C.K., W.M., S.D.M.B., R.E. and M.R.B. and R.H. wrote the manuscript.

**Author information** Reprints and permissions information is available at [www.nature.com/reprints](http://www.nature.com/reprints). The authors declare no competing financial interests. Correspondence and requests for materials should be addressed to M.R.B. ([m.bowl@har.mrc.ac.uk](mailto:m.bowl@har.mrc.ac.uk)) or R.H. ([RHertzano@som.umaryland.edu](mailto:RHertzano@som.umaryland.edu)).

## Figures and Legends

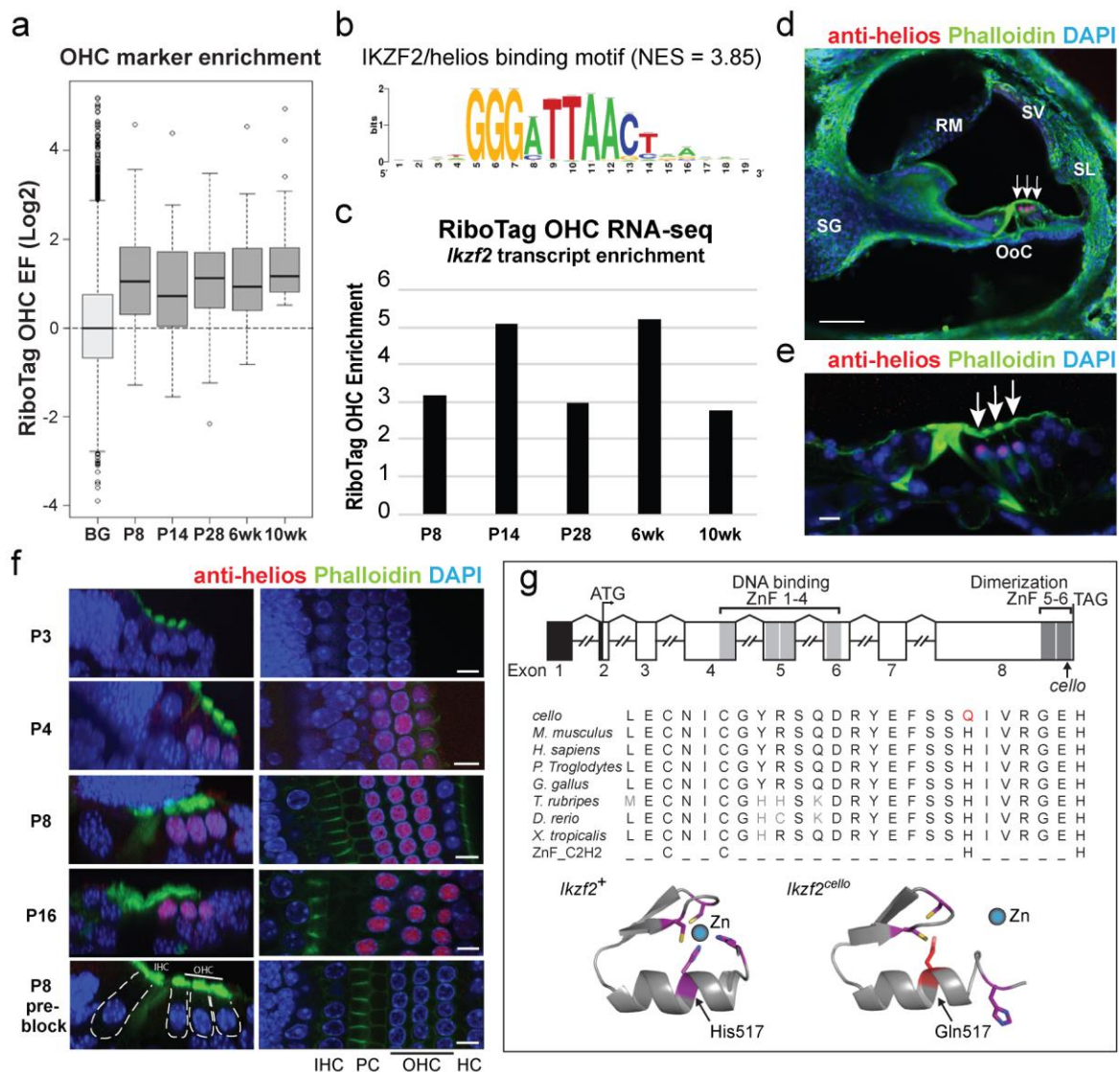


### Figure 1. Helios is a candidate regulator of OHC genes.

(a) The 100 OHC marker genes ( $n=100$ ) are enriched in OHCs at all RiboTag OHC dataset time points compared to expression of all other genes detected (background, BG) ( $n=13,044$ ).  $p$ -values: P8 =  $1.73E-17$ , P14 =  $6.55E-12$ , P28 =  $1.60E-18$ , 6wk =  $7.79E-18$ , 10wk =  $1.43E-33$  (two-sided Wilcoxon's test). Black center line represents median enrichment factor (EF,  $\log_2$  fold change), box demarcates 1<sup>st</sup> and 3<sup>rd</sup> quartiles, whiskers demarcate 1<sup>st</sup> and 3<sup>rd</sup> quartile  $\pm 1.5 \times \text{IQR}$  values, dots represent single outliers.

(b) Transcription factor binding motif analysis using the 100 highly confident OHC marker genes identifies the binding signature for IKZF2/helios as significantly overrepresented. NES = normalized enrichment score.  $\text{NES} \geq 3.0$  corresponds to a false discovery rate of 3-9% (see Janky et al., 2014).

(c) *Ikzf2* transcript enrichment in OHCs as measured by the RiboTag OHC RNA-seq.

(d) Specific expression of helios in the nuclei of wild-type P8 OHCs (white arrows,  $n=3$  biologically independent samples). Scale=50  $\mu\text{m}$ .

(e) Helios expression is maintained in wild-type OHCs at 1-month (white arrows,  $n=3$  biologically independent samples). Scale=10  $\mu\text{m}$ .

(f) Helios is detected in wild-type OHCs from P4 and is maintained in mature P16 OHCs (P3 n=2, P4 n=4, P8 n=4, P16 n=4 biologically independent samples). Loss of labelling when the anti-helios antibody is 'pre-blocked' with its immunizing peptide confirms specificity (n=5 biologically independent samples). Scale=10  $\mu$ m.

(g) The genomic/domain structure of *Ikzf2*/helios. Black = 5' untranslated region, light grey = N-terminal DNA-binding domain, dark grey = C-terminal dimerization domain. The *Ikzf2<sup>cello</sup>* mutation lies in ZnF6. Further alignment of the helios ZnF6 sequence with its paralogues and the classical Cys<sub>2</sub>His<sub>2</sub> ZnF motif shows that the H517Q *cello* mutation causes substitution of a highly conserved zinc-coordinating histidine residue. 3D modelling of wild-type *Ikzf2<sup>+</sup>* ZnF6 and mutant *Ikzf2<sup>cello</sup>* ZnF6 illustrates the requirement of residue His517 for zinc-coordination, which is not possible when residue Gln517 is substituted.

HC, Hensen's cells; IHC, inner hair cells; OoC, organ of Corti; OHC, outer hair cells; PC, pillar cells; RM, Reissner's membrane; SG, spiral ganglion; SL, spiral ligament; SV, stria vascularis.

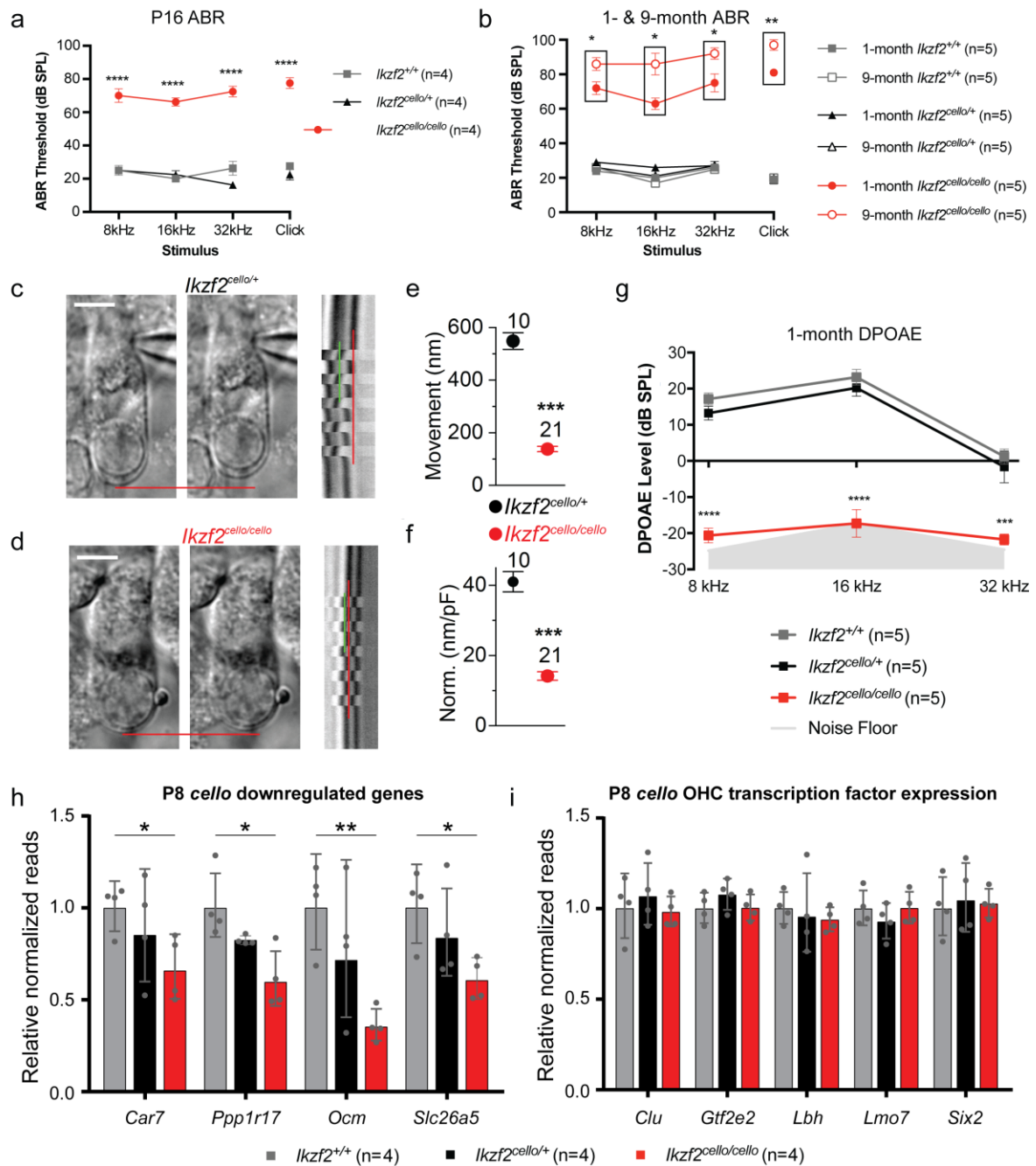


**Figure 2. *Ikzf2/helios* is required for hearing and OHC electromotility.**

(a-b) Averaged ABR thresholds for *cello* mice at P16 (a, n=4 biologically independent animals per genotype) and 1- and 9-months of age (b, n=5 biologically independent animals per genotype for each time point). Age-matched *Ikzf2*<sup>+/+</sup> and *Ikzf2*<sup>cello/+</sup> controls display thresholds within the expected range (15 – 30 dB SPL) at all time-points tested. Data shown are averaged thresholds ± s.e.m. P16 *Ikzf2*<sup>cello/cello</sup> vs *Ikzf2*<sup>+/+</sup> (a) p-values: 8 kHz <0.0001, 16 kHz <0.0001, 32 kHz <0.0001, Click <0.0001. P16 *Ikzf2*<sup>cello/cello</sup> vs *Ikzf2*<sup>cello/+</sup> (a) p-values: 8 kHz <0.0001, 16 kHz <0.0001, 32 kHz <0.0001, Click <0.0001. 1-month *Ikzf2*<sup>cello/cello</sup> vs 9-month *Ikzf2*<sup>cello/cello</sup> (b) p-values: 8 kHz = 0.0284, 16 kHz = 0.0166, 32 kHz = 0.0303, Click = 0.0042. Significance was assessed by one-way ANOVA with Tukey post-hoc test (a) or two-sided Welch's t-test (b). See also Extended Data Figure 4.

(c-d) Images showing a patch pipette attached to an OHC from control *Ikzf2*<sup>cello/+</sup> (c) and mutant *Ikzf2*<sup>cello/cello</sup> (d) cochleae at P16–P18. Red lines indicate the position of the OHC basal

membrane before (left) and during (right) a depolarizing voltage from step from  $-64$  mV to  $+56$  mV, highlighting the shorting of the cells. Scale= $5$   $\mu$ m. Also shown are time-based z-stack projections (right), where red lines indicate the resting position of the basal membrane and the green lines indicate the movement.  $Ikzf2^{cello/+}$   $n = 10$  and  $Ikzf2^{cello/cello}$   $n = 21$  z-stack projections (one set per OHC) from 5 biologically independent animals per genotype.

(e-f) Average movement was significantly reduced in  $Ikzf2^{cello/cello}$  OHCs compared to  $Ikzf2^{cello/+}$  at P16–P18 (e), even after normalization to respective membrane capacitance (f) (for this set of recordings,  $Ikzf2^{cello/+}$ :  $13.6 \pm 0.4$  pF;  $Ikzf2^{cello/cello}$ :  $10.0 \pm 0.3$  pF). Data shown are averaged movement  $\pm$  s.e.m.  $Ikzf2^{cello/+}$   $n = 10$  and  $Ikzf2^{cello/cello}$   $n = 21$  OHCs from 5 biologically independent animals per genotype.  $p$ -value  $< 0.0001$ , two-sided Welch's t-test.

(g) Averaged DPOAE responses for *cello* mice at 1-month of age ( $n=5$  biologically independent animals per genotype). Data shown are averaged thresholds  $\pm$  s.e.m.  $Ikzf2^{cello/cello}$  vs  $Ikzf2^{+/+}$   $p$ -values: 8 kHz  $< 0.0001$ , 16 kHz  $< 0.0001$ , 32 kHz = 0.0004. P16  $Ikzf2^{cello/cello}$  vs  $Ikzf2^{cello/+}$   $p$ -values: 8 kHz  $< 0.0001$ , 16 kHz  $< 0.0001$ , 32 kHz = 0.0012. Significance was assessed by one-way ANOVA with Tukey post-hoc test.

(h-i) NanoString validations of genes downregulated in  $Ikzf2^{cello/cello}$  cochleae at P8 (h) and results showing no change in expression of other OHC TFs (i). Data shown are mean normalized reads relative to wild-type  $\pm$  SD ( $n=4$  biologically independent samples per genotype).  $Ikzf2^{cello/cello}$  vs  $Ikzf2^{+/+}$   $p$ -values: *Car7* = 0.028, *Ppp17r1* = 0.006, *Ocm* = 0.017, *Slc26a5* = 0.017 (two-sided Welch's t-test).

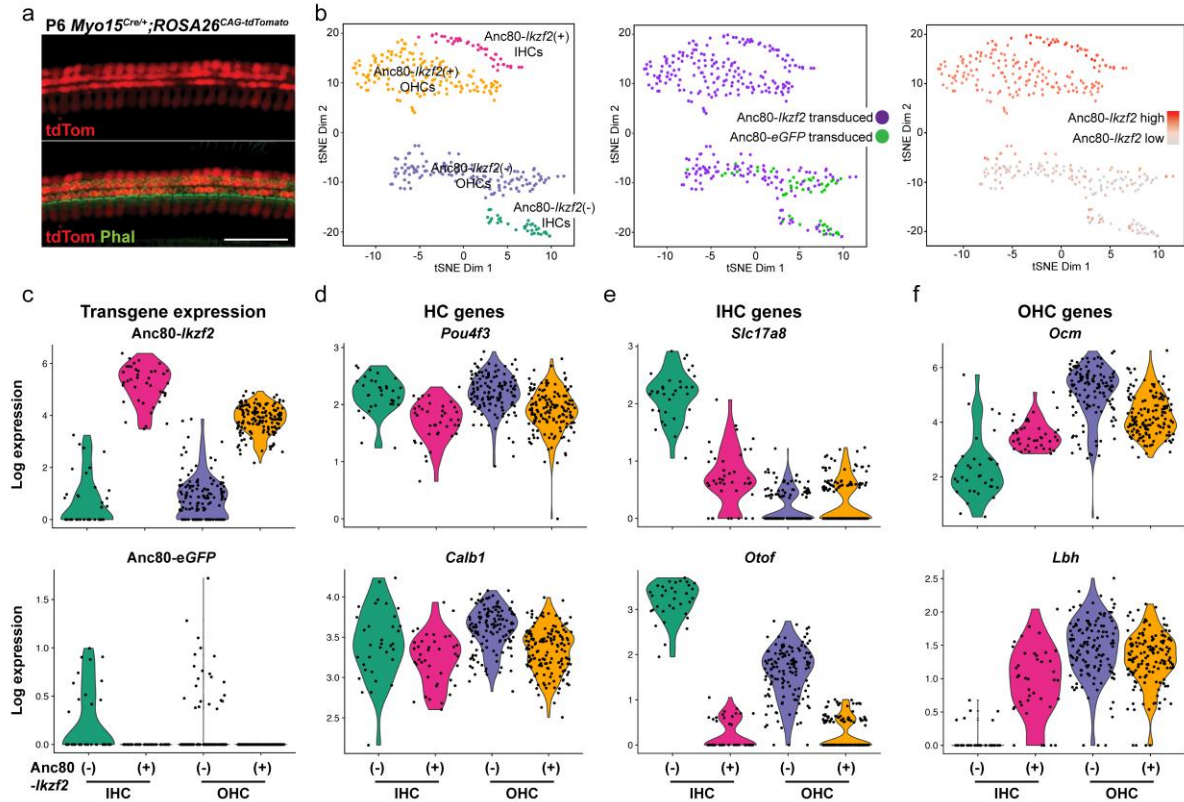


**Figure 3. Partial transcriptional conversion of *Anc80-Ikzf2* transduced IHCs identified by scRNA-seq.**

(a) Representative *Myo15<sup>Cre/+</sup>;ROSA26<sup>CAG-tdTomato</sup>* cochlear whole-mount. *Myo15-Cre*-driven tdTomato expression is HC specific at P6 (n=3 biologically independent samples with similar results). Scale=50  $\mu$ m.

(b) tSNE plots of all cochlear HCs profiled by scRNA-seq, including the cluster to which each cell was assigned, the experimental origin of each cell (*Anc80-Ikzf2* or *Anc80-eGFP* injected cochlea), and the relative transcript abundance of *Anc80-Ikzf2* measured in each cell.

(c) *Anc80-Ikzf2* is highly expressed in the *Anc80-Ikzf2*(+) IHCs and OHCs, whereas *Anc80-eGFP* expression is only seen in the cells assigned to the *Anc80-Ikzf2*(-) IHC and OHC clusters. Dots represent the expression values of individual cells, with width of violins summarizing overall relative distribution of expression.

(d) Canonical HC markers are highly expressed in all HC clusters, and not notably changed as a result of *Anc80-Ikzf2* expression.

(e) IHC-enriched genes that are highly expressed in control IHCs vs control OHCs, but are significantly reduced in *Anc80-Ikzf2*(+) IHCs. *Anc80-Ikzf2*(-) IHC (n=34) vs. *Anc80-Ikzf2*(+) IHC (n=40) FDR: *Slc17a8* = 2.25E-12, *Otof* = 6.76E-14. Significance was assessed by Kruskal-Wallis test followed by post-hoc pairwise Wilcoxon Ranked Sum test adjusted for multiple comparisons.

(f) OHC-enriched genes that are induced in *Anc80-Ikzf2*(+) IHCs. *Anc80-Ikzf2*(-) IHC (n=34) vs. *Anc80-Ikzf2*(+) IHC (n=40) FDR: *Ocm* = 3.65E-08, *Lbh* = 1.81E-10. Significance was assessed by Kruskal-Wallis test followed by post-hoc pairwise Wilcoxon Ranked Sum test adjusted for multiple comparisons.

See also Extended Data Figures 8 and 9.

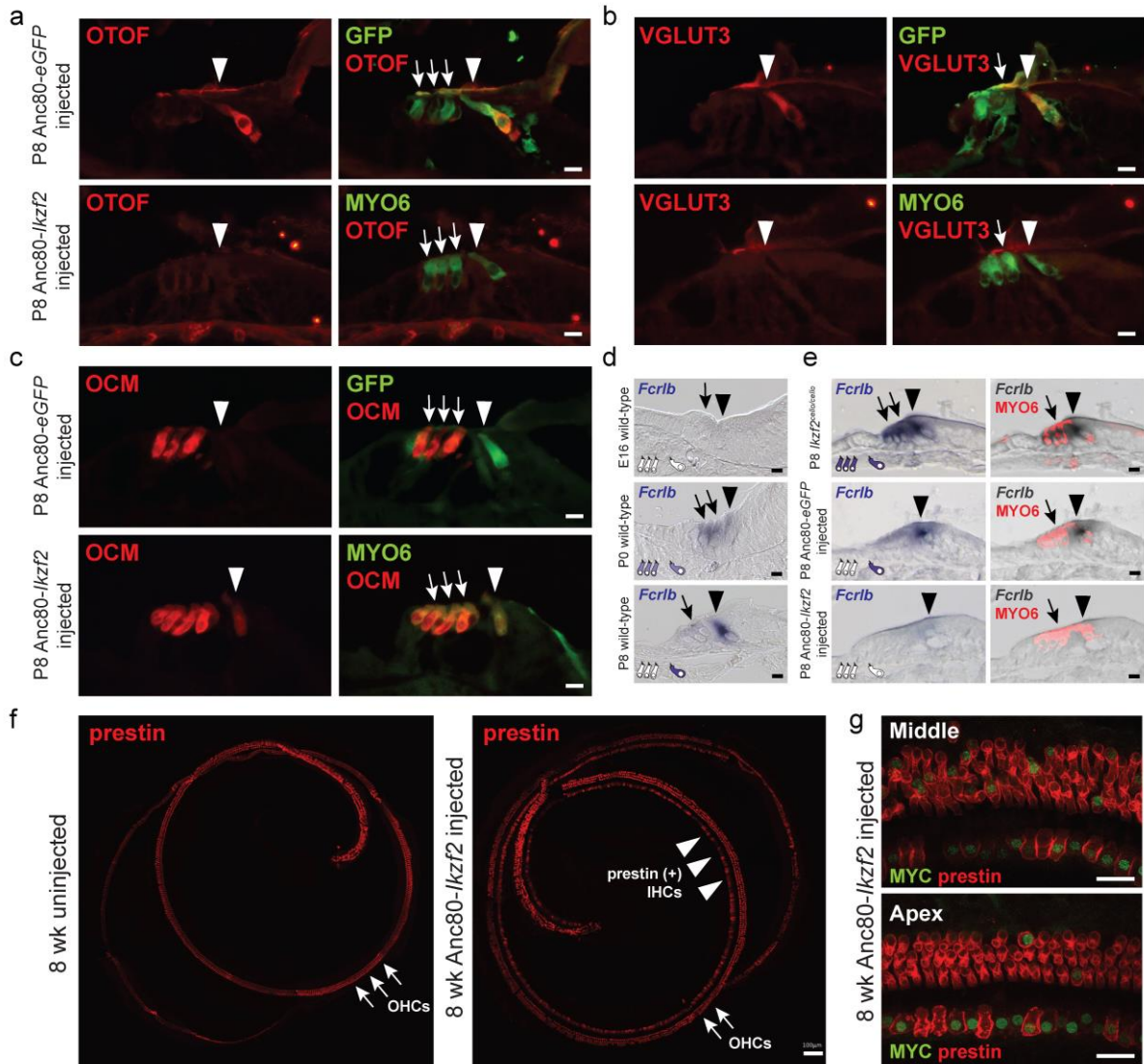


**Figure 4. Helios overexpression modulates expression of HC markers.**

(a-b) IHC markers OTOF and VGLUT3 are downregulated in Anc80-*Ikzf2* transduced IHCs (n=3 biologically independent samples). Arrows = OHCs, arrowheads = IHCs. Scale=10 $\mu$ M. (c) The OHC marker OCM is expressed in Anc80-*Ikzf2* transduced IHCs (n=3 biologically independent samples per condition). Arrows = OHCs, arrowheads = IHCs. Scale=10  $\mu$ m. (d) *Fcrlb* expression during wild-type mouse inner ear development as detected by *in situ* hybridization. While at E16, *Fcrlb* expression is not detected in the inner ear, by P0 it is detected in both IHCs and OHCs and by P8, *Fcrlb* expression is largely restricted to the IHCs (n=3 biologically independent samples per time point). Scale=10  $\mu$ m. (e) In the absence of functional helios (*Ikzf2*<sup>cello/cello</sup> mouse), *Fcrlb* is robustly expressed in IHCs and OHCs at P8. IHC expression of *Fcrlb* is not affected by Anc80-*eGFP* transduction, whereas *Fcrlb* expression is lost in Anc80-*Ikzf2* transduced HCs (n=3 biologically independent samples per condition). Scale=10  $\mu$ m. (f-g) Expression of prestin can be seen in Anc80-*Ikzf2* transduced IHCs up to 8-weeks of age (n=3 biologically independent samples at 6-8 weeks) (f, scale=100  $\mu$ m), and overlaps with Myc staining (g, scale=20  $\mu$ m). See also Extended Data Figure 10.

## Methods

### *Animal procedures*

Animal procedures performed at the University of Maryland School of Medicine were carried out in accordance with the National Institutes of Health Guide for the Care and Use of Laboratory Animals and have been approved by the Institutional Animal Care and Use Committee at the University of Maryland, Baltimore (protocol numbers 1112005 and 1015003). The RiboTag (maintained on a C57BL/6N background), prestin-CreERT2 and Myo15-Cre mouse models (maintained on a C57BL/6J background) have been described previously<sup>5,6,22</sup>, and were generously provided for this study by Dr. Mary Kay Lobo, Dr. Jian Zuo, and Drs. Christine Petit and Thomas Friedman, respectively. CBA/CaJ mice (stock #000654) and B6.Cg-*Gt(ROSA)26Sor<sup>tm14(CAG-tdTomato)Hze</sup>/J* mice (stock #007914, referred to as *ROSA26<sup>CAG-tdTomato</sup>*) were procured from the Jackson Laboratory (Bar Harbor, ME). Prestin<sup>CreERT2</sup> specificity was determined by crossing *prestin<sup>CreERT2/CreERT2</sup>* mice to *ROSA26<sup>CAG-tdTomato</sup>* mice, and resulting offspring were dissected at P21 for whole-mount immunohistochemistry. To generate animals for the RiboTag OHC RNA-seq dataset, *RiboTag<sup>HA/HA</sup>* mice were crossed to *prestin<sup>CreERT2/CreERT2</sup>* mice to produce *RiboTag<sup>HA/+</sup>;prestin<sup>CreERT2/+</sup>* mice. These mice were further intercrossed to obtain double homozygous *RiboTag<sup>HA/HA</sup>;prestin<sup>CreERT2/CreERT2</sup>* animals, which were then crossed to CBA/CaJ mice to generate F1 *RiboTag<sup>HA/+</sup>;prestin<sup>CreERT2/+</sup>* offspring on a mixed CBA/C57BL/6 background, avoiding the recessively inherited age related hearing loss phenotype inherent to C57BL/6 mice<sup>23</sup>. Recombination was induced by tamoxifen injection (3 mg/40 g body weight in mice younger than 21 days, 9 mg/40 g body weight in mice 21 days or older), and cochlear tissues were collected at the following ages: P8, P14, P28, 6 weeks, and 10 weeks. For the *cello* RNA-seq and NanoString experiments, cochlear ducts from *Ikzf2<sup>+/+</sup>*, *Ikzf2<sup>cello/+</sup>* and *Ikzf2<sup>cello/cello</sup>* mice were dissected at P8 and P16. CD-1 or C57BL/6 pregnant females were procured from Charles River (Frederick, MD) or the University of Maryland School of Medicine Veterinary Resources (Baltimore, MD). Resulting neonates were injected with Anc80L65 virus between P1 – P3, and dissected for later analyses between P8 and 8wk. For the Anc80L65 transduced IHC scRNA-seq experiment, *Myo15<sup>Cre/Cre</sup>* mice were crossed to *ROSA26<sup>CAG-tdTomato</sup>* mice, resulting offspring were injected with Anc80L65 virus between P1-P3, and the cochlear epithelium was collected at P8. Additionally, a number of litters with Anc80-*Ikzf2* injected pups and their control littermates (aged P7 – P8), together with a mother, were sent to the University of Kentucky for the measurements of non-linear (voltage-dependent) capacitance, an electrical “signature” of electromotility. All animal procedures for these experiments were approved by the Institutional Animal Care and Use Committee at the University of Kentucky (protocol 00903M2005). Both male and female animals were used for all experiments.

Animal procedures performed at the MRC Harwell Institute were licenced by the Home Office under the Animals (Scientific Procedures) Act 1986, UK and additionally approved by the relevant Institutional Ethical Review Committees. The *cello* mutant mouse was originally identified from the MRC Harwell Institute phenotype-driven *N*-ethyl-*N*-nitrosourea (ENU) Ageing Screen<sup>11</sup>. In this screen, ENU-mutagenized C57BL/6J males were mated with wild-type ‘sighted C3H’ (C3H.Pde6b+) females<sup>24</sup>. The resulting G<sub>1</sub> males were crossed with C3H.Pde6b+ females to produce G<sub>2</sub> females, all of which were screened for the *Cadherin23<sup>ahl</sup>* allele<sup>23</sup>. *Cadherin23<sup>+/+</sup>* G<sub>2</sub> females were then backcrossed to their G<sub>1</sub> fathers to generate recessive G<sub>3</sub> pedigrees, which entered a longitudinal phenotyping pipeline. Auditory phenotyping comprised clickbox testing at 3-, 6-, 9- and 12-months of age and ABR at 9-months of age. The *Ikzf2<sup>del1890</sup>* mutant line was generated by the Molecular and Cellular Biology

group at the MRC Harwell Institute using a CRISPR-Cas9-mediated deletion approach. Both male and female mice were used for experiments.

### ***RiboTag immunoprecipitations***

RiboTag immunoprecipitations were performed as described in Sanz et al., 2009<sup>6</sup>. Briefly, for one biological sample, 10 cochlear ducts from 5 mice were pooled and homogenized in 1 ml of supplemented homogenization buffer (50 mM Tris-HCl pH.7, 100 mM KCl, 12 mM MgCl<sub>2</sub>, 1% Nonidet P-40, 1 mM 1,4-Dithiothreitol, 1X protease inhibitor cocktail, 200 U/mL RNaseOUT, 100 µg/ml cycloheximide, 1 mg/ml heparin). Homogenates were spun down (10,000 rpm for 10 minutes at 4°C) to remove particulates. 40 µl of homogenate was reserved for total RNA isolation (input control), and the remaining homogenate was incubated with 5 µg HA antibody (BioLegend) at 4°C under gentle rotation for 4 – 6 hours. The supernatant was then added to 300 µl of rinsed Invitrogen Dynabeads Protein G magnetic beads (Thermo Fisher), and incubated overnight at 4°C under gentle rotation. The following day, bound beads were rinsed three times with 800 µl high salt buffer (50 mM Tris-HCl pH.7, 300 mM KCl, 12 mM MgCl<sub>2</sub>, 1% Nonidet P-40, 1 mM 1,4-Dithiothreitol, 100 µg/ml cycloheximide) at 4°C for 10 minutes, rotating. 350 µl of buffer RLT from the RNeasy Plus Micro kit (Qiagen) was then added to the beads or reserved input sample, and vortexed for 30 seconds to bound ribosomes and RNA. RNA was extracted according to the manufacturer's instructions for the RNeasy Plus Micro kit (Qiagen), using 16 µl of nuclease free water for elution as recommended by Sanz et al. This method yielded an average of 10.9 ng of IP RNA (average concentration = 0.68 ng/µl) and 185.6 ng of input RNA (average concentration = 10.9 ng/µl) for downstream analyses. All RNA samples used for RNA-seq had a minimum RNA integrity number (RIN) of 8.

### ***cello cochlear RNA extractions***

For the *cello* RNA-seq, cochlear ducts from P8 *Ikzf2*<sup>+/+</sup> and *Ikzf2*<sup>cello/cello</sup> mice were dissected and pooled (6 cochlear ducts/sample) to generate two biological replicates per genotype. For the NanoString validations, cochlear ducts from P8 *Ikzf2*<sup>cello/cello</sup>, *Ikzf2*<sup>cello/+</sup> and *Ikzf2*<sup>+/+</sup> mice were dissected and pooled (2 – 4 cochlear ducts/sample) to generate four biological replicates per genotype. RNA was extracted using the Direct-zol™ RNA MiniPrep kit (Zymo Research) following the manufacturer's instructions. RNA quality and concentration were assessed using the Agilent RNA Pico kit (Agilent Technologies). All RNA samples used for RNA-seq had a minimum RNA integrity number (RIN) of 8.

### ***RNA-seq and normalization***

RiboTag OHC RNA-seq libraries were prepared using the NEBNext® Ultra™ Directional RNA Library Prep Kit for Illumina (New England Biolabs), and samples were sequenced in at least biological duplicates on a HiSeq 4000 system (Illumina) using a 75 bp paired end read configuration. P8 *Ikzf2*<sup>+/+</sup> and *Ikzf2*<sup>cello/cello</sup> RNA libraries were prepared using the TruSeq RNA Sample Prep kit (Illumina), and samples were sequenced in biological duplicates on a HiSeq 2000 system (Illumina) and a 125 bp paired end read configuration. Reads were aligned to the *Mus musculus* reference genome (assembly GRCm38.87 [RiboTag] or GRCm38.84 [P8 *cello*]) using TopHat v2.0.8<sup>25</sup>, and HTSeq was used to quantify the number of reads aligning to predicted coding regions<sup>26</sup>. See Supplementary Table 12 for alignment statistics. Expression levels were normalized using quantile normalization. In downstream analyses, only genes covered by at least 20 reads in a minimum of two samples from the same

biological condition were considered as expressed. Significant differential gene expression between samples was assessed using DEseq<sup>27</sup>. In addition to statistical significance between samples ( $FDR \leq 0.05$ ), we also required a complete separation of expression levels between compared conditions for a gene to be called as differentially expressed. That is, for a gene to be called downregulated in condition A compared to condition B, we required that all normalized expression levels measured in the samples of condition A to be lower than all normalized expression levels measured in the samples of condition B. To avoid inflation of fold change estimates for lowly expressed genes, a floor level equal to the 10<sup>th</sup> percentile of the distribution of the expression levels was applied (i.e., all expression values below the 10<sup>th</sup> percentile were set to the 10<sup>th</sup> percentile value). The OHC enrichment factors (EF) were calculated for each gene and time point by comparing the RiboTag IP samples to matched input samples, and are defined as the  $\text{Log}_2$  ratio of expression levels between the IP and input samples. Inspection of these EFs revealed a systematic association to transcripts length (Supplementary Fig.2a). Therefore, we used a locally weighted regression, implemented by the R lowess function, to remove this systematic effect (Supplementary Fig.2b). The RiboTag OHC RNA-seq and P8 *cello* cochlea RNA-seq data have been submitted to the Gene Expression Omnibus database (GEO accession numbers GSE116703 and GSE116702), and are additionally available for viewing through the gEAR Portal (<https://umgear.org/>).

### ***Gene expression analyses***

Genes with a changed level of expression in OHC IP samples at any time point relative to P8 were subjected to a clustering analysis using the CLICK algorithm, implemented in the EXPANDER package<sup>28,29</sup>. Gene Ontology (GO) enrichment analysis was carried out using the EXPANDER implemented tool TANGO<sup>28</sup>. The adult mouse IHC and OHC transcriptomic dataset used for comparisons was generated by Liu et al., 2014 and can be accessed through the Gene Expression Omnibus database (GEO accession number GSE111348)<sup>7</sup>. The expanded motif prediction analysis was performed using iRegulon<sup>10</sup> through the Cytoscape visualization tool<sup>30</sup>. The analysis was performed on the putative regulatory region of 20 kb centered around the TSS using default settings.

### ***Immunohistochemistry***

For cochlear sections, mice were culled by cervical dislocation and inner ears fixed in 4% paraformaldehyde (PFA) overnight at 4°C then decalcified in 4% ethylenediaminetetraacetic acid (EDTA) in PBS. Ears were positioned in 4% low melting temperature agarose (Sigma-Aldrich) in upturned BEEM® capsules (Agar Scientific) at a 45° diagonal angle, with the apex of the cochlea facing down and the vestibular system uppermost. Once set, the agarose block was removed from the BEEM® capsule and 200 µm sections were cut through the mid-modiolar plane of the cochlea using a Leica VT1000S Vibratome. Sections were simultaneously permeabilized and blocked with 10% donkey serum (Sigma) in 0.3% Triton-X for 30 minutes at room temperature (RT) then labelled with primary antibodies for 3 hours at RT. To enable detection, samples were incubated with fluorophore-coupled secondary antibodies for 2 hours at RT then stained with DAPI (1:2500, Thermo Fisher) for 5 minutes. Sections were transferred to WillCo glass bottom dishes (Intracel) and visualized free-floating in PBS using a Zeiss 700 inverted confocal microscope (10x – 40x magnification). Primary antibodies: goat anti-Helios M-20 (1:400, Santa Cruz Biotechnology); mouse anti-β-Actin (1:500, Abcam). Secondary antibodies: Alexa Fluor® 568 donkey anti-goat (Invitrogen, 1:200) and Alexa Fluor® 488 donkey anti-mouse (Invitrogen, 1:200).

For cochlear whole-mounts, mice were euthanized by cervical dislocation and inner ears fixed in 2% PFA for 30 minutes at 4°C. Post-fixation, ears were fine dissected to expose the sensory epithelium then immediately permeabilized in 0.2% Triton-X for 10 minutes and blocked with 10% donkey serum (Sigma) for 1 hour at RT. Cochleae were immunolabelled with goat anti-Helios M-20 (1:400, Santa Cruz Biotechnology) overnight at 4°C then incubated with Alexa Fluor® 568 donkey anti-goat secondary (1:200, Invitrogen) and the F-actin marker Alexa Fluor® 488 Phalloidin (1:200, Invitrogen) for 1 hour at RT. Samples were washed with DAPI (1:2500, Thermo Fisher) for 60 seconds to stain nuclei then mounted onto slides with SlowFade® Gold (Life Technologies) and visualized using a Zeiss LSM 710 fluorescence confocal microscope and 63x oil magnification.

### ***Identification of the cello mutation***

DNA was extracted from ear biopsies of affected G<sub>3</sub> mice using the DNeasy Blood and Tissue Kit (Qiagen) and used for an initial genome-wide linkage study, employing SNP markers polymorphic between the parental strains C57BL/6J and C3H.Pde6b+ (Tepnel Life Sciences). Following linkage to a 21.57 Mb region on Chromosome 1, additional SNP markers were identified and genotyped using standard PCR and restriction endonuclease protocols in order to delineate an 8.4 Mb critical interval between SNPs rs31869113 and rs13475914. Subsequently, high-quality DNA was extracted from the tail of an affected G<sub>3</sub> mouse using the Illustra™ Nucleon BACC2 Genomic DNA Extraction Kit (GE Healthcare) and sequenced by the Oxford Genomics Centre (Wellcome Trust Centre for Human Genetics, Oxford, UK) using the HiSeq system (Illumina). Sequencing reads were aligned to the mouse reference genome (assembly GRCm38) and known C57BL/6J and C3H.Pde6b+ SNPs were filtered out, leaving variants that were then given a quality score based on their sequencing read depth. Variants within the 8.4 Mb critical region which were deemed heterozygous, low-confidence (quality score <200), non-coding or synonymous were discounted. The putative *Ikzf2* lesion was amplified by standard PCR (see Supplementary Table 13 for genotyping primers) and validated by Sanger sequencing, using DNA from an affected G<sub>3</sub> animal, as well an unaffected G<sub>3</sub> (control). Sequence gaps that spanned coding regions were amplified by PCR using DNA from an affected G<sub>3</sub> mouse and analysed by Sanger sequencing. In all cases, sequence data were assessed for variation using DNASTAR Lasergene software (version 12.0.0).

### ***In silico analyses***

Three independent online tools were used to predict the functional effect of the *cello* mutation *in silico*: Sorting Intolerant From Tolerant (SIFT); Polymorphism Phenotyping version 2 (PolyPhen-2); and Protein Variation Effect Analyser (PROVEAN)<sup>31-33</sup>. Structural 3D representations of wild-type and H517Q helios ZnF6 were predicted with RaptorX<sup>34</sup>, using peptide sequences as input, and visualized using pyMOL software (version 1.7).

### ***In vitro analyses***

A full-length *Ikzf2*<sup>+</sup> helios construct was prepared using the pGEM®-T Vector System II Kit (Promega) and used as a template for the generation of an *Ikzf2*<sup>cello</sup> helios construct with the QuikChange® Lightning Site-Directed Mutagenesis Kit (Agilent Technologies). Plasmid DNA was prepared using the Wizard® Plus SV Miniprep Purification System (Promega) and validated by Sanger sequencing. Sequence-verified *Ikzf2*<sup>+</sup> and *Ikzf2*<sup>cello</sup> constructs were subcloned in-frame into pCMV-Myc and pEGFP-C3 mammalian expression vectors

(generously provided by Dr. Chris Esapa), to yield N-terminally tagged *Ikzf2*<sup>+</sup> and *Ikzf2*<sup>cello</sup> helios. See Supplementary Table 13 for cloning and mutagenesis oligonucleotide sequences.

Constructs were subsequently employed for subcellular localization studies using male *Cercopithecus aethiops* SV40 transformed kidney cells (Cos-7) cells (generously provided by Dr. Chris Esapa) that had been seeded onto 22 x 22 mm glass coverslips in six-well plates, at a volume of 1x10<sup>5</sup> cells per well. After 24 hours (or when at 50 – 60% confluency), cells were transiently transfected with 1 µg DNA of *Ikzf2*<sup>+</sup>-Myc or *Ikzf2*<sup>cello</sup>-Myc helios construct using JetPEI® DNA Transfection Reagent (Polyplus Transfection). At 24 hours post-transfection, cells were fixed in 4% PFA for 10 minutes and permeabilised with 1% Triton-X for 15 minutes at RT. After blocking in 10% donkey serum (Sigma) for 1 hour at RT, cells were immunolabelled with goat anti-Helios M-20 primary antibody (1:600, Santa Cruz Biotechnology) overnight at 4°C then incubated with Alexa Fluor® 488 donkey anti-goat secondary antibody (1:200, Invitrogen) and F-actin marker Texas Red®-X Phalloidin (1:200, Invitrogen) for 1 hour at RT. Cells were washed with DAPI (1:2500, Thermo Fisher) for 60 seconds. Coverslips were mounted onto slides with SlowFade® Gold (Life Technologies) and cells were visualized using a Zeiss LSM 710 multiphoton fluorescence confocal microscope and 63x oil magnification.

Constructs were also utilized for co-immunoprecipitation studies using *Homo sapiens* embryonic kidney cells (HEK293T) cells (generously provided by Dr. Chris Esapa) that had been seeded directly onto six-well plates at a volume of 5x10<sup>5</sup> cells per well. Cells were transiently co-transfected 24 hours later with a total of 2 µg plasmid DNA to mimic the wild-type (1 µg *Ikzf2*<sup>+</sup>-Myc helios + 1 µg *Ikzf2*<sup>+</sup>-GFP helios), heterozygous (1 µg *Ikzf2*<sup>+</sup>-Myc helios + 1 µg *Ikzf2*<sup>cello</sup>-GFP helios; 1 µg *Ikzf2*<sup>cello</sup>-Myc helios + 1 µg *Ikzf2*<sup>+</sup>-GFP helios) or homozygous (1 µg *Ikzf2*<sup>cello</sup>-Myc helios + 1 µg *Ikzf2*<sup>cello</sup>-GFP helios) states using JetPEI® DNA Transfection Reagent (Polyplus Transfection). Single transfections with either 1 µg *Ikzf2*<sup>+</sup>-GFP helios or 1 µg *Ikzf2*<sup>+</sup>-Myc helios were also carried out for negative controls. Cells were lysed in 250 µl of 1x RIPA buffer (150 mM NaCl, 1% NP-40, 0.5% deoxycholate, 0.1% SDS, 50 mM Tris pH 7.5 in milliQ water) at 48 hours post-transfection, then incubated with Protein G Sepharose® Beads (Sigma) for 2 hours at 4°C. The beads were pelleted by centrifugation and the supernatant incubated with either 1 µg of mouse anti-cMyc 9E10 antibody (Developmental Studies Hybridoma Bank) or 1-2 µg of custom-made rabbit anti-GFP antibody overnight at 4°C. The immunoprecipitation complexes were captured using Protein G beads, washed with RIPA buffer and released by incubation with NuPAGE Reducing Agent (Novex). Immunoprecipitation reactions and their corresponding reduced cell lysate were analysed by western blotting. Samples were electrophoresed on NuPage 4 – 12% Bis-Tris gels (Invitrogen) and transferred onto nitrocellulose membranes using the iBlot® system (Invitrogen). Membranes were incubated with mouse anti-cMyc 9E10 antibody (1:5000, Developmental Studies Hybridoma Bank) and custom-made rabbit anti-GFP (1:1000, CUK-1819 MGU-GFP-FL) primary antibodies. Mouse 12G10 anti-α-Tubulin (1:10,000, Developmental Studies Hybridoma Bank) was also used as a loading control. For detection, membranes were incubated with goat anti-mouse IRDye 680RD (1:15000, LI-COR) and goat anti-rabbit IRDye 800CW secondary antibodies (1:15000, LI-COR) and imaged using the Odyssey® CLx Infrared Imaging System (LI-COR). For quantification, band intensities were determined using the Image Studio Lite Ver 5.2 software and used to calculate the relative ratio of Co-IP to IP signal. Cos-7 and HEK293T cells were grown at 37°C under 5% carbon dioxide (CO<sub>2</sub>) conditions in Dulbecco's Modified Eagle Medium (Invitrogen) containing 10% heat-inactivated foetal bovine serum (FBS) (Invitrogen) and 1X penicillin/streptomycin (Invitrogen).

### ***Auditory brainstem response (ABR)***

ABR tests were performed using a click stimulus in addition to frequency-specific tone-burst stimuli to screen mice for auditory phenotypes and investigate auditory function<sup>35</sup>. Mice were anaesthetized by intraperitoneal injection of ketamine (100 mg/ml at 10% v/v) and xylazine (20 mg/ml at 5% v/v) administered at the rate of 0.1 ml/10 g body mass. Animals were placed on a heated mat inside a sound-attenuated chamber (ETS Lindgren) and electrodes were placed subdermally over the vertex (active), right mastoid (reference) and left mastoid (ground). ABR responses were collected, amplified and averaged using TDT System 3 (Tucker Davies Technology, Alachua, FL, USA) in conjunction with either BioSig RP (version 4.4.11) or BioSig RZ (version 5.7.1) software. The TDT system click ABR stimuli comprised clicks of 0.1 ms broadband noise spanning ~2-48 kHz, presented at a rate of 21.1/sec with alternating polarity. Tone-burst stimuli were of 7 ms duration, inclusive of 1 ms rise/fall gating using a Cos<sup>2</sup> filter, presented at a rate of 42.5/s and were measured at 8, 16, and 32 kHz. All stimuli were presented free-field to the right ear of the mouse, starting at 90 dB SPL and decreasing in 5 dB increments. Auditory thresholds were defined as the lowest dB SPL that produced a reproducible ABR trace pattern and were determined manually. All ABR waveform traces were viewed and re-scored by a second operator blind to genotype. Animals were recovered using 0.1 ml of anaesthetic reversal agent atipamezole (Antisedan™, 5 mg/ml at 1% v/v), unless aged P16, when the procedure was performed terminally.

### ***Generation of *Ikzf2*<sup>del890</sup> mice***

The *Ikzf2*<sup>del890</sup> mutant line was generated by the Molecular and Cellular Biology group at the Mary Lyon Centre, MRC Harwell Institute using CRISPR-Cas9 gene editing, as in Mianné et al., 2016 (see Supplementary Table 13 for single guide RNA (sgRNA) sequences, donor oligonucleotide sequences and genotyping primers)<sup>36</sup>. For construction of each sgRNA plasmid, a pair of single-stranded donor oligonucleotides (IDT) was hybridized and cloned using Gibson Assembly® Master Mix (NEB) into linearized p\_1.1 plasmid digested with *StuI* and *AflIII* in order to express sgRNAs under the T7 promoter.

The p\_1.1\_sgRNA plasmids were linearized with *XbaI*, phenol-chloroform purified and the products used as templates from which sgRNAs were *in vitro* transcribed. sgRNAs were synthesized using MEGAshortscript™ T7 Transcription Kit (Ambion). RNAs were purified using MEGAclean™ Transcription Clean-Up Kit (Ambion). RNA quality was assessed using a NanoDrop (Thermo Scientific) and by electrophoresis on 2% agarose gel containing Ethidium Bromide (Fisher Scientific).

As this exon deletion mutant was generated as part of an experiment to generate a floxed mutant, a *Ikzf2* flox long single-stranded DNA (lssDNA) donor was also synthesized as per Codner et al., 2018, for inclusion in the microinjection mix<sup>37</sup>.

For microinjections, the pronucleus of one-cell stage C57BL/6NTac embryos were injected with a mix containing Cas9 mRNA (5meC,Ψ, Tebu-Bio/TriLink Biotechnologies) at 100 ng/μl, the four *Ikzf2* sgRNAs, each at 50 ng/μl and the *Ikzf2* flox lssDNA donor at 50 ng/μl prepared in microinjection buffer. Injected embryos were re-implanted in pseudo-pregnant CD1 females, which were allowed to litter and rear F<sub>0</sub> progeny.

For genotyping, genomic DNA was extracted from ear biopsies of F<sub>0</sub> and F<sub>1</sub> mice using DNA Extract All Reagents Kit (Applied Biosystems) and amplified by PCR using high fidelity Expand Long Range dNTPack (Roche) and specific genotyping primers (see Supplementary

Table 13). PCR products were further purified using QIAquick Gel Extraction Kit (Qiagen) and analysed by Sanger sequencing. Copy counting experiments by ddPCR against a known two copy reference (*Dot1l*) were also carried out to confirm the exon deletion and that there were no additional integrations of the lssDNA donor. Mice carrying the *del890* deletion allele were subsequently mated with mice carrying the *cello* mutation in order to generate *Ikzf2<sup>cello/del890</sup>* compound heterozygotes for complementation testing.

### **Scanning electron microscopy**

Mice were culled by cervical dislocation and inner ears were removed and fixed in 2.5% glutaraldehyde (TAAB Laboratories Equipment Ltd.) in 0.1 M phosphate buffer for 4 hours at 4°C. Following decalcification in 4.3% EDTA, cochleae were dissected to expose the organ of Corti, and subjected to ‘OTO’ processing (1 hour incubation in 1% osmium tetroxide (TAAB Laboratories Equipment Ltd.), 30 minute incubation in 1% thiocarbohydrazide (Sigma), 1 hour incubation in 1% osmium tetroxide), before dehydration in increasing concentrations of ethanol (25%, 40%, 60%, 80%, 95%, 2 x 100%) at 4°C. Samples were critical point dried with liquid CO<sub>2</sub> using an Emitech K850 (EM Technologies Ltd), then mounted on stubs using silver paint (Agar Scientific) and sputter coated with platinum using a Quorum Q150R S sputter coater (Quorum Technologies). Samples were examined using a JEOL JSM-6010LV Scanning Electron Microscope. Hair cell bundle counts were performed by counting the number of OHC and IHC bundles adjacent to ten pillar cells in the apical (<180° from apex), mid (180 – 450° from apex) and basal (> 450° from apex) regions of the cochlea. At least three ears (one ear per mouse) were analysed for each genotype at each time point.

### **Electrophysiological analyses**

Electrophysiological recordings were made from OHCs of *cello* mice aged P9 – P18. Cochleae were dissected in normal extracellular solution (in mM): 135 NaCl, 5.8 KCl, 1.3 CaCl<sub>2</sub>, 0.9 MgCl<sub>2</sub>, 0.7 NaH<sub>2</sub>PO<sub>4</sub>, 5.6 D-glucose, 10 Hepes-NaOH. Sodium pyruvate (2 mM), MEM amino acids solution (50X, without L-Glutamine) and MEM vitamins solution (100X) were added from concentrates (Fisher Scientific, UK). The pH was adjusted to 7.5 (osmolality ~308 mmol kg<sup>-1</sup>). The dissected cochleae were transferred to a microscope chamber, immobilized as previously described<sup>38</sup> and continuously perfused with a peristaltic pump using the above extracellular solution. The organs of Corti were viewed using an upright microscope (Nikon FN1, Japan) with Nomarski optics (x60 objective).

MET currents were elicited by stimulating the hair bundles of P9 OHCs in the excitatory and inhibitory direction using a fluid jet from a pipette (tip diameter 8 – 10 µm) driven by a piezoelectric disc<sup>38</sup>. The pipette tip of the fluid jet was positioned near to the bundles to elicit a maximal MET current. Mechanical stimuli were applied as 50 Hz sinusoids (filtered at 0.25 kHz, 8-pole Bessel) with driving voltages of ± 40 V. MET currents were recorded with a patch pipette solution containing (in mM): 106 Cs-glutamate, 20 CsCl, 3 MgCl<sub>2</sub>, 1 EGTA-CsOH, 5 Na<sub>2</sub>ATP, 0.3 Na<sub>2</sub>GTP, 5 Hepes-CsOH, 10 sodium phosphocreatine (pH 7.3). Membrane potentials were corrected for the liquid junction potential (-11 mV).

Patch clamp recordings were performed using an Optopatch (Cairn Research Ltd, UK) amplifier. Patch pipettes were made from soda glass capillaries (Harvard Apparatus Ltd, UK) and had a typical resistance in extracellular solution of 2-3 MΩ. In order to reduce the electrode capacitance, patch electrodes were coated with surf wax (Mr Zoggs SexWax, USA). Potassium current recordings were performed at RT (22 – 24°C) and the intracellular solution contained

(in mM): 131 KCl, 3 MgCl<sub>2</sub>, 1 EGTA-KOH, 5 Na<sub>2</sub>ATP, 5 Hepes-KOH, 10 Na<sub>2</sub>-phosphocreatine (pH 7.3; osmolality ~296 mmol kg<sup>-1</sup>). Data acquisition was controlled by pClamp software (version 10) using Digidata 1440A boards (Molecular Devices, USA). Recordings were low-pass filtered at 2.5 kHz (8-pole Bessel), sampled at 5 kHz and stored on computer for off-line analysis (Origin: OriginLab, USA). Membrane potentials in voltage clamp were corrected for the voltage drop across the uncompensated residual series resistance and for a liquid junction potential (−4 mV).

The presence of electromotile activity in P16 – P18 OHCs was estimated by applying a depolarizing voltage step from the holding potential of −64 mV to +56 mV. Changes in cell length were viewed and recorded with a Nikon FN1 microscope (75x magnification) with a Flash 4.0 SCCD camera (Hamamatsu, Japan). Cell body movement was tracked using Fiji software. Lines were drawn across the basal membrane of patched OHCs, perpendicular to the direction of cell motion, and a projected time-based z-stack of the pixels under the line was made. Cell movement was measured with Photoshop as a pixel shift and then converted to nm (290 pixels = 10 μm).

Non-linear (voltage-dependent) capacitance of IHCs in *Anc80-Ikzf2* injected mice and their non-injected littermates was studied at P12 – P16 using conventional whole cell patch clamp recordings. Apical turn of the organ of Corti was carefully dissected in Leibovitz's L-15 cell culture medium (Cat #21083027, Gibco/ThermoFisher, USA) containing the following inorganic salts (in mM): NaCl (137), KCl (5.4), CaCl<sub>2</sub> (1.26), MgCl<sub>2</sub> (1.0), Na<sub>2</sub>HPO<sub>4</sub> (1.0), KH<sub>2</sub>PO<sub>4</sub> (0.44), MgSO<sub>4</sub> (0.81) and placed into the custom-made recording chamber, where it was held by two strands of dental floss. The organ of Corti explants were viewed with an upright microscope (BX51WIF, Olympus, Japan), equipped with a high numerical aperture (NA) objective (100x, 1.0 NA). To block voltage-gated ion channels in IHCs, the bath solution was made of L-15 medium supplemented with 10 mM tetraethylammonium-Cl, 2 mM CoCl<sub>2</sub>, 10 mM CsCl, and 0.1 mM Nifedipine (all from Sigma, USA), while the intrapipette solution contained (in mM): CsCl (140), MgCl<sub>2</sub> (2.5), Na<sub>2</sub>ATP (2.5), EGTA (1.0), HEPES (5). During recordings, the organs of Corti were continuously perfused with the above extracellular bath solution. Whole cell current responses were recorded with MultiClamp 700B patch clamp amplifier (Molecular Devices, USA), controlled by jClamp software (SciSoft, USA). Membrane capacitance was measured during the voltage ramp with a dual sinusoidal, FFT-based method<sup>39</sup>. The recorded capacitance was fitted to the first derivative of a two-state Boltzmann function that is typically used to fit non-linear capacitance of OHCs plus a small correction for the membrane area changes between expanded and contracted states of prestin<sup>40</sup>, as follows:

$C_m = C_v + C_{lin}$ , where  $C_m$  is the total membrane capacitance,  $C_v$  is a voltage-dependent (non-linear) component, and  $C_{lin}$  is a voltage-independent (linear) component.

$$C_v = Q_{max} \frac{ze}{kT} \frac{b}{(1+b)^2} + \frac{\Delta C_{sa}}{(1+b^{-1})}; \quad b = \exp\left(\frac{-ze(V - V_{pk})}{kT}\right)$$

where,  $Q_{max}$  is the maximum nonlinear charge moved,  $V_{pk}$  is a voltage at peak capacitance,  $V$  is membrane potential,  $z$  is valence,  $e$  is electron charge,  $k$  is Boltzmann's constant,  $T$  is absolute temperature, and  $\Delta C_{sa}$  is the maximum increase in capacitance that occurs when all prestin molecules change from compact to expanded state. To account for some variability in sizes of IHCs, statistical data are shown as the maximum of voltage-dependent component of capacitance ( $C_v$ ) normalized to the linear capacitance of the cell ( $C_v/C_{lin}$ ).

### ***Distortion Product Oto-Acoustic Emissions (DPOAEs)***

DPOAE tests were performed using frequency-specific tone-burst stimuli at 8, 16 and 32 kHz with the TDT RZ6 System 3 hardware and BioSig RZ (version 5.7.1) software (Tucker Davis Technology, Alachua, FL, USA). An ER10B+ low noise probe microphone (Etymotic Research) was used to measure the DPOAE near the tympanic membrane. Tone stimuli were presented via separate MF1 (Tucker Davis Technology) speakers, with f1 and f2 at a ratio of  $f2/f1 = 1.2$  ( $L1=65$  dB SPL,  $L2=55$  dB SPL), centred around the frequencies of 8, 16 and 32 kHz. Surgical anaesthesia was achieved by intraperitoneal injection of ketamine (100 mg/ml at 10% v/v), xylazine (20 mg/ml at 5% v/v) and acepromazine (2 mg/ml at 8% v/v) administered at a rate of 0.1 ml/10 g body mass. Once the required depth of anaesthesia was confirmed by the lack of the pedal reflex, a section of pinna was removed to allow unobstructed access to the external auditory meatus. Mice were then placed on a heated mat inside a sound-attenuated chamber (ETS-Lindgren) and the DPOAE probe assembly was inserted into the ear canal using a pipette tip to aid correct placement. In-ear calibration was performed before each test. The f1 and f2 tones were presented continuously and a fast-Fourier transform was performed on the averaged response of 356 epochs (each ~21 ms). The level of the 2f1-f2 DPOAE response was recorded and the noise floor calculated by averaging the four frequency bins either side of the 2f1-f2 frequency.

### ***NanoString validation***

Cochlear RNA extracted from biological triplicates of *Ikzf2*<sup>cello/cello</sup>, *Ikzf2*<sup>cello/+</sup> and *Ikzf2*<sup>+/+</sup> animals at P8 were processed for NanoString validation at the UMSOM Institute for Genome Sciences using the nCounter Master Kit per manufacturer's instructions, and quantified using the NanoString nCounter platform. See Supplementary Table 13 for NanoString probe sequences. Data were analyzed using nSolver 4.0 software (NanoString).

### ***Anc80L65 AAV vector construction***

The Anc80L65-*Myc-Ikzf2*<sup>+</sup> (Anc80-*Ikzf2*) expression vector was designed to drive expression of a Myc-tagged *Ikzf2* construct followed by a bovine Growth Hormone polyadenylation (BGH pA) site under control of the cytomegalovirus (CMV) promoter. The Anc80L65-*eGFP* (Anc80-*eGFP*) expression construct also contained a Woodchuck Hepatitis Virus Posttranscriptional Regulatory Element (WPRE) preceding the BGH pA site. Anc80L65 AAV vectors<sup>16,17</sup> were produced by the Gene Transfer Vector Core, Grousbeck Gene Therapy Center at the Massachusetts Eye and Ear Infirmary (Boston, MA) (<http://vector.meei.harvard.edu/>).

### ***Inner ear gene delivery***

For in vivo HC transductions, mice were injected with Anc80L65 AAVs between P1 to P3 via the posterior semicircular canal following the injection method described in Isgrig et al., 2017<sup>41</sup>. Briefly, animals were anesthetized on ice before a post-auricular incision was made on either the left or right side. Tissues were further dissected to reveal the posterior semicircular canal, and a Nanoliter 2010 microinjection system (World Precision Instruments) equipped with a loaded glass needle was used to inject 700 nl of 1.13E+13GC/ml Anc80-*Ikzf2* or 500 nl of 4.85E+12GC/ml Anc80-*eGFP*. Injections into the inner ear were performed in 50 nl increments over the course of 2 minutes. The needle was then removed, the incision sutured, and animals were placed on a 37°C heating pad to recover before being returned to their cage.

## ***Fluorescence activated cell sorting (FACS)***

For the scRNA-seq analysis of *Anc80-Ikzf2* transduced HCs, inner ears of neonatal *Myo15<sup>Cre/+</sup>;ROSA26<sup>CAG-tdTomato</sup>* mice were injected with *Anc80-Ikzf2* (4 mice) or control *Anc80-eGFP* (2 mice) via the posterior semicircular canal. Cochlear tissues from both injected and uninjected ears were harvested at P8 and further dissected to reveal the sensory epithelium. Inclusion of the uninjected ear in the single cell analysis allowed for the study of changes in gene expression that occur in response to a gradient of transgene expression. This is because, in mice, inner ear gene delivery often results in transduction in the contralateral ear, albeit at a lower intensity<sup>17</sup>. Cochlear tissues were then dissociated for fluorescence activated cell sorting (FACS) following the method described in Elkon et al., 2015<sup>8</sup>. Briefly, the sensory epithelia from *Anc80-eGFP* and *Anc80-Ikzf2* injected mice were pooled separately into 2 wells of a 48-well plate containing 0.5 mg/ml Thermolysin (Sigma). Tissues were incubated at 37°C for 20 minutes, after which the Thermolysin was removed and replaced with Accutase enzyme (MilliporeSigma). After a 3 minute incubation at 37°C, tissues were mechanically disrupted using a 23G blunt ended needle connected to a 1 ml syringe. This step was performed twice. After confirming tissue dissociation by direct visualization, the dissociation reaction was stopped by adding an equal volume of IMDM supplemented with 10% heat-inactivated FBS to the Accutase enzyme solution. Cells were passed through a 40 mm cell strainer (BD) to remove cell clumps. tdTomato expressing HCs were sorted into ice cold tubes containing IMDM with 10% FBS on a BD FACSAria II (BD Biosciences) and processed for scRNA-seq. Flow cytometry analyses were performed with assistance from Dr. X. Fan at the University of Maryland Marlene and Stewart Greenebaum Comprehensive Cancer Center Flow Cytometry Shared Service.

## ***Single cell RNA-seq (scRNA-seq)***

tdTomato positive sorted HCs were pelleted once (300 g at 4°C) and resuspended in a minimal remaining volume (~30 µl). HC-enriched single cell suspensions were then used as input on the 10X Genomics Chromium platform with 3' Single Cell v2 chemistry (10X Genomics). Following capture and library preparation, single cell RNA-seq libraries were sequenced on a NextSeq 500 (Illumina) in collaboration with the NIDCD Genomics and Computational Biology Core. Samples were sequenced to an average depth of over 300,000 reads per cell, which resulted in detection of a median of >3,000 genes (*Anc80-eGFP*) and >4,000 genes (*Anc80-Ikzf2*) per cell, ensuring maximal transcriptional complexity and detection of low-abundance transcripts (see Extended Data Fig.9b-c). Reads were aligned to a modified mm10 mouse reference containing the sequences for the *Ai14* locus, as well as *Anc80-eGFP* and *Anc80-Ikzf2* viral sequences (Extended Data Fig.9a) using the 10X Genomics cellranger (version 2.0.2) package to generate the read counts matrix files. Read counts from viral and *Ai14* loci were removed from the expression matrix before dimensionality reduction so as to not influence data clustering. Cells from these HC clusters were determined to be *Anc80-Ikzf2*(+) versus *Anc80-Ikzf2*(-), and IHCs versus OHCs, based on their expression of *Anc80-Ikzf2* and *Slc17a8*, respectively (Fig.3, Extended Data Fig.8 and 9, Supplementary Table 9). *Slc26a5* was not well detected in the scRNA-seq dataset and was therefore not used as an OHC marker. After clustering, four HCs were excluded based on co-expression of a contaminating cell type. Secondary analyses, including shared nearest neighbor (SNN) clustering, tSNE embedding, and differential expression testing (using either Wilcoxon Ranked Sum for marker gene identification or MAST for pairwise comparison between control inner and outer HCs) were performed in R with Seurat (version 2.1.0)<sup>42,43</sup>. Non-parametric

analysis of variance between the four classified groups of HCs (IHCs and OHCs with either high or low *Anc80-Ikzf2* expression) using a Kruskal-Wallis test was performed to help qualify genes that had statistical difference across these cell populations. This was followed by post-hoc pairwise Wilcoxon Ranked Sum comparisons to assess multiple-comparison-adjusted *p*-values. Additional plots were generated by NMF (version 0.20.6) and ggplot2 (version 2.2.1)<sup>44,45</sup>. These analyses utilized the computational resources of the NIH HPC Biowulf cluster (<http://hpc.nih.gov>). scRNA-seq data have been submitted to the Gene Expression Omnibus database (GEO accession number GSE120462), and are additionally available for viewing through the gEAR Portal (<https://umgear.org/>).

### ***Immunohistochemistry of AAV-injected cochleae***

Mouse inner ears injected with either *Anc80-Ikzf2* or *Anc80-eGFP* were between P8 and 8 weeks, fixed in 4% PFA in PBS overnight at 4°C, and decalcified in a solution of 5% EDTA in RNAlater (Invitrogen). Decalcified ears were processed by sucrose gradient and embedded in OCT compound (Tissue-Tek) for cryosectioning, or fine dissected for whole-mount immunohistochemistry. 10 µm sections on positively charged glass slides were used for *in situ* hybridization (ISH) and section immunohistochemistry. For whole-mount immunolabeling at 6-8 weeks, HC loss was observed in the injected ear and therefore the contralateral ear, expressing a lower level of the *Anc80-Ikzf2* virus, was used. Primary antibodies: goat anti-prestin N-20 (1:200, Santa Cruz Biotechnology), goat anti-Oncomodulin N-19 (1:100, Santa Cruz Biotechnology), rabbit anti-Myosin VI (1:1000, Proteus BioSciences), rabbit anti-GFP (1:100, Life Technologies), mouse anti-cMyc 9E10 (1:100, Santa Cruz Biotechnology), and mouse anti-Otoferlin (1:100, Abcam). Dr. Rebecca Seal generously donated the guinea pig anti-Vglut3 antibody used in this study (1:5000). Corresponding Alexa Fluor® 488 and 546 (1:800, Invitrogen) were used for secondary detection, Alexa Fluor® 488 Phalloidin (1:1000, Invitrogen) was used to mark F-actin, and 4',6-Diamidino-2-Phenylindole Dihydrochloride (DAPI, 1:20,000, Thermo Fisher) was used to mark cell nuclei. Images were acquired using a Nikon Eclipse E600 microscope (Nikon, Tokyo, Japan) equipped with a Lumenera Infinity 3 camera. Whole-mount images were acquired using a Zeiss LSM DUO confocal microscope, located at the UMSOM Confocal Microscopy Core, at 63x oil magnification. Images were processed using Infinity Capture and Infinity Analyze software (Lumenera, Ottawa, ON), and ImageJ software.

### ***RNA in situ hybridization (ISH)***

ISH was performed as described in Geng et al., 2016<sup>46</sup>. Briefly, slides were re-fixed in 4% PFA, and then treated with 2 µg/ml Proteinase-K for 10 minutes. Proteinase-K reaction was stopped by soaking slides again in 4% PFA, followed by acetylation and permeabilization. Hybridization for the digoxigenin labelled *Fcrlb* probe was performed overnight at 65°C (see Supplementary Table 13 for *Fcrlb* probe primers). Following a series of washes in saline sodium citrate, slides were incubated with sheep-anti-digoxigenin antibody conjugated to alkaline phosphatase (Sigma-Aldrich, 1:100) overnight at 4°C. Slide were then incubated in BM purple AP substrate precipitating solution (Roche) to localize bound anti-digoxigenin antibody.

## Methods references

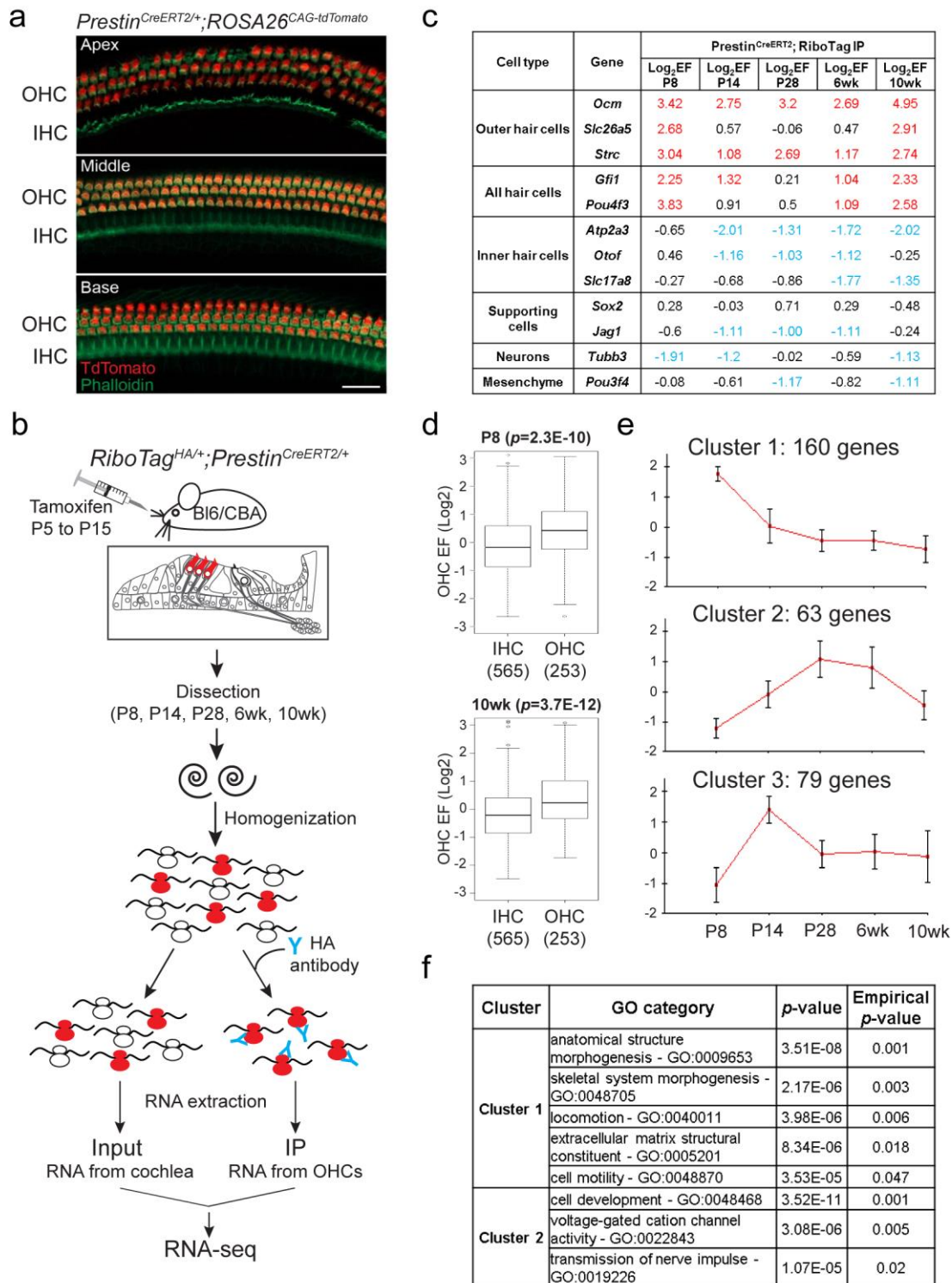
22. Caberlotto, E. *et al.* Usher type 1G protein sans is a critical component of the tip-link complex, a structure controlling actin polymerization in stereocilia. *Proc. Natl. Acad. Sci. U. S. A.* **108**, 5825–30 (2011).
23. Johnson, K. R., Zheng, Q. Y. & Noben-Trauth, K. Strain background effects and genetic modifiers of hearing in mice. *Brain Res.* **1091**, 79–88 (2006).
24. Hoelter, S. M. *et al.* Sighted C3H mice--a tool for analysing the influence of vision on mouse behaviour? *Front. Biosci.* **13**, 5810–23 (2008).
25. Kim, D. *et al.* TopHat2: accurate alignment of transcriptomes in the presence of insertions, deletions and gene fusions. *Genome Biol.* **14**, R36 (2013).
26. Anders, S., Pyl, P. T. & Huber, W. Genome analysis HTSeq — a Python framework to work with high-throughput sequencing data. *Bioinformatics* **31**, 166–169 (2015).
27. Anders, S. & Huber, W. Differential expression analysis for sequence count data. *Genome Biol.* **11**, R106 (2010).
28. Ulitsky, I. *et al.* Expander: from expression microarrays to networks and functions. *Nat. Protoc.* **5**, 303–322 (2010).
29. Sharan, R., Maron-Katz, A. & Shamir, R. CLICK and EXPANDER: a system for clustering and visualizing gene expression data. *Bioinformatics* **19**, 1787–99 (2003).
30. Shannon, P. *et al.* Cytoscape : A Software Environment for Integrated Models of Biomolecular Interaction Networks. *Genome Res.* **12**, 2498–2504 (2003).
31. Adzhubei, I. A. *et al.* A method and server for predicting damaging missense mutations. *Nat. Methods* **7**, 248–9 (2010).
32. Choi, Y., Sims, G. E., Murphy, S., Miller, J. R. & Chan, A. P. Predicting the Functional Effect of Amino Acid Substitutions and Indels. *PLoS One* **7**, e46688 (2012).
33. Kumar, P., Henikoff, S. & Ng, P. C. Predicting the effects of coding non-synonymous variants on protein function using the SIFT algorithm. *Nat. Protoc.* **4**, 1073–1081 (2009).
34. Källberg, M. *et al.* Template-based protein structure modeling using the RaptorX web server. *Nat. Protoc.* **7**, 1511–22 (2012).
35. Hardisty-Hughes, R. E., Parker, A. & Brown, S. D. M. A hearing and vestibular phenotyping pipeline to identify mouse mutants with hearing impairment. *Nat. Protoc.* **5**, 177–190 (2010).
36. Mianné, J. *et al.* Correction of the auditory phenotype in C57BL/6N mice via CRISPR/Cas9-mediated homology directed repair. *Genome Med.* **8**, 16 (2016).
37. Codner, G. F. *et al.* Application of long single-stranded DNA donors in genome editing: generation and validation of mouse mutants. *BMC Biol.* **16**, (2018).
38. Corns, L. F., Johnson, S. L., Kros, C. J. & Marcotti, W. Calcium entry into stereocilia drives adaptation of the mechano-electrical transducer current of mammalian cochlear hair cells. *Proc. Natl. Acad. Sci.* **111**, 14918–14923 (2014).
39. Santos-Sacchi, J. Determination of cell capacitance using the exact empirical solution of partial differential Y/partial differential Cm and its phase angle. *Biophys. J.* **87**, 714–27 (2004).
40. Santos-Sacchi, J. & Navarrete, E. Voltage-dependent changes in specific membrane capacitance caused by prestin, the outer hair cell lateral membrane motor. *Pflügers Arch.* **444**, 99–106 (2002).
41. Isgrig, K. *et al.* Gene Therapy Restores Balance and Auditory Functions in a Mouse Model of Usher Syndrome. *Mol. Ther.* **25**, 780–791 (2017).
42. Finak, G. *et al.* MAST: a flexible statistical framework for assessing transcriptional

- changes and characterizing heterogeneity in single-cell RNA sequencing data. *Genome Biol.* **16**, 278 (2015).
43. Satija, R., Farrell, J. A., Gennert, D., Schier, A. F. & Regev, A. Spatial reconstruction of single-cell gene expression data. *Nat. Biotechnol.* **33**, 495–502 (2015).
  44. Wickham, H. *ggplot2: Elegant Graphics for Data Analysis*. (Springer, 2009).
  45. Gaujoux, R. & Seoighe, C. A flexible R package for nonnegative matrix factorization. *BMC Bioinformatics* **11**, 367 (2010).
  46. Geng, R. *et al.* Comprehensive Expression of Wnt Signaling Pathway Genes during Development and Maturation of the Mouse Cochlea. *PLoS One* **11**, e0148339 (2016).

### **Data Availability**

The RiboTag OHC RNA-seq, P8 cello cochlea RNA-seq, and P8 Anc80-*Ikzf2* and Anc80-*eGFP* injected cochlea scRNA-seq data have been submitted to the Gene Expression Omnibus database (GEO Accession # GSE116703, GSE116702, and GSE120462), and are additionally available for viewing through the gEAR Portal (<https://umgear.org/>).

## Extended Data Figure and Legends



### Extended Data Figure 1. RiboTag immunoprecipitation enriches for known OHC-expressed transcripts.

(a) Representative *prestin*<sup>CreERT2/+</sup>; *ROSA26*<sup>CAG-tdTomato</sup> cochlear whole-mount. *Prestin*-*CreERT2*-driven tdTomato expression is OHC-specific at P21 (n=1). Scale=20 μm.

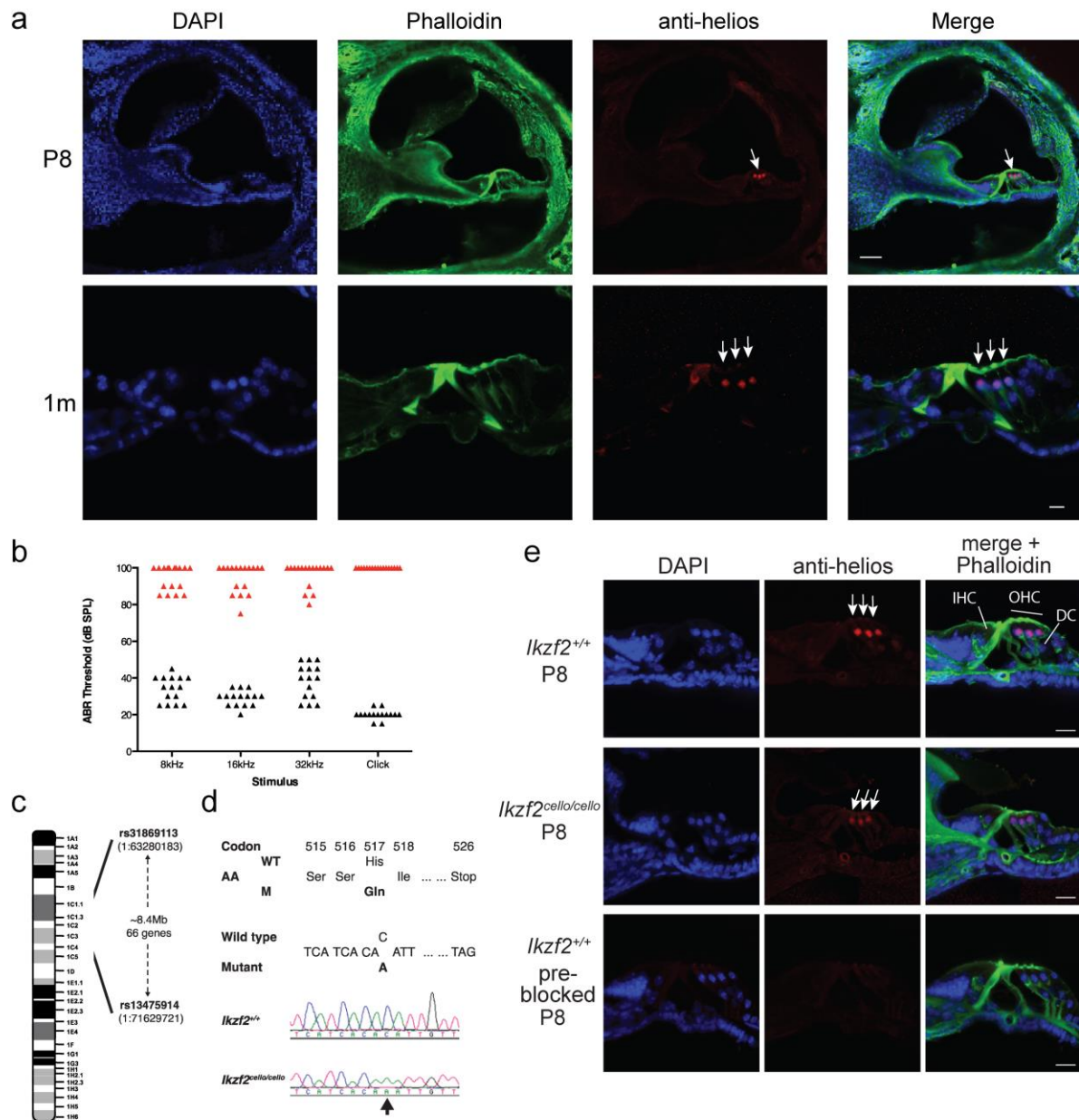
(b) Schematic of the RiboTag immunoprecipitation protocol. Red OHCs represent Cre/HA-tagged ribosome expression.

(c) RiboTag RNA-seq  $\log_2$  enrichment and depletion of transcripts for known inner ear cell type markers (enrichment factor (EF) =  $\log_2(\text{IP}/\text{input})$ ).

(d) Genes at least 2-fold enriched in IHCs (n = 565 genes) or OHCs (n = 253 genes) in the dataset of Liu et al. are significantly depleted and enriched, respectively, by the RiboTag OHC immunoprecipitation (two-sided Wilcoxon's test). This was true for all time points examined. Black line represents median EF, box demarcates 1<sup>st</sup> and 3<sup>rd</sup> quartiles, whiskers demarcate 1<sup>st</sup> and 3<sup>rd</sup> quartiles  $\pm 1.5 \times \text{IQR}$  values, dots represent single outliers.

(e) Clustering of genes differentially expressed across OHC postnatal development (error bars = SD). Prior to clustering, expression levels were standardized to mean=0 and SD=1.

(f) Enriched gene ontology (GO) functional categories identified for the gene clusters in (e) (cluster 1 n=160 genes, cluster 2 n=63 genes). No significantly enriched GO categories were found for cluster 3 (n=79 genes). Enrichment and statistical analyses were performed using the EXPANDER implemented tool TANGO.



**Extended Data Figure 2. Auditory phenotyping, SNP mapping and whole-genome sequencing of mouse pedigree MPC173, subsequently named *cello*.**

(a) Specific expression of helios can be seen in the nuclei of wild-type P8 OHCs (white arrow, n=3 biologically independent samples, scale=50  $\mu$ m), and is maintained in wild-type OHCs at 1-month (white arrows, n=3 biologically independent samples, scale=10  $\mu$ m).

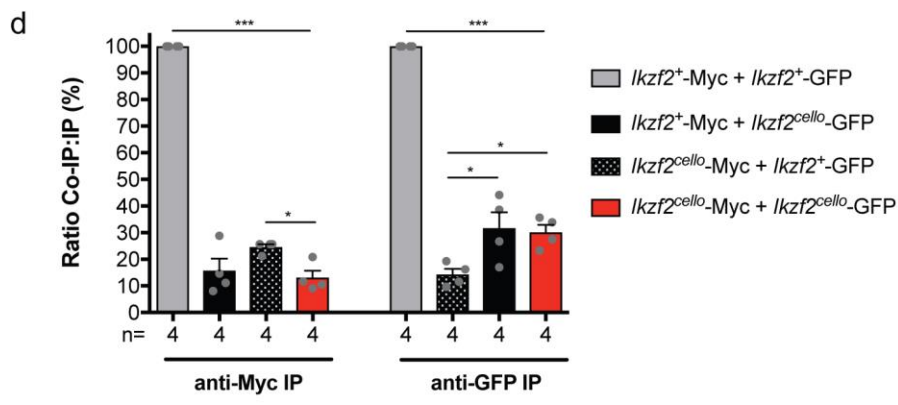
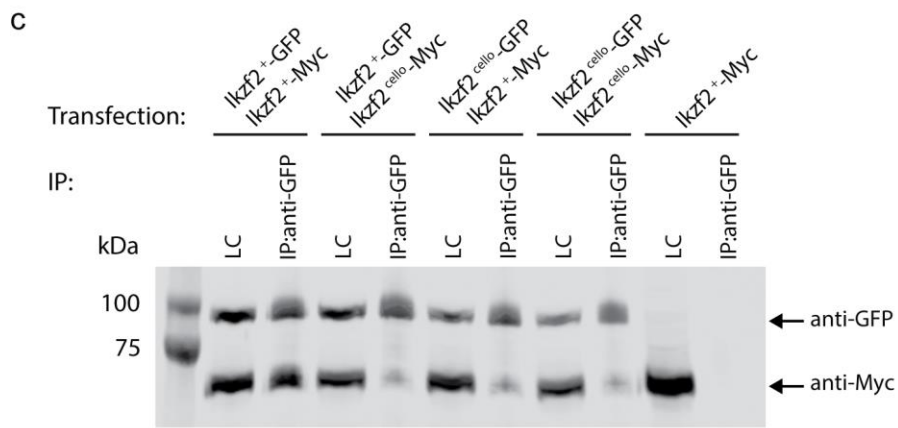
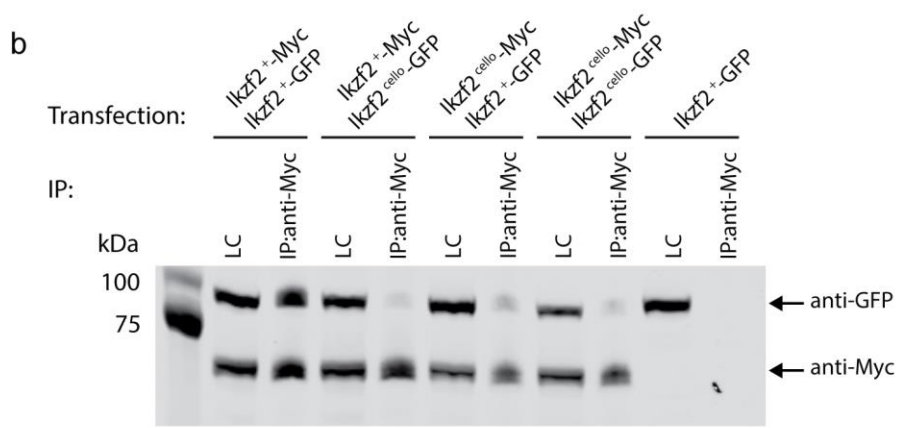
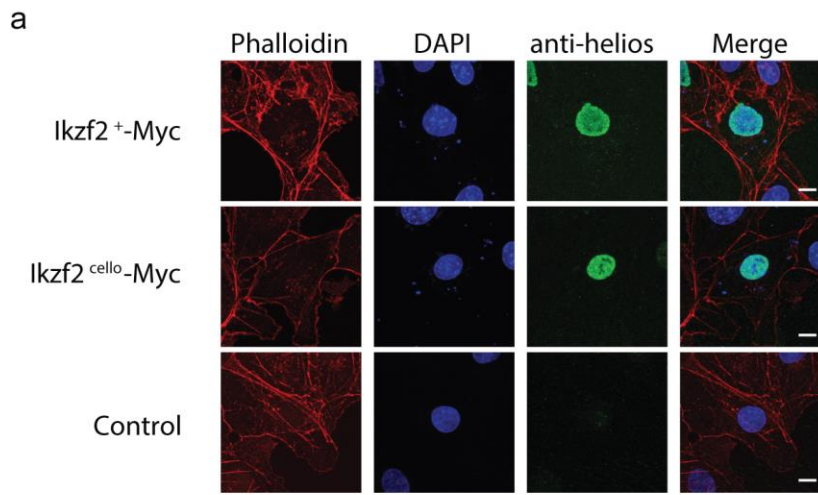
(b) Auditory brainstem response phenotyping of pedigree MPC173 at 9-months of age identified 17 biologically independent animals with elevated hearing thresholds (red triangles) compared to their normal hearing colony mates (n=15 biologically independent animals, black triangles).

(c) The mutation mapped to an 8.4 Mb region on Chromosome 1 between SNPs rs31869113 and rs13475914 (Chr1:63280183-71629721), containing 66 genes.

(d) Detection of a non-synonymous mutation in *cello*. DNA sequencing identified a nucleotide transversion (c.1551C>A) in the *Ikzf2* gene at codon 517, thus altering the wild-type (WT) sequence CAC, encoding a histidine (His), to the mutant (M) sequence CAA, encoding a glutamine (Gln). Electropherograms derived from a *cello* mutant mouse

(*Ikzf2<sup>cello/cello</sup>*) and a wild-type colony mate (*Ikzf2<sup>+/+</sup>*) control showing the sequence surrounding *Ikzf2* nucleotide 1551 (indicated by an arrow).

(e) Helios is expressed in the OHC nuclei of both *Ikzf2<sup>+/+</sup>* and *Ikzf2<sup>cello/cello</sup>* mice at P8 (n=3 biologically independent samples per genotype). Loss of labelling when the anti-helios antibody is 'pre-blocked' confirms specificity (n=1 biologically independent sample). Scale=20  $\mu$ m.



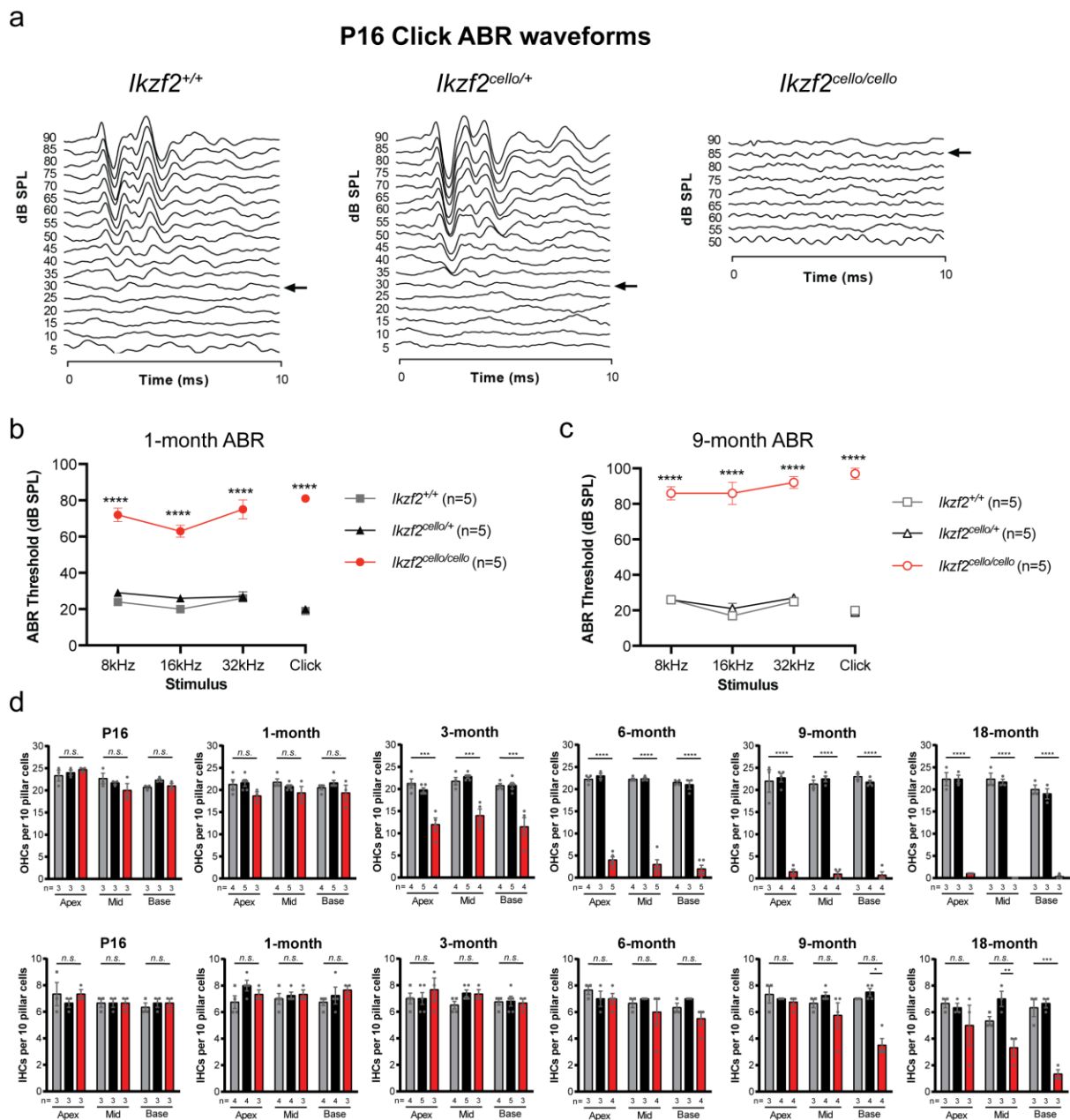
**Extended Data Figure 3. The *Ikzf2<sup>cello</sup>* mutation disrupts helios homodimerization.**

(a) Cos-7 cells transfected with *Ikzf2<sup>+</sup>*- or *Ikzf2<sup>cello</sup>*-Myc. Nuclear localization is unaffected by the *Ikzf2<sup>cello</sup>* mutation (n=2 biologically independent experiments). Scale=10  $\mu$ m.

(b) Co-immunoprecipitation (IP) of Myc-tagged (~62 kDa) and GFP-tagged (~88 kDa) *Ikzf2<sup>+</sup>* and *Ikzf2<sup>cello</sup>* constructs. Transfected cell lysates were immunoprecipitated using an anti-Myc antibody and analysed by western blotting with both anti-Myc and anti-GFP antibodies. Results show that wild-type *Ikzf2<sup>+</sup>* helios can dimerize, but that dimerization is impaired by the *cello* mutation. kDa = kilodaltons, LC = cell lysate loading control.

(c) Reciprocal immunoprecipitation reactions using an anti-GFP antibody confirm dimerization of wild-type *Ikzf2<sup>+</sup>* helios and reduced dimerization of mutant *Ikzf2<sup>cello</sup>* helios. kDa = kilodaltons, LC = cell lysate loading control.

(d) Quantification of Co-IP western blots. Band intensities were determined and used to calculate the relative ratio of Co-IP to IP signal. Data shown are averaged percentages  $\pm$  s.e.m. (n=4 biologically independent experiments). Myc IP *p*-values: *Ikzf2<sup>+</sup>*-Myc + *Ikzf2<sup>+</sup>*-GFP vs *Ikzf2<sup>+</sup>*-Myc + *Ikzf2<sup>cello</sup>*-GFP <0.0001, *Ikzf2<sup>+</sup>*-Myc + *Ikzf2<sup>+</sup>*-GFP vs *Ikzf2<sup>cello</sup>*-Myc + *Ikzf2<sup>+</sup>*-GFP <0.0001, *Ikzf2<sup>+</sup>*-Myc + *Ikzf2<sup>+</sup>*-GFP vs *Ikzf2<sup>cello</sup>*-Myc + *Ikzf2<sup>cello</sup>*-GFP <0.0001, *Ikzf2<sup>+</sup>*-Myc + *Ikzf2<sup>cello</sup>*-GFP vs *Ikzf2<sup>cello</sup>*-Myc + *Ikzf2<sup>+</sup>*-GFP = 0.1488, *Ikzf2<sup>+</sup>*-Myc + *Ikzf2<sup>cello</sup>*-GFP vs *Ikzf2<sup>cello</sup>*-Myc + *Ikzf2<sup>cello</sup>*-GFP = 0.9020, *Ikzf2<sup>cello</sup>*-Myc + *Ikzf2<sup>+</sup>*-GFP vs *Ikzf2<sup>cello</sup>*-Myc + *Ikzf2<sup>cello</sup>*-GFP = 0.0476. GFP IP *p*-values: *Ikzf2<sup>+</sup>*-GFP + *Ikzf2<sup>+</sup>*-Myc vs *Ikzf2<sup>+</sup>*-GFP + *Ikzf2<sup>cello</sup>*-Myc <0.0001, *Ikzf2<sup>+</sup>*-GFP + *Ikzf2<sup>+</sup>*-Myc vs *Ikzf2<sup>cello</sup>*-GFP + *Ikzf2<sup>+</sup>*-Myc <0.0001, *Ikzf2<sup>+</sup>*-GFP + *Ikzf2<sup>+</sup>*-Myc vs *Ikzf2<sup>cello</sup>*-GFP + *Ikzf2<sup>cello</sup>*-Myc <0.0001, *Ikzf2<sup>+</sup>*-GFP + *Ikzf2<sup>cello</sup>*-Myc vs *Ikzf2<sup>cello</sup>*-GFP + *Ikzf2<sup>+</sup>*-Myc = 0.0202, *Ikzf2<sup>+</sup>*-GFP + *Ikzf2<sup>cello</sup>*-Myc vs *Ikzf2<sup>cello</sup>*-GFP + *Ikzf2<sup>cello</sup>*-Myc = 0.0346, *Ikzf2<sup>cello</sup>*-GFP + *Ikzf2<sup>+</sup>*-Myc vs *Ikzf2<sup>cello</sup>*-GFP + *Ikzf2<sup>cello</sup>*-Myc = 0.9894. Significance was assessed by one-way ANOVA with Tukey post-hoc test. See Supplementary Fig.1 for source images.



**Extended Data Figure 4. Auditory function and HC bundle survival in *cello* mice.**

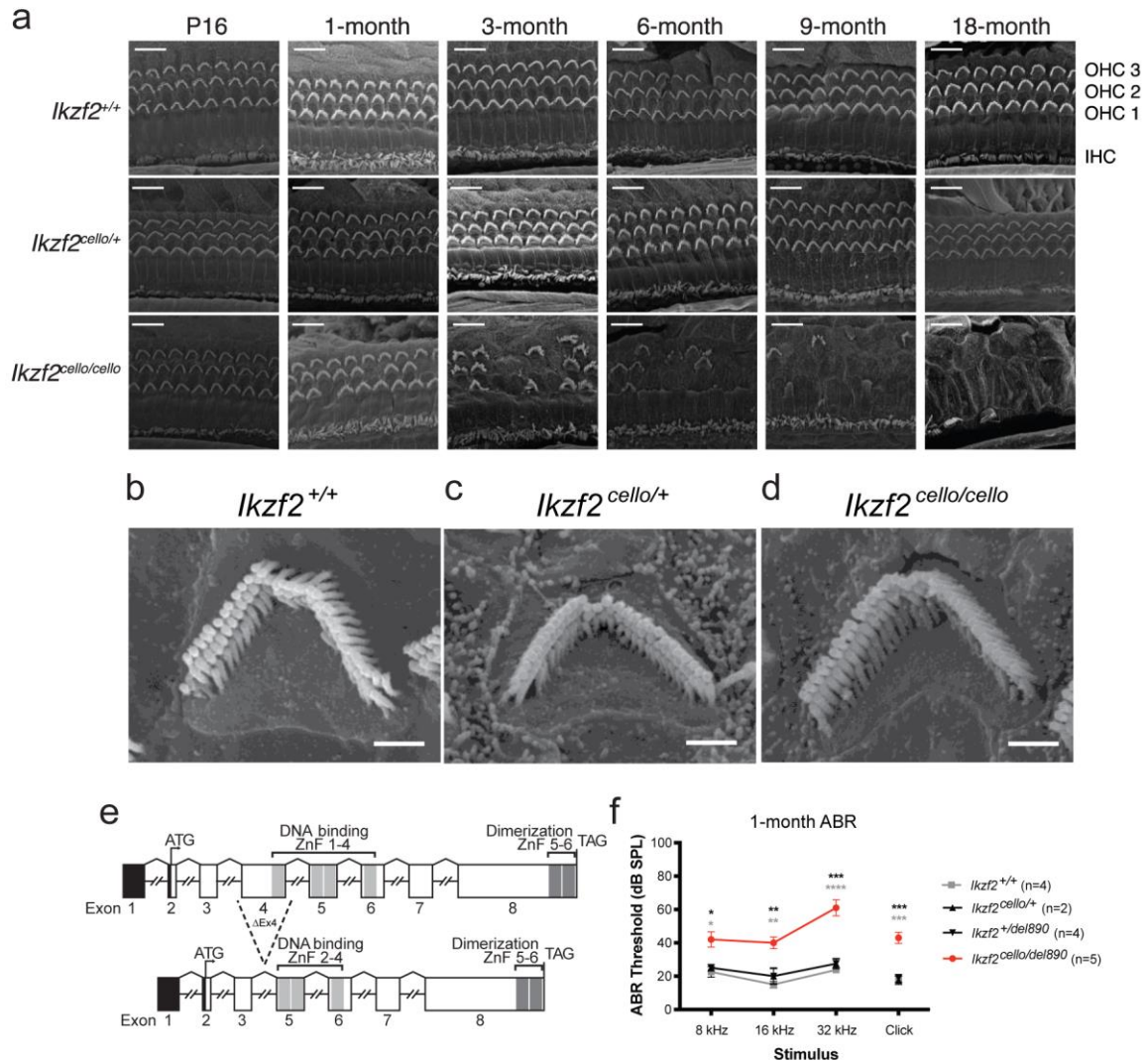
(a) Representative click ABR waveforms for *Ikzf2*<sup>+/+</sup>, *Ikzf2*<sup>cello/+</sup> and *Ikzf2*<sup>cello/cello</sup> littermates at P16 (n=4 biologically independent animals per genotype).

(b-c) Averaged ABR thresholds for *cello* mice at 1-month of age (b, n=5 biologically independent animals per genotype) and 9-months of age (c, n=5 biologically independent animals per genotype). Age-matched *Ikzf2*<sup>+/+</sup> and *Ikzf2*<sup>cello/+</sup> controls display thresholds within the expected range (15 – 30 dB SPL) at all time-points tested. Data shown are averaged thresholds ± s.e.m. 1-month *Ikzf2*<sup>cello/cello</sup> vs 1-month *Ikzf2*<sup>+/+</sup> (b) *p*-values: 8 kHz <0.0001, 16 kHz <0.0001, 32 kHz <0.0001, Click <0.0001. 1-month *Ikzf2*<sup>cello/cello</sup> vs 1-month *Ikzf2*<sup>cello/+</sup> (b) *p*-values: 8 kHz <0.0001, 16 kHz <0.0001, 32 kHz <0.0001, Click <0.0001. 9-month *Ikzf2*<sup>cello/cello</sup> vs 9-month *Ikzf2*<sup>+/+</sup> (b) *p*-values: 8 kHz <0.0001, 16 kHz <0.0001, 32 kHz <0.0001, Click <0.0001. 9-month *Ikzf2*<sup>cello/cello</sup> vs 9-month *Ikzf2*<sup>cello/+</sup> (b) *p*-values: 8 kHz <0.0001, 16 kHz <0.0001, 32 kHz <0.0001, Click <0.0001. Significance was assessed by one-way ANOVA with Tukey post-hoc test.

(d) OHC and IHC bundle counts for *cello* mice from P16 to 18-months of age. Data shown are averaged number of HC bundles adjacent to ten pillar cells ± s.e.m. *n.s.* non-significant,

\* $p < 0.05$ , \*\* $p < 0.01$ , \*\*\* $p < 0.001$ , \*\*\*\* $p < 0.0001$ , one-way ANOVA with Tukey post-hoc test. Number of biologically independent samples for OHC bundle counts: P16  $Ikzf2^{+/+}$   $n=3$ , P16  $Ikzf2^{cello/+}$   $n=3$ , P16  $Ikzf2^{cello/cello}$   $n=3$ ; 1-month  $Ikzf2^{+/+}$   $n=4$ , 1-month  $Ikzf2^{cello/+}$   $n=5$ , 1-month  $Ikzf2^{cello/cello}$   $n=3$ ; 3-month  $Ikzf2^{+/+}$   $n=4$ , 3-month  $Ikzf2^{cello/+}$   $n=5$ , 3-month  $Ikzf2^{cello/cello}$   $n=4$ ; 6-month  $Ikzf2^{+/+}$   $n=4$ , 6-month  $Ikzf2^{cello/+}$   $n=3$ , 6-month  $Ikzf2^{cello/cello}$   $n=5$ ; 9-month  $Ikzf2^{+/+}$   $n=3$ , 9-month  $Ikzf2^{cello/+}$   $n=4$ , 9-month  $Ikzf2^{cello/cello}$   $n=4$ ; 18-month  $Ikzf2^{+/+}$   $n=3$ , 18-month  $Ikzf2^{cello/+}$   $n=3$ , 18-month  $Ikzf2^{cello/cello}$   $n=3$ . Number of biologically independent samples for IHC bundle counts: P16  $Ikzf2^{+/+}$   $n=3$ , P16  $Ikzf2^{cello/+}$   $n=3$ , P16  $Ikzf2^{cello/cello}$   $n=3$ ; 1-month  $Ikzf2^{+/+}$   $n=4$ , 1-month  $Ikzf2^{cello/+}$   $n=4$ , 1-month  $Ikzf2^{cello/cello}$   $n=3$ ; 3-month  $Ikzf2^{+/+}$   $n=4$ , 3-month  $Ikzf2^{cello/+}$   $n=5$ , 3-month  $Ikzf2^{cello/cello}$   $n=3$ ; 6-month  $Ikzf2^{+/+}$   $n=3$ , 6-month  $Ikzf2^{cello/+}$   $n=3$ , 6-month  $Ikzf2^{cello/cello}$   $n=4$ ; 9-month  $Ikzf2^{+/+}$   $n=3$ , 9-month  $Ikzf2^{cello/+}$   $n=4$ , 9-month  $Ikzf2^{cello/cello}$   $n=4$ ; 18-month  $Ikzf2^{+/+}$   $n=3$ , 18-month  $Ikzf2^{cello/+}$   $n=3$ , 18-month  $Ikzf2^{cello/cello}$   $n=3$ .

See also Supplementary Table 5 and 6.



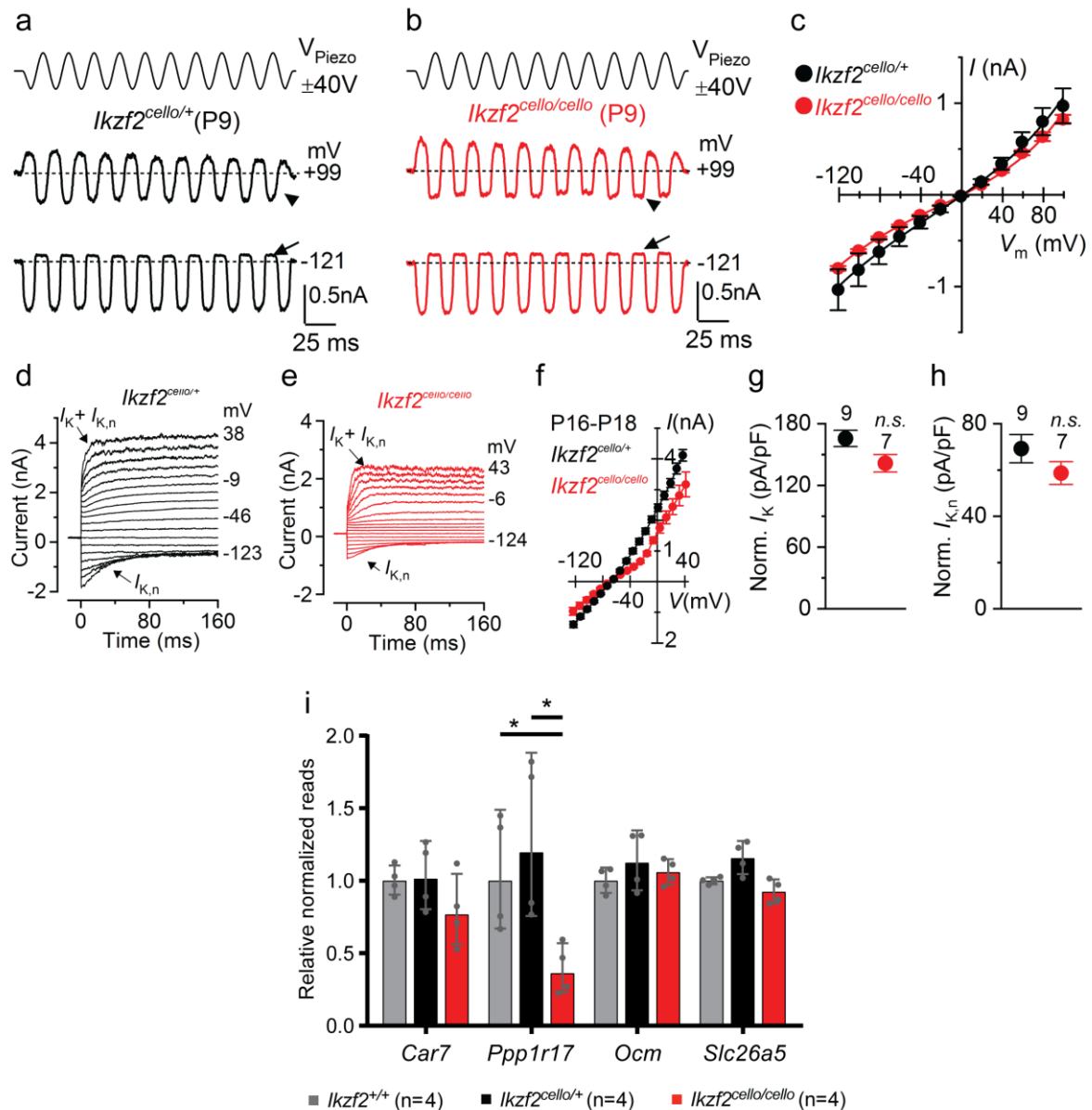
**Extended Data Figure 5. Scanning electron microscopy of *cello* mice and auditory function of *Ikzf2<sup>cello/del890</sup>* compound heterozygotes.**

(a) Scanning electron micrographs of the organ of Corti of *cello* mice from P16 to 18-months of age. Representative images from the mid region of the cochlear spiral are shown. Scale = 10  $\mu$ m. Number of biologically independent samples: P16 *Ikzf2<sup>+/+</sup>* n=4, P16 *Ikzf2<sup>cello/+</sup>* n=3, P16 *Ikzf2<sup>cello/cello</sup>* n=3; 1-month *Ikzf2<sup>+/+</sup>* n=4, 1-month *Ikzf2<sup>cello/+</sup>* n=5, 1-month *Ikzf2<sup>cello/cello</sup>* n=3; 3-month *Ikzf2<sup>+/+</sup>* n=4, 3-month *Ikzf2<sup>cello/+</sup>* n=5, 3-month *Ikzf2<sup>cello/cello</sup>* n=4; 6-month *Ikzf2<sup>+/+</sup>* n=4, 6-month *Ikzf2<sup>cello/+</sup>* n=5, 6-month *Ikzf2<sup>cello/cello</sup>* n=4; 9-month *Ikzf2<sup>+/+</sup>* n=3, 9-month *Ikzf2<sup>cello/+</sup>* n=4, 9-month *Ikzf2<sup>cello/cello</sup>* n=4; 18-month *Ikzf2<sup>+/+</sup>* n=3, 18-month *Ikzf2<sup>cello/+</sup>* n=3, 18-month *Ikzf2<sup>cello/cello</sup>* n=3.

(b-d) Scanning electron micrographs of OHC stereocilia bundles of *cello* mice at P16, showing that wild-type *Ikzf2<sup>+/+</sup>* (b), *Ikzf2<sup>cello/+</sup>* (c) and mutant *Ikzf2<sup>cello/cello</sup>* (d) mice display overall expected bundle patterning. Images are from the mid region of the cochlear spiral. Scale = 1  $\mu$ m. Number of biologically independent samples: *Ikzf2<sup>+/+</sup>* n=3, *Ikzf2<sup>cello/+</sup>* n=3, *Ikzf2<sup>cello/cello</sup>* n=3.

(e) The genomic/domain structure of the *Ikzf2<sup>del890</sup>* allele/protein. Black = 5' untranslated region, light grey = N-terminal DNA-binding domain, dark grey = C-terminal dimerization domain. The *Ikzf2<sup>cello</sup>* mutation lies in ZnF6. The *del890* mutation deletes exon 4 and surrounding intronic sequence.

(f) Averaged ABR thresholds for  $Ikzf2^{cello/del890}$  compound heterozygotes at 1-month of age, showing significantly elevated thresholds ( $\geq 40$  dB SPL) at all frequencies tested compared to  $Ikzf2^{+/+}$ ,  $Ikzf2^{cello/+}$  and  $Ikzf2^{del890/+}$  control colony mates. Data shown are averaged thresholds  $\pm$  s.e.m. Number of biologically independent samples:  $Ikzf2^{+/+}$  n=4,  $Ikzf2^{cello/+}$  n=2,  $Ikzf2^{+/del890}$  n=4,  $Ikzf2^{cello/del890}$  n=5.  $Ikzf2^{cello/del890}$  vs  $Ikzf2^{+/+}$  p-values: 8 kHz = 0.011, 16 kHz = 0.002, 32 kHz <0.0001, Click = 0.0001;  $Ikzf2^{cello/del890}$  vs  $Ikzf2^{cello/+}$  p-values: 8 kHz = 0.078, 16 kHz = 0.034, 32 kHz = 0.001, Click = 0.001;  $Ikzf2^{cello/del890}$  vs  $Ikzf2^{+/del890}$  p-values: 8 kHz = 0.025, 16 kHz = 0.009, 32 kHz = 0.0002, Click = 0.0002. Significance was assessed by one-way ANOVA with Tukey post-hoc test.



### Extended Data Figure 6. The MET current is normal in $I_{kzf2}^{cello}$ mice.

(a-b) MET currents were recorded from OHCs of P9  $I_{kzf2}^{cello/cello}$  and  $I_{kzf2}^{cello/+}$  (control) littermates. During voltage steps, hair bundles were displaced by applying a 50 Hz sinusoidal force stimuli (the driver voltage to the fluid jet is shown above the traces)<sup>47</sup>. At hyperpolarised membrane potentials ( $-121$  mV), saturating excitatory bundle stimulation (i.e., towards the taller stereocilia) elicited a large inward MET current from both  $I_{kzf2}^{cello/+}$  and  $I_{kzf2}^{cello/cello}$  OHCs, while inhibitory bundle stimulation (i.e. away from the taller stereocilia) closed the MET channels and reduced the resting current. Because the MET current reverses near 0 mV, it became outward when excitatory bundle stimulation was applied during voltage steps positive to its reversal potential. At positive membrane potentials ( $+99$  mV), excitatory bundle stimulation now elicited similar outward MET currents with larger resting amplitudes. Arrows indicate closure of the MET channels (i.e., disappearance of the resting current) during inhibitory bundle displacements, arrowheads indicate the larger resting MET current at  $+99$  mV compared to  $-121$  mV.

(c) Peak-to-peak current-voltage curves obtained from  $I_{kzf2}^{cello/+}$  (n=10 biologically independent samples) and  $I_{kzf2}^{cello/cello}$  (n=8 biologically independent samples) OHCs at P9.

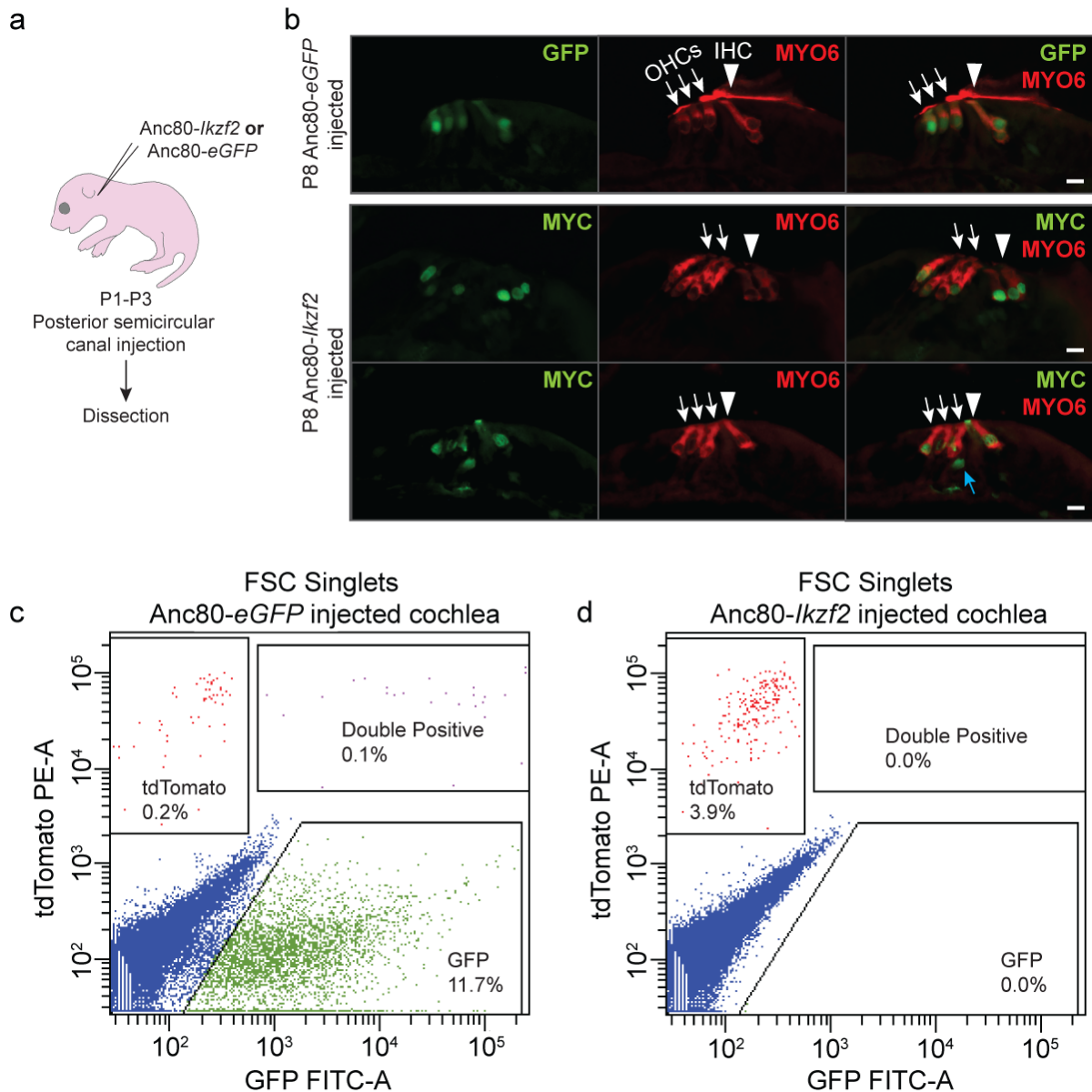
The maximal MET current and the resting open probability of the MET channel were found to be similar between the two genotypes. Data shown are mean values  $\pm$  s.e.m.

(d-e) Total  $K^+$  currents recorded from P18 *Ikzf2<sup>cello/+</sup>* control (d) and *Ikzf2<sup>cello/cello</sup>* mutant (e) OHCs. The size of the  $K^+$  current, which is mainly due to the negatively-activated  $I_{K,n}$  (in addition to a small delayed rectifier  $I_K$ : Marcotti and Kros, 1999), was smaller in *Ikzf2<sup>cello/cello</sup>* OHCs.

(f) Average peak current-voltage relationship for the total  $K^+$  current recorded from the OHCs of *Ikzf2<sup>cello/+</sup>* (n = 9 OHCs from 6 biologically independent animals) and *Ikzf2<sup>cello/cello</sup>* (n = 7 OHCs from 5 biologically independent animals) mice at P16–P18. Data shown are mean values  $\pm$  s.e.m.

(g-h) After normalization to the significantly reduced surface area of *Ikzf2<sup>cello/cello</sup>* OHCs (for this set of experiments: *Ikzf2<sup>cello/+</sup>*:  $14.2 \pm 0.4$  pF; *Ikzf2<sup>cello/cello</sup>*:  $11.2 \pm 0.5$  pF;  $p < 0.0005$ ), both the total  $I_K$  (g) and isolated  $I_{K,n}$  (h) were not significantly different between the two genotypes at P16–P18. Data shown are mean values  $\pm$  s.e.m. n.s. non-significant, two-sided Welch's t-test.

(i) NanoString validations of genes downregulated in P8 *Ikzf2<sup>cello/cello</sup>* cochleae at P16. Data shown are mean normalized reads relative to wild-type  $\pm$  SD (n = 4 biologically independent samples per genotype). *Ppp17r1* in *Ikzf2<sup>cello/cello</sup>* vs *Ikzf2<sup>+/+</sup>* p-value = 0.038, *Ppp17r1* in *Ikzf2<sup>cello/cello</sup>* vs *Ikzf2<sup>cello/+</sup>* p-value = 0.037. Significance was assessed by two-sided Welch's t-test.



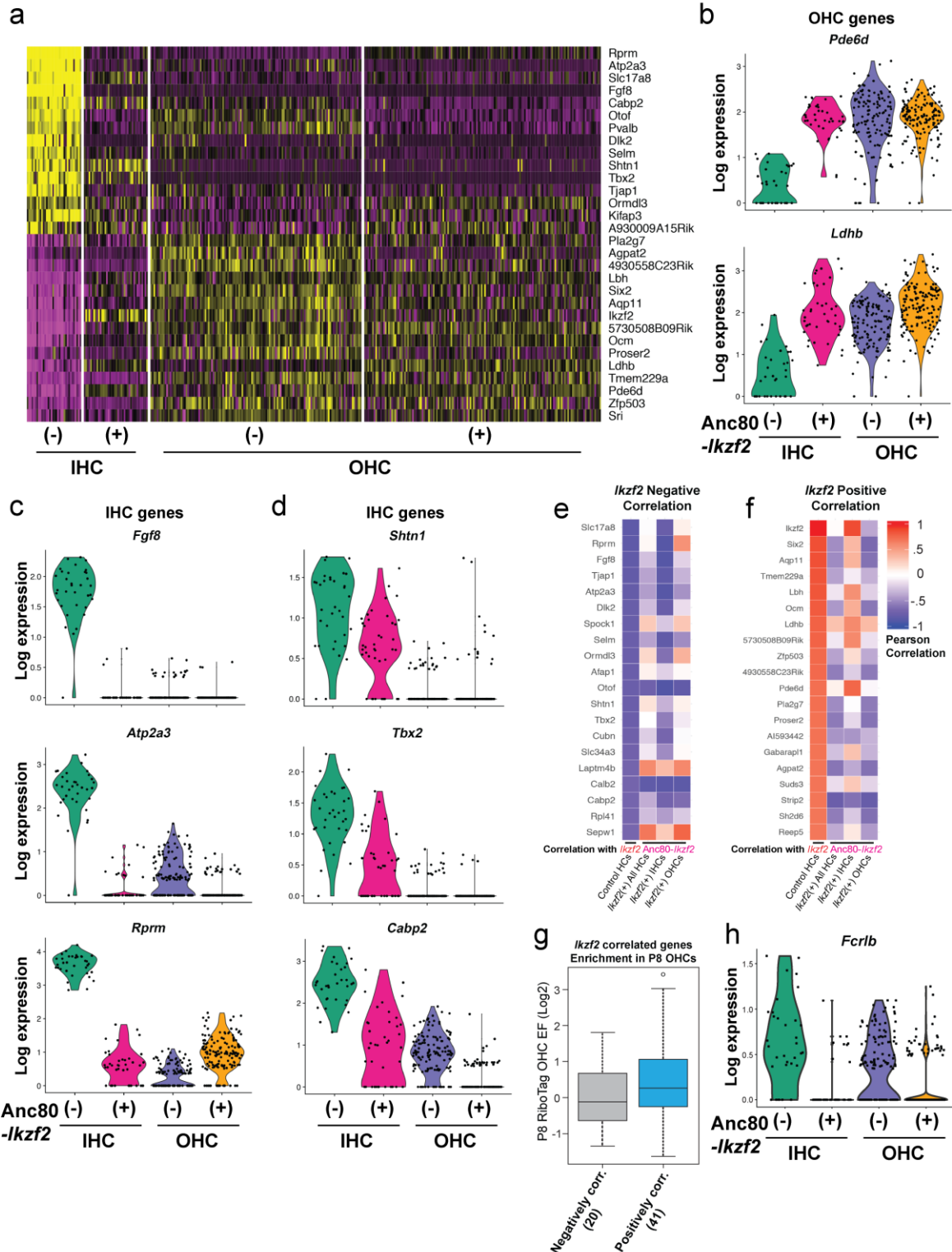
**Extended Data Figure 7. Transduction of cochlear HCs using Anc80L65 and HC enrichment by flow cytometry.**

(a) Schematic representation of inner ear viral gene delivery via the posterior semicircular canal of CD-1 mice for HC marker immunolabeling.

(b) Immunolabeling for GFP in the *Anc80-eGFP* injected, and MYC in the *Anc80-Ikzf2* injected ears, showed mainly HC transduction, although some MYC staining could also be observed in supporting cells (blue arrow) ( $n=3$  biologically independent samples per condition). Nuclear MYC staining suggests proper trafficking of the MYC-tagged helios protein in transduced cells. White arrows indicate OHCs and white arrowheads indicate IHCs. Scale = 10  $\mu\text{m}$ .

(c-d) Fluorescence activated cell sorting (FACS) of dissociated cochlear GFP positive and tdTomato positive cells from P8 *Myo15<sup>Cre/+</sup>; ROSA26<sup>CAG-tdTomato</sup>* mice injected with either *Anc80-eGFP* (c, 2 mice) or *Anc80-Ikzf2* (d, 4 mice). Cells were first gated by forward and side scatter to exclude doublets. For the *Anc80-eGFP* transduced cochlear sample, transduced cells were identified based on GFP expression, and hair cells were further identified by tdTomato expression. tdTomato single positive, GFP single positive and

tdTomato+GFP double positive cells were collected. For the *Anc80-Ikzf2* transduced cochlear sample, HCs were gated based on tdTomato single positive expression and collected.



**Extended Data Figure 8. Transcriptional conversion of Anc80-*Ikzf2* transduced IHCs.**

(a) Heatmap for the top 30 differently expressed genes between all HCs profiled. Scaled expression values shown as z-scores, with yellow indicating higher and purple indicating lower expression than the mean.

(b) OHC enriched genes that are induced in Anc80-*Ikzf2*(+) IHCs. Anc80-*Ikzf2*(-) IHC (n=34) vs. Anc80-*Ikzf2*(+) IHC (n=40) FDR: *Pde6d* = 2.03E-12, *Ldhb* = 3.74E-11. Dots represent the expression values of individual cells, with width of violins summarizing overall relative distribution of expression.

(c) IHC enriched genes that are highly expressed in control IHCs vs control OHCs, but are significantly reduced in Anc80-*Ikzf2*(+) IHCs. Anc80-*Ikzf2*(-) IHC (n=34) vs. Anc80-*Ikzf2*(+) IHC (n=40) FDR: *Fgf8* = 3.30E-14, *Atp2a3* = 2.46E-13, *Rprm* = 2.27E-13 (Kruskal-Wallis test followed by post-hoc pairwise Wilcoxon Ranked Sum test adjusted for multiple comparisons).

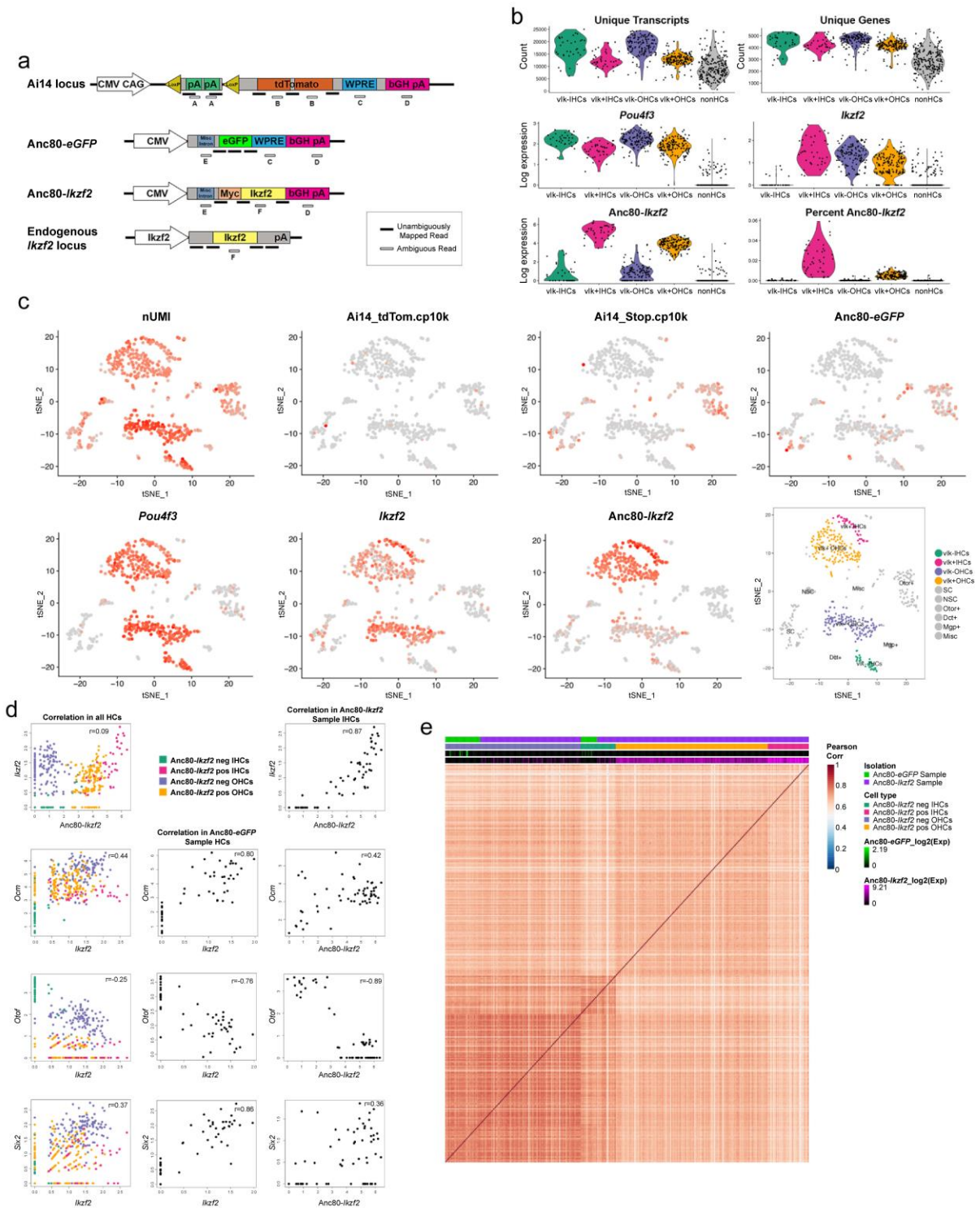
(d) IHC enriched genes that show only moderately reduced expression in Anc80-*Ikzf2*(+) IHCs. Anc80-*Ikzf2*(-) IHC (n=34) vs. Anc80-*Ikzf2*(+) IHC (n=40) FDR: *Shtn1* = 8.59E-05, *Tbx2* = 3.88E-08, *Cabp2* = 1.40E-10 (Kruskal-Wallis test followed by post-hoc pairwise Wilcoxon Ranked Sum test adjusted for multiple comparisons).

(e-f) Top 20 genes negatively (e) or positively (f) correlated with *Ikzf2* expression in control HCs, shown alongside corresponding correlations of gene expression within all Anc80-*Ikzf2* transduced HCs, Anc80-*Ikzf2* transduced IHCs, or Anc80-*Ikzf2* transduced OHCs. See also Extended Data Figure 9.

(g) Genes that are negatively correlated with *Ikzf2* (n=20, Pearson correlation < -0.6) are not enriched in OHCs at P8 compared to all other genes detected in the RiboTag OHC dataset (background genes, BG, n=13,124). Genes that are positively correlated with *Ikzf2* (n=41, Pearson correlation > 0.6) are significantly enriched in OHCs at P8 compared to BG (n=13,103) ( $p = 0.025$ , two-sided Wilcoxon's test). Black line represents median enrichment factor (EF, log<sub>2</sub> fold change), box demarcates 1<sup>st</sup> and 3<sup>rd</sup> quartiles, whiskers demarcate 1<sup>st</sup> and 3<sup>rd</sup> quartile  $\pm 1.5 \times$  IQR values, dots represent single outliers.

(h) One of the most differentially expressed genes we observed in our scRNA-seq experiment was *Fcrlb*, a gene which encodes an Fc receptor like protein, and whose expression in the ear has not been previously described. *Fcrlb* is significantly downregulated in Anc80-*Ikzf2*(+) HCs. Anc80-*Ikzf2*(-) IHC (n=34) vs. Anc80-*Ikzf2*(+) IHC (n=40) FDR= 4.89E-06. Anc80-*Ikzf2*(-) OHC (n=132) vs. Anc80-*Ikzf2*(+) OHC (n=148) FDR= 6.88E-08 (Kruskal-Wallis test followed by post-hoc pairwise Wilcoxon Ranked Sum test adjusted for multiple comparisons).

See also Supplementary Tables 8-11.



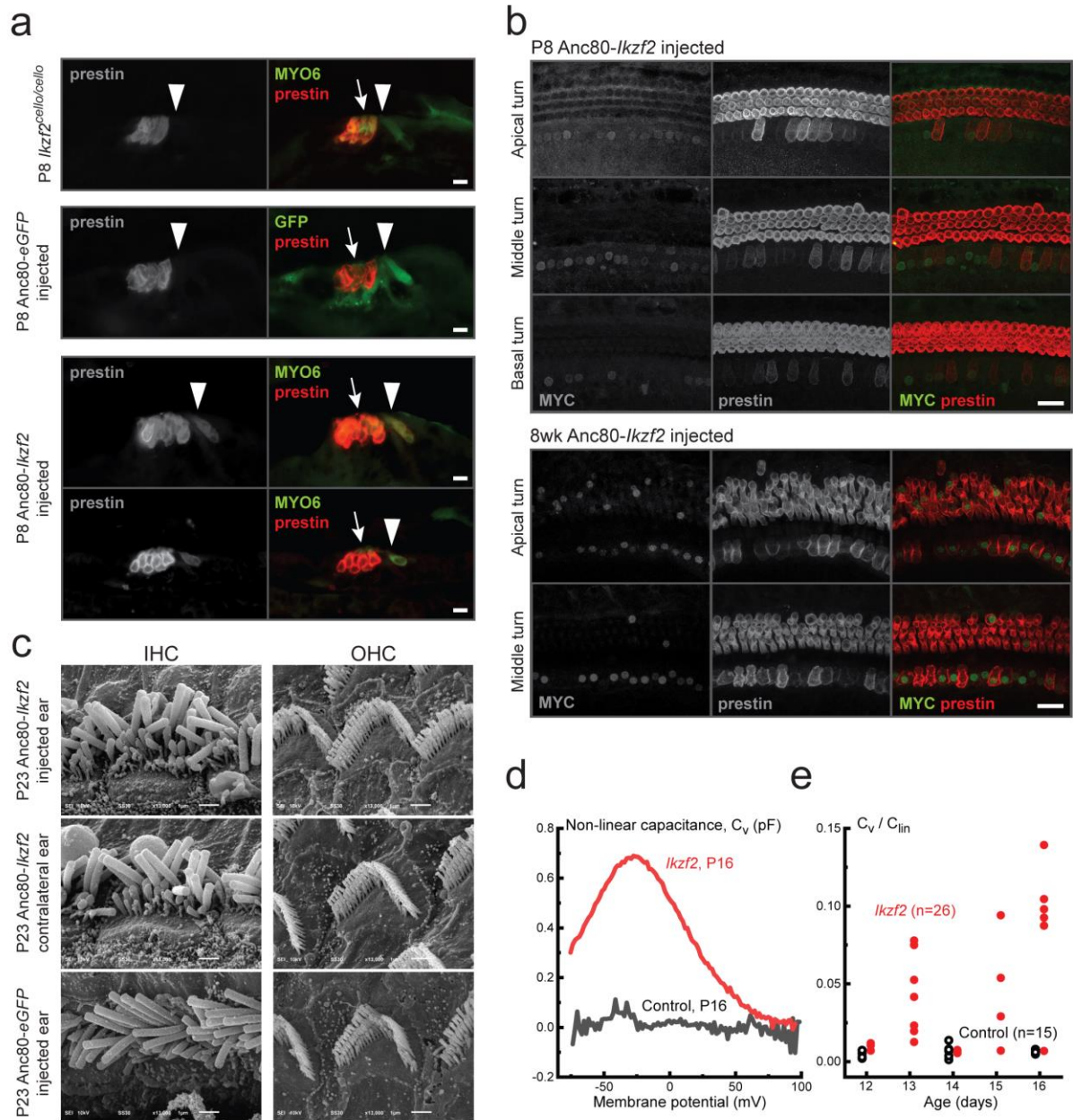
**Extended Data Figure 9. Single cell RNA-seq allows for high-resolution discrimination of cell types and their transcriptional changes due to overexpression of *Ikzf2*/helios.** (a) Custom annotation strategy with theoretical reads mapping to unambiguous regions of the various custom viral loci, as well as those regions that get discarded because of endogenous sequence similarity (i.e. ambiguous reads). (b) Violin plots of the overall scRNA-seq detection metrics, including number of unique molecules detected in each of the major cell type cluster identified (low Anc80-*Ikzf2* expressing IHCs: vIk- IHCs n=34; low Anc80-*Ikzf2* expressing OHCs: vIk- OHCs n=132;

high *Anc80-Ikzf2* expressing IHCs: vIk+ IHCs n=40; high *Anc80-Ikzf2* expressing OHCs: vIk+ OHCs n=140; and non-HCs: NonHCs n=219).

(c) FeaturePlots with red showing higher expression across all profiled cells, including cells identified as non-HCs. Expression from loci captured with custom annotation shown to support cluster identification. A final labeled tSNE plot shows all cells profiled clustered by predicted cell type. (Misc: Cells from all miscellaneous clusters with fewer than 5 cells, NSC: Non-Sensory Epithelial Cell, SC: Organ of Corti Supporting Cell, and other clusters defined by the highest differentially expressed marker gene).

(d) Pearson correlation scatter plots for selected genes within all profiled HCs, HCs from the *Anc80-eGFP* sample, or IHCs from the *Anc80-Ikzf2* sample.

(e) A Pearson correlation heatmap of all HCs detected showing overall transcriptional similarities between the non-transduced IHCs and OHCs, along with the *Anc80-Ikzf2* transduced IHCs and OHCs.



**Extended Data Figure 10: Helios overexpression induces prestin expression and electromotility in IHCs but does not affect hair bundle morphology.**

(a) The OHC electromotility protein prestin is expressed in the OHCs of *Ikrzf2<sup>cello/cello</sup>* mutants (n=6 biologically independent samples). Additionally, the pattern of prestin expression is not affected by Anc80-*eGFP* transduction, but is induced in Anc80-*Ikrzf2* transduced IHCs (n=3 biologically independent samples per condition). Scale=10  $\mu$ m

(b) Expression of prestin can be seen in Anc80-*Ikrzf2* transduced IHCs as early as P8, and up to 8-weeks of age and overlaps with MYC staining (n=6 biologically independent samples at P8, n=3 biologically independent samples at 6-8 weeks). Scale = 20  $\mu$ m.

(c) Scanning electron micrographs of IHC and OHC stereocilia bundles of Anc80-*Ikrzf2* and Anc80-*eGFP* injected mice at P23 showing expected bundle patterning. Images are from the mid – basal region of the cochlear spiral. Scale=1  $\mu$ m. Number of biologically independent samples (P16-P23): Anc80-*Ikrzf2* injected cochlea n=8, Anc80-*Ikrzf2* contralateral cochlea n=6, Anc80-*GFP* injected cochlea n=3.

(d) Representative traces of the voltage-dependent (non-linear) component of the membrane capacitance (an electrical “signature” of electromotility) in the IHCs of *Anc80-Ikzf2* injected mouse (red) and its non-injected littermate (black). Mice were injected with *Anc80-Ikzf2* at P2 and recorded at P16.

(e) Normalized maximal non-linear capacitance in all recorded IHCs of mice injected with *Anc80-Ikzf2* at P2 (red) at different ages after injection and their non-injected littermates (black). Each symbol represents one biologically independent cell, the total number of cells is indicated in parentheses. Since *Anc80-Ikzf2* transduction is not 100% efficient in the apical turn of the cochlea at the time points tested, some IHCs of *Anc80-Ikzf2* injected mice do not show prominent non-linear capacitance while the other IHCs do. In the IHCs with maximal non-linear capacitance of more than 0.25 pF (due to presumable *Ikzf2* expression), the parameters of the Boltzmann fit were as following (Mean±SEM):  $Q_{max} = 0.10 \pm 0.02$  pC;  $V_{pk} = -31 \pm 1$  mV;  $z = 0.91 \pm 0.02$ ;  $C_{lin} = 11.7 \pm 1.2$  pF;  $\Delta C_{sa} = 0.14 \pm 0.07$  pF (n=12). For information on the fitting procedure, see methods.

### Extended Data References

47. Corns, L. F., Johnson, S. L., Kros, C. J. & Marcotti, W. Calcium entry into stereocilia drives adaptation of the mechano-electrical transducer current of mammalian cochlear hair cells. *Proc. Natl. Acad. Sci.* **111**, 14918–14923 (2014).

RESEARCH

Open Access



# The impact of biological sex on the response to noise and otoprotective therapies against acoustic injury in mice

Béatrice Milon<sup>1</sup>, Sunayana Mitra<sup>1</sup>, Yang Song<sup>2</sup>, Zachary Margulies<sup>1</sup>, Ryan Casserly<sup>1</sup>, Virginia Drake<sup>1</sup>, Jessica A. Mong<sup>3</sup>, Didier A. Depireux<sup>1,4</sup> and Ronna Hertzano<sup>1,2,5\*</sup>

## Abstract

**Background:** Noise-induced hearing loss (NIHL) is the most prevalent form of acquired hearing loss and affects about 40 million US adults. Among the suggested therapeutics tested in rodents, suberoylanilide hydroxamic acid (SAHA) has been shown to be otoprotective from NIHL; however, these results were limited to male mice.

**Methods:** Here we tested the effect of SAHA on the hearing of 10-week-old B6CBAF1/J mice of both sexes, which were exposed to 2 h of octave-band noise (101 dB SPL centered at 11.3 kHz). Hearing was assessed by measuring auditory brainstem responses (ABR) at 8, 16, 24, and 32 kHz, 1 week before, as well as at 24 h and 15–21 days following exposure (baseline, compound threshold shift (CTS) and permanent threshold shift (PTS), respectively), followed by histologic analyses.

**Results:** We found significant differences in the CTS and PTS of the control (vehicle injected) mice to noise, where females had a significantly smaller CTS at 16 and 24 kHz ( $p < 0.0001$ ) and PTS at 16, 24, and 32 kHz (16 and 24 kHz  $p < 0.001$ , 32 kHz  $p < 0.01$ ). This sexual dimorphic effect could not be explained by a differential loss of sensory cells or synapses but was reflected in the amplitude and amplitude progression of wave I of the ABR, which correlates with outer hair cell (OHC) function. Finally, the frequency of the protective effect of SAHA differed significantly between males (PTS, 24 kHz,  $p = 0.002$ ) and females (PTS, 16 kHz,  $p = 0.003$ ), and the magnitude of the protection was smaller in females than in males. Importantly, the magnitude of the protection by SAHA was smaller than the effect of sex as a biological factor in the vehicle-injected mice.

**Conclusions:** These results indicate that female mice are significantly protected from NIHL in comparison to males and that therapeutics for NIHL may have a different effect in males and females. The data highlight the importance of analyzing NIHL experiments from males and females, separately. Finally, these data also raise the possibility of effectors in the estrogen signaling pathway as novel therapeutics for NIHL.

**Keywords:** Noise-induced hearing loss, Sex differences, SAHA, B6CBAF1/J mice, Inner ear, ABR

## Background

Noise-induced hearing loss (NIHL) is a form of an acquired hearing deficit that underlies 16% of adult sensorineural hearing loss worldwide [1]. In the US adult population, NIHL is second only to age-related hearing loss (ARHL) [2]. NIHL as an occupational hazard is widespread in the

military, construction, agriculture, and in other fields with high noise exposure, causing hearing loss in 7–21% of the exposed population [3]. Health problems secondary to noise exposure are particularly frequent in the military. In the USA, hearing loss and tinnitus rank as the most prevalent service-connected disabilities for veterans [4]. Untreated hearing loss adversely impacts social, psychological, and cognitive functioning of affected individuals [5].

Small animal models such as the guinea pig, gerbil, chinchilla, mouse, and ferrets are commonly used to conduct auditory research and, in particular, studies on

\* Correspondence: [rhertzano@som.umaryland.edu](mailto:rhertzano@som.umaryland.edu)

<sup>1</sup>Department of Otorhinolaryngology - Head and Neck Surgery, University of Maryland, 16 South Eutaw Street, Suite 500, Baltimore, MD 21201, USA

<sup>2</sup>Institute for Genome Science, University of Maryland School of Medicine, Baltimore, MD 21201, USA

Full list of author information is available at the end of the article

NIHL [6–8]. Mouse models have proven especially useful because of the ease in generating inbred strains with low genetic variability, the ability to manipulate the mouse genome, as well as structural, molecular and functional similarity to the human ear [9–11]. The current study stemmed from research that was designed to analyze the molecular mechanism of action of drugs with a protective effect from NIHL. Suberoylanilide hydroxamic acid (SAHA) is a histone deacetylase inhibitor and thus functions through modulating gene expression by changing the accessibility of the DNA to transcription factors [12, 13]. SAHA has been shown to be protective against hearing loss caused by exposure to chemicals/medications (ototoxic hearing loss) *in vivo* in mice of both sexes [12] as well as from NIHL in male mice [14]. Little is known, however, about the differential responses of male and female mice to noise and its potential therapeutics as historically most studies of acquired hearing loss using animal model were performed exclusively on males [14–19]. This is in part because the fluctuating hormone levels during an estrous cycle could introduce a confounding variable in the response to trauma or treatment [20]. Of relevance, sex differences have been described in age-related hearing loss (presbycusis) as well as in NIHL, where pre-menopausal women are protected in comparison to age-matched men [21, 22].

Here we initially tested the efficacy of SAHA as a protective agent from NIHL in young adult B6CBAF1/J mice of both sexes. We exposed mice of both sexes, who were treated with SAHA or its carrier, DMSO, to a permanent threshold-shift inducing noise exposure. We compared hearing function by analysis of auditory brainstem responses, and histological outcomes of the noise exposures by inner and outer hair cell counts and inner hair cell synapse analysis. Our results indicate a differential response to both noise and SAHA treatment between sexes, where female mice exhibit less hearing loss following noise (i.e., less damage) and have less therapeutic benefit from SAHA, when compared to males. Interestingly, the effect of sex on the degree of hearing loss following noise exposure was greater than the effect of the tested drug. This is the first detailed report comparing and characterizing such differences between sexes.

## Methods

### Animals

All procedures involving animals were carried out in accordance with the National Institutes of Health Guide for the Care and Use of Laboratory Animals and were approved by the Animal Care Committee at the University of Maryland (protocol numbers 0915006 and 1015003) and the Animal Care and Use Review Office (Department of Defense, USA).

All experiments were performed on B6CBAF1/J mice (Stock No: 100011, Jackson Laboratories, ME). We use B6CBAF1/J mice, which are F1 progeny of a cross between C57BL/6J and CBA/J (CBA) for most of our experiments for NIHL. We choose this combination of strains because, while the C57BL/6 mice are used extensively to generate transgenic animals for auditory research owing to availability of its complete genome information [23], long life span and resistance to sound induced seizures [24, 25]; C57BL/6 mice also suffer from early onset age-related hearing loss (ARHL) due to recessively inherited mutation in the *Cdh23* gene [26] underlying the *Ahl* locus [27]. In contrast, the CBA strain is relatively resistant to ARHL [28]. The B6CBAF1/J mice therefore enable the use of Cre-lines (originating from C57BL/6 mice) and have been previously used and characterized in studies of NIHL [29]. Mice were obtained at 7–8 weeks of age and kept in our facility 1–2 weeks for acclimatization before any procedures. The facility is controlled for temperature and humidity, has a 12h light/12 h dark cycle (lights on at 6 am), and mice were provided with food and water *ad libitum*.

### Study design

The experiment consisted of two separate cohorts of animals, to ascertain reproducibility of data. Each cohort consisted of (a) three male and three female mice that were not exposed to noise and used only for histology, (b) six or eight mice from each sex that were all exposed to noise and treated with SAHA, and (c) six or eight mice from each sex that were all exposed to noise and treated with vehicle (DMSO). Noise exposures were performed on 3 to 4 mice at a time, which consisted of a mixture of mice that were treated with either SAHA or DMSO. The phase of the estrus cycle was not recorded for the female mice. One male in the DMSO group was removed from all analyses because it did not present a threshold shift at 24 h after noise exposure. A second person who was blinded with respect to the animal groups determined the ABR thresholds and counted outer hair cells and synapses.

### Noise trauma

All noise exposures were performed on mice at 10 weeks of age. Noise trauma was induced with a 2-h duration, octave band of noise centered at 11.3 kHz (8–16 kHz) at 101 dB sound pressure level (SPL) using the Fostex FT17H tweeter [30] (Fostex, Tokyo, Japan). Output stimuli were calibrated with a measurement microphone (PCB Piezoelectronics, NY) placed at the same distance as the mouse ears. Mice were placed in a custom-made animal holder made of a perforated aluminum sheet, 18 × 15 × 5 cm in size with eight equal-sized chambers

measuring  $4.5 \times 7.5 \times 5$  cm, which was itself placed in a soundproof box (IAC Acoustics, IL). Only the four center chambers immediately inferior to the speaker were used to house mice during the noise exposures. Sound level was measured to be within 0.5 dB of the target level throughout the holding cells, with the speaker situated 20 cm above the mice. The mice were awake and unrestrained throughout the noise exposure. All mice were exposed to noise at the same time of the day (8 am) for each of the experimental groups.

#### **SAHA treatment**

Mice were injected intraperitoneally with suberoylanilide hydroxamic acid (SAHA) (Selleckchem, TX), (100 mg/kg body weight) dissolved in DMSO (MilliporeSigma, MA), or with DMSO alone (vehicle) 3 days before exposure to noise and 2 h after the end of the noise exposure. The SAHA dosing amount was based on a previous publication using SAHA as an otoprotective agent, where the authors tried different dose concentrations of SAHA and reported a 100 mg/kg dose to be most efficacious without cytotoxicity [12]. Because studies vary in their dosing regimen for SAHA, the frequency of the dosing was based on the published literature with minor modifications [14, 31].

#### **Determination of auditory brainstem response**

Auditory brainstem responses (ABR) were recorded after induction of anesthesia using an intraperitoneal injection of a mixture of ketamine (100 mg/kg) (VetOne, ID) and xylazine (20 mg/kg) (Anased, IL). Hearing thresholds were determined at 8, 16, 24, and 32 kHz using the RZ6 recording system (Tucker-Davis Technologies, FL). Recording electrodes were inserted under the skin at the inferior post-auricular area of the left and right ears, and a reference was placed under the skin at the vertex region of the skull. A ground electrode was inserted near the base of the tail. The animals were placed in a soundproof box (IAC Acoustics, IL) for the recordings. Stimuli were presented via a speaker situated in front of the mouse, 10 cm from the ears. Frequency-specific tone bursts 2.5 ms long, with a 0.5 ms sinusoidal on and off ramp, were presented to the mice at varying intensities beginning at 90 dB SPL and proceeding in 5 dB decrements down to 10 dB below the measurable hearing threshold for each mouse. Output stimuli were calibrated with a one-quarter inch microphone (model PCB-378C01; PCB Piezotronics, NY) placed at the same distance from the speaker as the mouse ears would be. Electrophysiological signals in response to each tone stimulus were recorded for 10 ms starting at the onset of the tone. A total of 512 sweeps were presented at the rate of 21 sweeps/s, and responses were averaged at each level and frequency tested. Responses from both ears

were recorded simultaneously and used for data acquisition [32]. Hearing thresholds were determined as the lowest level at which definite ABR waves I and II response patterns could be identified for each frequency. Importantly, wave I and II of the ABR are generated from the contributions of the uncrossed fibers of spiral ganglion and cochlear nucleus, respectively. This allowed for hearing thresholds to be determined from both ears simultaneously, with each ear considered a separate data point. The results section shows the data with each ear counting as an individual biological replicate because both ears were exposed to noise and thresholds were obtained from the two ears separately, as previously described [33, 34]. In addition, the supplementary data reports the hearing threshold results where the thresholds from both ears of each mouse are averaged and each mouse is counted as an individual biological sample. Body temperature of the animals was maintained constant at 37.0 °C by a feedback heating pad placed under the animal while recording (FHC, ME). Baseline ABR thresholds were determined 1 week prior to noise exposure when the mice were 9 weeks of age. After the noise exposure, ABR thresholds were recorded at 24 h, 8 days, and 15 to 21 days, corresponding to 10–13 weeks of age. These permitted measurement of the compound threshold shift (CTS) as well as permanent threshold shift (PTS), respectively [35].

#### **ABR wave I amplitude growth as a function of sound level**

Peak-to-trough amplitude values of wave I of the ABR traces were extracted using a custom MatLab (MathWorks, MA) script (Additional file 1). Briefly, the script extracted the first maximum deflection after the first millisecond (ms) of the recording (peak I) and the corresponding subsequent minimum deflection (trough I). Wave I peak-to-trough amplitudes were obtained for stimuli levels ranging from 55 dB SPL to 85 dB SPL for ABR recorded before and after noise exposure. In noise-exposed animals, the minimum hearing threshold averaged around 55 dB at 24 h. Thus, the linear regressions were performed setting the minimal value to 55 dB to allow for the comparison of data from all time points. Additionally, the data between these level ranges are linear for most of the level versus amplitude plot, allowing for the accurate calculation of the slope. The data were plotted to obtain the growth of amplitude as a function of sound level for each experimental group at 16 kHz, which was the frequency with the maximal permanent threshold shift. Linear regression analyses were performed using the Prism 7 software (GraphPad, CA) to obtain slope values. The slopes were compared between conditions at each frequency analyzed. Slopes were considered significantly different if  $p < 0.05$  calculated by a two-tailed paired  $t$  test [36].

### Immunostaining

Within 1 week of the final ABR recording, mice were euthanized by CO<sub>2</sub> asphyxiation followed by cervical dislocation. Immediately after euthanasia, the temporal bones were dissected in ice-cold phosphate-buffered saline (PBS) (Corning, MA), a small hole was made in the bony apex of the cochlea, and the round and oval windows were opened for subsequent perfusion of the fixative. The temporal bones were fixed overnight at 4 °C in 4% paraformaldehyde (Alfa Aesar, MA) solution in PBS and then decalcified by immersion in 500 mM EDTA at 4 °C until adequate decalcification. Each cochlear duct was dissected according to the method described by the Eaton-Peabody Laboratories [37]. Briefly, each cochlear duct was first bisected across the oval window. The resulting halves were further dissected to obtain the apical turn of the basilar membrane as a single piece, the middle turn and the basal turns in two halves as well as the basal hook as a final piece, exposing the organ of Corti in its entirety. The tissue was permeabilized for 1 h in PBST ((PBS (CorningCellgro, VA) with 0.3% Triton X-100 (MiliporeSigma, MA)) and blocked for 1 h in PBST with 5% normal goat serum (Cell Signaling Technologies, MA) at room temperature.

For pre-synaptic ribbon and post-synaptic density staining, cochlear segments were incubated overnight at 37 °C with a monoclonal mouse anti-CtBP2 antibody (1:200, BD Biosciences, CA) and a monoclonal mouse anti-GluR2 antibody (1:2000, MiliporeSigma), diluted in blocking buffer. Labeling was performed by incubating the tissue with the corresponding secondary antibodies, goat anti-mouse IgG2 Alexa Fluor® 488 and goat anti-mouse IgG1 Alexa Fluor® 568 (1:1000, ThermoFisher Scientific, MA) supplemented with DAPI (1:20,000, ThermoFisher Scientific) in PBST for 2 h at room temperature. Tissue was mounted with the ProLong Gold antifade reagent (ThermoFisher Scientific).

### Frequency-specific pre-synaptic ribbon and post-synaptic density (PSD) counts

Following immunostaining, tissue was imaged at a ×20 magnification using a Nikon Eclipse E600 fluorescence microscope (Nikon, NY) equipped with an Infinity 3 camera (Lumenera, Canada) to allow for frequency mapping. Cochlear frequencies were mapped onto the images using the Measure Line plugin, developed by the Eaton-Peabody Laboratories [38] on the software ImageJ [39]. Subsequently, confocal Z-stacks in the regions of 15 to 17 kHz, 22 to 26 kHz, and 32 kHz were obtained using a 63X oil objective, 1.2 X digital zoom, and 42 μm sections using the LSM 5 Duo confocal microscope (Zeiss). Ribbons and PSDs were counted using the ImageJ Cell Counter plugin.

### Cytochrome c

Fluorescence images of the outer hair cell nuclei counterstained with DAPI were captured using an Eclipse E600 microscope (20 X objective) (Nikon) equipped with an Infinity 3 camera (Lumenera). Cochlear frequencies were mapped as described above for the ribbon and PSD counts. Missing outer hair cells (OHCs) were counted throughout the entire length of the basilar membrane from the apex towards the base at the following frequency intervals: 4–5.6 kHz, 5.6–8 kHz, 8–11.3 kHz, 11.3–16 kHz, 16–22.6 kHz, 22.6–32 kHz, 32–45.2 kHz, 45.2–51 kHz, and 51–55 kHz. These counts were expressed as the percentage of missing OHCs with respect to their position along the length of the basilar membrane.

### Statistical analysis

The ABR data comparisons between groups were made by a two-way ANOVA followed by a Tukey post hoc test for multiple pair-wise comparisons [40]. ABR data comparing threshold shifts within a group before and after noise exposure were analyzed by a two-way ANOVA with Sidak's post hoc test for multiple comparisons. An adjusted *p* value of < 0.05 was set as the threshold for significance. The *F* values for main effects are listed in the main text, and the interactions are listed in Additional file 2. The value of Cohen's *d* (*d*) was calculated when the data reach significance following the post hoc test. All ABR data analyses and figures were generated using Prism 7 software (GraphPad, CA) with the recommended settings for post hoc tests.

For the ABR wave I amplitude analysis, the growth of the amplitude as a function of stimuli levels was expressed as a slope, obtained by linear regression of amplitude versus stimuli level plots from noise-exposed animals (DMSO treated) of each sex, before and after noise exposure, at 16 kHz. Two-tailed *t* test was used to compare the slopes between groups using Prism 7 software (GraphPad, CA).

Comparisons of OHCs and synapse counts between male and female mice were made using Student's *t* test assuming unequal variance using Prism 7 software (GraphPad, CA).

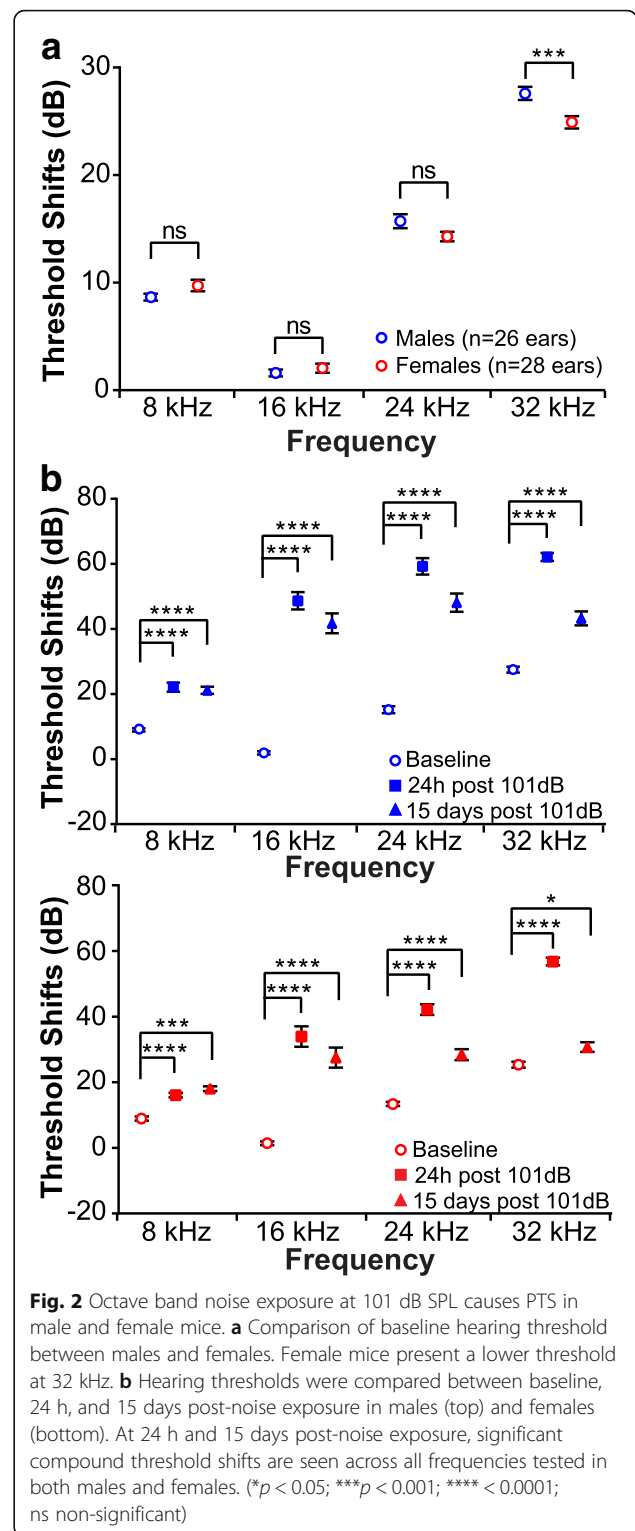
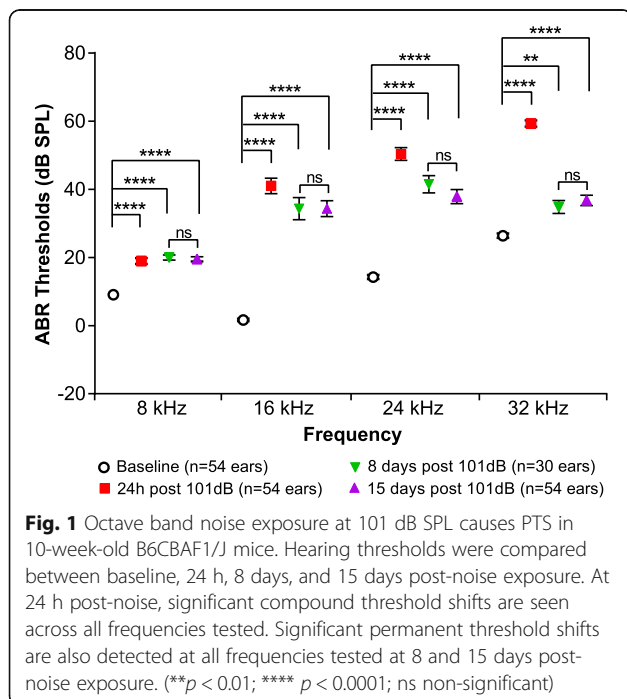
## Results

### Differential response of male and female mice to noise trauma

In the present study, 10-week-old male and female mice were exposed to 101 dB SPL octave band noise centered at around 11.3 kHz, for 2 h. The mice received either SAHA (100 mg/kg) dissolved in DMSO, or DMSO alone as a control (vehicle) 3 days before and 2 h after the end of noise exposure. Hearing thresholds were measured using ABRs at 8, 16, 24, and 32 kHz. Thresholds measured

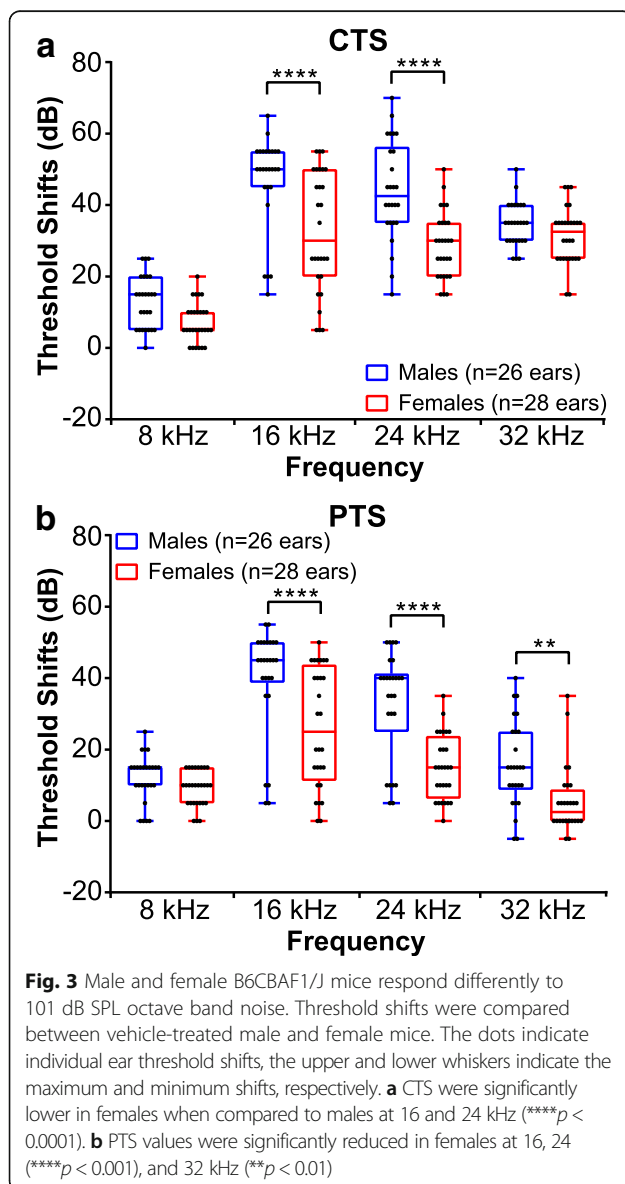
at 24 h, 8 days, and 15 days after noise exposure were compared to the baseline thresholds to calculate the compound (24 h) and permanent (8 and 15 days) threshold shifts, respectively (CTS and PTS) [35]. The CTS reflects the change in hearing threshold shortly following noise exposure, which is normally higher than the final change in hearing threshold, whereas the PTS reflects what is considered a “final” change in hearing threshold following noise exposure [35]. In vehicle-treated mice, a two-way ANOVA revealed main effects of frequency and time on the hearing thresholds (frequency:  $F_{3, 752} = 155.1$ ;  $p < 0.0001$ ; time:  $F_{3, 752} = 284$ ;  $p < 0.0001$ ). A post hoc comparison showed that the noise exposure induced a significant CTS and PTS at all frequencies measured (Fig. 1). In addition, there were no statistically significant differences in the hearing thresholds at 8 and 15 days post-exposure; therefore, subsequent measures for PTS are reported at 15 days only (Fig. 1).

To test whether male and female mice have a differential response to noise, we first compared baselines in males and females to rule out a possible difference in hearing thresholds before noise exposure (Fig. 2a and Additional file 2: Table S1). A two-way ANOVA followed by a post hoc analysis detected a small but significant lower threshold in females at 32 kHz ( $p = 0.0008$ ;  $d = 0.357$ ) but not at 8, 16, and 24 kHz. We next assessed the CTS and PTS for each sex separately (Fig. 2b and Additional file 2: Table S2). Similar to the results obtained with both sexes combined, males and females had



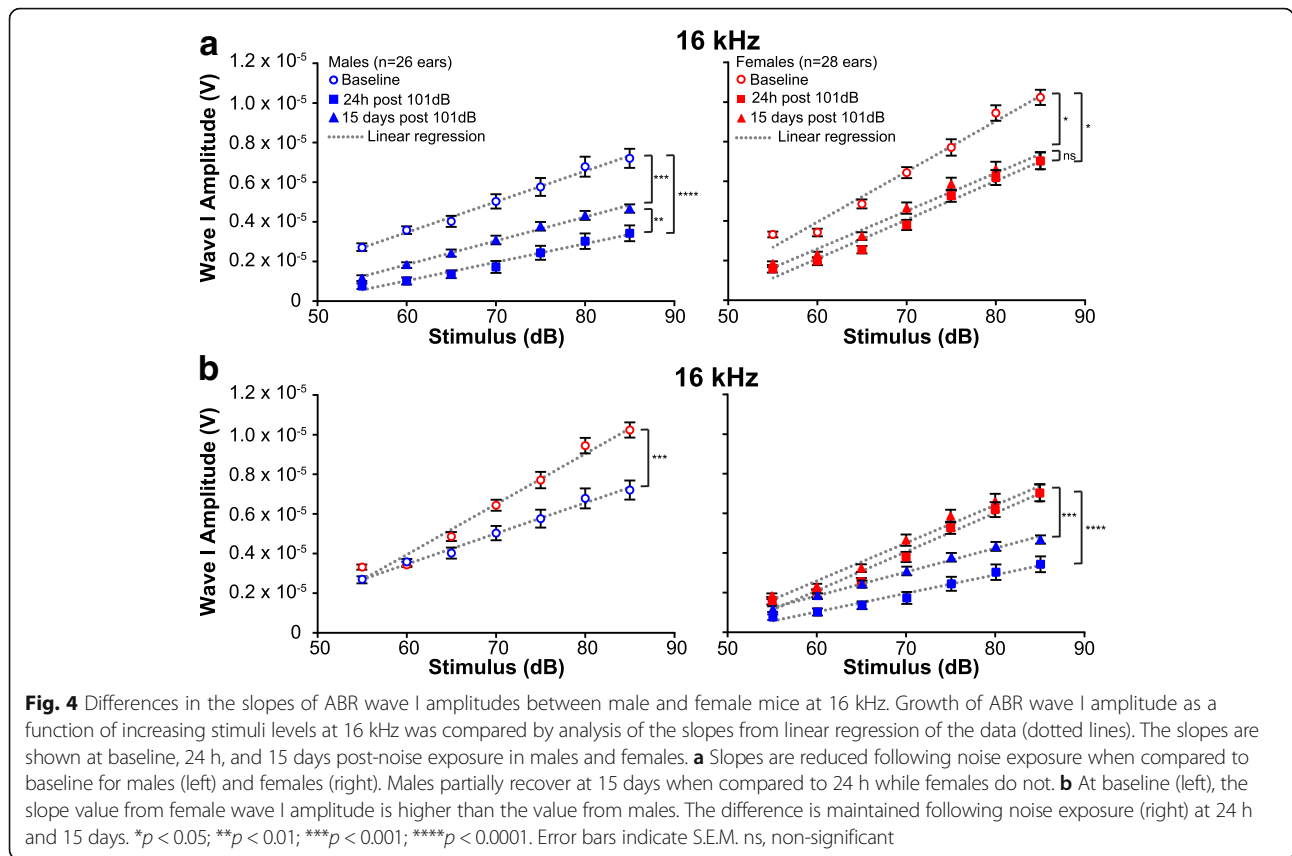
significant CTS and PTS at all frequencies measured when compared to pre-noise baseline. However, when male and female threshold shifts following noise exposure were compared to each other, a two-way ANOVA revealed main effects of frequency and sex on both CTS

(frequency:  $F_{3, 208} = 84.84$ ;  $p < 0.0001$ ; sex:  $F_{1, 208} = 43.41$ ;  $p < 0.0001$ ) and PTS (frequency:  $F_{3, 208} = 47.46$ ;  $p < 0.0001$ ; sex:  $F_{1, 208} = 49.58$ ;  $p < 0.0001$ ) (Fig. 3 and Additional file 2: Table S3). A *post hoc* comparison revealed that 24 h after noise exposure, females have a significantly lower CTS at 16 and 24 kHz ( $p < 0.0001$  for both frequencies;  $d = 0.676$  for 16 kHz and  $d = 0.727$  for 24 kHz) compared to males (Fig. 3 and Additional file 2: Table S4). This difference is extended to the 32 kHz frequency as well 15 days post-noise exposure ( $p < 0.0001$  for 16 and 24 kHz;  $p = 0.005$  for 32 kHz;  $d = 0.598$  for 16 kHz,  $d = 0.779$  for 24 kHz, and  $d = 0.453$  for 32 kHz). These data suggest that females have a less severe hearing loss following noise exposure compared to males.



### Effect of noise on ABR wave I amplitude in male and female mice

The cochlea has two types of sensory cells—inner hair cells (IHC) and outer hair cells (OHC). The OHC function primarily as signal amplifiers, whereas the IHC receive primarily afferent innervation and are the main source of auditory sensory input to the brain [41]. The ABR wave I amplitude is primarily a reflection of the frequency-specific activity at the spiral ganglion (SG), which is the ganglion that houses the cell bodies of the afferent neurons that come in contact mainly with the IHC. This activity is a compound of the levels of IHC and OHC activity (as IHC activity is influenced by OHC function), the number of active auditory nerve fibers present, functional synapses, as well as the endocochlear potential [17, 42]. To assess whether the difference in the male and female response to noise correlates with a difference in the synchronous activity at the SG, the increase in ABR wave I amplitude as a function of increasing sound level was measured in the vehicle-treated noise-exposed mice. A change in amplitude can result from changes in any of the factors that contribute to wave I. We analyzed wave I amplitude at the frequency with the maximal threshold shift, which was 16 kHz in this study. Average peak-to-trough wave I amplitudes were extracted for stimuli levels 55 dB to 85 dB for each animal at baseline (prior to noise exposure), 24 h, and 15 days post-noise exposure. A change in the slope of the amplitude as a function of sound level would most likely reflect a change in active processes in the cochlea, primarily attributed to OHC function [43, 44]. (Fig. 4). A linear regression analysis showed a decrease in the slope 24 h post-noise exposure for both males and females. At baseline, males had an average slope of  $155 \pm 6$  nV/dB, while at 24 h post-noise exposure, this slope significantly decreased to  $93 \pm 6$  nV/dB ( $p < 0.0001$ ) (Fig. 4a). The average slope at baseline for females was  $255 \pm 16$  nV/dB as compared to  $196 \pm 14$  nV/dB for 24 h post-noise exposure ( $p = 0.0022$ ) (Fig. 4a). At 15 days post-noise exposure, the slope value partially recovered in males when compared to 24 h, averaging  $120 \pm 4$  nV/dB ( $p = 0.0051$ ), but remained significantly lower than baseline ( $p = 0.0008$ ) (Fig. 4a). While males recovered partially, the average slope for females at 15 days post-noise exposure was similar to the slope at 24 h with a value of  $191 \pm 13$  nV/dB ( $p = 0.7959$ ). Interestingly, when we directly compared the slopes between males and females from the same time point, a two-tailed *t* test revealed significant differences between the slopes (Fig. 4b). At baseline, females have a slope of  $255 \pm 16$  nV/dB as compared to a slope of  $155 \pm 6$  nV/dB for males ( $p = 0.0002$ ). This difference is maintained after noise exposure at 24 h and 15 days (Fig. 4b). Comparison of the absolute amplitude of wave I at 85 dB SPL shows permanent lower



amplitude in the males compared with the female mice (Fig. 4b and Table 1).

**Effect of noise on OHC loss**

To identify possible causes for the differential response to noise between male and female mice, we performed cytochrome c oxidase II (COX II) immunohistochemistry to compare hair cell loss throughout the cochlear duct (up to a frequency position corresponding to 55 kHz) (Additional file 3). For unexposed controls, we used strain (B6CBAF1/J) and age-matched (12 weeks old) mice. As expected, 12-week-old control mice (males and females) showed little to no OHC loss along the organ of Corti (0 to 0.34% loss) (Table 2 and Additional file 4). Similarly, 2 weeks following a 101 dB noise exposure, there was no significant OHC loss (less

than 1%) in either sex up to 32 kHz (Fig. 5). While an OHC loss was measured at 32–55 kHz (Table 2 and Additional file 4), no sex-specific differences were measured with respect to OHC loss (Table 2, Additional file 4 and Additional file 2: Table S5). These results suggest that the sex difference seen in response to noise exposure is not explained by a divergence in OHC loss in males and females. Interestingly, the pattern of OHC loss seen in noise-exposed animals does not match the frequency-specific PTS. The cochlea is organized such that high-frequency sounds are sensed at the base of the organ, close to the “entry of sound,” and low-frequency sounds at the apex (also known as a tonotopic organization) [45]. While the highest PTS is measured at 16 and 24 kHz, only minimal OHC loss is observed around these frequencies (Table 2 and Additional file 4). Therefore, our data indicate that the OHC loss at the 16 and the 24 kHz location is not sufficient to explain the PTS at these frequencies when measured 15 days post-noise exposure.

**Effect of noise trauma on IHC synapses**

Our data indicate that 2 weeks after noise exposure, at a time a PTS is already obtained, the OHC loss does not account for either the significant PTS at 16 and 24 kHz or the sex differences observed in the PTS and wave I

**Table 1** Values for the wave I absolute amplitudes at 85 dB SPL

	Wave I amplitudes at a 85 dB stimulus (volt)		
	Baseline	24 h post 101 dB	15 days post 101 dB
Males	$7.21 \times 10^{-6}$	$3.42 \times 10^{-6}$	$4.67 \times 10^{-6}$
Females	$10.2 \times 10^{-6}$	$7.04 \times 10^{-6}$	$7.04 \times 10^{-6}$
<i>p</i> value	< 0.0001	< 0.0001	< 0.0001
<i>d</i> value	1.380	1.719	1.317

Females have a higher amplitude at baseline, 24 h, and 15 days post-noise exposure (unpaired *t* test)

**Table 2** Values for the percentage of OHC loss within nine frequency ranges measured

		OHC loss by frequency range								
		4–5.6 kHz	5.6–8 kHz	8–11.3 kHz	11.3–16 kHz	16–22.6 kHz	22.6–32 kHz	32–45.2 kHz	45.2–51 kHz	51–55 kHz
Controls	Males	0.12 ± 0.12	0.23 ± 0.23	0.34 ± 0.21	0.03 ± 0.03	0.26 ± 0.16	0.23 ± 0.08	0.29 ± 0.10	0.34 ± 0.34	0.15 ± 0.15
	Females	0.00 ± 0.00	0.13 ± 0.09	0.06 ± 0.06	0.09 ± 0.06	0.07 ± 0.05	0.10 ± 0.07	0.18 ± 0.12	0.00 ± 0.00	0.18 ± 0.18
DMSO + noise	Males	0.29 ± 0.20	0.23 ± 0.12	0.16 ± 0.08	0.15 ± 0.05	0.22 ± 0.07	0.77 ± 0.23	4.76 ± 1.17	21.8 ± 4.57	45.7 ± 10.3
	Females	0.00 ± 0.00	0.02 ± 0.02	0.20 ± 0.08	0.10 ± 0.06	0.35 ± 0.11	0.43 ± 0.16	5.36 ± 2.32	22.4 ± 7.73	45.3 ± 14.2

Progressive OHC loss is seen beginning from 32 kHz. Both male and female animals show a similar pattern of OHC loss. ± represent S.E.M

amplitude progression. Loss of IHC functional synapses has been shown to account for the decrease in wave I amplitude following lower intensity noise exposures, a phenomenon also known as cochlear synaptopathy [46]. We therefore focused our analysis on the IHC synapses. We first quantified the number of pre-synaptic ribbons in the IHCs. For this purpose, whole mount cochleae were fluorescently immunolabeled with an antibody directed against CtBP2 to visualize the pre-synaptic ribbons. Pre-synaptic ribbons were counted on Z-stacks created from confocal sections in the regions of 16, 24, and 32 kHz (Additional file 5). In the region where the maximal threshold shift is detected (16 kHz location),

no significant change in the pre-synaptic ribbons was recorded following noise in either sex (Table 3 and Additional file 6). However, a significant decrease in the pre-synaptic ribbons per IHC was observed in the region of 24 and 32 kHz in both male and female mice (Table 3 and Additional file 6). Interestingly, no difference was detected between males and females at the three frequencies analyzed in either the controls or noise-exposed animals ( $p > 0.05$ ), suggesting that the change in pre-synaptic ribbons does not account for the sex differences in hearing following noise exposure.

Recent evidence suggests that noise exposure reduces the number of active IHC synapses by inducing the

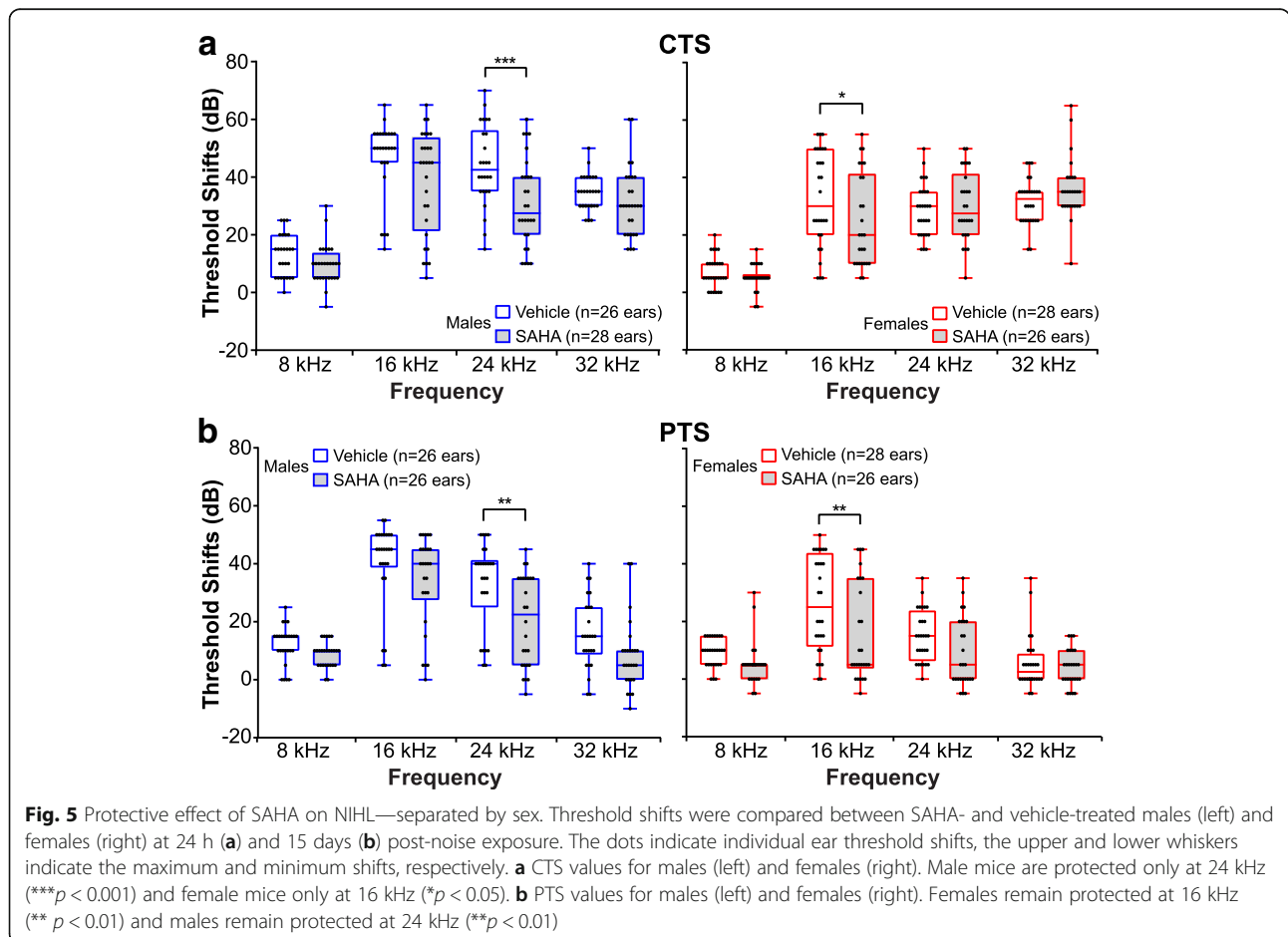


**Fig. 5** Protective effect of SAHA on NIHL—separated by sex. Threshold shifts were compared between SAHA- and vehicle-treated males (left) and females (right) at 24 h (a) and 15 days (b) post-noise exposure. The dots indicate individual ear threshold shifts, the upper and lower whiskers indicate the maximum and minimum shifts, respectively. **a** CTS values for males (left) and females (right). Male mice are protected only at 24 kHz ( $***p < 0.001$ ) and female mice only at 16 kHz ( $*p < 0.05$ ). **b** PTS values for males (left) and females (right). Females remain protected at 16 kHz ( $**p < 0.01$ ) and males remain protected at 24 kHz ( $**p < 0.01$ )

**Table 3** Pre-synaptic ribbon counts per IHC in the 16, 24 and 32 kHz regions in male and female mice

	Total IHC ribbons								
	16 kHz location			24 kHz location			32 kHz location		
	Males	Female	<i>p</i> value	Males	Females	<i>p</i> value	Males	Females	<i>p</i> value
Controls	15.00 ± 0.72	15.86 ± 0.53	0.34	16.16 ± 0.78	15.85 ± 0.61	0.76	15.60 ± 0.98	13.78 ± 0.92	0.20
DMSO + Noise	15.25 ± 0.86	14.60 ± 0.87	0.60	11.38 ± 0.74	11.95 ± 0.95	0.64	7.65 ± 0.88	8.11 ± 0.78	0.71

± represent S.E.M. (unpaired *t* test to compare males versus females)

retraction of some of the neurons that come in contact with the IHC. Shortly after noise exposure, while the synaptic ribbons may persist, loss of neuronal contact can be identified by loss of post-synaptic densities [47]. We therefore analyzed the number of pre-synaptic ribbons paired with post-synaptic glutamate receptor (GluR2) to determine if the different response to noise exposure between male and female mice can be attributed to the number of active synapses (Additional file 5). Similar to pre-synaptic ribbons, noise exposure induced a significant decrease in the number of active synapses at the regions of 24 and 32 kHz but not 16 kHz. However, again, there was no sexual dimorphism in the number of active synapses (Table 4 and Additional file 6). These data indicate that the noise-induced synaptopathy is not the main underlying cause for the PTS seen at 16 kHz, which is the frequency with the maximal threshold shift, and is not the culprit of the sexual dimorphism in the response to noise.

#### Sex influences the measured effect of SAHA treatment on mice exposed to noise

To date, most studies on noise exposure and its treatments were performed on male mice only or mice of both sexes combined. Because our data show a differential response to noise between male and female mice, we next explored whether sex influences the measured response to treatment. This is important for proper testing of therapeutics. To determine whether SAHA has a protective effect from noise exposure, CTS (Fig. 5a) and PTS values (Fig. 5b) were compared between vehicle and SAHA-treated animals. A two-way ANOVA revealed main effects of SAHA and sex on CTS at 8, 16, and 24 kHz (Table 5 and Additional file 2: Table S3). Main effects of SAHA and sex 15 days post-noise exposure is significant at all frequencies tested (Table 5).

Post hoc comparisons revealed that CTS of SAHA-treated males were significantly lower at 24 kHz ( $p = 0.0006$ ;  $d = 0.536$ ) compared to vehicle-treated controls, whereas in females, CTS values were significantly lower at 16 kHz ( $p = 0.04$ ;  $d = 0.359$ ) (Fig. 5a, Additional file 2: Table S6). Comparisons of PTS suggested that the protective effect of SAHA in male mice is maintained at 24 kHz ( $p = 0.002$ ;  $d = 0.489$ ) and at 16 kHz in female mice ( $p = 0.003$ ;  $d = 0.482$ ) compared to the vehicle-treated controls (Fig. 5b, Additional file 2: Table S6). These data indicate a difference in the response to SAHA between male and female mice.

Next, we re-analyzed the data, this time combining mice from both sexes, to assess whether this might change the measured response to treatment. A two-way ANOVA revealed significant main effects of SAHA and frequency at 24 h (SAHA:  $F_{1, 424} = 9.576$ ,  $p = 0.0021$ ; frequency:  $F_{3, 424} = 110.1$ ,  $p < 0.0001$ ) and 15 days (SAHA:  $F_{1, 416} = 22.67$ ,  $p < 0.0001$ ; frequency:  $F_{3, 416} = 57.36$ ,  $p < 0.0001$ ) post-noise exposure. Compared to vehicle-treated controls, SAHA significantly decreased the CTS only at 16 kHz ( $p = 0.0074$ ) (Fig. 6a, Additional file 2: Table S7) while a significant decrease in PTS was observed at 16 and 24 kHz ( $p = 0.0095$  and  $0.0024$ , respectively) (Fig. 6b, Additional file 2: Table S7). Thus, these findings indicate that when combining mice from both sexes, the measured response to treatment is different from the response when each sex is analyzed separately. This is critically important as it may lead to misinterpretation of biological data.

#### Discussion

The major finding reported here is the identification and characterization of a sexually dimorphic response to PTS-inducing noise exposure and its candidate therapeutics in mice. Sex is an important biological variable

**Table 4** Active synapse counts per IHC at 16, 24, and 32 kHz in male and female mice

	Active synapses								
	16 kHz location			24 kHz location			32 kHz location		
	Males	Females	<i>p</i> value	Males	Females	<i>p</i> value	Males	Females	<i>p</i> value
Control	13.26 ± 1.75	14.51 ± 2.82	0.63	14.84 ± 1.91	13.64 ± 1.11	0.60	11.36 ± 1.38	9.73 ± 1.07	0.41
DMSO + Noise	11.66 ± 1.38	11.39 ± 1.50	0.89	8.47 ± 1.28	7.34 ± 2.13	0.66	3.94 ± 1.18	4.86 ± 0.99	0.58

± represent S.E.M. (unpaired *t* test to compare males versus females)

**Table 5** Main effects of SAHA and sex on CTS and PTS following a two-way ANOVA

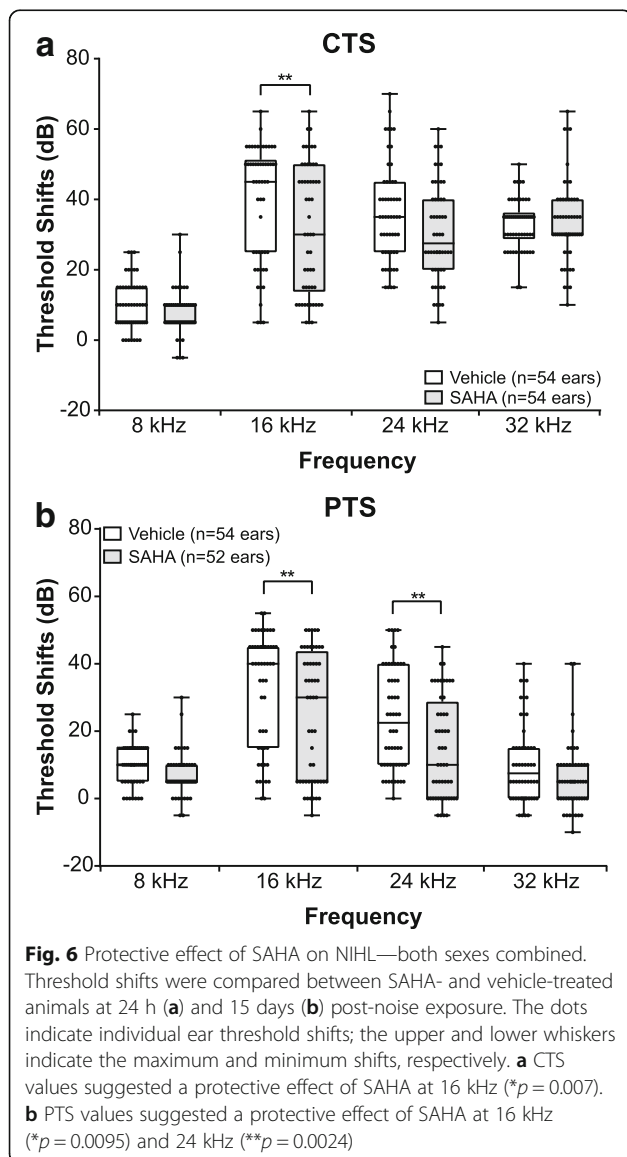
		8 kHz		16 kHz		24 kHz		32 kHz	
		F	<i>p</i> value	F	<i>p</i> value	F	<i>p</i> value	F	<i>p</i> value
CTS	Sex	18.67	<b>&lt; 0.0001</b>	20.06	<b>&lt; 0.0001</b>	11.07	<b>0.001</b>	0.174	ns
	SAHA	4.845	<b>0.030</b>	6.728	<b>0.011</b>	5.678	<b>0.020</b>	0.102	ns
PTS	Sex	6.885	<b>0.010</b>	26.35	<b>&lt; 0.0001</b>	22.14	<b>&lt; 0.0001</b>	14.02	<b>0.0003</b>
	SAHA	9.089	<b>0.003</b>	6.723	<b>0.011</b>	13.18	<b>0.0004</b>	5.174	<b>0.025</b>

For CTS and PTS, the degree of freedom for the numerator is 1. The degrees of freedom for the denominator are 104 and 102 for CTS and PTS, respectively. Significant results are shown in bold font (ns non-significant)

with effects on a wide range of physiological processes, and it must be considered in the experimental design to allow study results to relate to both male and female biology [48]. Importantly, the National Institutes of Health has added consideration of sex as a biological

factor in all applications considered for funding [49, 50]. We tested the efficacy of SAHA on prevention of noise-induced hearing loss in mice of both sexes. SAHA has been previously shown to be otoprotective against ototoxic drugs [51–54] and NIHL in male mice [14, 31]. Our results confirmed the efficacy of SAHA in male mice, albeit possibly to a lesser degree than previously reported [14, 31], and revealed only a small protective effect in females. Importantly, our treatment paradigm differed from previously published work and could account for some of the difference in efficacy. When the PTS from both sexes were analyzed together, 15 days post-noise exposure, a statistically significant protective effect of SAHA was found at both 16 and 24 kHz. However, when the data were separated by sex, we found that the protective effect of SAHA in males was limited to 24 kHz while in females to 16 kHz. Female mice demonstrated less hearing loss in response to noise at 16 and 24 kHz, in comparison to males, suggesting a sex-specific difference in the response to PTS-inducing noise trauma. This sex difference may explain the differential frequency-specific therapeutic efficacy of SAHA, where males at 16 kHz may have suffered too much damage to allow for SAHA-dependent rescue, and females at 24 kHz have too little PTS to allow a therapeutic effect to be detected with the number of mice tested. Concomitantly, previous studies suggested a level-specific limitation to the therapeutic effect of SAHA [14, 31].

To further investigate the sex-specific differences in hearing following PTS-inducing noise exposure, we compared OHC loss, wave I amplitude, and amplitude progression, as well as IHC pre-synaptic ribbons and active synapses. To our surprise, we found a significant difference between the sexes only in the wave I amplitude and amplitude progression. Wave I amplitude is an indicator of activity at the level of the SG, whereas wave I amplitude progression reflects the OHC contribution to the active process of hearing. Since the number of hair cells and synapses following noise exposure was not different across sexes, a decrease in wave I amplitude and amplitude progression suggests a greater decrease in OHC activity in the male mice. The suggested decrease in OHC function may be primary and represent a



dysfunction resulting from injury to the stereocilia or cell bodies [46], or secondary as a consequence of changes in the endocochlear potential. A recent study in F344 rats shows that the difference in hearing loss between aging male and female animals results in part from cellular degeneration at the level of the stria vascularis [55]. However, in this strain of rats OHC loss progressed from apex to base, indicating that the pathophysiology underlying the ARHL in the F344 rats may not be generalizable. Additional studies using inbred mouse strains revealed a divergent pathophysiology for male and female age-related loss [56, 57]. These observations suggest that outbred mice such as the B6CBAF1/J may prove particularly useful in the study of NIHL, as the effect of strain-specific recessively inherited mutations on the auditory system will be largely avoided. Future studies comparing changes in OHC and stria vascularis morphology and ultrastructure, as well as measurement of the endocochlear potential and distortion product otoacoustic emissions (DPOAE), are necessary to further define the underlying sex-specific differences following noise exposure [58, 59].

We employed an octave band (8–16 kHz) noise exposure paradigm that results in PTS in the B6CBAF1/J mouse strain. As expected following these type of exposures, we measured a maximal threshold shift at 16 and 24 kHz. A smaller threshold shift was measured at 32 kHz, the highest frequency analyzed in this study. A marked and significant loss of OHC was seen in both sexes in regions that correspond to frequencies higher than 32 kHz; however, only a minimal loss of OHC was measured in areas that map to 16 and 24 kHz. Taken together, these data suggest that two weeks following noise exposure, there are two types of hearing loss that differ in their underlying mechanisms. A loss of OHC in the base of the cochlea underlies a high-frequency hearing

loss, which is not directly related to the frequency of the noise exposure. Rather, it represents a non-specific acoustic injury likely secondary to the position and physical characteristics of the cells in the base of the cochlea. In addition, a frequency-specific PTS, which is the focus of this manuscript, is not secondary to loss of OHC. More importantly, these findings suggest a possible therapeutic window to treat the OHC and possibly prevent the frequency-specific PTS, as OHC in the frequency-specific PTS are still present 2 weeks following exposure. Later degeneration of OHC following PTS has been observed when ears are analyzed 1 year following noise exposure [18]. Similar to the lack of OHC loss at 16 kHz, the frequency where maximal PTS is found in both sexes, we did not observe a significant loss of active synapses in either sex. A progressive loss of active synapses was seen at 24 and 32 kHz. These data suggest that at least 2 weeks following PTS-inducing noise exposure, synaptopathy preferentially affects higher frequencies and does not explain the loss of hearing at 16 kHz or the sex-specific differences in the response to noise trauma (Fig. 7).

Differences in circulating levels of the steroid hormone estradiol and/or sensitivity to estradiol via its receptor activation may account for the observed sex difference in PTS as a result of noise trauma. Evidence from both clinical and basic studies clearly demonstrates that estradiol plays an important role in modulating auditory function in vertebrates as well as conferring a protective function in the female auditory system [60]. Estradiol signaling primarily occurs via two cognate receptors that are ligand-activated transcription factors. Estrogen receptor 1 (ERS1) and estrogen receptor 2 (ERS2) are widely distributed throughout the body and both have been reported in the cochlea of rodents and humans [61–64]. In mice, ESR1

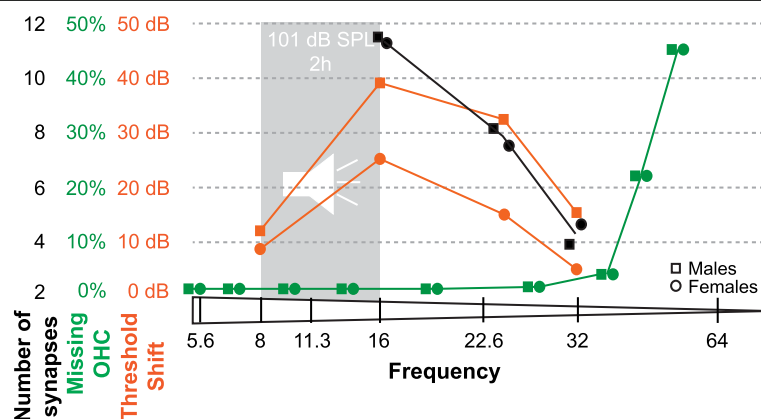


**Fig. 7** Schematic showing the threshold shifts in relation to missing outer hair cells and number of active synapses. Loss of OHC (green) and decrease in the number of active synapses (black) does not correlate with the highest threshold shift (orange) following noise exposure detected at 16 kHz. The difference in threshold shifts between male and female mice is not explained by a difference in OHC loss or active synapse numbers

and ESR2 are present in both the inner and outer hair cells, as well as the spiral ganglion neurons [61, 63, 65]. ESR2 and not ESR1 has been implicated in conferring the protective actions of estradiol against temporary hearing loss as result of a noise trauma in male and female mice [65] and age-related hearing loss in female mice [66]. However, the exact mechanisms through which estradiol is acting to confer protection is not well understood. In addition, molecular differences independent of the estradiol signaling pathway should also be considered in the underpinning mechanisms of the sexual dimorphic response to noise exposure.

## Conclusions

In conclusion, this study documents significant sex-specific differences in the response of the mouse cochlea to damaging noise exposure. These findings have implications on future study design for proper interpretation of the data. In particular, male and female mice should be tested and analyzed separately when used to study NIHL. As females demonstrate less noise-induced hearing damage in comparison to males, they may require exposure to a higher sound level to assess therapeutic effects. In addition, understanding the underpinnings of the females' relative protection from NIHL could lead to the development of new therapeutics to ameliorate the outcomes of noise exposures. Classic approaches to interrogate sex differences such as studying gonadectomized mice with and without supplemental sex hormones might be particularly useful to overcome challenges related to fluctuation of circulating sex hormones [67].

## Additional files

**Additional file 1:** Schematic showing ABR wave I extraction and analysis. Peak (P1) and trough (T1) values of wave I of the ABR traces (wave shaded in blue) were automatically extracted at stimuli levels from 55 to 85 dB SPL using a MatLab script. Wave I amplitudes were then plotted as a function of the stimuli levels. SigmaPlot was used to perform linear regression (dotted line) and calculate the slope (solid lines). Slopes were then compared between the different groups at 16 kHz. (PDF 471 kb)

**Additional file 2:** **Table S1.** Comparison of average hearing thresholds at baseline in male and female mice (Sidak's multiple comparison test; ns: non-significant). **Table S2.** Average threshold shift values in dB at 24 h post-noise exposure (CTS) and 15 days post-noise exposure (PTS) in vehicle-treated males and females (Tukey's multiple comparisons test). **Table S3.** Statistical values for interactions between the two factors following a two-way ANOVA. The degrees of freedom for the numerator (DFn) and denominator (DFd) are shown in parenthesis before the *F* value. Significant results are shown in bold font. **Table S4.** Comparison of average ABR thresholds shifts at 24 h (CTS) and 15 days (PTS) post-noise exposure in male and female mice treated with vehicle only (Sidak's multiple comparison test; ns: non-significant). **Table S5.** Values for the percentage of OHC loss within 32–45.2 kHz, 45.2–51 kHz, and 51–55 kHz. Progressive OHC loss is seen up to 55 kHz which is the highest frequency counted. Both male and female animals show a similar pattern of OHC loss.  $\pm$  represent S.E.M. (unpaired *t* test to compare male and female mice). **Table S6.** Comparison of average threshold shift values in dB at 24 h post-noise exposure (CTS) and 15 days post-noise exposure (PTS)

between vehicle- and SAHA-treated males and females separately (Sidak's multiple comparisons test; ns: non-significant). **Table S7.** Comparison of average threshold shift values in dB at 24 h post-noise exposure (CTS) and 15 days post-noise exposure (PTS) between vehicle- and SAHA-treated animals (Sidak's multiple comparisons test; ns: non-significant). (PDF 257 kb)

**Additional file 3:** OHC loss along the cochlear duct. Representative fluorescence microscopy images of the Organ of Corti at the level of the OHC (counter-stained with DAPI) at different frequency bands from controls and mice exposed at 101 dB SPL. There is little to no OHC loss in the control animals, whereas extensive OHC loss is seen above 32 kHz in animals exposed to noise. Scale bar represents 20  $\mu$ m. (PDF 1120 kb)

**Additional file 4:** OHC loss does not account for the frequency-specific PTS at 16 and 24 kHz or the sex differences in NIHL. Line graph indicating the percentage of OHC loss from apex to base in vehicle-treated noise-exposed animals compared to control non-noise-exposed animals. The frequency range of noise exposure is shaded gray and a gray dotted line outlines the frequency range where significant PTS is seen. Error bars indicate S.E.M. (PDF 396 kb)

**Additional file 5:** Pre-synaptic ribbons and active synapses at 16 kHz and 24 kHz. Representative fluorescence microscopy images of IHC stained for CtBP2 (red) and GluR2 (green) at 16 kHz (left) and 24 kHz (right) from control and noise-exposed mice. The dotted lines represent the approximate border of one IHC. The inset in the bottom left corner image represent a zoom in of active synapses where CtBP2 and GluR2 partially co-localize. Scale bar represents 10  $\mu$ m. (PDF 1242 kb)

**Additional file 6:** Effect of noise on pre-synaptic ribbons and active synapses in IHC. Graphs representing the number of pre-synaptic ribbons (a) and active synapses (b) in IHC of control and vehicle-treated noise-exposed animals. A significant decrease in pre-synaptic ribbons and active synapses is observed at 24 and 32 kHz in both males and females, but no difference is seen between sexes. Error bars indicate S.E.M. (PDF 418 kb)

## Abbreviations

ABR: Auditory brainstem response; ARHL: Age-related hearing loss; CTS: Compound threshold shift; dB: Decibel; DMSO: Dimethyl sulfoxide; DPOAE: Distortion product otoacoustic emissions; IHC: Inner hair cell; NIHL: Noise-induced hearing loss; OHC: Outer hair cell; PTS: Permanent threshold shift; SAHA: Suberoylanilide hydroxamic acid; SPL: Sound pressure level

## Acknowledgements

We would like to thank Lisa Cunningham, PhD and Kevin Ohlemiller, PhD for critically reviewing this manuscript.

## Funding

This work was supported by R01DC03544 (NIDCD), R01DC013817 (NIDCD), and MR130240 (CDMRP/DoD).

## Availability of data and materials

The datasets supporting the conclusions of this article are included within the article and its additional files (Additional files 1, 2, 3, 4, 5, and 6).

## Authors' contributions

SM and ZM contributed to the treatments, noise exposure, and ABR; BM and SM contributed to the histology and data analysis; RC and VD contributed to the blinded thresholds determination; DAD contributed to the MatLab script and data analysis; YS and JAM contributed to the statistical analysis; RH contributed to the experimental design and data analysis; and SM, RH, BM, JAM, and DAD wrote the manuscript. All the authors read and approved the final manuscript.

## Ethics approval

All procedures involving animals were carried out in accordance with the National Institutes of Health Guide for the Care and Use of Laboratory Animals and have been approved by the Institutional Animal Care and Use Committee at the University of Maryland, Baltimore (protocol numbers 1015003 and 0915006).

## Consent for publication

Not applicable.

**Competing interests**

The authors declare that they have no competing interests.

**Publisher's Note**

Springer Nature remains neutral with regard to jurisdictional claims in published maps and institutional affiliations.

**Author details**

<sup>1</sup>Department of Otorhinolaryngology - Head and Neck Surgery, University of Maryland, 16 South Eutaw Street, Suite 500, Baltimore, MD 21201, USA.

<sup>2</sup>Institute for Genome Science, University of Maryland School of Medicine, Baltimore, MD 21201, USA.

<sup>3</sup>Department of Pharmacology, University of Maryland School of Medicine, Baltimore, MD 21201, USA. <sup>4</sup>Institute for Systems Research, University of Maryland, College Park, MD 20742, USA.

<sup>5</sup>Department of Anatomy and Neurobiology, University of Maryland School of Medicine, Baltimore, MD 21201, USA.

Received: 26 January 2018 Accepted: 27 February 2018

Published online: 12 March 2018

**References**

- Nelson DI, Nelson RY, Concha-Barrientos M, Fingerhut M. The global burden of occupational noise-induced hearing loss. *Am J Ind Med.* 2005;48:446–58. <http://doi.wiley.com/10.1002/ajim.20223>
- Carroll YI, Eichwald J, Scincariello F, Hoffman HJ, Deitchman S, Radke MS, et al. Vital signs: noise-induced hearing loss among adults—United States 2011–2012. *MMWR Morb Mortal Wkly Rep.* 2017;66:139–44.
- Lie A, Skogstad M, Johannessen HA, Tynes T, Mehlum IS, Nordby K-C, et al. Occupational noise exposure and hearing: a systematic review. *Int Arch Occup Environ Health.* 2016;89:351–72.
- U.S. Department of Veterans Affairs. Veterans benefit administration, annual benefits report, fiscal year 2016. 2016. [https://www.benefits.va.gov/REPORTS/abr/ABR-All\\_Sections\\_FY16\\_06292017.pdf](https://www.benefits.va.gov/REPORTS/abr/ABR-All_Sections_FY16_06292017.pdf)
- Lin FR, Hazzard WR, Blazer DG. Priorities for improving hearing health care for adults: a report from the National Academies of Sciences, Engineering, and Medicine. *JAMA J Am Med Assoc.* 2016;316:819–20.
- Salvi R, Boettcher FA. Animal models of noise-induced hearing loss. In: Conn PM, editor. *Sourcebook. Model. Biomed. Res.* 1st ed. Totowa: Humana Press; 2008. p. 289–301.
- Nodal FR, King AJ. Hearing and auditory function in ferrets. In: Fox JG, Marini R, editors. *Biol Dis Ferret.* 3rd ed. Ames: Wiley; 2014. p. 685–710.
- Depireux DA, Simon JZ, Klein DJ, Shamma SA. Spectro-temporal response field characterization with dynamic ripples in ferret primary auditory cortex. *J Neurophysiol.* 2001;85:1220–34. United States
- Chen G-D, Fechter LD. The relationship between noise-induced hearing loss and hair cell loss in rats. *Hear Res.* 2003;177:81–90.
- Ohlemiller KK. Contributions of mouse models to understanding of age- and noise-related hearing loss. *Brain Res.* 2006;1091:89–102.
- Ahituv N, Avraham KB. Auditory and vestibular mouse mutants: models for human deafness. *J Basic Clin Physiol Pharmacol.* 2000;11:181–92.
- Layman WS, Williams DM, Dearman JA, Saucedo MA, Zuo J. Histone deacetylase inhibition protects hearing against acute ototoxicity by activating the NF- $\kappa$ B pathway. *Cell Death Discov.* 2015;1:15012. <http://www.nature.com/articles/cddiscovery201512>
- Xu WS, Parmigiani RB, Marks PA. Histone deacetylase inhibitors: molecular mechanisms of action. *Oncogene.* 2007;26:5541–52.
- Chen J, Hill K, Sha S-H. Inhibitors of histone deacetylases attenuate noise-induced hearing loss. *JARO.* 2016;17:289–302.
- Yoshida N, Kristiansen A, Liberman MC. Heat stress and protection from permanent acoustic injury in mice. *J Neurosci.* 1999;19:10116–24.
- Tahera Y, Meltser I, Johansson P, Canlon B. Restraint stress modulates glucocorticoid receptors and nuclear factor kappa B in the cochlea. *Neuroreport.* 2006;17:879–82.
- Kujawa S, Liberman C. Adding insult to injury: cochlear nerve degeneration after “temporary” noise-induced hearing loss. *J Neurosci.* 2009;29:14077–85.
- Fernandez KA, Jeffers PWC, Lall K, Liberman MC, Kujawa SG. Aging after noise exposure: acceleration of cochlear synaptopathy in “recovered” ears. *J Neurosci.* 2015;35:7509–20.
- Lauer AM, Schrode KM. Sex bias in basic and preclinical noise-induced hearing loss research. *Noise Health.* 2017;19:207–12. <http://www.noiseandhealth.org/text.asp?2017/19/90/207/215156>
- Canlon B, Meltser I, Johansson P, Tahera Y. Glucocorticoid receptors modulate auditory sensitivity to acoustic trauma. *Hear Res.* 2007;226:61–9.
- Jerger J, Chmiel R, Stach B, Spretnjak M. Gender affects audiometric shape in presbycusis. *J Am Acad Audiol.* 1993;4:42–9. [https://www.audiology.org/sites/default/files/journal/JAAA\\_04\\_01\\_07.pdf](https://www.audiology.org/sites/default/files/journal/JAAA_04_01_07.pdf)
- Ward WD, Royster JD, Royster LH. Auditory and nonauditory effects of noise. In: Berger EH, Royster LH, Royster JD, Driscoll DP, Layne M, editors. *Noise Man.* 5th ed: Fairfax: American Industrial Hygiene Association; 2000. p. 101–47.
- Waterston RH, Lindblad-Toh K, Birney E, Rogers J, Abril JF, Agarwal P, et al. Initial sequencing and comparative analysis of the mouse genome. *Nature.* 2002;420:520–62. England
- Brown SDM, Hardisty-Hughes RE, Mburu P. Quiet as a mouse: dissecting the molecular and genetic basis of hearing. *Nat Rev Genet.* 2008;9:277–90. England
- Scimemi P, Santarelli R, Selmo A, Mammano F. Auditory brainstem responses to clicks and tone bursts in C57 BL/6J mice. *Acta Otorhinolaryngol Ital.* 2014;34:264–71.
- Noben-Trauth K, Zheng QY, Johnson KR. Association of cadherin 23 with polygenic inheritance and genetic modification of sensorineural hearing loss. *Nat Genet.* 2003;35:21–3. United States.
- Davis RR, Newlander JK, Ling XB, Cortopassi GA, Krieg EF, Erway LC. Genetic basis for susceptibility to noise-induced hearing loss in mice. *Hear Res.* 2001;155:82–90.
- Johnson KR, Zheng QY, Noben-Trauth K. Strain background effects and genetic modifiers of hearing in mice. *Brain Res.* 2006;1091:79–88. Netherlands
- Ou HC, Bohne BA, Harding GW. Noise damage in the C57BL/CBA mouse cochlea. *Hear Res.* 2000;145:111–22.
- Longenecker RJ, Galazyuk AV. Methodological optimization of tinnitus assessment using prepulse inhibition of the acoustic startle reflex. *Brain Res.* 2012;1485:54–62. Netherlands
- Wen L-T, Wang J, Wang Y, Chen F-Q. Association between histone deacetylases and the loss of cochlear hair cells: role of the former in noise-induced hearing loss. *Int. J. Mol. Med.* 2015;36:534–40. Athens, Greece: Spandidos Publ LTD
- Ponton CW, Moore JK, Eggermont JJ. Auditory brain stem response generation by parallel pathways: differential maturation of axonal conduction time and synaptic transmission. *Ear Hear.* 1996;17:402–10.
- Zuccotti A, Lee SC, Campanelli D, Singer W, Sathesh SV, Patriarchi T, et al. L-type CaV1.2 deletion in the cochlea but not in the brainstem reduces noise vulnerability: implication for CaV1.2-mediated control of cochlear BDNF expression. *Front Mol Neurosci.* 2013;6:20. <https://www.frontiersin.org/articles/10.3389/fnmol.2013.00020/full>
- Fuchs JC, Zinnamon FA, Taylor RR, Ivins S, Scambler PJ, Forge A, et al. Hearing loss in a mouse model of 22q11.2 deletion syndrome. *PLoS One.* 2013;8:e80104. <http://journals.plos.org/plosone/article?id=10.1371/journal.pone.0080104>
- Ohlemiller KK, Jones SM, Johnson KR. Application of mouse models to research in hearing and balance. *JARO - J. Assoc. Res. Otolaryngol.* 2016;17:493–523.
- Zar JH. *Biostatistical analysis.* Upper Saddle River: Prentice-Hall; 1984.
- Massachusetts Eye and Ear. Video tutorial for mouse cochlear dissection. 2015.
- Massachusetts Eye and Ear. ImageJ Plugin Measure\_Line for mapping cochlear frequencies on whole mounts. <https://www.masseyeandear.org/research/otology/investigators/laboratories/eaton-peabody-laboratories/epl-histology-resources/imagej-plugin-for-cochlear-frequency-mapping-in-whole-mounts>
- Abràmoff MD, Magalhães PJ, Ram SJ. Image processing with imageJ: *Biophotonics Int.* 2004;11:36–42.
- Abdi H. The Bonferroni and Šidák corrections for multiple comparisons. In: Salkind N, editor. *Encycl Meas Stat.* Thousand Oaks: Sage Publications; 2007. p. 103–7. <https://www.utd.edu/~herve/Abdi-Bonferroni2007-pretty.pdf>
- Goutman JD, Elgoyhen AB, Gómez-Casati ME. Cochlear hair cells: the sound-sensing machines. *FEBS Lett.* 2015;589:3354–61. <http://onlinelibrary.wiley.com/doi/10.1016/j.febslet.2015.08.030/full>
- Henry KS, Kale S, Scheidt RE, Heinz MG. Auditory brainstem responses predict auditory nerve fiber thresholds and frequency selectivity in hearing impaired chinchillas. *Hear Res.* 2011;280:236–44.
- Hudspeth A. Mechanical amplification of stimuli by hair cells. *Curr Opin Neurobiol.* 1997;7:480–6. Available from: <https://www.sciencedirect.com/science/article/pii/S0959438897800268?via%3Dihub>
- Martin P, Hudspeth AJ. Active hair-bundle movements can amplify a hair cell's response to oscillatory mechanical stimuli. *Proc Natl Acad Sci U S A.* 1999;96:14306–11. <http://www.pnas.org/content/96/25/14306.long>
- Mann ZF, Kelley MW. Development of tonotopy in the auditory periphery. *Hear Res.* 2011;276:2–15. [cited 2018 Jan 17]. <http://linkinghub.elsevier.com/retrieve/pii/S037859511000141>

46. Kujawa SG, Liberman MC. Synaptopathy in the noise-exposed and aging cochlea: primary neural degeneration in acquired sensorineural hearing loss. *Hear Res.* 2015;330:191–9.
47. Suzuki J, Corfas G, Liberman MC. Round-window delivery of neurotrophin 3 regenerates cochlear synapses after acoustic overexposure. *Sci Rep.* 2016;6:24907. <http://www.nature.com/articles/srep24907>.
48. Karp NA, Mason J, Beaudet AL, Benjamini Y, Bower L, Braun RE, et al. Prevalence of sexual dimorphism in mammalian phenotypic traits. *Nat Commun.* 2017;8:15475. England
49. Hultcrantz M, Simonoska R, Stenberg AE. Estrogen and hearing: a summary of recent investigations. *Acta Otolaryngol.* 2006;126:10–4.
50. Clayton JA, Collins FS. Policy: NIH to balance sex in cell and animal studies. *Nature.* 2014;509:282–3. England
51. Drottar M, Liberman MC, Ratan RR, Roberson DW. The histone deacetylase inhibitor sodium butyrate protects against cisplatin-induced hearing loss in guinea pigs. *Laryngoscope.* 2006;116:292–6.
52. Chen FQ, Schacht J, Sha SH. Aminoglycoside-induced histone deacetylation and hair cell death in the mouse cochlea. *J Neurochem.* 2009;108:1226–36.
53. Wang J, Wang Y, Chen X, Zhang PZ, Shi ZT, Wen LT, et al. Histone deacetylase inhibitor sodium butyrate attenuates gentamicin-induced hearing loss in vivo. *Am J Otolaryngol Head Neck Med Surg.* 2015;36:242–8. Elsevier Inc
54. Layman WS, Zuo J. Preventing ototoxic hearing loss by inhibiting histone deacetylases. *Cell Death Dis.* 2015;6:e1882. <http://www.nature.com/doi/10.1038/cddis.2015.252>
55. Balogová Z, Popelář J, Chiumenti F, Chumak T, Burianová JS, Rybalko N, et al. Age-related differences in hearing function and cochlear morphology between male and female Fischer 344 rats. *Front Aging Neurosci.* 2018;9:428. <http://journal.frontiersin.org/article/10.3389/fnagi.2017.00428/full>.
56. Henry KR. Males lose hearing earlier in mouse models of late-onset age-related hearing loss; females lose hearing earlier in mouse models of early-onset hearing loss. *Hear Res.* 2004;190:141–8. <https://www.sciencedirect.com/science/article/pii/S0378595503004015?via%3Dihub>
57. Ohlemiller KK, Dahl AR, Gagnon PM. Divergent aging characteristics in CBA/J and CBA/CaJ mouse cochleae. *J Assoc Res Otolaryngol.* 2010;11:605–23. <https://link.springer.com/article/10.1007%2Fs10162-010-0228-1>.
58. Hirose K, Liberman MC. Lateral wall histopathology and endocochlear potential in the noise-damaged mouse cochlea. *JARO J Assoc Res Otolaryngol.* 2003;4:339–52. <https://link.springer.com/article/10.1007%2Fs10162-002-3036-4>.
59. Wang Y, Hirose K, Liberman MC. Dynamics of noise-induced cellular injury and repair in the mouse cochlea. *J Assoc Res Otolaryngol.* 2002;3:248–68. <https://link.springer.com/article/10.1007%2Fs101620020028>.
60. Caras ML. Estrogenic modulation of auditory processing: a vertebrate comparison. *Front. Neuroendocrinol.* San Diego, Academic Press INC Elsevier Science; 2013;34:285–299.
61. Charitidi K, Meltser I, Canlon B. Estradiol treatment and hormonal fluctuations during the estrous cycle modulate the expression of estrogen receptors in the auditory system and the prepulse inhibition of acoustic startle response. *Endocrinology.* 2012;153:4412–21.
62. Simonoska R, Stenberg A, Masironi B, Sahlin L, Hultcrantz M. Estrogen receptors in the inner ear during different stages of pregnancy and development in the rat. *Acta Otolaryngol.* 2009;129:1175–81.
63. Stenberg AE, Wang H, Fish J, Schrott-Fisher A, Sahlin L, Hultcrantz M. Estrogen receptors in the normal adult and developing human inner ear and in Turner's syndrome. *Hear Res.* 2001;157:87–92.
64. Motohashi R, Takumida M, Shimizu A, Konomi U, Fujita K, Hirakawa K, et al. Effects of age and sex on the expression of estrogen receptor  $\alpha$  and  $\beta$  in the mouse inner ear. *Acta Otolaryngol.* 2010;130:204–14. <https://www.tandfonline.com/doi/full/10.3109/00016480903016570>.
65. Meltser I, Tahera Y, Simpson E, Hultcrantz M, Charitidi K, Gustafsson J-A, et al. Estrogen receptor beta protects against acoustic trauma in mice. *J Clin Invest.* 2008;118:1563–70.
66. Simonoska R, Stenberg AE, Duan M, Yakimchuk K, Fridberger A, Sahlin L, et al. Inner ear pathology and loss of hearing in estrogen receptor-beta deficient mice. *J Endocrinol.* 2009;201:397–406. <http://joe.endocrinology-journals.org/cgi/doi/10.1677/JOE-09-0060>
67. Willott JF. Effects of sex, gonadal hormones, and augmented acoustic environments on sensorineural hearing loss and the central auditory system: insights from research on C57BL/6J mice. *Hear Res.* 2009;252:89–99. <https://www.sciencedirect.com/science/article/pii/S037859550800258X?via%3Dihub>.

Submit your next manuscript to BioMed Central and we will help you at every step:

- We accept pre-submission inquiries
- Our selector tool helps you to find the most relevant journal
- We provide round the clock customer support
- Convenient online submission
- Thorough peer review
- Inclusion in PubMed and all major indexing services
- Maximum visibility for your research

Submit your manuscript at  
[www.biomedcentral.com/submit](http://www.biomedcentral.com/submit)



RESEARCH ARTICLE

Open Access



# A comparative analysis of library prep approaches for sequencing low input transcriptome samples

Yang Song<sup>1</sup>, Beatrice Milon<sup>2</sup>, Sandra Ott<sup>1</sup>, Xuechu Zhao<sup>1</sup>, Lisa Sadzewicz<sup>1</sup>, Amol Shetty<sup>1</sup>, Erich T. Boger<sup>3</sup>, Luke J. Tallon<sup>1</sup>, Robert J. Morell<sup>3</sup>, Anup Mahurkar<sup>1</sup> and Ronna Hertzano<sup>1,2,4\*</sup>

## Abstract

**Background:** Cell type-specific ribosome-pulldown has become an increasingly popular method for analysis of gene expression. It allows for expression analysis from intact tissues and monitoring of protein synthesis in vivo. However, while its utility has been assessed, technical aspects related to sequencing of these samples, often starting with a smaller amount of RNA, have not been reported. In this study, we evaluated the performance of five library prep protocols for ribosome-associated mRNAs when only 250 pg–4 ng of total RNA are used.

**Results:** We obtained total and RiboTag-IP RNA, in three biological replicates. We compared 5 methods of library preparation for Illumina Next Generation sequencing: NuGEN Ovation RNA-Seq system V2 Kit, TaKaRa SMARTer Stranded Total RNA-Seq Kit, TaKaRa SMART-Seq v4 Ultra Low Input RNA Kit, Illumina TruSeq RNA Library Prep Kit v2 and NEBNext<sup>®</sup> Ultra<sup>™</sup> Directional RNA Library Prep Kit using slightly modified protocols each with 4 ng of total RNA. An additional set of samples was processed using the TruSeq kit with 70 ng, as a ‘gold standard’ control and the SMART-Seq v4 with 250 pg of total RNA. TruSeq-processed samples had the best metrics overall, with similar results for the 4 ng and 70 ng samples. The results of the SMART-Seq v4 processed samples were similar to TruSeq (Spearman correlation > 0.8) despite using lower amount of input RNA. All RiboTag-IP samples had an increase in the intronic reads compared with the corresponding whole tissue, suggesting that the IP captures some immature mRNAs. The SMARTer-processed samples had a higher representation of ribosomal and non-coding RNAs leading to lower representation of protein coding mRNA. The enrichment or depletion of IP samples compared to corresponding input RNA was similar across all kits except for SMARTer kit.

**Conclusion:** RiboTag-seq can be performed successfully with as little as 250 pg of total RNA when using the SMART-Seq v4 kit and 4 ng when using the modified protocols of other library preparation kits. The SMART-Seq v4 and TruSeq kits resulted in the highest quality libraries. RiboTag IP RNA contains some immature transcripts.

**Keywords:** RiboTag, Library preparation kits, Low-input RNA-seq, RNA-seq, Coverage bias

\* Correspondence: [rhertzano@som.umaryland.edu](mailto:rhertzano@som.umaryland.edu)

<sup>1</sup>Institute for Genome Sciences, University of Maryland School of Medicine, Baltimore, MD 21201, USA

<sup>2</sup>Department of Otorhinolaryngology-Head & Neck Surgery, University of Maryland School of Medicine, Baltimore, MD 21201, USA

Full list of author information is available at the end of the article



## Background

Considerable scientific effort has been dedicated to understanding cell type-specific expression profiles from complex tissues, such as brain, liver, pancreas, testes, eye or ear [1–7]. To overcome the issue of cellular heterogeneity within complex tissues, two methods have been traditionally used in mice: Laser-Capture Microdissection (LCM) [8, 9] and Fluorescence Activated Cell Sorting (FACS) [10, 11]. However, LCM is a laborious and time-consuming procedure with low yield of mRNA; and FACS requires tissue dissociation – which may lead to changes in gene expression – and requires dedicated equipment [12]. More recently, single cell RNA-seq has been introduced. However, this technique too requires tissue dissociation and is currently limited by the number of genes detected per sequenced cell [13, 14]. To overcome these limitations, Translating Ribosome Affinity Purification (TRAP) [15] and RiboTag [16] have been recently developed to study cell type-specific transcriptome profiles. Both methods rely on immunoprecipitation of ribosome-attached RNA (also named ‘translatome’) by cell type-specific molecular targeting of the ribosomal proteins, often in a Cre-lox based system [15–17]. These methods have the advantage of not requiring tissue dissociation, thus allowing for cell type-specific translatome analysis from intact tissues.

While ribosome-attached RNA sequencing for expression analysis has been validated from a biological standpoint [18, 19], the technical aspects of its library construction and sequencing have not been studied. In instances where small complex tissues are studied, the amount of starting material after immunoprecipitation may be limited (e.g., less than 5 ng). When starting from low amounts of RNA, additional cycles of amplification using PCR are performed after adapter ligation to amplify the cDNA to generate enough material for sequencing. Multiple commercial kits are available in the market to build cDNA libraries from samples with low amounts of RNA, including kits from NuGEN, New England Biolabs (NEB), Illumina and TaKaRa. Standard protocols for library construction are commonly designed to start with more than 100 ng of total RNA [20, 21] and only a few studies have been conducted to compare the performance of library preparation kits using less than 5 ng of total RNA as their starting amount [22, 23]. In this study, we selected four of the commonly used library preparation kits that are also suitable for lower-input samples for comparison. We modified the standard protocols for NEB and Illumina library preparation kits to enable them to work with smaller amounts of RNA than the recommended amounts down to as little as 4 ng of total RNA. We included one kit, SMART-Seq v4, that was designed for single cell RNA-seq and tested it with 4 ng and 250 pg of

total RNA. We evaluated the performance of the different kits based on duplication rate, percentage of intronic and exonic regions being detected, the evenness of coverage of transcripts and ribosomal RNA read-count in comparison to total reads. We also compared the reproducibility of the enrichment or depletion effect based on ribotag-translatome profile for the first time.

## Methods

### Animals

The *Gfi1*-Cre knock-in mice generated by Dr. Lin Gan (University of Rochester) were kindly provided by Dr. Jian Zuo of the Developmental Neurobiology Department at St. Jude Children’s Research Hospital. RiboTag mice generated by Dr. Paul S Amieux (University of Washington) were kindly provided by Dr. Mary-Kay Lobo of the Department of Neurobiology and Anatomy at University of Maryland Baltimore. B6.Cg-Gt(ROSA)26-Sor<sup>tm14(CAG-tdTomato)Hze/J</sup> mice (also referred to as Ai14) were purchased from the Jackson Laboratory (stock #007914, Bar Harbor, ME). Experimental animals for RNA-seq, *Gfi1*<sup>Cre/+</sup>;*RiboTag*<sup>HA/HA</sup>, were obtained by crossing RiboTag mice with *Gfi1*-Cre mice. Animals for immunostaining, *Gfi1*<sup>Cre/+</sup>;*Ai14*, were obtained by crossing *Gfi1*-Cre mice with Ai14 mice [24]. All procedures involving animals were carried out in accordance with the National Institutes of Health Guide for the Care and Use of Laboratory Animals and have been approved by the Institutional Animal Care and Use Committee at the University of Maryland, Baltimore (protocol numbers 1015003 and 0915006).

### Ribosome immunoprecipitation and RNA extraction

Three 30-day old *Gfi1*<sup>Cre/+</sup>;*RiboTag*<sup>HA/HA</sup> mice were euthanized by CO<sub>2</sub> asphyxiation followed by cervical dislocation. Livers were harvested and immediately frozen on dry ice. Equal amounts of liver were used for input RNA extractions (RNeasy Plus Micro kit, QIAGEN USA, Germantown, MD, USA) or further processed for ribosome immunoprecipitation (5 µg of purified anti-HA.11, BioLegend, San Diego, CA, USA) followed by RNA extraction as previously described in Sanz et al., 2009 [16]. The RNeasy Plus Micro kit is optimized for the removal of genomic DNA through a combination of high salt buffer and the gDNA Eliminator spin column. Quality of the RNA was assessed on an Agilent Technologies Bioanalyzer 2100 RNA pico chip as per the manufacturer’s instructions (Agilent Technologies, Palo Alto, CA, USA). All samples had a RIN score of 10 and no evidence of DNA contamination in the form of a high molecular weight DNA band. All RNA was equally aliquoted to test for the performance of five commercial kits and seven protocols.

### Real-time RT-PCR

Efficiency of the ribosome immunoprecipitation was assessed by reverse transcription followed by real time PCR. One nanogram of total RNA from the input and the IP samples was used for reverse transcription using the Maxima First Strand cDNA Synthesis Kit for RT-qPCR (Thermo Fisher Scientific, Waltham, MA, USA). The real time PCR was performed on an Applied Biosystems® StepOnePlus™ Real-Time PCR System with the Maxima SYBR Green/ROX qPCR Master Mix (Thermo Fisher Scientific, Waltham, MA, USA) and the following primers: *Gapdh*-Fw 5'-GGAGAAACCTGCCAAGTATGA-3'; *Gapdh*-Rv 5'-T CCTCAGTGTAGCCCAAGA-3'; *Gfi1*-Fw 5'-AATGCA GCAAGGTGTTCTC-3'; *Gfi1*-Rv 5'-CTTACAGTCAAA GCTGCGT-3'.

### Immunostaining

Progeny from a cross between *Gfi1*<sup>Cre/+</sup> mice and TdTomato reporter mice Ai14 were euthanized at P1 and their livers were harvested. Following fixation in 4% paraformaldehyde overnight at 4 °C, livers were cryoprotected through incubation in PBS with increasing amount of sucrose before being embedded in O.C.T. compound (Scigen, Gardena, CA, USA). Ten μm cryosections were permeabilized with PBS supplemented with 0.2% Tween-20 for 1 h at room temperature and incubated with Alexa Fluor™ 488 Phalloidin (1/800, Thermo Fisher Scientific, Waltham, MA, USA) and DAPI (1/20,000, Thermo Fisher Scientific, Waltham, MA, USA). Samples were mounted with ProLong Gold antifade reagent (Thermo Fisher Scientific, Waltham, MA, USA). Images were acquired using a Nikon Eclipse E600 microscope (Nikon, Tokyo, Japan) equipped with a Lumenera Infinity 3 camera (Lumenera, Ottawa, ON).

### RNA-Seq library construction

Below are the experimental methods for RNA-Seq library construction. We followed the manufacturer's instructions with minor modifications, as noted below. The shearing approach was not altered and remains different between kits.

#### **Ovation® RNA-Seq system V2 combined with TruSeq RNA library prep kit v2**

We performed a hybrid library preparation by using Ovation® RNA-Seq System V2 (NuGEN, San Carlos, CA, USA) to synthesize cDNA and the TruSeq RNA Library Preparation Kit v2 to construct the sequencing library (Illumina, San Diego, CA, USA), consistent with the NuGEN manufacturer protocol (See Additional file 1: Table S1). Briefly, 4 ng of total RNA or RiboTag IP RNA were used to synthesize cDNA following the NuGEN's instructions. Subsequently, 200 ng of cDNA were sheared to an average size of 300 bp with a Covaris E220

Focused-Ultrasonicator (Covaris Inc., Woburn, MA, USA). Following the manufacturer protocol, the library was prepared from the sheared cDNA using the Illumina TruSeq RNA Library Prep Kit with 8 cycles of PCR.

#### **SMARTer® stranded total RNA-Seq kit-Pico input mammalian**

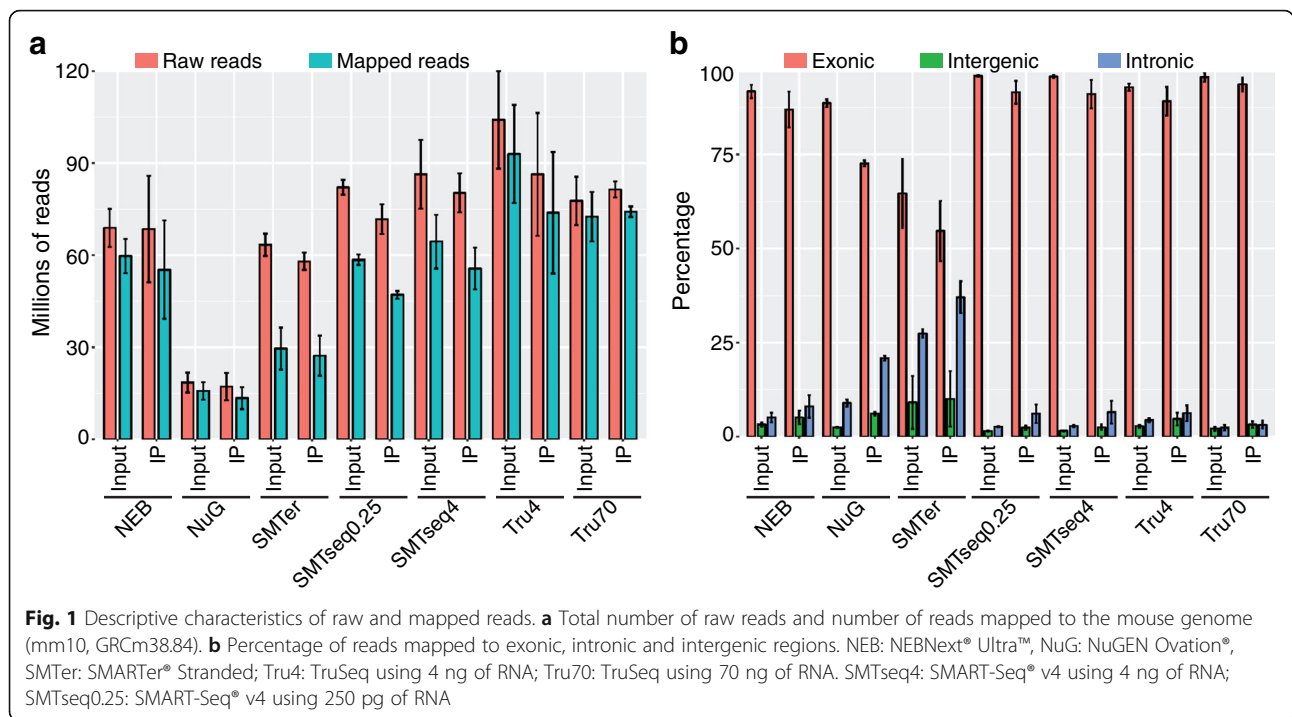
Four nanograms of RNA were used as input material and libraries were prepared by following the SMARTer Stranded Total RNA-Seq kit-Pico Input Mammalian user manual (Takara Bio USA, Mountain View, CA, USA). In brief, samples were fragmented at 94 °C for 4 min prior to first-strand synthesis. Illumina adaptors and indexes were added to single-stranded cDNA via 5 cycles of PCR. Libraries were hybridized to R-probes for fragments originating from ribosomal RNA to be cleaved by ZapR. The resulting ribo-depleted library fragments were amplified with 15 cycles of PCR.

#### **SMART-Seq® v4 ultra® low input RNA kit for sequencing**

Two types of libraries were prepared by using 4 ng or 250 pg RNA from each sample. Libraries were prepared by following the SMART-Seq v4 Ultra Low Input RNA Kit (Takara Bio USA, Mountain View, CA, USA) user manual. The cDNA was amplified with 11 cycles of PCR. Nextera XT kit (Nextera XT DNA Library Preparation Kit (Illumina, San Diego, CA) was used to make cDNA libraries suitable for Illumina sequencing.

#### **TruSeq RNA library prep kit v2**

Two types of libraries were prepared by using 70 ng or 4 ng RNA from each sample. The 70 ng libraries were built using TruSeq RNA Library Prep Kit v2 (Illumina, San Diego, CA, USA) according to the manufacturer protocol. Size selection was performed using SPRIselect beads (Beckman Coulter, Indianapolis, IN, USA) and in-house calibration values (first round selection to select the upper or right limit of the distribution), salt unit equals to 0.427 and second round selection to select the lower or left limit of the distribution, salt unit = 0.455). The cDNA was amplified with 19 cycles of PCR. Libraries were prepared using 4 ng of RNA with modifications to the standard protocol by reducing the end-repair reaction to 1/2 the recommended amounts of enzyme mix and sample volume. In addition A-tail ligation followed the standard protocol without the use of internal control mixes. Due to the low input amount, no size selection was applied to the 4 ng libraries. The cDNA was amplified with 22 cycles of PCR. Libraries prepared using 70 ng of RNA were prepared following the standard protocol and cDNA was amplified with 14 cycles as suggested by manufacture protocol.



**NEBNext® ultra™ directional RNA library prep kit for Illumina**

Four nanograms of total RNA were used for NEBNext® Ultra™ Directional RNA Library Prep Kit (New England Biolabs, Ipswich, MA, USA). Poly-A selection and cDNA synthesis were performed according to NEB protocol. The adaptors were diluted with a 1:30 ratio instead of the recommended 1:10 ratio. Size selection was performed using SPRIselect beads. (Beckman Coulter, Indianapolis, IN, USA) with in-house calibration values. The cDNA was amplified with 22 cycles of PCR.

**Sequencing**

Samples prepared by TruSeq, NEB, NuGEN and SMARTer were sequenced at the Institute for Genome Sciences (IGS) Genomics Resource Center (Baltimore, MD) on a HiSeq 4000 using 75 base read lengths in paired-end mode. Samples prepared by SMART-Seq v4 were sequenced by the Genomics and Computational Biology Core (GCBC) at the National Institute on Deafness and Other Communication Disorders (NIDCD/NIH) on a HiSeq 1500 using a read length of 126 bases in paired-end mode.

**RNA-Seq analyses**

The Illumina adapters used during the library construction were removed from the reads using Trimmomatic [1]. In order to reduce the impact of lower quality reads on the alignment, all reads were trimmed to 60 bp

**Table 1** Duplication rate of libraries prepared by different kits

Kit	Sample type	PCR cycles for lib prep	Percent_Duplication (%)			
			replicate			avg
			1	2	3	
NEB <sup>a</sup>	Input	22	97	99	97	97
	IP		99	99	99	99
NuG/Tru <sup>b</sup>	Input	8	52	53	52	53
	IP		36	31	26	31
SMTer <sup>c</sup>	Input	15	83	86	85	85
	IP		86	83	68	79
Tru4 <sup>d</sup>	Input	22	67	77	71	72
	IP		85	82	99	89
Tru70 <sup>e</sup>	Input	19	90	94	92	92
	IP		98	97	96	97
SMTseq4 <sup>f</sup>	Input	11	40	38	40	40
	IP		60	49	48	52
SMTseq0.25 <sup>f</sup>	Input	11	37	37	41	38
	IP		59	50	47	52

<sup>a</sup>NEBNext® Ultra™ Directional RNA Library Prep Kit for Illumina

<sup>b</sup>Nugen Ovation® RNAseq System v2

<sup>c</sup>SMARTer® Stranded Total RNA-Seq Kit-Pico Input Mammalian User

<sup>d</sup>TruSeq® RNA sample preparation v2,4 ng

<sup>e</sup>TruSeq® RNA sample preparation v2,70 ng

<sup>f</sup>SMART-Seq v4 Ultra Low Input RNA Kit

using the FASTX Toolkit v-0.0.13 [25] resulting in a Phred-Quality-Score greater than 30. The reads generated for each RNA sample were analyzed and compared using an Ergatis-based RNA-Seq analysis pipeline [26] where sequencing reads were aligned and annotated to the UCSC mouse reference genome (mm10, GRCm38.84) from Ensembl (<http://www.ensembl.org>) using TopHat v-2.0.8 [27] (maximum number of mismatches = 2; segment length = 30; maximum multi-hits per read = 25; maximum intron length = 50,000) and the number of reads that aligned to the predicted coding regions were determined using HTSeq [28]. Bedtools (v-2.7.1) [29] was used to count the reads mapping to exons according to Ensembl gene annotations (March 2016, Mus\_musculus.GRCm38.84, with 47,729 genes annotated). Read counts per million mapped reads values (CPM) [28] or reads per kilobase of transcripts per million mapped reads (RPKM) [30] were calculated and used for downstream analyses. 5'-3' exonic coverage was calculated using CollectRnaSeqMetrics component of picard-tools (v-1.60, <https://broadinstitute.github.io/picard/>), and duplication rate was calculated using EstimateLibraryComplexity of Picard-tools.

**Statistical analysis**

All plots were generated using R (v-3.2.4), including the following R packages ggplot2, ComplexHeatmap for producing bar plots or heat maps, and limma to generate Venn diagrams. The difference among groups in boxplots was evaluated based on the overlapping of the notch region [31]. The notch is defined as median  $m \pm 1.58IQR/\sqrt{n}$

[31]. The significance test is evaluated using a non-parametric Wilcoxon test with  $p < 0.05$ .

**Accession number**

All of the processed gene expression data from this study have been submitted to the NCBI Gene Expression Omnibus (GEO) under accession number GSE104213.

**Results**

**Sample preparation for sequencing**

In order to evaluate the efficiency of different library preparation kits with low amounts of RNA obtained after ribosome immunoprecipitation, we crossed RiboTag mice with *Gfi1*-Cre mice to obtain progeny that expressed HA-tagged ribosomes in cells with *Gfi1* expression. We obtained RNA from liver because it is a tissue that, at least during embryogenesis, expresses *Gfi1*, thus allowing for early induced recombination in a subset of the liver cells for permanent expression of a reporter gene [32] (Additional file 2: Figure S1a). Additionally, the size of the liver would provide enough material to test five different kits with varying amounts of starting RNA from individually processed samples. Livers were processed for HA-tagged ribosome immunoprecipitation (IP) followed by RNA extraction as previously described [16]. Prior to sequencing, the efficacy of the IP was confirmed by comparing the level of *Gfi1* transcripts in the input and IP samples using real time RT-PCR (Additional file 2: Figure S1b). The profiles generated by the five different commercial library preparation kits, from four different manufacturers, were compared in this study (See Additional file 1: Table S1). NEBNext® Ultra™

**Table 2** Number of features with CPM > 0

Kit	Sample type	Number of features with coverage (CPM > 0)				Number of reads of all expressed features (CPM > 0)			
		Replicate			avg	Replicate			avg
		1	2	3		1	2	3	
NEB	Input	13,543	12,464	11,419	12,475	22,373,163	26,292,017	22,305,929	23,657,036
	IP	11,059	12,165	14,331	12,518	16,668,355	27,323,849	15,122,257	19,704,820
NuG	Input	16,946	16,458	15,624	16,343	5,529,417	7,615,866	7,482,819	6,876,034
	IP	17,715	17,841	18,198	17,918	3,223,153	5,319,712	5,141,329	4,561,398
SMTer	Input	12,281	10,184	10,929	11,131	759,221	762,562	750,159	757,314
	IP	12,422	11,168	15,684	13,091	701,059	645,414	464,199	603,557
Tru4	Input	19,906	19,863	19,631	19,800	35,368,451	45,466,334	31,299,550	37,378,112
	IP	17,467	18,899	21,161	19,176	36,785,680	28,571,125	18,031,264	27,796,023
Tru70	Input	15,957	15,577	16,082	15,872	32,103,296	33,797,108	25,797,283	30,565,896
	IP	14,430	15,213	15,680	15,108	31,150,532	29,799,544	27,902,766	29,617,614
SMTseq4	Input	19,111	19,287	19,630	19,343	23,573,272	24,615,731	30,217,161	26,135,388
	IP	19,835	20,551	20,488	20,291	14,407,184	19,577,709	17,262,557	17,082,483
SMTseq0.25	Input	16,834	16,742	16,117	16,564	23,815,261	24,347,672	22,951,893	23,704,942
	IP	16,827	16,870	16,527	16,741	13,971,566	15,047,219	14,691,099	14,569,961

Directional RNA Library Prep Kit for Illumina (NEB) with 4 ng of RNA, NuGEN Ovation® RNA-Seq System V2 with 4 ng of RNA (NuGEN) with 4 ng of RNA, TaKaRa SMARTer® Stranded Total RNA-Seq Kit-Pico Input Mammalian with 4 ng of RNA (SMARTer), TaKaRa SMART-Seq® v4 Ultra® Low Input RNA Kit for Sequencing with 4 ng and 0.25 ng of RNA (SMARTseq4 and SMARTseq0.25) and Illumina TruSeq RNA Library Prep Kit v2 with 4 ng and 70 ng of RNA (TruSeq4 and TruSeq70). Of these kits only the SMARTer kit produced strand specific libraries and we therefore did not analyze the data for strandness.

**Comparison of mapping efficiency and duplication rate**

The number of reads varied widely among samples being prepared by different library preparation kits. Input RNA samples generated 14.7 to 122 million pair-end reads (2 × 60 bp) and IP RNA samples generated 12 to 108 million pair-end reads (2 × 60 bp). Overall, fewer raw/mapped reads were generated when using the NuGEN kit. Of the raw reads, 12.5 to 111 million reads mapped to mouse genome for input RNA samples while 9.2 to 94.6 million reads mapped for IP RNA samples (Fig. 1a).

In order to evaluate the expression profile composition and library complexity, we assessed the duplication rate of the read pairs (Table 1) as lower duplication rates usually indicate a higher complexity of the sample and better representation of RNA present in a sample [20]. In this study, duplication rate ranged from 26 to 99% (Table 1). However, the duplication we observed was not well correlated with the numbers of PCR cycles and was more dependent on the library prep kit. For instance, while NEB and TruSeq4 samples both had the highest number of PCR cycles (22), their duplication rates differed (Table 1). Indeed, NEB-input samples had the highest duplication rate of 99% with the overall largest number of reads duplicated more than 200 times while the TruSeq4 samples had a duplication rate of 72% with a substantially smaller number of reads with greater than 200 duplications (Table 1 and Additional file 3: Figure S2).

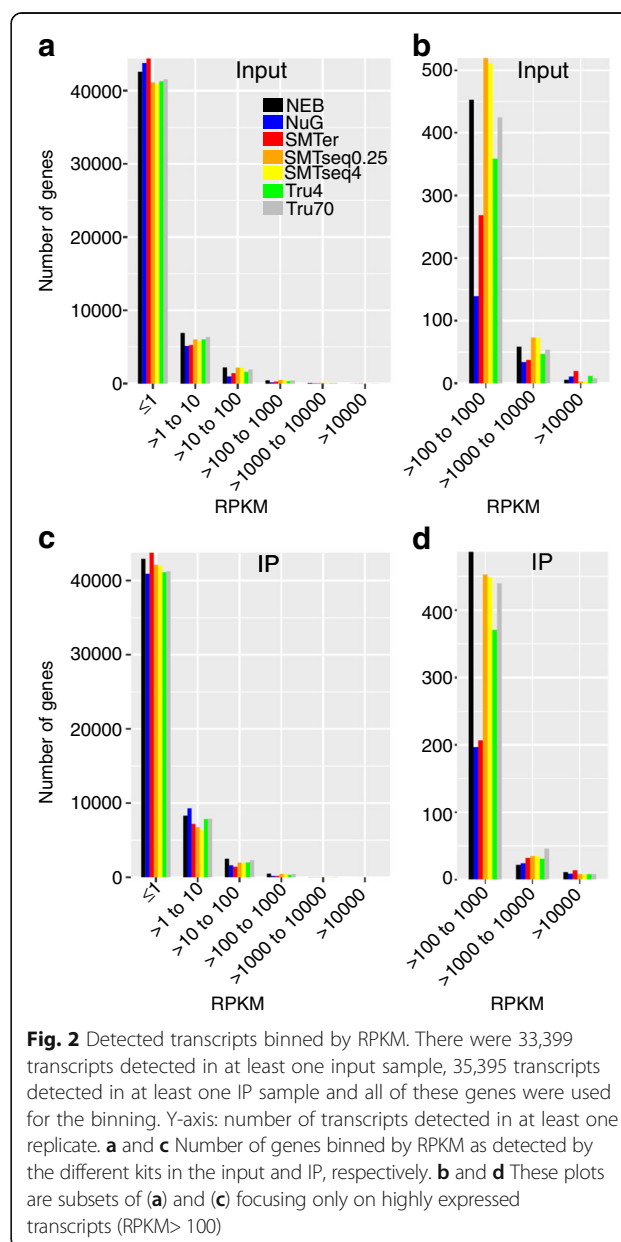
**Detection of exonic, intergenic and intronic regions**

Among the mapped reads, SMARTer samples showed the lowest alignment to exonic regions. The percentage of reads aligned to exonic regions was greater than 85% in samples prepared with NEB, TruSeq and SMARTseq library kits and less than 70% in samples prepared with the SMARTer and NuGEN kits (Fig. 1b). As expected, the overall percentage of reads aligning to intronic regions detected in input samples was less than 10% for most samples, except for samples prepared by the SMARTer kit, where more than 20% of the reads align to intronic regions. IP samples had roughly twice as many reads aligning to intronic regions, or 10% more

intronic reads compared with the corresponding input RNA samples, which may suggest that the IP captures some immature mRNAs. In particular, the percentage of intronic reads from the SMARTer samples increased from 22% for the input RNA to 41% for the IP RNA. The percentage of intronic reads for the NuGEN samples ranged from 8% for the input RNA and 22% for the IP RNA.

**Number of genes being detected as expressed**

Because of the differences in sequencing efficiency and library complexity, we examined the number of features detected in samples prepared with each library kit. After removing ambiguous reads or reads mapped to multiple



features using HTSeq, we detected between 10,184 to 21,161 genes where the CPM values were greater than zero (Table 2). The corresponding average raw read counts ranged from 0.76 to 37 million reads. Fewer features were detected in SMARTer and NEB samples. All of the annotated genes (47,729) were binned into 6 groups ( $RPKM \leq 1$ ,  $1 < RPKM \leq 10$ ,  $10 < RPKM \leq 100$ ,  $100 < RPKM \leq 1000$ ,  $1000 < RPKM \leq 10,000$  and  $RPKM > 10,000$ . Fig. 2). SMARTer, NuGEN, and NEB samples had more genes that were entirely missed or had low expression levels ( $RPKM \leq 1$ ) in comparison to the other kits in the input samples (Fig. 2a). The SMARTer and NEB samples had more genes with a lower expression levels ( $RPKM \leq 1$ ) also in the IP (Fig. 2c). The number of genes within RPKM range (100–10,000) was relatively low in SMARTer and NuGEN samples (Fig. 2b, d). Conversely,

SMARTer samples contained more highly expressed genes ( $RPKM > 10,000$ ) than others samples, but the majority of these were rRNA genes or genes encoding for hypothetical proteins (Fig. 2b, d and See Additional file 1: Table S2).

In order to compare the similarity of expression profiles of the different kits, we compared genes with at least 1 CPM in at least one replicate across all the samples. More than 60% of the genes were co-detected by all kits (Fig. 3). The median CPM for shared genes across all samples was 28 for input samples (Fig. 3a, c) and 36 for IP samples (Fig. 3b, d). Meanwhile, less than 10% of features were uniquely detected in NEB, NuGEN and TruSeq input samples, but over 20% of features were uniquely detected from the SMARTer samples. The median CPM of uniquely detected genes in SMARTer input samples was around 10, while the median for other kits was less than 3.

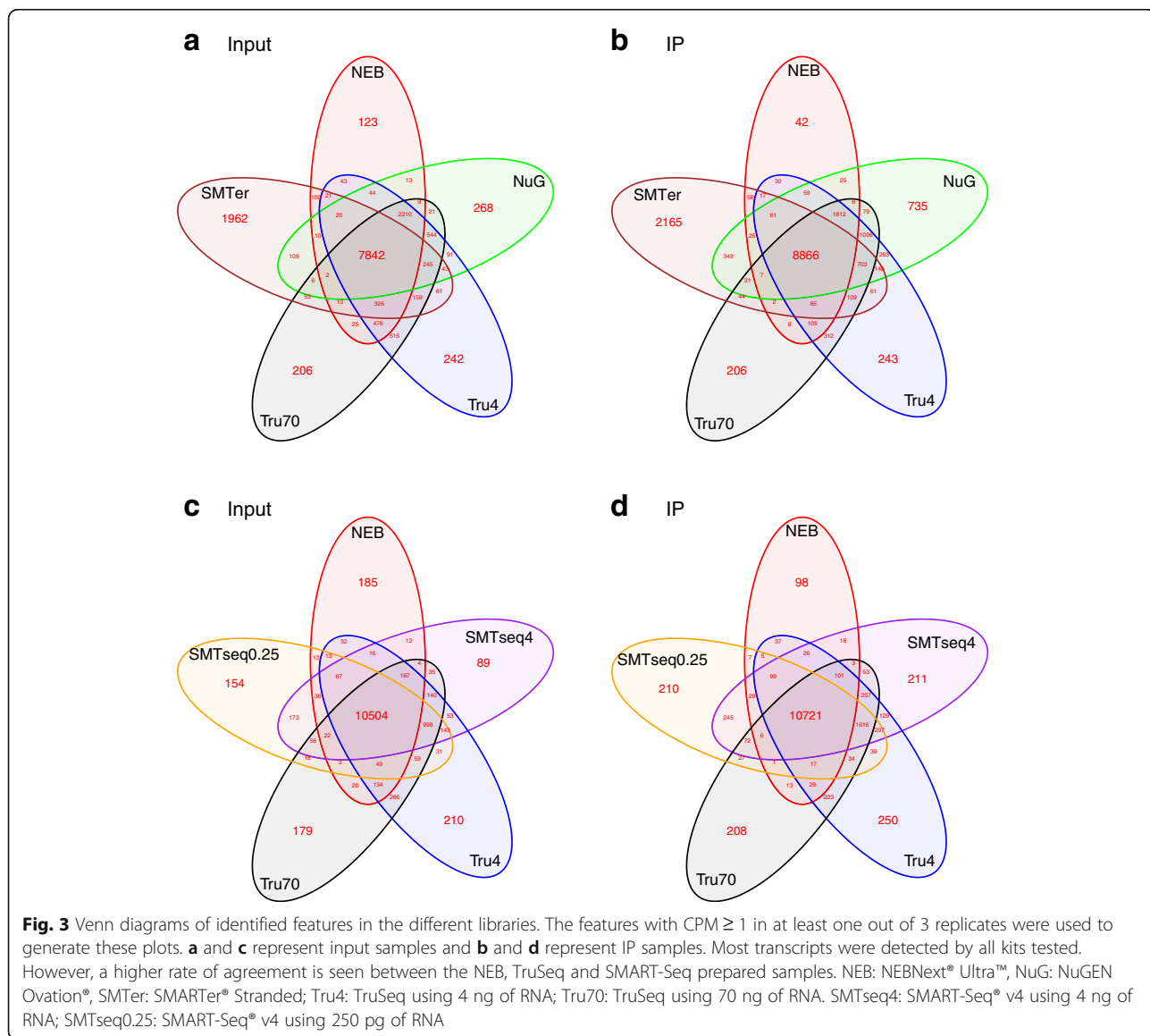


**Table 3** Descriptive statistic of non-coding detected features (CPM >=1)

Kit	Sample type	Total features of ribosomal RNA			Average CPM of ribosomal RNA			Total features of ribosomal RNA, lincRNA, microRNA			Average CPM of ribosomal RNA, lincRNA, microRNA		
		Replicate			Replicate			Replicate			Replicate		
		1	2	3	1	2	3	1	2	3	1	2	3
NEB	Input	3	3	3	73.87	67.33	72.15	233	186	140	46.01	29.22	28.34
	IP	3	3	4	14.24	6.15	7.80	128	157	268	78.05	28.33	34.25
NuG	Input	8	11	10	5533.70	5571.81	5603.65	552	488	415	272.73	274.17	276.54
	IP	13	11	17	1803.34	820.73	863.91	583	593	637	97.91	48.26	51.37
SMTer	Input	8	5	6	4282.62	7858.83	4641.15	440	359	377	247.75	429.65	261.04
	IP	12	6	17	4880.27	7906.14	3936.78	467	411	599	282.51	429.64	240.08
Tru4	Input	17	17	13	232.50	120.94	169.47	804	786	767	13.96	7.59	10.29
	IP	8	7	19	415.93	129.19	168.59	546	650	927	26.49	8.94	11.45
Tru70	Input	6	4	4	102.39	28.55	58.50	410	363	406	6.34	2.08	3.81
	IP	3	3	4	141.53	54.91	65.21	265	295	341	9.24	3.97	5.10
SMTseq4	Input	13	13	21	214.51	159.76	185.17	750	764	803	11.78	8.93	10.54
	IP	7	11	10	851.62	63.75	92.92	844	881	889	46.39	5.91	8.73
SMTseq0.25	Input	6	7	3	224.50	191.46	235.20	531	515	461	12.32	10.52	13.04
	IP	6	6	7	886.27	73.72	99.28	476	502	457	48.03	6.43	8.88

A similar trend is observed in IP samples (Fig. 3b, d and See Additional file 1: Table S3).

We also grouped all of the detected features into ribosomal RNA, non-coding (ribosomal RNA, lincRNA, microRNA) and protein-coding groups. The average CPM of ribosomal RNA and non-coding gene groups were 2-fold higher in NuGEN and SMARTer samples than in other samples (Table 3). Conversely, the average CPMs for the protein-coding group were similar across most samples, except for SMARTer prepared samples

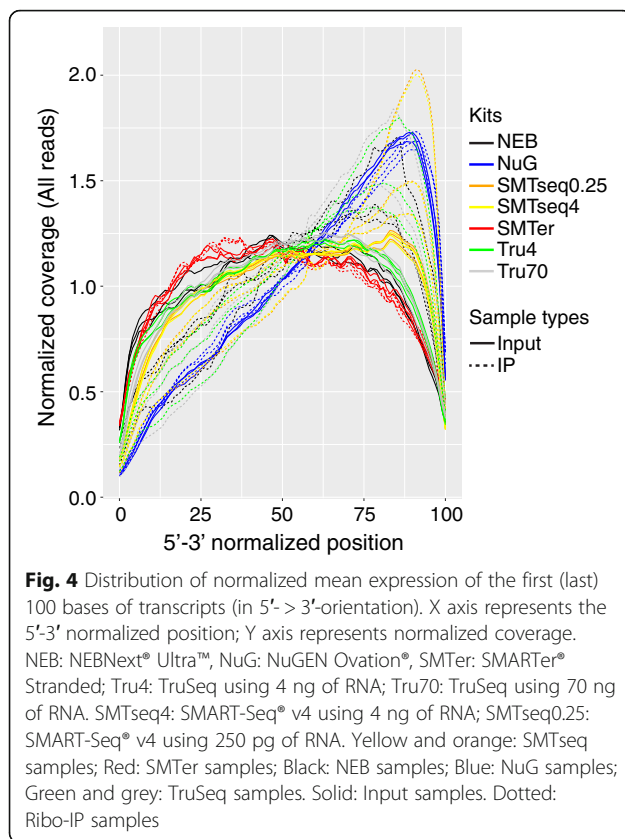
(Table 4). By comparing IP samples with input samples, it is interesting that the CPMs of IP samples are relatively lower than input samples, except for NuGEN prepared samples.

#### Coverage uniformity relative to 5' and 3' ends

The evenness of transcript coverage was calculated by dividing the mean coverage of first (last) 100 bases (5' or 3') of transcripts divided by the mean coverage of all bases across the corresponding transcript (Fig. 4). The median

**Table 4** Descriptive statistic of protein-coding detected features (CPM ≥ 1)

Kit	Sample type	Total features of protein-coding RNA			Average CPM of protein-coding RNA		
		Replicate			Replicate		
		1	2	3	1	2	3
NEB	Input	11,316	10,551	9789	36.51	37.77	37.83
	IP	8740	10,252	12,435	34.13	37.84	37.39
NuG	Input	10,921	10,828	10,656	19.61	19.50	19.32
	IP	12,970	13,142	13,318	32.65	36.35	36.12
SMTer	Input	11,136	9368	10,019	21.47	7.90	20.48
	IP	11,826	11,860	11,824	18.88	7.90	22.02
Tru4	Input	11,826	11,860	11,824	38.90	39.38	39.18
	IP	12,360	12,842	12,941	37.97	39.28	39.09
Tru70	Input	11,690	11,691	11,611	39.47	39.79	39.66
	IP	11,996	12,493	12,660	39.26	39.65	39.56
SMTseq4	Input	11,659	11,499	11,578	39.07	39.28	39.16
	IP	12,443	12,579	12,587	36.50	39.51	39.01
SMTseq0.25	Input	11,500	11,475	11,384	39.03	39.16	38.97
	IP	12,648	12,846	12,940	36.38	39.47	39.29



was calculated and plotted for the 1000 most highly expressed transcripts. Most of the input RNA samples showed even coverage from 5' to 3' end, except for all NuGEN samples which had pronounced increase in coverage at the 3' end. Additionally, consistently higher coverage at the 3' end was observed among IP RNA samples, except for SMARTer samples with even coverage across 5' and 3' extremities.

#### Similarity of expression profiles

In order to assess the similarity of expression profiles being generated by different library preparation kits, we applied Spearman correlation coefficients as a measure of similarity. The Spearman coefficient was calculated based on the rank of the CPM value as opposed to using the absolute values. This was done to accommodate the difference in CPM values due to differences in duplication rates observed among the kits (Fig. 5). The correlation coefficient for input samples ranged from 0.5 to 0.9, where SMARTseq profiles were better correlated with TruSeq70 than others (Spearman correlation coefficient  $\geq 0.9$ ). SMARTer samples had the lowest correlation (0.5) with the control library TruSeq70 (Fig. 5 and See Additional file 1: Table S4). Overall, as expected, input profiles are less correlated to corresponding IP profiles (See Additional file 1: Table S4). When we compared

input samples with corresponding IP samples for each individual kit respectively, all input samples were clustered separately from IP samples except for the SMARTer samples (Additional file 4: Figure S3).

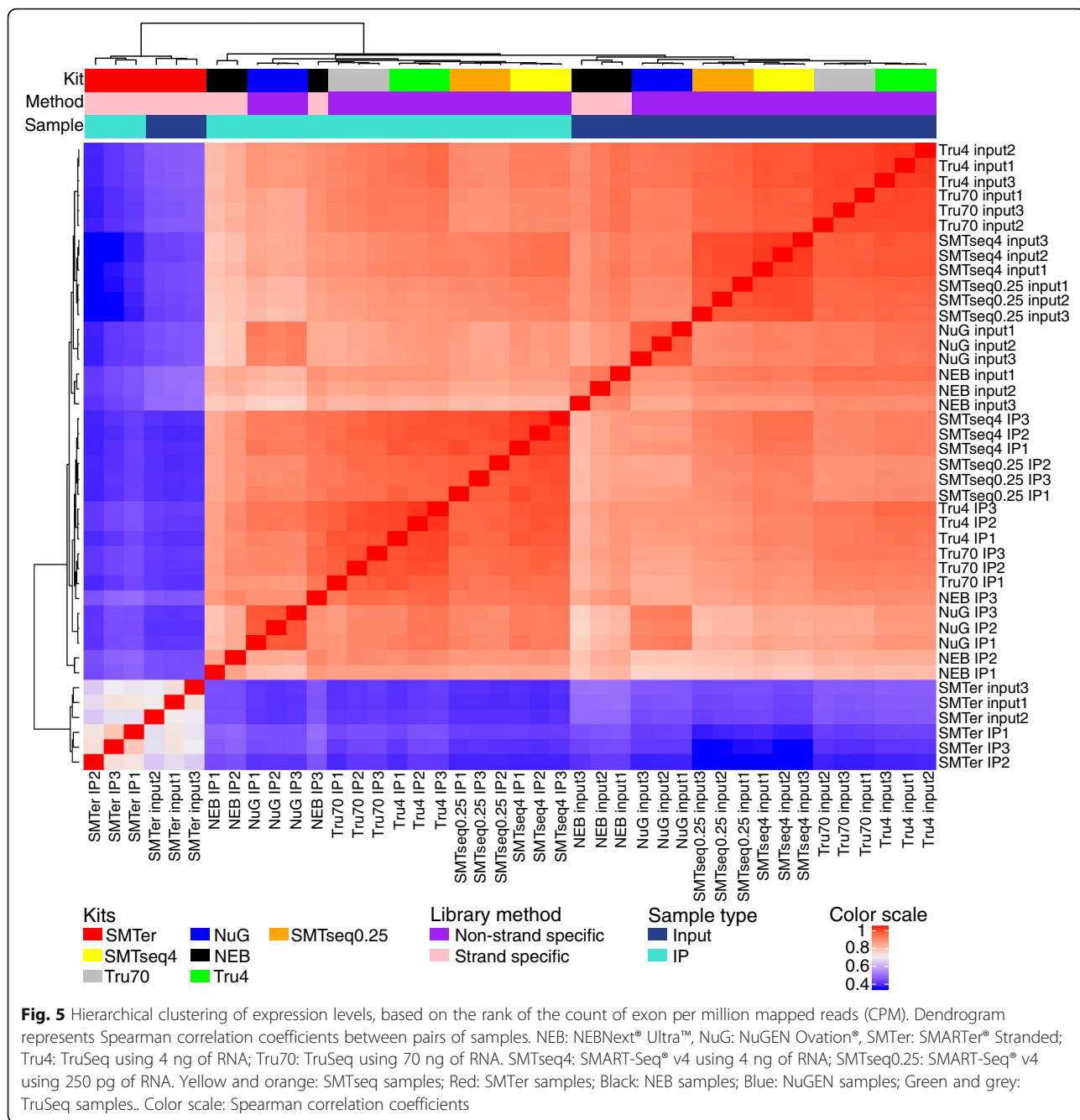
Although two different amounts of RNA were used for the TruSeq library kit, TruSeq 4 ng samples were well correlated with TruSeq 70 ng samples (Spearman correlation coefficient was  $0.96 \pm 0.002$  for input;  $0.946 \pm 0.01$  for IP). Similarly, the SMARTseq samples with 0.25 ng and 4 ng were highly correlated (Spearman correlation coefficient was  $0.95 \pm 0.004$  for input and  $0.95 \pm 0.005$  for IP) (See Additional file 1: Table S4).

#### Transcript enrichment is better represented than transcript depletion in the IP samples

We evaluated the robustness of different kits for detecting enrichment (IP/input RNA  $> 1$ ) or depletion (IP/input RNA  $< 1$ ) of transcripts in the transcriptome (IP samples) compared to the transcriptome (input samples). Features with raw read counts  $\geq 20$  in input samples and with an enrichment or depletion factor  $\geq 2$  were included as enriched (IP/Input  $\geq 2$ ) or depleted transcripts (IP/Input  $\leq 0.5$ ). Of note, more transcripts were enriched than depleted (Fig. 6a and Additional file 5: Figure S4). NuGEN produced the greatest number of enriched transcripts (mean 4270) and smallest number of depleted transcripts (mean 74) as compared with other kits (Fig. 6b). Among the enriched transcripts from NuGEN, 60% were enriched less than 4-fold whereas only 25% of transcripts prepared by other kits were enriched less than 4-fold (Fig. 6b). NEB samples had the highest percentage of enriched/depleted transcripts ( $\log_2(\text{IP}/\text{INPUT}) > 5$  or  $\log_2(\text{INPUT}/\text{IP}) > 5$ ) when compared to samples obtained from the other kits (Fig. 6b, Fig. 7a). Conversely, the enrichment profile of the SMARTer samples showed fewer enriched or depleted transcripts compared with the rest of the samples. Indeed, when plotting for the top 50 enriched transcripts (Fig. 7b), the median enrichment value for the SMARTer profile was significantly lower than other profiles ( $p < 0.05$ ).

We also compared the number of transcripts being enriched or depleted across samples (Additional file 6: Figure S5). NuGEN had the highest number of uniquely enriched transcripts that were detected (accounting for 25% of its total enriched transcripts, 95% of which are protein-coding genes). TruSeq4 and TruSeq70 had around 5% uniquely enriched transcripts (Additional file 6: Figure S5a,b).

We also clustered all the transcripts based on the rank of enrichment factor or depletion factor greater than 2 in at least one sample (Fig. 8). As expected, the profiles for TruSeq4 and TruSeq70 were most similar to each other (Spearman correlation coefficient  $> 0.7$ ). The same is true for SMARTseq4 and SMARTseq0.25. On the

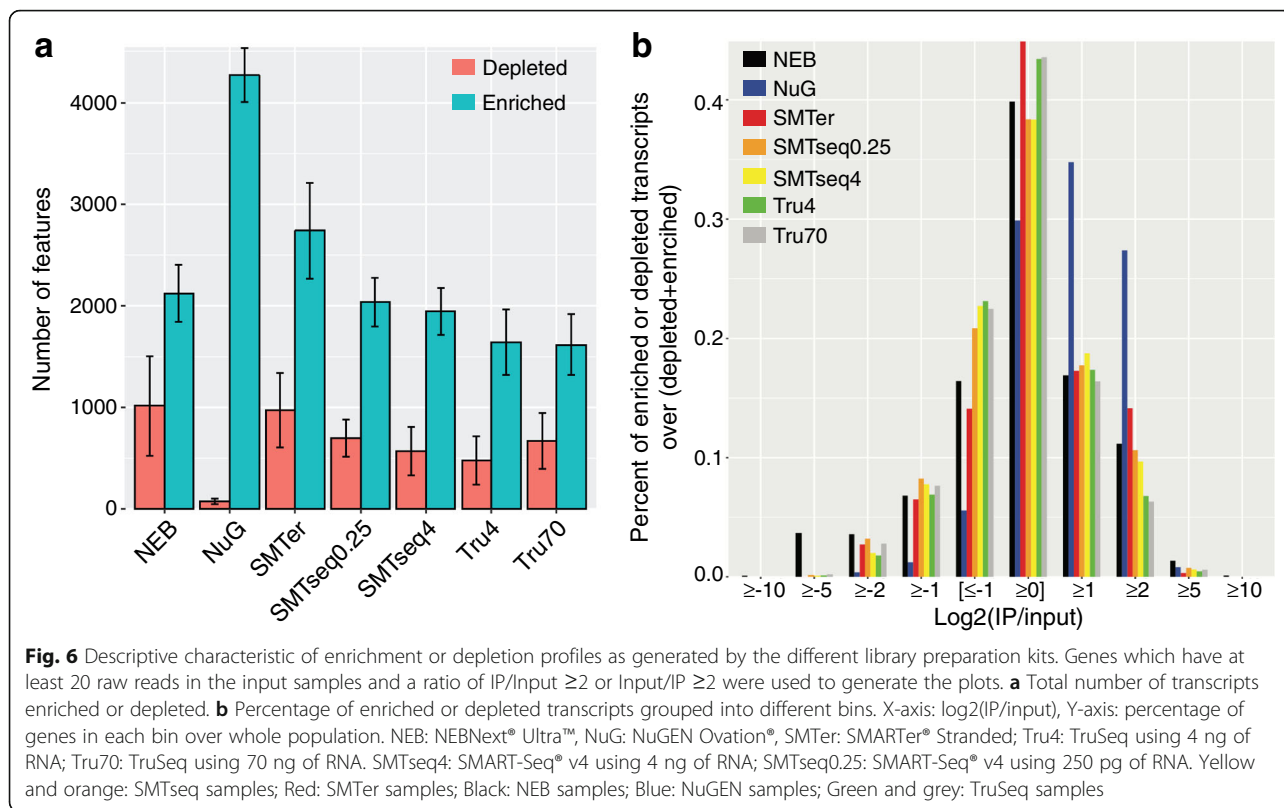


other hand, the enrichment/depletion profile for SMARTer was the least similar to the other profiles (Spearman correlation coefficient < 0.2).

**Transcript-length dependent enrichment/depletion**

We examined whether the enrichment or depletion effects observed in the transcriptome were affected by the transcript length. Based on size distribution of the enriched/depleted transcripts (the majority being between 0.5 and 10 kb, Additional file 7: Figure S6), we grouped the transcripts into four bins (≤0.5 kb, 0.5–1 kb, 1 kb–10 kb, and >

10 kb) (Fig. 9). The median enrichment for transcripts was relatively higher in the longer transcript (> 10 kb) except in TruSeq70 samples (Fig. 9a). Within each transcript length bin, the median enrichment effect from NuGEN and SMARTer samples was much higher than TruSeq70 samples for transcripts less than 10 kb (Fig. 9b). For longer transcripts (> 10 kb), NEB, NuGEN, SMARTer and SMARTseq samples had a median enrichment that is much higher than those of TruSeq70 (Fig. 9b). Additionally, the enrichment effect for NEB samples distributed wider than all the other samples (Fig. 9).

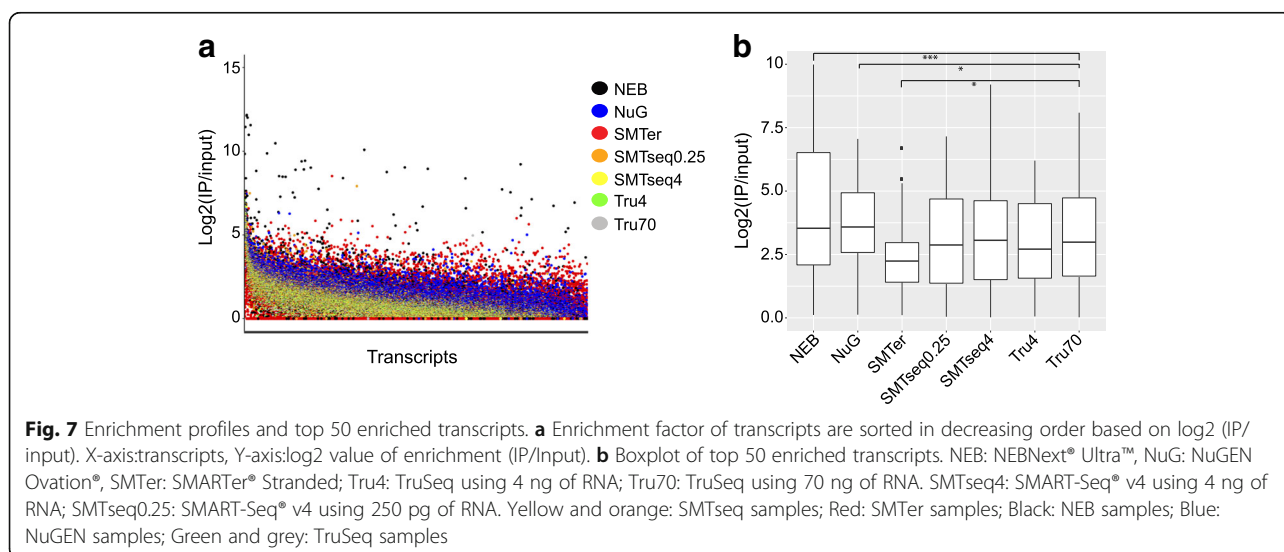


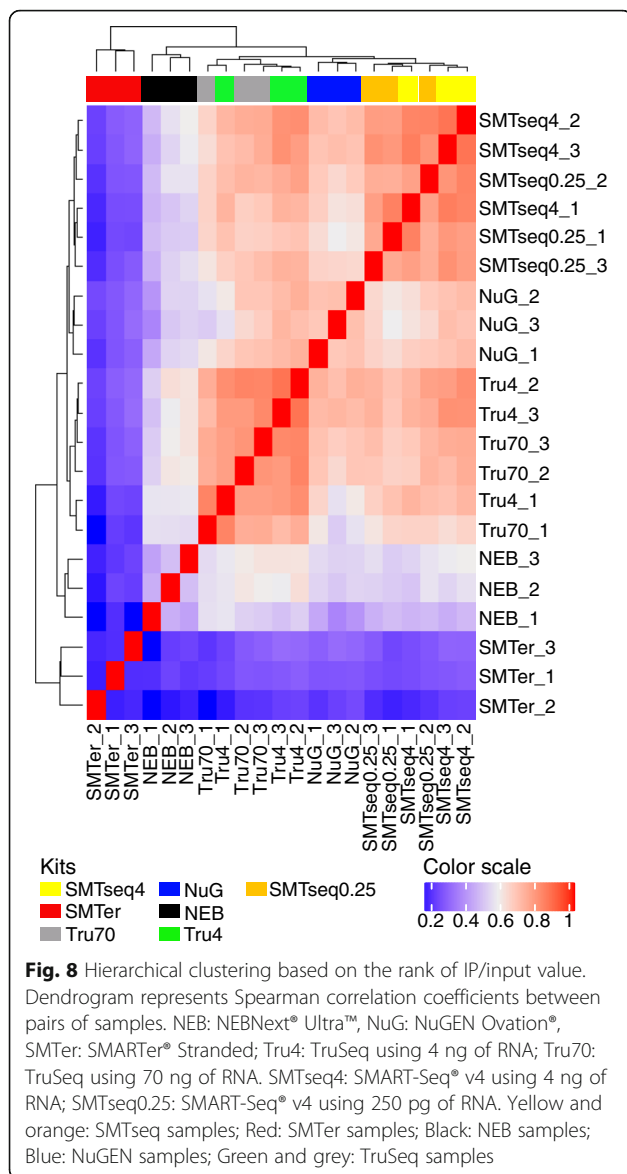
A similar trend was also observed in depleted transcripts. Across all transcript lengths, the range of depletion effect for NuGEN and SMARTer samples was less than for other samples (Fig. 10a). For NEB samples, the depletion effect distribution was wider than all the other samples (Fig. 10b). For longer transcripts (> 10 kb), NEB, NuGEN, SMARTer and SMARTseq samples

showed fewer depletion effects than those from TruSeq70 (Fig. 10b).

### Discussion

In this study, we compared five library-preparation kits for RNA-seq, using low-quantity input or RiboTag IP RNA, by applying a comprehensive set of quality





measures. One of the major differences among library preparation kits was whether oligo (dT) is used to select mRNA. Among the kits tested, the NEBNext® Ultra™, the Illumina TruSeq® and the TaKaRa SMART-Seq® v4 Ultra® use oligo-dT primers to select for polyA mRNA. Conversely, the TaKaRa SMARTer® kit depends on locked nucleic acid (LNA) technology and random primers to capture both products with classical long polyA(+) and those with short poly(A) tails or polyA(-) transcripts and employs a ribosomal depletion step. Although the NuGEN Ovation® V2 kit uses a combination of semi-random hexamers and a poly-dT chimeric primer for 1st strand cDNA amplification in an effort to mitigate bias, 3' end bias was still observed. Shanker, et al.(2015), also observed 3' end bias using the NuGEN Ovation V2 kit with low input samples [22]. Interestingly, we observed

greater 3' end bias in IP samples (except for SMARTer prepared samples) than in the input samples, possibly suggesting some degradation of the RNA.

A higher percentage of reads mapped to the intronic and intergenic region in the samples derived from the TaKaRa SMARTer® kit in comparison to samples derived from the other five kits. Adiconis, et al., 2013 [23], also found a similar difference by comparing the SMARTer® kit to the TruSeq® kit. In our study, among the top-100 highly expressed transcripts in SMARTer samples, 30% were miRNA, lincRNA and rRNA. It is known that the source of miRNA or lincRNA is mainly from intergenic or intronic region, and that certain ribosomal RNAs generated by RNA polymerase I and III are without polyA tails. Therefore, we propose that the SMARTer® kit may be useful for studies which aim to focus on poly(A) negative transcripts or transcripts derived from non-exon-coding regions.

We observed lower duplication rates for the SMART-Seq® v4 Ultra (SMARTseq) and NuGEN prepared samples as compared to samples prepared with the other kits. A possible explanation to this observed lower duplication rate may relate to the protocols of these two kits. The mRNA is pre-amplified to cDNA, before fragmentation, making the duplication rate resulting from the amplification harder to identify based on mapping position. Conversely, in other methods including the TruSeq kit, mRNA is fragmented first and the amplification only happens during the library construction step, making it easier to identify duplication based on the mapping position. For this study, the comparisons among different kits were achieved by using the rank-based method without removal of duplicate reads. Parekh et al., also showed that removal of duplicates improved neither accuracy nor precision and can actually worsen the power and the False Discovery Rate (FDR) for differential gene expression [33].

While Combs et al., (2015) [34] reported the use of the TruSeq kit with 100 ng of RNA, our modification of the TruSeq protocol provides the possibility to use the kit with RNA amounts as low as 4 ng. Indeed, our study, for the first time, shows that with protocol modifications, TruSeq with 4 ng of RNA performs similarly to the TruSeq with 70 ng of RNA with respect to the number of genes being captured and overall profile composition.

Comparing transcriptome (IP samples) against corresponding transcriptome (input samples), we find a relative higher intronic percentage in the transcriptome profiles, which might indicate that some non-mature RNA are precipitated during the IP process. Overall, we detected more enriched transcripts than depleted transcripts in the IP samples. Roh et al., report a similar result although the fold-change was greater in the depleted genes than the enriched genes [35]. This difference may result from the

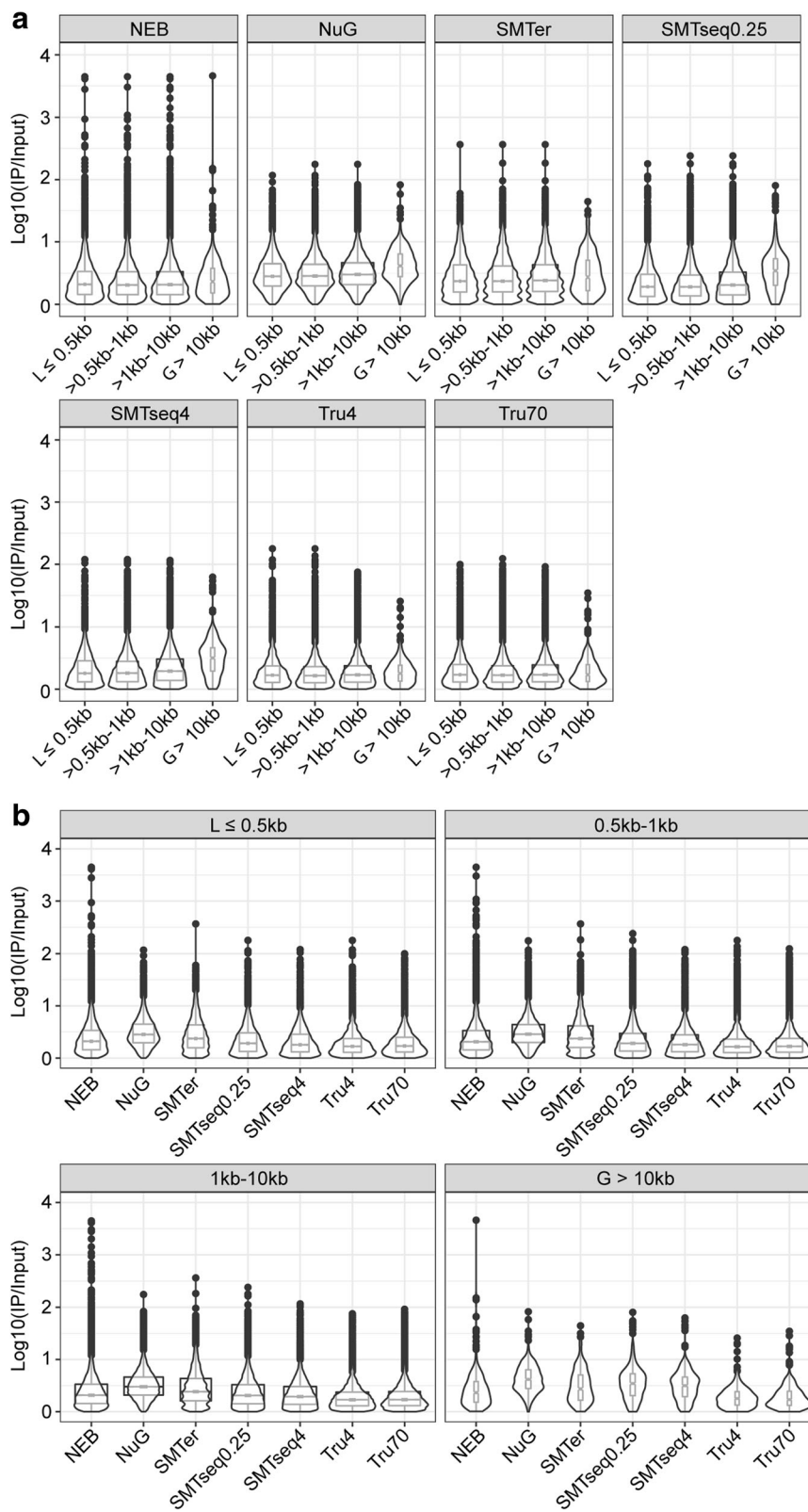


**Fig. 9** Boxplot and violin plots of enriched features over different transcript lengths. **a** Boxplots of enrichment factor of different transcripts within each kit. **b** Boxplots of enrichment factor of different kits at each transcript length bin. The notch represents the median  $\pm 1.58IQR/\sqrt{n}$ . The width of boxplot is proportion to sample size of each group

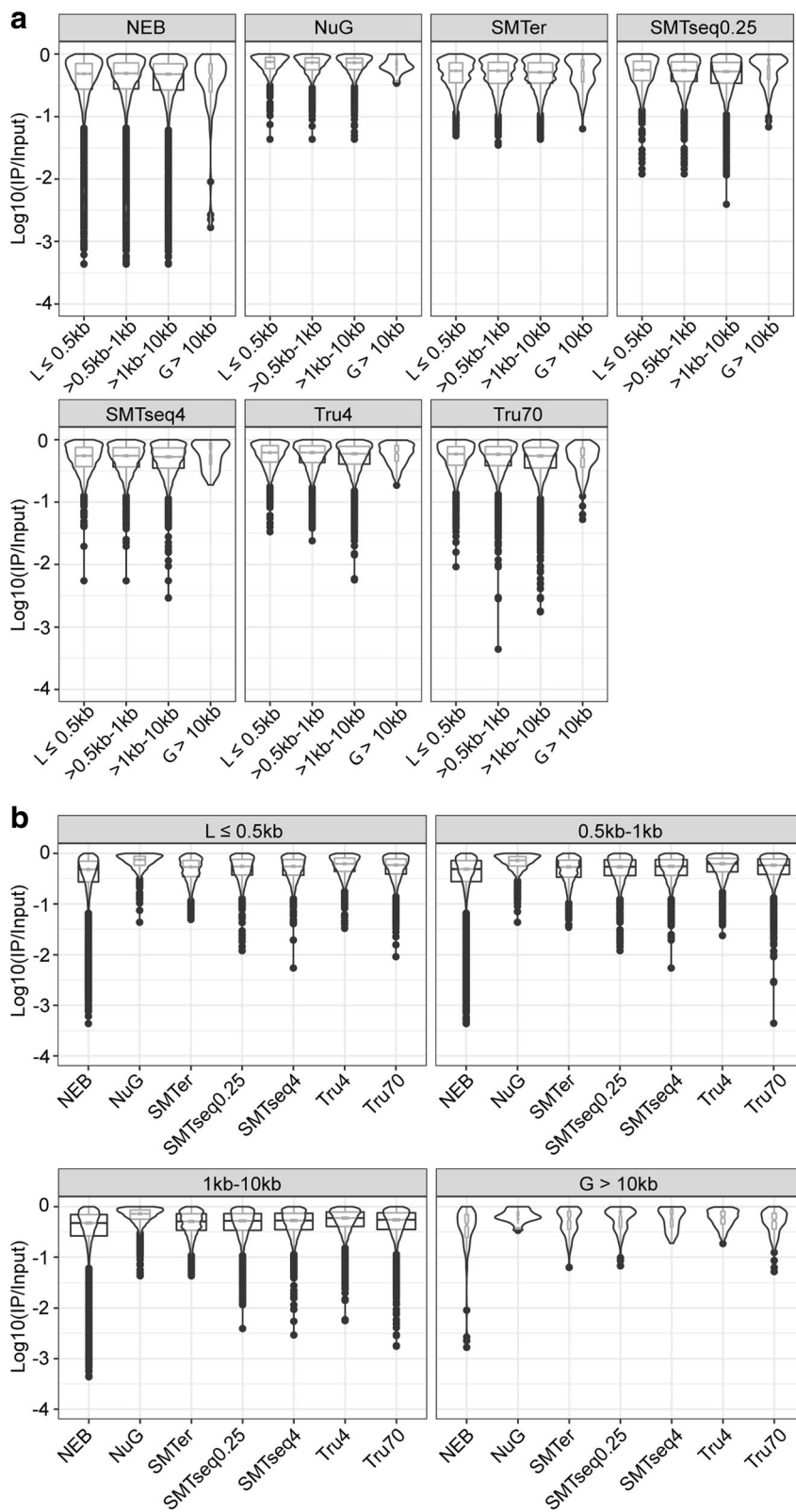


**Fig. 10** Boxplot and violin plots of depletion features over different transcript lengths. **a** Boxplots of depletion factor of different transcripts within each kit. **b** Boxplots of depletion factor of different kits at each transcript length bin. The notch represents the median  $\pm 1.581\text{QR}/\sqrt{n}$ . The width of boxplot is proportion to sample size of each group

different tissues being used, and more specifically the percent of cells that express the tagged ribosomes. Among enriched transcripts, we observed an enrichment effect bias toward longer transcripts (> 10 kb) (Fig. 9a). This may relate to the nature of RiboTag IP since it is a method to detect polysome profiles during translation [16]. It is possible that the higher number of ribosomes on longer transcripts leads to a higher enrichment. In addition, the greater enrichment effect of longer transcript is slightly higher for samples prepared by SMARTer and SMARTseq kits. This may be related to the template-switch oligonucleotide with one locked nucleic acid (LNA) technique applied in these kits, which is aimed to improve the hybridization between the template-switch oligonucleotide and the cDNA product [36, 37], increasing full coverage for longer transcripts.

## Conclusion

Amongst the kits and library prep protocols analyzed in this manuscript, SMART-Seq v4 and TruSeq offer the best sequencing results for library preparation from smaller amounts of RNA as starting material. Indeed, the overall profile of 250 pg/4 ng samples from SMART-Seq v4 was similar to the TruSeq 70, here used as a gold-standard control. SMARTer Stranded Total RNA-Seq Kit might be a good choice to study both polyA(+) mRNA and non-polyA mRNA, especially non-coding RNAs. Since there is a coverage bias towards 3' for IP samples and more enrichment for longer transcripts, correction should be included during comparison among samples, for example, using the bias correction function in Cufflink [38]. Finally, IP RNA from RiboTag samples is likely to include a higher rate of immature RNAs, given the observed increase in intronic sequences in the IP samples across all library prep approaches. Overall, we were able to observe both enriched and depleted transcripts of transcriptome profiles using all kits. Greater enrichment effects were detected than depletion, however this may be related to the percent of tagged ribosomes in the tissue and therefore tissue and Cre-driver specific. In summary, by considering the evenness of coverage, number of detected features, low CPM of non-coding genes, and similar enrichment profiles comparing to standard TruSeq70 prepared samples, the SMARTseq and NEB kits performed the best in comparison to the other kits tested. However, the SMARTseq kit had a lower duplication rate and allows reactions to start with as little as 250 pg, significantly decreasing the necessary amount of starting material. In addition, the modified TruSeq4 protocol provides good results based on the relative high number of detected features, low CPM of non-coding genes, and similarity of the enrichment profile to the standard TruSeq70.

## Additional files

**Additional file 1: Table S1.** Library preparation performed in this study. Table S2 Gene list with RPKM greater than 10,000. Table S3 Median of genes from unique and shared regions of Venn diagram. Table S4 Spearman correlation coefficients between different profiles. (XLSX 28 kb)

**Additional file 2: Figure S1.** Cre recombination in liver cells expressing Gfi1. (a) Cryosection of liver from a cross between a Gfi1-Cre mouse and a TdTomato reporter mouse (Ai14) stained with DAPI and phalloidin. TdTomato is found in a subset of cells in the liver that is likely consistent with Kupffer or endothelial cells. (b) Enrichment of *Gfi1* transcripts in the IP samples as compared to the input samples was assessed by reverse-transcription followed by real time PCR. (PDF 2947 kb)

**Additional file 3: Figure S2.** Duplication rate of each library. X-axis: duplication rate, Y-axis: log10 of reads at different duplication rates. (PDF 622 kb)

**Additional file 4: Figure S3.** Hierarchical clustering of expression levels, based on the rank of the count of exon per million mapped reads (CPM). Dendrograms represent Spearman correlation coefficients between pairs of samples that is 3 replicates for input and 3 replicates for IP. (PDF 233 kb)

**Additional file 5: Figure S4.** Bland-Altman plot (MA plot) of transcriptome (IP samples) and transcriptome (input samples) profiles for each kit. The red lines represent the boundary cutoff [-1,1]. Dots above or below the red line represent the enriched or depleted transcripts. (JPG 587 kb)

**Additional file 6: Figure S5.** Venn diagram of enriched/depleted transcripts (CPM  $\geq 20$  in at least one replicate, mean ratio of enrichment/depletion of the three replicates). The mean ratio IP/input is  $\geq 2$  or input/IP is  $\geq 2$ . (PDF 1063 kb)

**Additional file 7: Figure S6.** Histogram of length distribution for enriched or depleted transcripts. (PDF 353 kb)

## Abbreviations

NEB: NEBNext® Ultra™ Directional RNA Library Prep Kit for Illumina with 4 ng of RNA; NuGEN: NuGEN Ovation® RNA-Seq System V2 with 4 ng of RNA; SMARTer: TaKaRa SMARTer® Stranded Total RNA-Seq Kit-Pico Input Mammalian with 4 ng of RNA; SMARTseq4 and SMARTseq0.25: TaKaRa SMART-Seq® v4 Ultra® Low Input RNA Kit for Sequencing with 4 ng and 0.25 ng of RNA; TruSeq4 and TruSeq70: Illumina TruSeq RNA Library Prep Kit v2 with 4 ng and 70 ng of RNA

## Acknowledgements

We would like to thank Maggie Matern and Benjamin Shuster for critically reviewing this manuscript. This work was supported by R01DC03544 (NIDCD), R01DC013817 (NIDCD) and MR130240 (CDMRP/DoD).

## Funding

This work was supported by R01DC03544 (NIDCD), R01DC013817 (NIDCD) and MR130240 (CDMRP/DoD). The funding sources provided the support for effort and materials, and did not have a role in study design, data collection and analysis, decision to publish or preparation of the manuscript.

## Availability of data and materials

The datasets supporting the conclusions of this article are available in the NCBI Gene Expression Omnibus (GEO) repository under accession number GSE104213 <https://www.ncbi.nlm.nih.gov/geo/query/acc.cgi?acc=GSE104213>. The datasets supporting the conclusions of this article are included within the article and its additional files (Additional files 1, 2, 3, 4, 5, 6, and 7).

## Authors' contributions

YS, BM, ETB, SO, XZ performed the experiments, YS, AS and AM performed the analysis, YS, BM and RH wrote the manuscript, AM, RJM, LT, LS and RH designed and oversaw the project. All the authors read and approved the final manuscript.

## Ethics approval and consent to participate

All procedures involving animals were carried out in accordance with the National Institutes of Health Guide for the Care and Use of Laboratory

Animals and have been approved by the Institutional Animal Care and Use Committee at the University of Maryland, Baltimore (protocol numbers 1,015,003 and 0915006).

#### Consent for publication

Not applicable.

#### Competing interests

The authors declare that they have no competing interests.

#### Publisher's Note

Springer Nature remains neutral with regard to jurisdictional claims in published maps and institutional affiliations.

#### Author details

<sup>1</sup>Institute for Genome Sciences, University of Maryland School of Medicine, Baltimore, MD 21201, USA. <sup>2</sup>Department of Otorhinolaryngology-Head & Neck Surgery, University of Maryland School of Medicine, Baltimore, MD 21201, USA. <sup>3</sup>Genomics and Computational Biology Core, National Institute on Deafness and Other Communication Disorders, Bethesda, MD 20892, USA. <sup>4</sup>Department of Anatomy and Neurobiology, University of Maryland School of Medicine, Baltimore, MD 21201, USA.

Received: 10 November 2017 Accepted: 11 September 2018

Published online: 21 September 2018

#### References

- JM S: Using fluorescence activated cell sorting to examine cell-type-specific gene expression in rat brain tissue. *J Vis Exp* 2015, 99:e52537.
- Jung J, Jung H. Methods to analyze cell type-specific gene expression profiles from heterogeneous cell populations. *Animal Cells and Systems*. 2016;20:113–7.
- Kim T, Lim CS, Kaang BK. Cell type-specific gene expression profiling in brain tissue: comparison between TRAP, LCM and RNA-seq. *BMB Rep*. 2015; 48(7):388–94.
- Chen L, Borozan I, Sun J, Guindi M, Fischer S, Feld J, Anand N, Heathcote J, Edwards AM, McGilvray ID. Cell-type specific gene expression signature in liver underlies response to interferon therapy in chronic hepatitis C infection. *Gastroenterology*. 2010;138(3):1123–33 e1121–1123.
- Li J, Klughammer J, Farlik M, Penz T, Spittler A, Barbieux C, Berishvili E, Bock C, Kubicek S. Single-cell transcriptomes reveal characteristic features of human pancreatic islet cell types. *EMBO Rep*. 2016;17(2):178–87.
- Li M, Jia C, Kazmierkiewicz KL, Bowman AS, Tian L, Liu Y, Gupta NA, Gudiseva HV, Yee SS, Kim M, et al. Comprehensive analysis of gene expression in human retina and supporting tissues. *Hum Mol Genet*. 2014;23(15):4001–14.
- Hertzano R, Elkon R, Kurima K, Morrisson A, Chan SL, Sallin M, Biedlingmaier A, Darling DS, Griffith AJ, Eisenman DJ, et al. Cell type-specific transcriptome analysis reveals a major role for Zeb1 and miR-200b in mouse inner ear morphogenesis. *PLoS Genet*. 2011;7(9):e1002309.
- Cheng L, Zhang S, MacLennan GT, Williamson SR, Davidson DD, Wang M, Jones TD, Lopez-Beltran A, Montironi R. Laser-assisted microdissection in translational research: theory, technical considerations, and future applications. *Appl Immunohistochem Mol Morphol*. 2013;21(1):31–47.
- Asano T, Masumura T, Kusano H, Kikuchi S, Kurita A, Shimada H, Kadowaki K. Construction of a specialized cDNA library from plant cells isolated by laser capture microdissection: toward comprehensive analysis of the genes expressed in the rice phloem. *Plant J*. 2002;32(3):401–8.
- Smalley MJ, Tittley J, O'Hare MJ. Clonal characterization of mouse mammary luminal epithelial and myoepithelial cells separated by fluorescence-activated cell sorting. *In Vitro Cell Dev Biol Anim*. 1998;34(9):711–21.
- Birnbaum K, Shasha DE, Wang JY, Jung JW, Lambert GM, Galbraith DW, Benfey PN. A gene expression map of the Arabidopsis root. *Science*. 2003; 302(5652):1956–60.
- Graham M, Richardson JL, Macara IG. Does facs change gene expression. *Cytometry*. 2015;87:166–75.
- Streets AM, Huang Y. How deep is enough in single-cell RNA-seq? *Nat Biotechnol*. 2014;32(10):1005–6.
- Wu AR, Neff NF, Kalisky T, Dalerba P, Treutlein B, Rothenberg ME, Mburu FM, Mantalas GL, Sim S, Clarke MF, et al. Quantitative assessment of single-cell RNA-sequencing methods. *Nat Methods*. 2014;11(1):41–6.
- Doyle JP, Dougherty JD, Heiman M, Schmidt EF, Stevens TR, Ma G, Bupp S, Shrestha P, Shah RD, Doughty ML, et al. Application of a translational profiling approach for the comparative analysis of CNS cell types. *Cell*. 2008; 135(4):749–62.
- Sanz E, Yang L, Su T, Morris DR, McKnight GS, Amieux PS. Cell-type-specific isolation of ribosome-associated mRNA from complex tissues. *Proc Natl Acad Sci U S A*. 2009;106(33):13939–44.
- Heiman M, Schaefer A, Gong S, Peterson JD, Day M, Ramsey KE, Suarez-Farinas M, Schwarz C, Stephan DA, Surmeier DJ, et al. A translational profiling approach for the molecular characterization of CNS cell types. *Cell*. 2008;135(4):738–48.
- Brar GA, Weissman JS. Ribosome profiling reveals the what, when, where and how of protein synthesis. *Nat Rev Mol Cell Biol*. 2015;16(11):651–64.
- Shigeoka T, Jung H, Jung J, Turner-Bridger B, Ohk J, Lin JQ, Amieux PS, Holt CE. Dynamic axonal translation in developing and mature visual circuits. *Cell*. 2016;166(1):181–92.
- Levin JZ, Yassour M, Adiconis X, Nusbaum C, Thompson DA, Friedman N, Gnirke A, Regev A. Comprehensive comparative analysis of strand-specific RNA sequencing methods. *Nat Methods*. 2010;7(9):709–15.
- Faherty SL, Campbell CR, Larsen PA, Yoder AD. Evaluating whole transcriptome amplification for gene profiling experiments using RNA-Seq. *BMC Biotechnol*. 2015;15:65.
- Shanker S, Paulson A, Edenberg HJ, Peak A, Perera A, Alekseyev YO, Beckloff N, Bivens NJ, Donnelly R, Gillaspay AF, et al. Evaluation of commercially available RNA amplification kits for RNA sequencing using very low input amounts of total RNA. *J Biomol Tech*. 2015;26(1):4–18.
- Adiconis X, Borges-Rivera D, Satija R, DeLuca DS, Busby MA, Berlin AM, Sivachenko A, Thompson DA, Wysoker A, Fennell T, et al. Comparative analysis of RNA sequencing methods for degraded or low-input samples. *Nat Methods*. 2013;10(7):623–9.
- Matern M, Vijayakumar S, Margulies Z, Milon B, Song Y, Elkon R, Zhang X, Jones SM, Hertzano R. Gfi1Cre mice have early onset progressive hearing loss and induce recombination in numerous inner ear non-hair cells. *Sci Rep*. 2017;7:42079.
- Pearson WR, Wood T, Zhang Z, Miller W. Comparison of DNA sequences with protein sequences. *Genomics*. 1997;46(1):24–36.
- Orvis J, Crabtree J, Galens K, Gussman A, Inman JM, Lee E, Nampally S, Riley D, Sundaram JP, Felix V, et al. Ergatis: a web interface and scalable software system for bioinformatics workflows. *Bioinformatics*. 2010;26(12):1488–92.
- Kim D, Perteu G, Trapnell C, Pimentel H, Kelley R, Salzberg SL. TopHat2: accurate alignment of transcriptomes in the presence of insertions, deletions and gene fusions. *Genome Biol*. 2013;14(4):R36.
- Anders S, Huber W. Differential expression analysis for sequence count data. *Genome Biol*. 2010;11(10):R106.
- Quinlan AR, Hall IM. BEDTools: a flexible suite of utilities for comparing genomic features. *Bioinformatics*. 2010;26(6):841–2.
- Mortazavi A, Williams BA, McCue K, Schaeffer L, Wold B. Mapping and quantifying mammalian transcriptomes by RNA-Seq. *Nat Methods*. 2008; 5(7):621–8.
- Krzywinski M, Altman N. Visualizing samples with box plots. *Nat Methods*. 2014;11(2):119–20.
- Yang H, Gan J, Xie X, Deng M, Feng L, Chen X, Gao Z, Gan L. Gfi1-Cre knock-in mouse line: a tool for inner ear hair cell-specific gene deletion. *Genesis*. 2010;48(6):400–6.
- Parekh S, Ziegenhain C, Vieth B, Enard W, Hellmann I. The impact of amplification on differential expression analyses by RNA-seq. *Sci Rep*. 2016;6:25533.
- Combs PA, Eisen MB. Low-cost, low-input RNA-seq protocols perform nearly as well as high-input protocols. *PeerJ*. 2015;3:e869.
- Roh HC, Tsai LT, Lyubetskaya A, Tenen D, Kumari M, Rosen ED. Simultaneous transcriptional and Epigenomic profiling from specific cell types within heterogeneous tissues in vivo. *Cell Rep*. 2017;18(4):1048–61.
- Picelli S, Bjorklund AK, Faridani OR, Sagasser S, Winberg G, Sandberg R. Smart-seq2 for sensitive full-length transcriptome profiling in single cells. *Nat Methods*. 2013;10(11):1096–8.
- Picelli S, Faridani OR, Bjorklund AK, Winberg G, Sagasser S, Sandberg R. Full-length RNA-seq from single cells using Smart-seq2. *Nat Protoc*. 2014;9(1): 171–81.
- Trapnell C, Williams BA, Pertea G, Mortazavi A, Kwan G, van Baren MJ, Salzberg SL, Wold BJ, Pachter L. Transcript assembly and quantification by RNA-Seq reveals unannotated transcripts and isoform switching during cell differentiation. *Nat Biotechnol*. 2010;28(5):511–5.

**Join us for the 3<sup>rd</sup> Auditory and Vestibular Translational Research Day, organized by the Center for Comparative and Evolutional Biology of Hearing, of the University of Maryland**

**Monday October 16, 2017, 8:15am-3:30pm**

Southern Management Corporate Center: 2<sup>nd</sup> floor - Elm Room 210B, 621 W. Lombard Street, Baltimore, MD 21201  
 Parking is available on Penn Street or Pratt Street Garage – 120 Penn Street.

**This year the meeting focus area is Noise Induced and Acquired Hearing Loss**

Time	Speaker	Title
8:15-8:45	Gathering and continental breakfast	
8:45-9:00	<b>Ronna Hertzano, MD PhD</b> <i>University of Maryland, Baltimore</i> <b>Catherine Carr, PhD</b> <i>University of Maryland, College Park</i>	Opening Remarks  CCEBH T32 Grant Updates
9:00-9:30	<b>Samira Anderson, AuD PhD</b> <i>University of Maryland, College Park</i>	Introduction to Occupational Noise Exposure
9:30-10:30	<b>Sharon Kujawa, PhD (Keynote)</b> <i>Harvard Medical School, Eaton-Peabody Laboratories</i>	Noise-Induced Cochlear Synaptopathy: Basic Observations Informing Clinical Translation
10:30-11:00	Coffee Break	
11:00-11:40	<b>Ronna Hertzano, MD PhD</b> <i>University of Maryland, Baltimore</i>	A Molecular Blueprint for Noise Induced Hearing Loss
11:40-12:20	<b>Lisa Cunningham, PhD</b> <i>NIDCD, NIH</i>	Cisplatin is Retained in the Cochlea Indefinitely Following Chemotherapy
12:20-13:00	Lunch Break	
13:00-14:00	<b>Colleen Le Prell, AuD PhD (Keynote)</b> <i>UT Dallas, School of Behavioral and brain Sciences</i>	Development of Novel Therapeutics for Prevention of Acquired Hearing Loss: From Animal Models to Clinical Trials
14:00-14:40	<b>Amanda Lauer, PhD</b> <i>Johns Hopkins University</i>	Effects of Hearing Loss and Noise on the Brainstem
14:40-15:20	<b>Doug Brungart, PhD</b> <i>Walter Reed National Military Medical Center</i>	Acoustic and Non-Acoustic Factors Influencing Speech Intelligibility in Real-World Environments
15:20-15:30	<b>Sandra Gordon-Salant, PhD</b> <i>University of Maryland, College Park</i>	Closing Remarks



UNIVERSITY OF MARYLAND  
SCHOOL OF MEDICINE  
Office of Animal Welfare Assurance

**COPY**

655 W. Baltimore Street  
BRB, Mezzanine Ste. M023  
Baltimore, MD 21201-1559

email: [iacuc@som.umaryland.edu](mailto:iacuc@som.umaryland.edu)  
voice: (410) 706-7859 / 8470  
Assurance Number: A3200-01

DATE: August 31, 2018

TO: Ronna Hertzano, M.D., Ph.D.  
Department of Otorhinolaryngology  
16 S Eutaw St. Suite 500

FROM: Institutional Animal Care and Use Committee

RE: IACUC PROTOCOL #0818004  
"Understanding the molecular basis of acquired hearing loss"

---

This is to certify that the Institutional Animal Care and Use Committee received your response to their queries and that your response was considered sufficient to grant FULL APPROVAL to your protocol.

An annual report must be submitted to the IACUC one month before each anniversary of the protocol. Please note that your protocol will expire on August 17, 2021. If you need to extend the protocol beyond this date, you must submit a new animal use protocol at least 3 months prior to the expiration.

*If you have any questions, please do not hesitate to contact the Office of Animal Welfare Assurance by email ([iacuc@som.umaryland.edu](mailto:iacuc@som.umaryland.edu)) or by phone (706-7859 / 8470).*



John B. Sacci, Jr., Ph.D.  
IACUC Chair

PN

AUG 30 2018

Office of Animal  
Welfare Assurance

# New Animal Use Protocol (AUP) Submission Checklist

\*\*\*This checklist has been prepared to assist PIs with a new AUP submission. Please check off each relevant item applicable to this protocol. The protocol will not be accepted without this form. Additionally, incomplete protocols will be returned.\*\*\*

- Animal Use Protocol (AUP) Form (*Version Date: 10/2017*)
- Flow Diagram for each experiment planned in the protocol
- Electronic copy of funded grant(s) supporting this work** (*Emailed to IACUC on: 8/27/2018*)
- All Species (x NHP) Enrichment / Socialization Form (*Version Date: 08/2014*)
- Non-Human Primate (NHP) Enrichment / Socialization Addendum (*Version Date: 06/2014*)
- Rodent Breeding Addendum (*Version Date: 07/2015*)
- Hazardous Agent Addendums (*Version Date: 10/2017*)
- Satellite Housing Addendum (*Version Date: 10/2017*)
- IBC Approval Letter or IBC application status: \_\_\_\_\_
- RSC Approval Letter or RSC application status: \_\_\_\_\_
- ESCRO Approval Letter or ESCRO application status: \_\_\_\_\_
- UMMC Administration Approval Letter or UMMC Review Status: \_\_\_\_\_
- Survival Surgery Consult *\*ALL SPECIES\**  
Date of Consult (*within last 3 months*): 8/1/18  
Veterinarian Consulted: Dr Turhan Coksaygan
- Non-survival Surgery Consult *\*USDA covered species only\**  
Date of Consult (*within last 3 months*): \_\_\_\_\_  
Veterinarian Consulted: \_\_\_\_\_
- BVAMC Attending Veterinarian Review & Signature (*on AUP form*)
- BVAMC SRS Approval or RPSS application status: \_\_\_\_\_

I certify that all required components of a new AUP submission (*as applicable*) are attached and complete.

Ronna Hertzano \_\_\_\_\_  
*PI or PI Designee Name (printed)*

OAWA Internal Use:

\_\_\_\_\_ All Relevant Items Attached  
\_\_\_\_\_ Current versions utilized  
\_\_\_\_\_ Adherence to AUP format

IACUC # \_\_\_\_\_

AUP Date Rec'd: \_\_\_\_\_

OAWA Staff Initials: \_\_\_\_\_  
Date: \_\_\_\_\_

**UNIVERSITY OF MARYLAND SCHOOL OF MEDICINE  
INSTITUTIONAL ANIMAL CARE AND USE COMMITTEE  
-- ANIMAL USE PROTOCOL --**

Principal Investigator: Ronna Hertzano Degree: MD PhD Employee ID#: n/a  
Campus Mail Address: 16 S Eutaw St. Suite 500 Dept: Otorhinolaryngology Head and Neck Surgery  
E-mail: rhertzano@som.umaryland.edu Office Phone: 410-706-4761  
Emergency Contact # (24 hr access): 410-608-9695  
Secondary Contact: Beatrice Milon Email: bmilon@som.umaryland.edu Phone: 410-706-2551

AUP Title: Understanding the molecular basis of acquired hearing loss

## I. RESEARCH CATEGORIES

Major Categories of Research: Please check all that apply.

- Antibody Production
- Behavioral Studies
- Breeding (*\*attach breeding protocol as an addendum to the experimental protocol. Breeding template on [OAWA Website](#)*)
- Chronic or Prolonged Restraint
- Exogenous Substances (*e.g., any substance administered to an animal except anesthetics or analgesics*)
- Euthanize and Harvest Tissue
- Food / Fluid Regulation
- Hazardous Agents
- Imaging
- Investigational Device
- Irradiation
- Non-Survival Surgery
- Oncology / Tumor Production
- Physiologic Measurements (*e.g., blood pressure, telemetry, electrophysiology, etc.*)
- Sampling** (*e.g., blood, urine, bone marrow, biopsies, etc. – collected antemortem*)
- Satellite Housing [*e.g. animals maintained outside animal facility >12 hours (USDA) or >24 hours (rodents)*]
- Specialized Diet
- Specialized Husbandry** (*e.g., Singly housed animals, BSL3 housing, metabolic cages, reverse light cycle, etc.*)
- Survival Surgery
  - Multiple Survival Surgery (*e.g., major + minor surgeries or multiple minor surgeries in one animal*)
  - Multiple Major Survival Surgery (*e.g., opening body cavity more than once in one animal*)
- Teaching / Training
- Use of Hospital Equipment [*(e.g., imaging or radiation producing equipment) \*refer to Use of Hospital Equipment Guidelines on [OAWA Website](#)*]

Will the animal work proposed in this protocol be carried out under Good Laboratory Practices (GLP) in support of, or intended to support, applications for research or marketing permits for products regulated by the Food and Drug Administration (FDA) or the Environmental Protection Agency (EPA), e.g., human and animal drugs, medical devices for human use, etc.?  YES or  NO

*If YES, please contact the [SOM GLP Office](#) (410-706-5180) for more information.*

## II. CATEGORY OF PAIN OR DISTRESS

Only the highest category of pain or distress should be indicated.

- CATEGORY B – Animals bred, conditioned or held for use in teaching, testing, research, but not yet used for such purposes. (*NOTE: If tail snips are necessary for genotyping, this category is not appropriate.*)

- CATEGORY C** – Procedures that involve no or only very brief pain or distress, with no need for or use of pain relieving drugs.
- CATEGORY D** – Procedures involving potential pain or distress for which appropriate anesthetics, analgesics, or tranquilizers are given. (NOTE: Contact Veterinary Resources for “appropriate” agents as needed)
- CATEGORY E** – Painful or distressful procedures for which drugs to relieve the pain or distress would adversely affect the research study. Under ‘Detailed Description of Animal Procedures’ in the written protocol, please include subheading Category E Justification and provide strong scientific justification for conducting procedures that involve unrelieved pain or distress. This justification should address a) why analgesics, anesthetic and/or sedatives cannot be used to relieve pain and/or distress, and b) what steps will be taken to minimize the time in which the animals experience unrelieved pain and/or distress, i.e., use of humane alternative endpoints. If death must be used as an endpoint, please justify.

**III. FUNDING SOURCE (CURRENT)**

Provide one copy of each funded grant for IACUC file. At a minimum, the Research Methods and Vertebrate Animal Section should be included with the submission.

- US Public Health Service (e.g., NIH)
- Department of Veterans Affairs
  - This research is funded by the Department of Veterans Affairs, or
  - This research is administered through the Baltimore BREF
- Private or Charitable Foundation
- Private Company
- Departmental Funds
- Other Department of Defense

Sponsor / Agency	Grant Identification Number*	Grant Title
Department of Defense	MR130240	Towards a Molecular Understanding of Noise Induced Hearing Loss
NIH	DC013817	Cell Type Specific Transcriptional Cascades in Inner Ear Development
NIH	DC003544	Autosomal Dominant Non-Syndromic Hearing Loss

Please add rows to these tables by placing cursor at end of last row and clicking return.

Does the PI or any of the research staff have a financial interest related to the proposed research or the sponsor that must be disclosed accordingly to UMB’s Policy on Conflicts of Interest in Research and Development and UMB’s Policy and Procedures on Financial Conflict of Interest to Promote Objectivity in Public Health Service-Funded Research?

YES or  NO

If YES, please contact the Research Integrity Office and speak with Alison Watkins (410-706-1266).

**IV. EXPERIMENTAL ANIMAL USAGE**

Each species (by age) should be listed separately. This table is for adult and/or juvenile (post-weaning) experimental animals only. \*\*Strain designations and the number of breeders are no longer required in this table. # of breeders should be provided in the Breeding Addendum only.

Species	Age	Weight range (USDA Covered Species Only)	Sex	Total # (for 3 yrs)	Max. Daily Census*

<b>Mouse</b>	<input checked="" type="checkbox"/> Juvenile ( <i>weaned</i> ) or Adult <input type="checkbox"/> Timed pregnant <input type="checkbox"/> Dams w/ pups <input type="checkbox"/> Other - <i>Specify</i> :		<input type="checkbox"/> Male <input type="checkbox"/> Female <input checked="" type="checkbox"/> Both	<b>736</b>	<b>88</b>
--------------	--	--	--	------------	-----------

\*Max. Daily Census = approximate number of animals to be housed in the facility on any given day. Please note that this information is necessary to plan for housing space and should be expressed in whole numbers.

\*\*Please add rows to these tables by placing cursor at end of last row and clicking return.

Will embryonic and/or pre-weaning animals be used at any time during this protocol?  YES  NO

If yes, state species, age and number required for 3-year protocol (estimations based upon species characteristics or lab experience are acceptable).

Species	Age (days)	Total # (for 3 yrs)
<b>Mouse</b>	<b>P10-P11 and P15-P16</b>	<b>32</b>

Will additional animals be required for training current or new staff on proposed animal procedures?  YES  NO

If yes, state species, age and number required for 3-year protocol. Under 'Detailed Description of Animal Procedures' in the written protocol, please discuss training procedures.

Species	Age (days)	Total # (for 3 yrs)

#### V. HAZARDOUS AGENT(S) IDENTIFICATION

Please contact [EHS](#) for assistance as needed. [Link to Hazardous Agent Addendums.](#)

Will pathogenic organisms be utilized in live animals in this protocol?  YES  NO

If yes, complete a hazardous agent addendum for each pathogenic organism.

Will recombinant DNA be utilized in live animals in this protocol?  YES  NO

If yes, complete a hazardous agent addendum for each category, e.g., rDNA, plasmids, siRNA, viral vectors, recombinant cells, etc.

Will radioactive materials be utilized in live animals in this protocol?  YES  NO

If yes, complete a hazardous agent addendum for each radioactive material.

Will hazardous chemicals be utilized in live animals in this protocol?  YES  NO

If yes, complete a hazardous agent addendum for each chemical level, e.g., CL1 or CL2.

Please refer to [EHS Hazardous Chemical Use in Animal Research](#) website for guidance.

#### VI. METHOD OF EUTHANASIA

Please list each method of euthanasia to be used in this protocol. Please refer to the [Recommended Methods of Euthanasia](#) located on the OAWA Website under Guidelines. *Method and description can be cut and pasted into the below table.*

SPECIES	METHOD	DESCRIPTION
<b>Adult mice</b>	<b>Asphyxiation using CO2 followed by cervical dislocation.</b>	<b>Using a non-precharged chamber, CO2 is dispensed from a commercial cylinder with fixed pressure regulator and inline restrictor controlling gas flow within 20%-30% of the chamber volume per minute to comply with 2013 AVMA Guidelines. CO2 flow will be maintained for &gt; 60 seconds following respiratory arrest (which may take up to 5 minutes), followed by cervical dislocation to assure euthanasia.</b>

<b>Neonate mice</b>	<b>Decapitation by sharp scissors of neonates</b>	<b>Neonates &lt; 7 days of age: decapitation performed with sharp scissors without sedation or anesthesia</b>

\*\*Please add rows to this table by placing cursor at end of last row and clicking return.

#### VII. LOCATION OF ANIMAL USAGE

BUILDING / RM #	LAB	ANIMAL FACILITY	LIST PROCEDURES TO BE PERFORMED IN LIVE ANIMALS IN THIS LOCATION (e.g., surgery, injections, behavior, imaging, euthanasia, etc.)
HSF1 Rm 643A	<input type="checkbox"/>	<input checked="" type="checkbox"/>	Housing of mice, euthanasia, Tamoxifen injection, <b>Auditory Brainstem Responses (ABR) and Distortion product otoacoustic emissions (DPOAE)</b> measurements, Heat Shock, Noise Exposure.
Biopark 1, Rm 404/405	<input checked="" type="checkbox"/>	<input type="checkbox"/>	Housing of mice up to 23 hours, euthanasia.
	<input type="checkbox"/>	<input type="checkbox"/>	
	<input type="checkbox"/>	<input type="checkbox"/>	
	<input type="checkbox"/>	<input type="checkbox"/>	

\*\*Please add rows to this table by placing cursor at end of last row and clicking return.

#### VIII. CONSIDERATION OF ALTERNATIVES TO POTENTIALLY PAINFUL / DISTRESSFUL PROCEDURES

Keep copies of computer database search results in your protocol file for a minimum of three years after the protocol has expired to demonstrate your compliance with the law if regulatory authorities or the IACUC should choose to audit your project. Refer to instructions for further information regarding the completion of this section.

- Does the study include procedures that have the potential for producing more than momentary or slight pain or distress?  YES or  NO If yes, complete questions 2-5.
- What are the potentially painful procedures or distressful conditions proposed in this animal use protocol?
  - measurement of hearing thresholds (animals are anesthetized);
  - Injection of Tamoxifen for induction of gene expression;
  - Noise exposures;
  - Heat shock (animals are anesthetized).
- A literature search for alternatives to the potentially painful or distressful procedures (listed above) was performed. Search methods and sources are documented in table below:

Name of Database Searched: (Minimum of 2)	Date search was performed: (mm/dd/yy)	Years covered by the search: (from yyyy to yyyy)	Search Strategies used: (including scientifically relevant terminology and Boolean operators)	# of hits:	# of relevant hits:
PubMed	07/18/18	1980-2018	Noise induced hearing loss AND Ribotag	0	
PubMed	07/18/18	1980-2018	Ribotag AND cochlea	0	
PubMed	07/18/18	1980-2018	RNA seq AND nihl	3	3
PubMed	07/18/18	1980-2018	nihl AND sex AND mouse	4	3
PubMed	07/18/18	1980-2018	nihl AND "cell-type"	6	4
PubMed	07/18/18	1980-2018	ribotag AND prestinCre	0	
PubMed	07/18/18	1980-2018	ribotag AND Sox2Cre	0	
Google Scholar	07/18/18	1980-2018	Noise induced hearing loss AND Ribotag	16	1
Google Scholar	07/18/18	1980-2018	Ribotag AND cochlea	13	1
Google Scholar	07/18/18	1980-2018	RNA seq AND nihl	260	12

Google Scholar	07/18/18	1980-2018	nihl AND sex AND mouse	513	7
Google Scholar	07/18/18	1980-2018	nihl AND "cell-type"	288	1
Google Scholar	07/18/18	1980-2018	ribotag AND prestinCre	0	
Google Scholar	07/18/18	1980-2018	ribotag AND Sox2Cre	3	0

Database Resources: [UMB HS-HSL Databases](#) and [AWIC](#)

4. Did the literature search reveal less painful or distressful alternatives to the potentially painful or distressful procedures that are proposed?

No alternatives, refinements, replacements or reduction methods were found.

Yes, but they cannot replace the procedures that are proposed. *See below explanation.*

a. If yes, identify the painful or distressful procedures(s) and provide a BRIEF explanation why the alternatives found to this potentially painful or distressful procedure(s) were not acceptable alternatives.

[Click here to enter text.](#)

5. List other sources of information used to refine this protocol, as applicable.

Since our previous protocol (#0915006), we have optimized the RNA-sequencing step to be able to use only 4 animals per replicate instead of 8 animals.

#### PRINCIPAL INVESTIGATOR'S ACKNOWLEDGEMENT OF RESPONSIBILITY

I acknowledge and accept the responsibilities associated with serving as the principal investigator of an IACUC protocol as delineated in the OAWA [Principal Investigator Manual](#).

I will conduct the project in accordance with the [PHS Policy on Humane Care and Use of Laboratory Animals](#), [USDA regulations \(9 CFR parts 1, 2, 3\)](#), the [Federal Animal Welfare Act \(7 USC 2131 et. Seq.\)](#), and the [Guide for the Care and Use of Laboratory Animals](#).

I authorize individuals listed on this application to conduct procedures involving animals and I accept responsibility for their oversight in the conduct of this proposal.

I confirm that all individuals working with animals have completed the [IACUC required training](#) and are participating in an appropriate [Occupational Health & Safety program](#). Further, I certify that those individuals are properly trained, or will receive such training prior to working with animals, in all areas relevant to their assigned work with animals (e.g., biology, handling, and care of the species used; aseptic surgical methods and techniques; the concept, availability, and use of research or testing methods that limit the use of animals or minimize distress; the proper use of anesthetics & analgesics; and procedures for reporting animal welfare concerns).

For animals under this proposal, I understand that in cases of necessary medical treatment, Vet Resources veterinarians are authorized to provide any treatment required to sustain life; or if necessary, provide humane euthanasia to prevent unapproved distress and/or pain. I recognize that the veterinary staff will contact me as soon as possible using the emergency contact information that I provide in this application, but I understand that such contact may not always be possible prior to providing treatment or performing euthanasia.

I will notify the IACUC of unanticipated outcomes of animals use, including protocol or non-protocol disease or injury. Unanticipated outcomes are generally defined as negative impacts to animal welfare or well-being.

I recognize that veterinary consultation must occur when pain or distress is beyond the level IACUC approved in this protocol, or when my staff are unable to provide interventional control (i.e., euthanasia, immediate removal from the study). I will notify VR veterinary staff when unanticipated pain or distress, unexpected morbidity, or unanticipated mortality occurs.

I will obtain approval from the IACUC before initiating any change in the study design or procedures by submitting an amendment request. I understand that work performed without IACUC approval cannot be published with certification of IACUC approval and may result in federally-required reporting of non-compliance.

I am familiar with the University of Maryland Baltimore Environmental Health and Safety (EHS) policies and procedures relative to laboratory safety, biohazards, radiation safety, occupational health and safety, laser safety, chemical and biological waste management practices, select agents, and shipping of infectious materials and clinical specimens. I will abide by the regulations, policies and procedures that relate to research, testing or training at UM. I will ensure that all laboratory personnel engaged in this project will be informed of potential hazards and adequately trained in procedures of animal experimentation involving hazardous agents.

*Ronna Hertzano*

\_\_\_\_\_  
Signature

8/27/2018  
Date

Ronna Hertzano  
Printed Name

\_\_\_\_\_  
Signature – VA Attending Veterinarian (*if animal work is funded by the VAMC or conducted in the VAMC*)

## WRITTEN PROTOCOL

### Lay Summary (limit response to ¼ - ½ page):

#### **1. Using non-technical (lay) language, please describe the purpose of the proposed study.**

Noise-induced hearing loss (NIHL) afflicts 5% of the population worldwide. However, to date, there are no treatments for reversal of NIHL in human. On the other hand, in mice, several treatments have been shown to prevent or ameliorate NIHL. These include previous exposure to lower intensity noise and heat shock. While these treatments are not applicable in human, by understanding the molecular cascades that are activated as a result of these treatments – we will be able to develop new drugs for prevention and treatment of NIHL. As hair cells and supporting cells likely have different roles in the response to noise and its treatments, the objectives of this project is to describe the molecular changes in response to noise in the hair cells and supporting cells, separately. The identified activated signaling cascades will be used as targets for therapeutic intervention.

#### **2. Describe the potential scientific benefit of the proposed study with respect to human and animal health, the advancement of knowledge, or the good of society.**

The goal of the proposed work is to understand the mechanisms that underlie (a) noise induced hearing loss and (b) treatments that in rodents prevent noise induced hearing loss. Once these are identified, the appropriate small molecules that modify these pathways could be studied as potential therapeutics. The importance of this study extends beyond noise induced hearing loss. We believe that the same interventions that will prevent noise induced hearing loss could be used to prevent age related hearing loss – a problems that affects over 50% of the population over 70 years of age.

### Justification for the use of animals and species (limit response to ¼ - ½ page):

#### **1. Please justify the use of animals in general. Discuss whether other alternatives (e.g., cell culture, computer modeling/simulation) to animal usage exist and if so, why they are not feasible, etc.**

To learn about the inner ear response to noise we have to use an animal model from which the different cell types can be extracted. As hair cells and supporting cells likely have different roles in the response to noise and its treatments, it is necessary to use a model organism that will allow expression analysis from hair cells and supporting cells, separately. Recently, we were able to develop such animal models in mice. We plan to use these mice to understand the molecular changes induced by noise exposure and its protective treatments in mouse. While we would like to avoid having to use mice, unfortunately neither cell lines, nor other lower organisms can be used to mimic the molecular changes resulting from exposure of intact ears to noise and its treatments. It is likely that in some of the treatments, a systemic effect (e.g. increase in cortisol level) has a role in the molecular changes induced in the ear further necessitating using a living animal model. Finally, as this is a discovery-project and the signaling cascades are unknown, computer modeling, at this point, is not applicable.

#### **2. Please document why a particular species was chosen for these studies (cost is not acceptable as the sole justification). Additionally, please justify the use of single sex / gender animals, e.g., experiments utilizing all males or all females.**

Species: mouse  
Stock/strain/breed -  $\text{Prestin}^{\text{creERT2/creERT2}}$ ,  $\text{Rpl22}^{\text{tm1.1Psam} / \text{tm1.1Psam}}$ ,  $\text{Sox2}^{\text{creERT2/+}}$ , CBA/CaJ and intercrosses between these mice.

Male and female mice will be used.

We have successfully applied the RiboTag mice ( $\text{Rpl22}^{\text{tm1.1Psam} / \text{tm1.1Psam}}$ ) to perform cell type-specific analyses in adult mice. In this protocol, we plan to study the inner ear outer hair cells (OHCs) and supporting cells (SCs)-specific responses to noise trauma. This can be achieved by crossing mice which express a cre-recombinase in the OHCs ( $\text{Prestin}^{\text{creERT2/creERT2}}$ ) or in the SC ( $\text{Sox2}^{\text{creERT2/+}}$ ) with the RiboTag mice. Our hypothesis is that as OHCs can be rescued by SCs when these are pre-conditioned (e.g. heat shock, lower intensity noise exposure), that by identifying

secreted factors from SCs we could identify candidates for therapeutic intervention to prevent and treat noise induced hearing loss (NIHL).

All of the genetically modified mice used in our studies are based on a C57BL/6 strain. This strain suffers from susceptibility to noise induced hearing loss and age related hearing loss. The genes that confer this susceptibility are inherited in a recessive fashion. We therefore plan to perform all of the experiments on F1 mice to BL/6 and CBA mice (CBA mice to not suffer from age related hearing loss).

We will also purchase F1 mice to C57BL/6 and CBA mice (B6CBAF1/J stock number 100011) to calibrate the conditions of our experiments.

### 3. Strain Identification (*Experimental & Breeder Animals*)

Strain	Brief description of relevance to the proposed research
<b>Prestin<sup>creERT2/creERT2</sup>;</b> <b>Rpl22<sup>tm1.1Psam/tm1.1Psam</sup></b> Breeders	These mice can be induced to express Cre-recombinase only in their outer hair cells, which lead to the expression of a protein tag (HA) on their ribosomes. Consequently, it is possible to immuno-precipitate the RNA from the cells of interest.
<b>Sox2<sup>creERT2/+</sup>;</b> <b>Rpl22<sup>tm1.1Psam/tm1.1Psam</sup></b> and <b>Sox2<sup>+/+</sup>;</b> <b>Rpl22<sup>tm1.1Psam/tm1.1Psam</sup></b> Breeders	These mice can be induced to express Cre-recombinase only in their supporting cells, which lead to the expression of a protein tag (HA) on their ribosomes. Consequently, it is possible to immuno-precipitate the RNA from the cells of interest.
<b>CBA/CaJ</b> (Jax stock number 000654) Breeders	These mice have excellent hearing and do not suffer from age-related hearing loss.
<b>B6.cg-GT(ROSA)26Sor<sup>tm14(CAG-tdTomato)/Hze/J</sup></b> Breeders	These mice, in the presence of Cre-recombinase express the reporter tdTomato. They are used to determine the specificity and the efficiency of a Cre animal models.
<b>Sox2<sup>creERT2/+</sup>;</b> <b>Rpl22<sup>tm1.1Psam/tm1.1Psam</sup></b> Experimental	These mice can be induced to express Cre-recombinase only in their supporting cells, which lead to the expression of a protein tag (HA) on their ribosomes. Consequently, it is possible to immuno-precipitate the RNA from the cells of interest.
<b>Prestin<sup>creERT2/+</sup>;</b> <b>Rpl22<sup>tm1.1Psam/tm1.1Psam</sup></b> Experimental	These mice can be induced to express Cre-recombinase only in their outer hair cells, which lead to the expression of a protein tag (HA) on their ribosomes. Consequently, it is possible to immuno-precipitate the RNA from the cells of interest.
<b>Prestin<sup>creERT2/creERT2</sup>;</b> <b>Rpl22<sup>tm1.1Psam/tm1.1Psam</sup>;</b> <b>CBACaJ</b> Experimental	These mice can be induced to express Cre-recombinase only in their outer hair cells, leading to the expression of HA-tagged ribosomes. Consequently, it is possible to immuno-precipitate the RNA from outer hair cells. Additionally, their mix background with CBACaJ protects them from the early age related hearing loss occurring in C57Bl/6.
<b>Sox2<sup>creERT2/+</sup>;</b> <b>Rpl22<sup>tm1.1Psam/tm1.1Psam</sup>;</b> <b>CBACaJ</b> Experimental	These mice can be induced to express Cre-recombinase only in their supporting cells, leading to the expression of HA-tagged ribosomes. Consequently, it is possible to immuno-precipitate the RNA from supporting cells. Additionally, their mix background with CBACaJ protects them from the early age related hearing loss occurring in C57Bl/6.
<b>Sox2<sup>+/+</sup>;</b> <b>Rpl22<sup>tm1.1Psam/tm1.1Psam</sup>;</b> <b>CBACaJ</b> Experimental	These mice do not expressed the Cre-recombinase and cannot be used for gene expression experiments but they are useful for validation with histology.
<b>Prestin<sup>creERT2/+</sup>;</b> <b>B6.cg-GT(ROSA)26Sor<sup>tm14(CAG-tdTomato)/Hze/J</sup></b>	These mice are used to determine the specificity and the efficiency of the Cre-recombinase expression from the prestinCreERT2 animal model.

Experimental	
Sox2 <sup>creERT2/+</sup> ; B6.cg- GT(ROSA)26Sor <sup>tm14(CAG-tdTomato)/Hze/J</sup>	These mice are used to determine the specificity and the efficiency of the Cre-recombinase expression from the Sox2CreERT2 animal model.
Experimental	

*\*\*Please add rows to this table by placing cursor at end of last row and clicking return.*

**Do any of the above strains exhibit any known phenotypic variations that could potentially affect animal health, well-being or longevity?**      YES\*    NO

\*If yes, please describe:

**Do any of the above strains require phenotype induction, e.g., pharmacologically activated, siRNA, viral induced, etc.?**      YES\*    NO

\*If yes, please include induction methods under *Detailed Description of Animal Procedures*.  
Induction by tamoxifen injection is described in *Detailed Description of Animal Procedures*.

**Experimental Summary / Animal Usage** (limit response to ¼ - ½ page):

- 1. What are the objectives or underlying hypothesis of the planned experiments? Provide background information on the science. Information provided will be similar to the background section on a grant application but abbreviated to convey what has already been done in the field at large and why these experiments should be done.**

Noise-induced hearing loss (NIHL) afflicts 5% of the population worldwide. From a functional standpoint, NIHL leads to tinnitus and difficulty with understanding speech, particularly in the presence of background noise, and is strongly associated with depression and social isolation. Noise exposure is inevitable. NIHL results from prolonged exposure to loud noise (such as the background noise in military aircraft, submarines and naval vessels) or intermittent exposure to very loud noise (such as machine gun firing or explosions). Similarly, in the public and private sectors, factory employees, construction workers, and aircrew staff are also exposed to sustained loud noise. The susceptibility to NIHL is highly heterogeneous, likely secondary to genetic variables. However, to date, there are no treatments for reversal of NIHL nor are there tools to confidently identify genetically susceptible individuals, limiting intervention primarily to hearing protection.

Physiologic pre-conditioning using temporary threshold shift (TTS)-inducing noise exposure and heat stress can partially protect from NIHL in diverse animal models. However, as these interventions are not clinically applicable, it is necessary to understand their mechanism of action to fulfill their translational potential. The mechanism of the well documented and paradoxical otoprotection obtained by TTS-inducing noise exposure is poorly understood. The otoprotection induced by heat stress is likely via glucocorticoid-related, or heat shock protein (HSP)-related pathways, which may function using common or independent mechanisms. Similarly, exogenous steroids can partially protect from NIHL, when administered before or immediately after the noise exposure. In vivo and in vitro works support a role for radical oxygen species in NIHL with promising results using anti-oxidant treatments. Genetic modifications of mice have shown that constitutive activation of protective mechanisms can render HCs resistant to NIHL without inducing toxicity or tachyphylaxis, supporting the idea that chemical prophylaxis for NIHL may be feasible. Finally, a member of the HSP pathway, HSP70, has been shown to be necessary and sufficient for induction of otoprotection from aminoglycosides in vitro. In the ear, HSP70 is induced and secreted by SCs to promote HC survival from aminoglycoside ototoxicity. The concept of SCs protecting sensory cells from damage is not new to the central or peripheral nervous systems (CNS and PNS, respectively). In the CNS, glial cells (which are akin to supporting cells) can rescue neurons by secretion of HSPs, while in the PNS, olfactory supporting cells (sustentacular cells) can rescue olfactory receptor neurons using a similar mechanism. These data suggest that SCs could adapt to compensate for noise exposure and function to rescue HCs. However, to date, the cell type-specific molecular pathophysiology of NIHL and its prevention/treatment are largely unknown, precluding the development of targeted treatments for prevention of, or early intervention following, noise trauma. Additionally, we have shown that male and female mice respond differently to noise exposure, with male mice being more sensitive.

Here we test two different pre-conditioning approaches (TTS and heat-shock) to verify their efficacy in our model, and then use them to understand the molecular mechanism by which their work to be able to develop new therapeutics. In parallel, we process tissue from male and female separately to decipher the molecular mechanism behind the sex difference in the response to noise exposure.

2. Does any of the proposed research duplicate previous work?  YES  NO

If yes, please discuss the rationale for this duplication.

Click here to enter text.

3. **Planned Experiments.** *The following information must be provided for each planned experiment. A flow diagram must also be incorporated into each experimental description or attached as an addendum to this protocol. Please label flow diagrams to be congruent with the experimental description(s) below.*

**Experiment 1 – Determine the outer hair cell (OHC)- and supporting cell (SC)-specific translatomes at 9-11 weeks of age (this experiment was approved in our previous protocol #0915006 as Experiment 1 and amendment dated 9/10/2016, we are transferring it to the new protocol).**

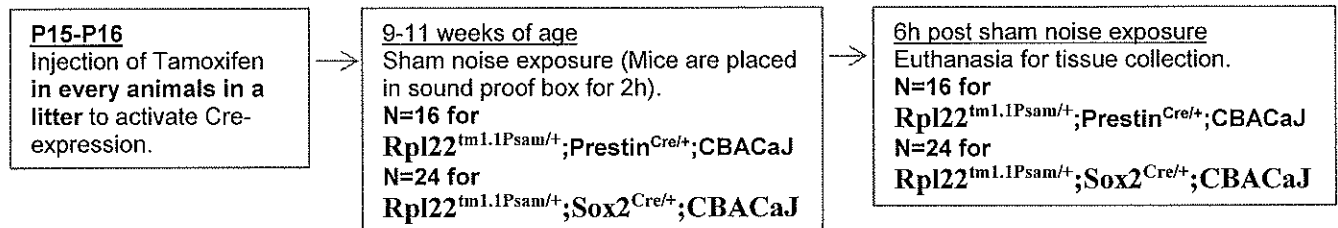
**Briefly describe the objective of this experiment.**

The goal of this experiment is to determine the gene expression patterns for OHC and SC of 9-11 week old mice that were not exposed to noise. In other words – the baseline gene expression.

**Describe what will happen to the animals from start to finish.** *Detailed animal procedures should NOT be described in this section.*

Mice are born, injected with tamoxifen at P15 and P16 and weaned at 21-28 days. At 10 weeks of age, mice will be placed in the sound proof box for 2h without noise exposure. Mice will be euthanized at 6h after the onset of the sham noise exposure and have their inner ears collected for cochlear tissue collection. Mice will be euthanized as described in “Method of euthanasia”.

Schematic:



**What is the longest that any one animal will be involved in an experiment?**

7 to 9 weeks – from tamoxifen injection to euthanasia. Following tamoxifen injection at P15-P16, mice will not be subjected to any procedure until they reach the age of 9-11 weeks, at which time the sham noise exposure will be performed. The mice will be euthanized 6h following sham noise exposure.

**List each experimental and control group, including the group size for each group (n=?).**

Based on tissue already collected as part of protocol #0915006, we need:

Rpl22<sup>tm1.1Psam/+</sup>;Prestin<sup>Cre/+</sup>;CBACaJ

Females: 4 females Rpl22<sup>tm1.1Psam/+</sup>;Prestin<sup>Cre/+</sup>;CBACaJ x 2 replicates x 1 time point = **8 females**

Males: 4 males Rpl22<sup>tm1.1Psam/+</sup>;Prestin<sup>Cre/+</sup>;CBACaJ x 2 replicates x 1 time point = **8 males**

Rpl22<sup>tm1.1Psam/+</sup>;Sox2<sup>Cre/+</sup>;CBACaJ

Females: 4 females Rpl22<sup>tm1.1Psam/+</sup>;Sox2<sup>Cre/+</sup>;CBACaJ x 3 replicates x 1 time point = **12 females**

Males: 4 males Rpl22<sup>tm1.1Psam/+</sup>;Sox2<sup>Cre/+</sup>;CBACaJ x 3 replicates x 1 time point = **12 males**

**Discuss what criteria were used to determine that the group size(s) proposed utilizes the minimal number of animals to generate statistically significant data (e.g., power analysis, reports in the literature, previous experience, etc.).**

3 main criteria were used for the number of animals needed.

- We optimized the tissue processing and we are now able to obtain enough RNA from 4 individual mice instead of 8 individual mice required at the time the previous protocol was written (Yang et al., under minor revision in BMC Genomics).
- We have recently shown that male and female mice respond differently to noise exposure with males being more sensitive (Milon et al., Biology of Sex Differences 2018). Therefore, we need to process male and female tissue separately.
- We have already collected tissues as part of our previous protocol #0915006, so the numbers reflect what still needs to be collected as part of this new protocol.

**Indicate whether the experiment must be repeated and justify the number of repetitions.**

The experiment is performed in three biological replicates for RNA-seq and one replicate for validation by NanoString technology.

**Indicate the species to be used, and how many will be used (e.g.,  $X$  # mice per experiment  $\times$   $X$  # strains of mice).**

We will use [8 females and 8 males from  $Rpl22^{tm1.1Psam/+};Prestin^{Cre/+};CBACaJ$  strain] + [12 females and 12 males from  $Rpl22^{tm1.1Psam/+};Sox2^{Cre/+};CBACaJ$  strain] = **40 mice**.

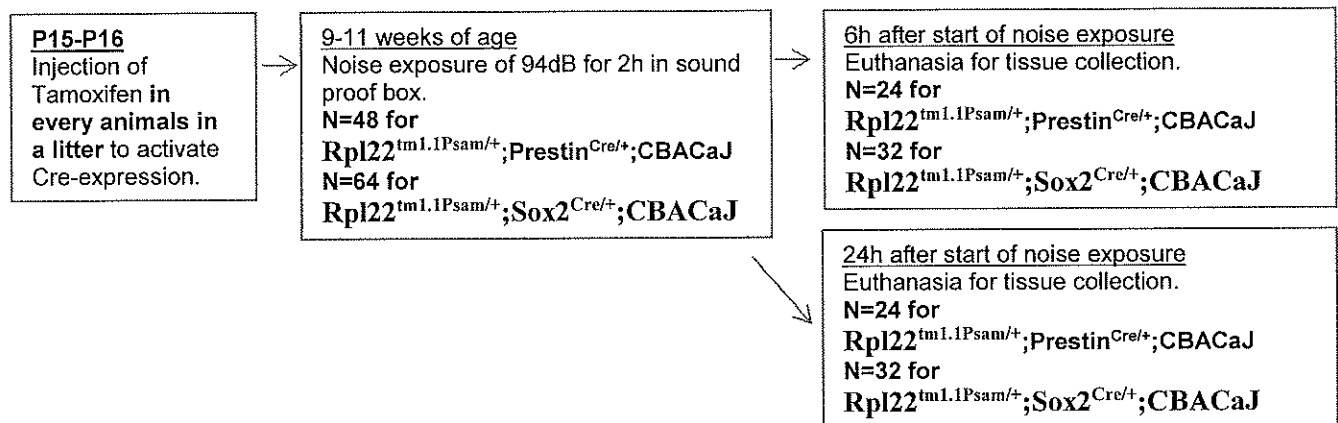
**Experiment 2 - Determine the OHC- and SC-specific response to Temporary Threshold Shift (TTS) (this experiment was approved in our previous protocol #0915006 as Experiment 2, we are transferring it to the new protocol).**

**Briefly describe the objective of this experiment.**

To determine the OHC- and SC-specific molecular changes in response to TTS-inducing noise exposure using  $Rpl22^{tm1.1Psam/+};Prestin^{Cre/+};CBACaJ$  mice and  $Rpl22^{tm1.1Psam/+};Sox2^{Cre/+};CBACaJ$ . This is a noise exposure that results in a temporary worsening in hearing.

**Describe what will happen to the animals from start to finish. Detailed animal procedures should NOT be described in this section.**

Mice are born, injected with Tamoxifen at **P15 and P16** and weaned at 21-28 days. At 10 weeks of age, mice will be exposed to a noise of 94dB for 2h. Mice will be euthanized at 6h or 24 hours after the onset of the noise exposure and have their inner ears collected for cochlear tissue collection. Mice will be euthanized as described in "Method of euthanasia".



**What is the longest that any one animal will be involved in an experiment?**

7 to 9 weeks – from tamoxifen injection to euthanasia. Following tamoxifen injection at **P15-P16**, mice will not be subjected to any procedure until they reach the age of 9-11 weeks, at which time the noise exposure will be performed. The mice will be euthanized 6h or 24h following noise exposure.

**List each experimental and control group, including the group size for each group (n=?).**

All experiments are done in triplicate for RNA-seq plus one replicate for validation using NanoString technology with each replicate consisting of 4 animals and based on tissue already collected as part of protocol #0915006, we are requesting:

Rpl22<sup>tm1.1Psam/+</sup>;Prestin<sup>Cre/+</sup>;CBACaJ

Females: 4 females Rpl22<sup>tm1.1Psam/+</sup>;Prestin<sup>Cre/+</sup>;CBACaJ x 3 replicates x 2 time points = **24 females**

Males: 4 males Rpl22<sup>tm1.1Psam/+</sup>;Prestin<sup>Cre/+</sup>;CBACaJ x 3 replicates x 2 time points = **24 males**

Rpl22<sup>tm1.1Psam/+</sup>;Sox2<sup>Cre/+</sup>;CBACaJ

Females: 4 females Rpl22<sup>tm1.1Psam/+</sup>;Sox2<sup>Cre/+</sup>;CBACaJ x 4 replicates x 2 time points = **32 females**

Males: 4 males Rpl22<sup>tm1.1Psam/+</sup>;Sox2<sup>Cre/+</sup>;CBACaJ x 4 replicates x 2 time points = **32 males**

**Discuss what criteria were used to determine that the group size(s) proposed utilizes the minimal number of animals to generate statistically significant data (e.g., power analysis, reports in the literature, previous experience, etc.).**

The same criteria as Experiment 1 were used.

**Indicate whether the experiment must be repeated and justify the number of repetitions.**

The experiment is performed in three biological replicates for RNA-seq and one replicate for validation by NanoString technology.

**Indicate the species to be used, and how many will be used (e.g., X # mice per experiment x X # strains of mice).**

We will use [24 females and 24 males from Rpl22<sup>tm1.1Psam/+</sup>;Prestin<sup>Cre/+</sup>;CBACaJ strain] + [32 females and 32 males from Rpl22<sup>tm1.1Psam/+</sup>;Sox2<sup>Cre/+</sup>;CBACaJ strain] = **112 mice**.

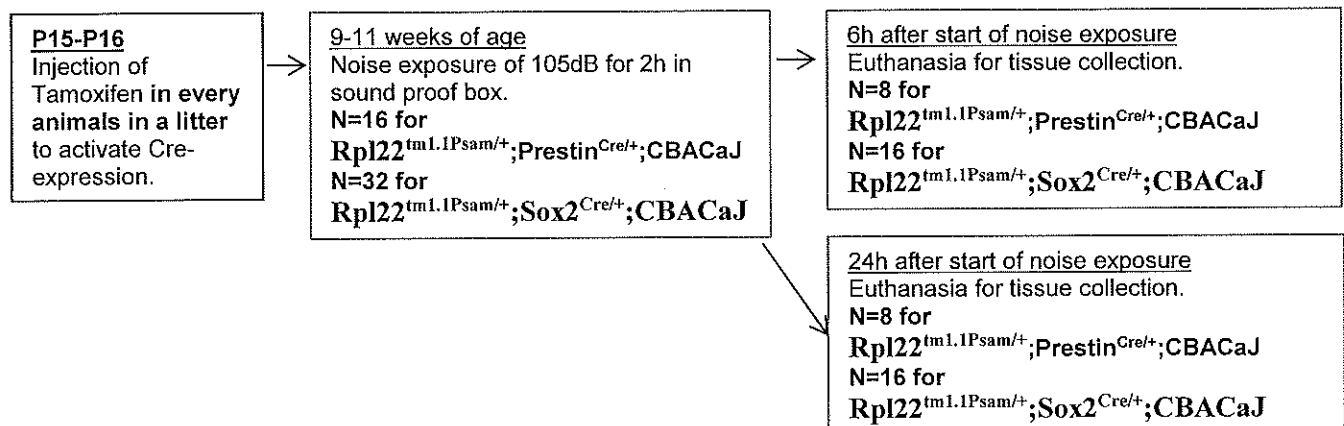
**Experiment 3 - Determine the OHC- and SC-specific response to Permanent Threshold Shift (PTS) (this experiment was approved in our previous protocol #0915006 as Experiment 3, we are transferring it to the new protocol)**

**Briefly describe the objective of this experiment.**

To determine the OHC and SC-specific molecular changes in response to PTS-inducing noise exposure. This is a noise exposure that results in a permanent worsening in hearing.

**Describe what will happen to the animals from start to finish. Detailed animal procedures should NOT be described in this section.**

Mice are born, injected with Tamoxifen at **P15 and P16** and weaned at 21-28 days. At 10 weeks of age, mice will be exposed to a noise of 105dB for 2h. Mice will be euthanized at 6h or 24 hours after the onset of the noise exposure and have their inner ears collected for cochlear tissue collection. Mice will be euthanized as described in "Method of euthanasia".



**What is the longest that any one animal will be involved in an experiment?**

7 to 9 weeks – from tamoxifen injection to euthanasia. Following tamoxifen injection at **P15-P16**, mice will not be subjected to any procedure until they reach the age of 9-11 weeks, at which time the noise exposure will be performed. The mice will be euthanized 6h or 24h following noise exposure.

**List each experimental and control group, including the group size for each group (n=?).**

All experiments are done in triplicate for RNA-seq plus one replicate for validation using NanoString technology with each replicate consisting of 4 animals and based on tissue already collected as part of protocol #0915006, we are requesting:

Rpl22<sup>tm1.1Psam/+</sup>;Prestin<sup>Cre/+</sup>;CBACaJ

Females: 4 females Rpl22<sup>tm1.1Psam/+</sup>;Prestin<sup>Cre/+</sup>;CBACaJ x 1 replicates x 2 time points = **8 females**

Males: 4 males Rpl22<sup>tm1.1Psam/+</sup>;Prestin<sup>Cre/+</sup>;CBACaJ x 1 replicates x 2 time points = **8 males**

Rpl22<sup>tm1.1Psam/+</sup>;Sox2<sup>Cre/+</sup>;CBACaJ

Females: 4 females Rpl22<sup>tm1.1Psam/+</sup>;Sox2<sup>Cre/+</sup>;CBACaJ x 2 replicates x 2 time points = **16 females**

Males: 4 males Rpl22<sup>tm1.1Psam/+</sup>;Sox2<sup>Cre/+</sup>;CBACaJ x 2 replicates x 2 time points = **16 males**

**Discuss what criteria were used to determine that the group size(s) proposed utilizes the minimal number of animals to generate statistically significant data (e.g., power analysis, reports in the literature, previous experience, etc.).**

The same criteria as Experiment 1 were used.

**Indicate whether the experiment must be repeated and justify the number of repetitions.**

The experiment is performed in three biological replicates for RNA-seq and one replicate for validation by NanoString technology.

**Indicate the species to be used, and how many will be used (e.g., X # mice per experiment x X # strains of mice).**

We will use [8 females and 8 males from Rpl22<sup>tm1.1Psam/+</sup>;Prestin<sup>Cre/+</sup>;CBACaJ strain] + [16 females and 16 males from Rpl22<sup>tm1.1Psam/+</sup>;Sox2<sup>Cre/+</sup>;CBACaJ strain] = **48 mice**.

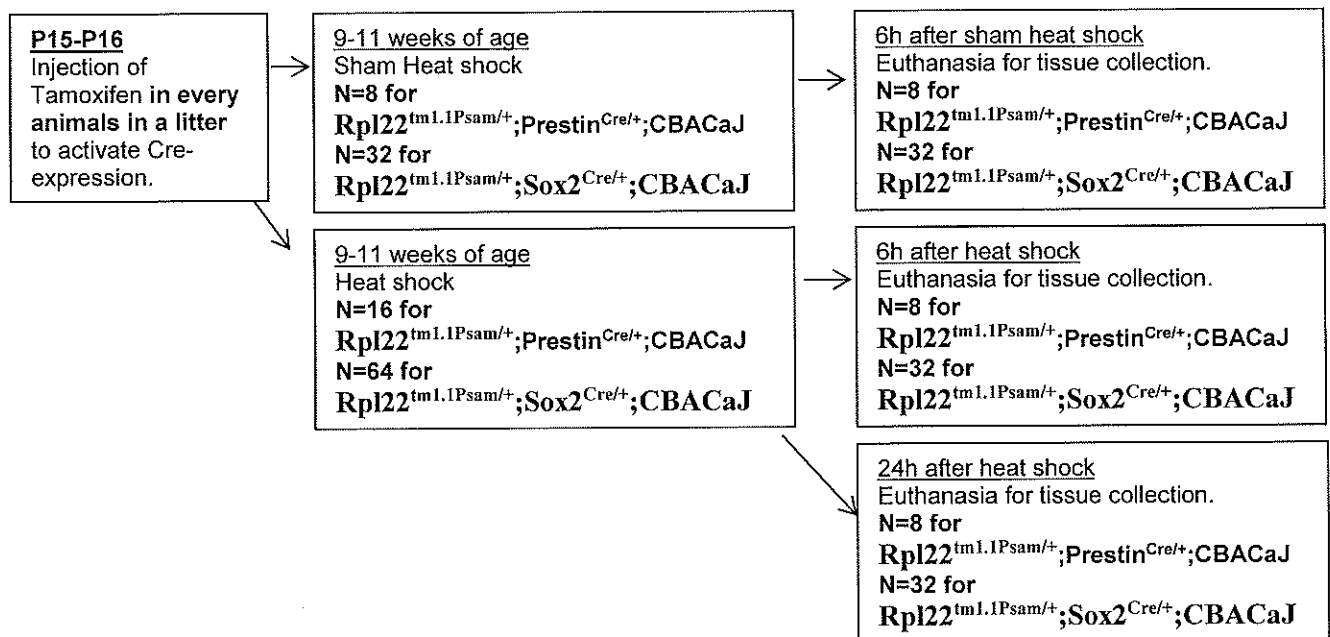
**Experiment 4 – Determine the OHC- and SC-specific response to Heat shock (Method was approved in amendment dated 4/3/17 related to previous protocol #0915006, we are transferring it to the new protocol).**

**Briefly describe the objective of this experiment.**

To determine the OHC and SC-specific molecular changes in response to Heat Shock. Heat shock is an intervention that has been shown to prevent noise induced hearing loss. However, the exact mechanism and changes happening in specific cell-types are not known. We will use two strains, Rpl22<sup>tm1.1Psam/+</sup>;Prestin<sup>CreERT2/+</sup> and Rpl22<sup>tm1.1Psam/+</sup>;Sox2<sup>CreERT2/+</sup> to determine the molecular changes occurring following heat shock in OHC and SC respectively.

**Describe what will happen to the animals from start to finish. Detailed animal procedures should NOT be described in this section.**

Mice are born, injected with Tamoxifen at **P15 and P16** and weaned at 21-28 days. Males and females will be treated separately. All mice will be anesthetized. Heat shock exposure will not be distressful and/ or painful to the animals due to being anesthetized during the procedure. At 9-11 weeks of age, experimental mice will have their body temperature increased by 3.3°C for 15 min (experimental) while control mice (sham heat) will be left on a 37°C pad. The mice will then be allowed to recover from anesthesia before being returned to their cage. Then, 6h or 24h post heat shock, mice will be euthanized as described in “Method of euthanasia” and their inner ear dissected to be processed for RNA extraction.



**What is the longest that any one animal will be involved in an experiment?**

7 to 9 weeks – from tamoxifen injection to euthanasia. Following tamoxifen injection at P15-P16, mice will not be subjected to any procedure until they reach the age of 9-11 weeks, at which time the heat shock experiment will be performed. The mice will be euthanized 6h or 24h following heat shock.

**List each experimental and control group, including the group size for each group (n=?).**

Tissue from male and female mice will be collected separately. Based on our previous experience with the amount of RNA obtained following immunoprecipitation from ribotag mice, we need 4 animals per sample. Experiments will be performed in three biological replicates, plus one replicate that will be used for validation of the results. Based on tissue already collected as part of protocol #0915006

$Rpl22^{tm1.1Psam/+}; Prestin^{CreERT2/+}$  strain

Based on the genotype of the parents ( $Rpl22^{tm1.1Psam}/tm1.1Psam \times Prestin^{CreERT2/CreERT2}$ ), all progeny will have the right genotype for the experiment.

Control group: [4 males x 1 replicate] + [4 females x 1 replicate] = 8 mice

Experimental group for 6h: [4 males x 1 replicate] + [4 females x 1 replicate] = 8 mice

Experimental group for 24h: [4 males x 1 replicate] + [4 females x 1 replicate] = 8 mice

Therefore, we are requesting **24 mice for the  $Rpl22^{tm1.1Psam/+}; Prestin^{CreERT2/+}$  strain.**

$Rpl22^{tm1.1Psam}/+; Sox2^{CreERT2/+}$  strain

Homozygote  $Sox2^{CreERT2/CreERT2}$  mice are not viable and are maintained as heterozygote  $Sox2^{CreERT2/+}$ . Therefore, based on the genotype of the parents ( $Rpl22^{tm1.1Psam}/tm1.1Psam \times Sox2^{CreERT2/+}$ ), 50% of the progeny will have the right genotype ( $Rpl22^{tm1.1Psam}/+; Sox2^{CreERT2/+}$ ) for the experiment.

We are still requesting 4 animals per samples but half of the animals in a litter will not be useful.

Control group: [4 males x 4 replicates] + [4 females x 4 replicates] = 32 mice

Experimental group for 6h: [4 males x 4 replicates] + [4 females x 4 replicates] = 32 mice

Experimental group for 24h: [4 males x 4 replicates] + [4 females x 4 replicates] = 32 mice

Therefore, we are requesting **96 mice for the  $Rpl22^{tm1.1Psam}/+; Sox2^{CreERT2/+}$  strain.**

**Discuss what criteria were used to determine that the group size(s) proposed utilizes the minimal number of animals to generate statistically significant data (e.g., power analysis, reports in the literature, previous experience, etc.).**

The same criteria as Experiment 1 were used.

**Indicate whether the experiment must be repeated and justify the number of repetitions.**

The experiment is performed in three biological replicates for RNA-seq and one replicate for validation by NanoString technology.

Indicate the species to be used, and how many will be used (e.g.,  $X\#$  mice per experiment  $\times X\#$  strains of mice).

We will use [24 mice from  $Rpl22^{tm1.1Psam/+}; Prestin^{Cre/+}$  strain] + [96 mice from  $Rpl22^{tm1.1Psam/+}; Sox2^{Cre/+}$  strain] = 120 mice.

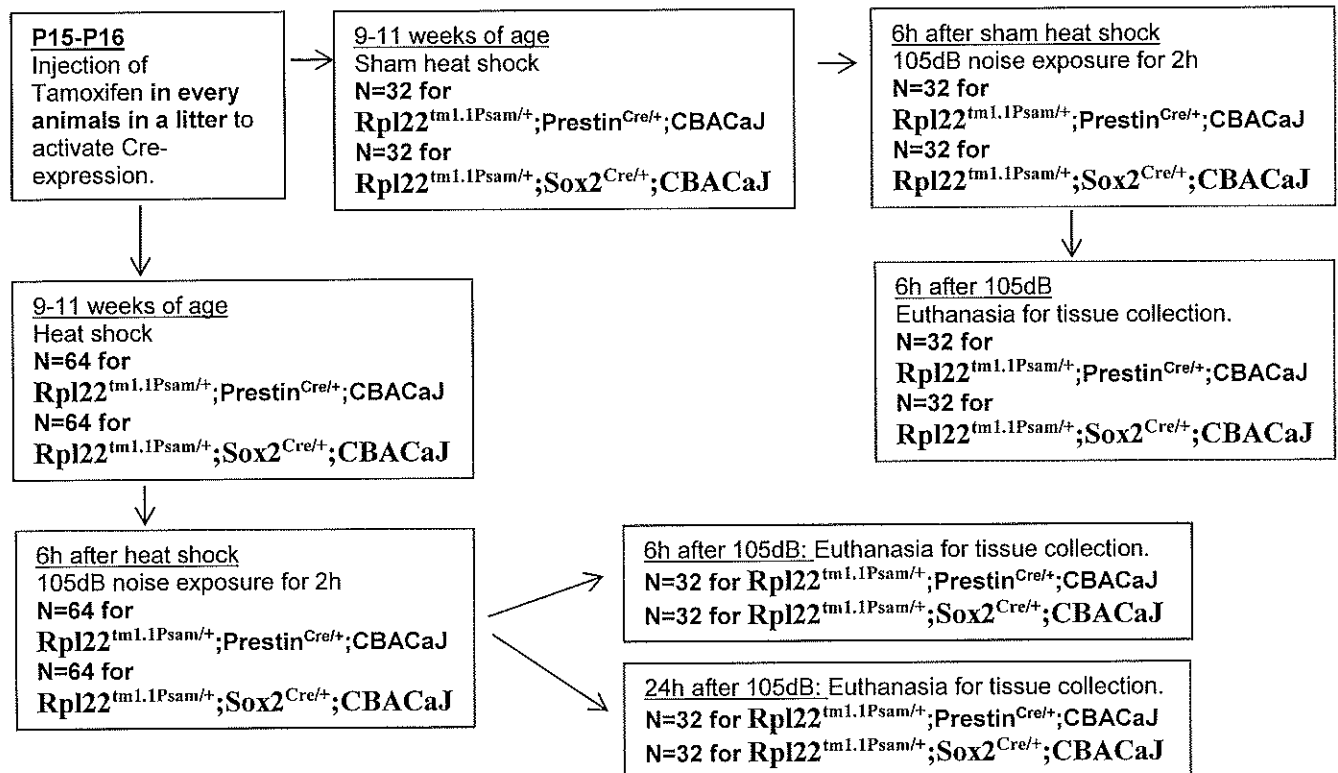
**Experiment 5 – Determine the OHC- and SC-specific response to Heat shock followed by Noise exposure** (Method was approved in previous protocol #0915006 – experiment 4, and related amendments dated 6/10/16 and 9/19/16, we are transferring it to the new protocol).

**Briefly describe the objective of this experiment.**

To determine the OHC and SC-specific molecular changes responsible for the protective effect of Heat Shock from noise exposure. Heat shock is an intervention that has been shown to prevent noise induced hearing loss. However, the exact mechanism and changes responsible for this protection in specific cell-types are not known. We will use two strains,  $Rpl22^{tm1.1Psam/+}; Prestin^{CreERT2/+}; CBACaJ$  and  $Rpl22^{tm1.1Psam/+}; Sox2^{CreERT2/+}; CBACaJ$  to determine the molecular changes occurring following heat shock in OHC and SC respectively.

**Describe what will happen to the animals from start to finish.** *Detailed animal procedures should NOT be described in this section.*

Mice are born, injected with Tamoxifen at P15 and P16 or at least five days before the experiment begins, separated at 21-28 days. Males and females will be treated separately. All mice will be anesthetized. Heat shock exposure will not be distressful and/or painful to the animals due to being anesthetized during the procedure. At 10 weeks of age, experimental mice will be placed on a Far-infrared warming pad connected to a Temperature Monitoring & Homeothermic Control Module (PhysioSuite from Kent Scientific Corporation) to have their body temperature increased by 3.3°C for 15 min while control mice (sham heat) will be left on a 37°C pad. The temperature of the animals will be monitored with a rectal probe. The mice will then be allowed to recover from anesthesia before being returned to their cage. Then, 6h post heat shock, the mice will be exposed to a noise of 105dB for two hours. 6h or 24h following the noise exposure, mice will be euthanized as described in “Method of euthanasia” and their inner ear dissected to be processed for RNA extraction or histology.



**What is the longest that any one animal will be involved in an experiment?**

7 to 9 weeks – from tamoxifen injection to euthanasia. Following tamoxifen injection at **P15-P16**, mice will not be subjected to any procedure until they reach the age of 9-11 weeks, at which time the heat shock and noise exposure experiment will be performed. The mice will be euthanized 6h or 24h following heat shock.

**List each experimental and control group, including the group size for each group (n=?).**

Tissue from male and female mice will be collected separately. Based on our previous experience with the amount of RNA obtained following immunoprecipitation from ribotag mice, we need 4 animals per sample. Experiments will be performed in three biological replicates, plus one replicate that will be used for validation of the results.

Rpl22<sup>tm1.1Psam<sup>+/+</sup></sup>;Prestin<sup>CreERT2/+</sup>;CBACaJ strain

Based on the genotype of the parents (Rpl22<sup>tm1.1Psam<sup>+/+</sup></sup>/tm1.1Psam<sup>+/+</sup> x Prestin<sup>CreERT2/CreERT2</sup>), all progeny will have the right genotype for the experiment.

Control group for 6h: [4 males x 4 replicates] + [4 females x 4 replicates] = 32 mice

Experimental group for 6h: [4 males x 4 replicates] + [4 females x 4 replicates] = 32 mice

Experimental group for 24h: [4 males x 4 replicates] + [4 females x 4 replicates] = 32 mice

Therefore, we are requesting **96 mice for the Rpl22<sup>tm1.1Psam<sup>+/+</sup></sup>;Prestin<sup>CreERT2/+</sup> strain.**

Rpl22<sup>tm1.1Psam<sup>+/+</sup></sup>;Sox2<sup>CreERT2/+</sup>;CBACaJ strain

Homozygote Sox2<sup>CreERT2/CreERT2</sup> mice are not viable and are maintained as heterozygote Sox2<sup>CreERT2/+</sup>. Therefore, based on the genotype of the parents (Rpl22<sup>tm1.1Psam<sup>+/+</sup></sup>/tm1.1Psam<sup>+/+</sup> x Sox2<sup>CreERT2/+</sup>), 50% of the progeny will have the right genotype (Rpl22<sup>tm1.1Psam<sup>+/+</sup></sup>;Sox2<sup>CreERT2/+</sup>) for the experiment.

We are still requesting 4 animals per samples but half of the animals in a litter will not be useful.

Control group for 6h: [4 males x 4 replicates] + [4 females x 4 replicates] = 32 mice

Experimental group for 6h: [4 males x 4 replicates] + [4 females x 4 replicates] = 32 mice

Experimental group for 24h: [4 males x 4 replicates] + [4 females x 4 replicates] = 32 mice

Therefore, we are requesting **96 mice for the Rpl22<sup>tm1.1Psam<sup>+/+</sup></sup>;Sox2<sup>CreERT2/+</sup> strain.**

**Discuss what criteria were used to determine that the group size(s) proposed utilizes the minimal number of animals to generate statistically significant data (e.g., power analysis, reports in the literature, previous experience, etc.).**

The same criteria as Experiment 1 were used.

**Indicate whether the experiment must be repeated and justify the number of repetitions.**

The experiment is performed in three biological replicates for RNA-seq and one replicate for validation by NanoString technology.

**Indicate the species to be used, and how many will be used (e.g., X # mice per experiment x X # strains of mice).**

We will use [96 mice from Rpl22<sup>tm1.1Psam<sup>+/+</sup></sup>;Prestin<sup>Cre/+</sup>;CBACaJ strain] + [96 mice from Rpl22<sup>tm1.1Psam<sup>+/+</sup></sup>;Sox2<sup>Cre/+</sup>;CBACaJ strain] = **192 mice.**

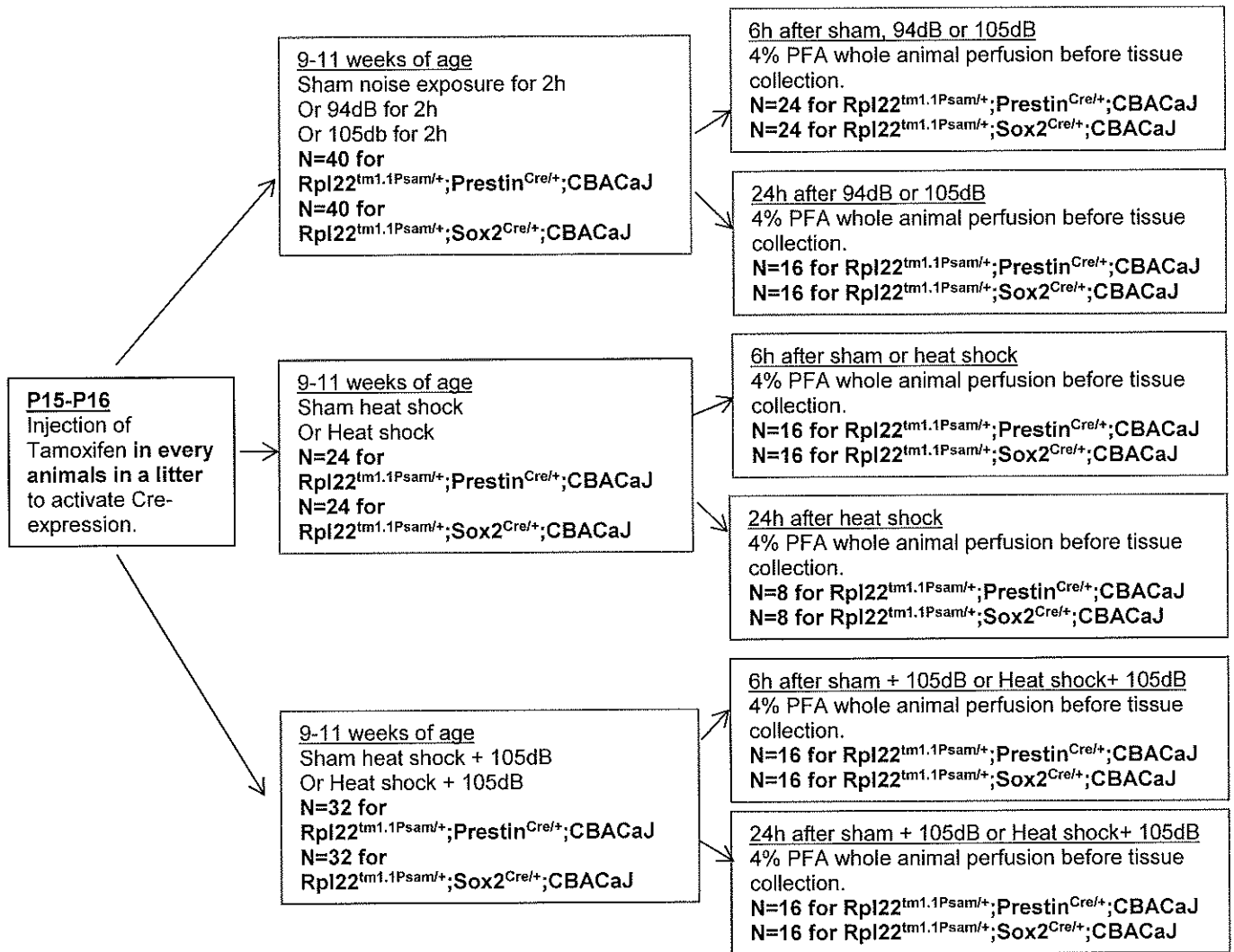
**Experiment 6 – Validation of the gene expression experiments by histological immunostaining**

**Briefly describe the objective of this experiment.**

Gene expression data need to be validated by immunohistochemistry or in situ hybridization for selected genes that are representative of the results or are of special interest to the field. For this experiment, we are requesting animals from each experiments described above (experiments 1 through 5).

**Describe what will happen to the animals from start to finish. Detailed animal procedures should NOT be described in this section.**

We will follow the same steps described for each experiment above. However, before euthanasia, the animals will be anesthetized and perfused by transcardial perfusion of 4% paraformaldehyde to fix tissues (see detailed description of animal procedures) prior collecting the inner ears for histological analysis.



**What is the longest that any one animal will be involved in an experiment?**

7 to 9 weeks – from tamoxifen injection to euthanasia. Following tamoxifen injection at P15-P16, mice will not be subjected to any procedure until they reach the age of 9-11 weeks.

**List each experimental and control group, including the group size for each group (n=?).**

We are requesting 4 animals per condition for histology.

Group 1 (noise exposure experiments)

(4 females sham + 4 males sham) + [(4 females + 4 males) x 2 time points x 2 conditions] = 40 mice x 2 strains = **80 mice**

Group 2 (heat shock experiments)

(4 females sham + 4 males sham) + [(4 females + 4 males) x 2 time points] = 24 mice x 2 strains = **48 mice**

Group 3 (heat shock + noise experiments)

(4 females + 4 males) x 2 time points x 2 conditions = 32 mice x 2 strains = **64 mice**

**Discuss what criteria were used to determine that the group size(s) proposed utilizes the minimal number of animals to generate statistically significant data (e.g., power analysis, reports in the literature, previous experience, etc.).**

Based on our previous experience, the hair cells in the cochlea of adult mice show signs of degeneration soon after euthanasia of the animals. This makes it challenging to obtain good immunostaining data. Therefore, we are requesting 4 animals per condition instead of 3 to account for any damage tissue.

**Indicate whether the experiment must be repeated and justify the number of repetitions.**

All the animals will be used and the experiment does not need to be repeated.

**Indicate the species to be used, and how many will be used (e.g.,  $X$  # mice per experiment  $\times$   $X$  # strains of mice).**

We will use [40 mice for Rpl22<sup>tm1.1Psam/+</sup>;Prestin<sup>Cre/+</sup>;CBACaJ strain + 40 mice for Rpl22<sup>tm1.1Psam/+</sup>;Sox2<sup>Cre/+</sup>;CBACaJ strain in group 1] + [24 mice for Rpl22<sup>tm1.1Psam/+</sup>;Prestin<sup>Cre/+</sup> strain + 24 mice for Rpl22<sup>tm1.1Psam/+</sup>;Sox2<sup>Cre/+</sup> strain in group 2] + [32 mice for Rpl22<sup>tm1.1Psam/+</sup>;Prestin<sup>Cre/+</sup>;CBACaJ strain + 32 mice for Rpl22<sup>tm1.1Psam/+</sup>;Sox2<sup>Cre/+</sup>;CBACaJ strain in group 3] = **192 mice**

**Experiment 7 – Determine the specificity and efficiency of the Cre-recombinase Prestin<sup>CreERT2/CreERT2</sup> mice (This experiment was approved in our previous protocol #0915006 for an earlier time point).**

**Briefly describe the objective of this experiment.**

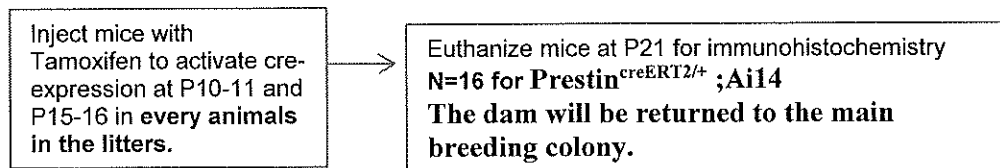
The goal of our project is to identify molecular changes after noise exposure in specific cell types of the inner ear. Therefore, this experiment is to verify that the Cre-recombinase from the **Prestin<sup>CreERT2/CreERT2</sup>** is efficiently and specifically expressed in outer hair cells when induced with tamoxifen at different time points using the reporter mouse **B6.cg-GT(ROSA)<sup>26Sortm14(CAG-tdTomato)/Hze/J</sup>**. These mice express the reporter TdTomato only in cells expressing the Cre-recombinase. This mouse strain is also known as Ai14 and will be referred as such in the remainder of the protocol.

**Describe what will happen to the animals from start to finish. Detailed animal procedures should NOT be described in this section.**

Experimental course for each animal:

Mice will be born, injected with Tamoxifen at P10-11 and P15-16. They will then be euthanized at P21 using CO<sub>2</sub> asphyxiation followed by cervical dislocation.

Schematic:



**What is the longest that any one animal will be involved in an experiment?**

For animals injected with tamoxifen at P10-11, they will be involved in the experiment for 12 days until P21. For animals injected with tamoxifen at P15-16, they will be involved in the experiment for 7 days until P21.

**List each experimental and control group, including the group size for each group (n=?).**

We will be checking the expression of the reporter protein TdTomato therefore no controls are needed.

We will use one litter for each time point. Assuming 8 mice per litter, we are requesting **16 mice** for this experiment.

**Discuss what criteria were used to determine that the group size(s) proposed utilizes the minimal number of animals to generate statistically significant data (e.g., power analysis, reports in the literature, previous experience, etc.).**

All mice from the progeny of the cross **Prestin<sup>CreERT2/CreERT2</sup> x Ai14** will express the reporter gene. Therefore, if we assume 8 mice per litter, we will have enough samples to generate significant data.

**Indicate whether the experiment must be repeated and justify the number of repetitions.**

All the animals in the litter will be used and the experiment does not need to be repeated.

**Indicate the species to be used, and how many will be used (e.g.,  $X$  # mice per experiment  $\times$   $X$  # strains of mice).**

**Prestin<sup>CreERT2/CreERT2</sup>** will be crossed with homozygous **Ai14** mice. Because we will use two litters for the experiment, we will need **one male (Ai14) and one female (Prestin<sup>CreERT2/CreERT2</sup>) breeders and 16 experimental mice.**

**Experiment 8 – Determine the specificity and efficiency of the Cre-recombinase expression from Sox2<sup>CreERT2/+</sup> mice.**

**Briefly describe the objective of this experiment.**

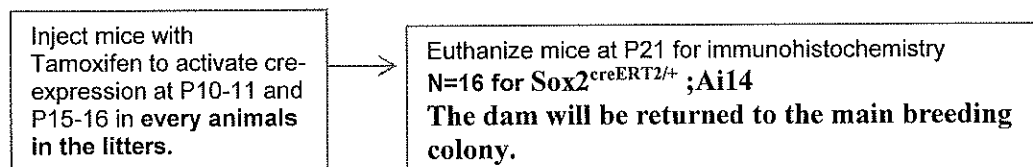
The goal of our project is to identify molecular changes after noise exposure in specific cell types of the inner ear. Therefore, this experiment is to verify that the Cre-recombinase from the Sox2<sup>CreERT2/+</sup> is efficiently and specifically expressed in the supporting cells when induced with tamoxifen at different time points using the reporter mouse Ai14. These mice express the reporter TdTomato only in cells expressing the Cre-recombinase.

**Describe what will happen to the animals from start to finish. Detailed animal procedures should NOT be described in this section.**

Experimental course for each animal:

Mice will be born, injected with Tamoxifen at P10-11 and P15-16. They will then be euthanized at P21 using CO<sub>2</sub> asphyxiation followed by cervical dislocation.

Schematic:



**What is the longest that any one animal will be involved in an experiment?**

For animals injected with tamoxifen at P10-11, they will be involved in the experiment for 12 days until P21. For animals injected with tamoxifen at P15-16, they will be involved in the experiment for 7 days until P21.

**List each experimental and control group, including the group size for each group (n=?).**

We will be checking the expression of the reporter protein TdTomato therefore no controls are needed.

We will use two litters per time point. Assuming 8 mice per litter, we are requesting 32 mice for this experiment of which **only 16 will be useful for the experiment.**

**Discuss what criteria were used to determine that the group size(s) proposed utilizes the minimal number of animals to generate statistically significant data (e.g., power analysis, reports in the literature, previous experience, etc.).**

Because Sox2CreERT2 homozygous mice are not viable, we will be using heterozygous. Therefore, only half the number of mice from the progeny of the cross Sox2<sup>CreERT2/+</sup> x Ai14 will express the reporter gene and be useful for experiment Therefore, two litters per time point (8 experimental + 8 unusable) will be enough samples to generate significant data.

**Indicate whether the experiment must be repeated and justify the number of repetitions.**

This experiment does not need to be repeated.

**Indicate the species to be used, and how many will be used (e.g., X# mice per experiment x X# strains of mice).**

Sox2<sup>CreERT2/+</sup> will be crossed with homozygous Ai14 mice. We will need **one male (Ai14) and one female (Sox2<sup>CreERT2/+</sup>) breeders and 16 experimental mice.**

4. **Animal Reuse – Will any of the proposed experiments utilize animals that have already undergone experimental procedures in this animal usage protocol or in a separate animal use protocol?**  YES  NO

**Detailed Descriptions of Animal Procedures:** Identify EACH procedure to be performed on an animal. List as a subheading and provide a detailed description of how the work will be performed. Please list procedures chronologically. The following items must be addressed.

### Animal Transport:

The mice will be transported to BioBark I, room 404/405 on campus by use of a cart. The cage tops will be secured, and the cage will be covered completely so that the animals are not visible to the public. The animals will be taken through as much of the campus buildings as possible to minimize their exposure to the public. The animals are transported to BioPark only to be euthanized. No other procedure will be performed at this site.

### Compounds and Substances Administered to Animals:

Tamoxifen powder (Sigma, St. Louis, MO; Cat #T5648) is dissolved in USP/ NF grade corn oil (Thermo Fisher) by putting the tube in a rotating oven at 56°C for 2 hr. Tamoxifen solution is then filter sterilized through a 0.22µm filter and stored at 4°C in the dark for up to 7 days. The tube containing the reconstituted tamoxifen will be labelled with the name of the drug, its concentration, the reconstitution date and the expiration date.

### Intraperitoneal (IP) Injections:

Prior to IP injections, the mouse will be restrained by scruffing, the abdomen will be prepped with a 70% alcohol pad and the mouse will be held at a 30 degrees angle with its head facing back and down and abdomen up. For adult mice, a 26G3/8 tuberculin syringe will be used to administer the injections. In pups, a 30G1/2 ultrafine needle insulin syringe will be used. For multiple injections, the injection sites will be alternated to minimize the adverse effects of serial injections.

### Tamoxifen Injections:

We will perform injections at 3mg/ 40g body weight in mice younger than 21 days old. The concentration used is 20mg/mL in order to keep the volume injected below 50 µL in young mice. For multiple injections, the injection sites will be alternated to minimize the adverse effects of serial injections.

Pups are intraperitoneally (IP) injected with a 30G1/2 ultrafine needle insulin syringe (Becton Dickinson). Prior to injection, the mouse will be restrained by scruffing, the abdomen will be prepped with a 70% alcohol pad and the mouse will be held at a 30 degrees angle with its head facing back and down and abdomen up.

**The research team is experienced with injections to pups and returning pups successfully to the litter.**

### Transcardial Perfusion of 4% paraformaldehyde (PFA) for fixation

Prior to injecting the mice with an anesthetic, the mouse will be restrained by the person handling the mouse, the abdomen will be prepped with a 70% alcohol pad and the mouse will be held at a 30 degrees angle with its head facing back and down and abdomen up. A tuberculin syringe with a 25G or smaller bore needle will be used to administer the anesthetic.

The mice will be anesthetized using intraperitoneal injection of Ketamine:Xylazine - Ketamine (80-150 mg/Kg) and Xylazine (10-16 mg/Kg) solution. The maximal volume that will be administered to any mouse is 0.3 ml IP. Xylazine in this mixture is at a concentration of 20 mg/ml. Xylazine is available at concentrations of 20 mg/ml and 100 mg/ml. If using 100 mg/ml the volume of Xylazine would be 0.2 ml with a volume of 1.8 ml of WFI (water for injection). The volume of Ketamine would remain the same.

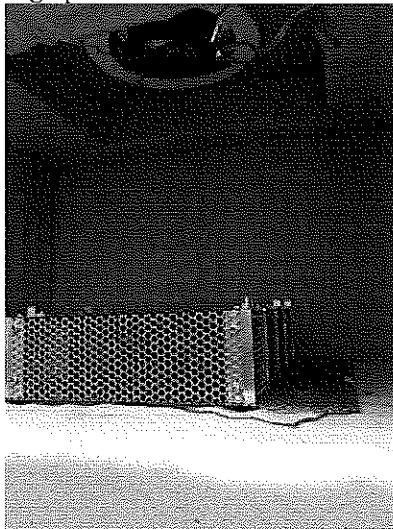
Perfusion will be performed in a fume hood as paraformaldehyde (PFA) is used as the fixative. The mouse to be perfused will be anesthetized using the ketamine/xylazine mixture as described in this protocol. Once deep anesthesia is verified by toe pinch, dissection will begin. Dissection through abdominal wall and the sternum will expose the heart. The left ventricle will be identified and punctured with a butterfly needle attached to a 50mL syringe filled with PBS. The right atrium is then cut to allow complete flow through the body. PBS will then be passed through the bloodstream to completely remove the blood from the body, during which time the mouse will die. Sufficient perfusion is verified by observing liver color change from deep red to pale (blanching). A second perfusion with 4% PFA will fix tissue throughout the mouse. The mouse will then be decapitated and the inner ears will be harvested for immunohistological analysis. The remaining carcass will then be properly disposed of in a carcass freezer

### Noise exposure

Noise exposure will be performed in HSF1, room 643. Mice will be placed, un-anaesthetized and unrestrained, into a cage with multiple compartments (one animal per compartment). The cage is 5.2"W x 8.3"L x 5.2"H. The cage is positioned inside of a reverberant noise exposure box. A noise stimulus, described as octave band of noise (8-16 kHz), is presented for 2 hours. The noise stimulus is delivered through a speaker, which is secured into the ceiling of the noise exposure box. Noise exposure sound levels are measured before every noise exposure with a calibration

microphone in order to ensure consistent and accurate sound levels. **Noise exposure will be performed in a soundproof box to ensure a constant level of noise. After one hour, the door of the box will be opened temporarily to monitor the animals. Continuous monitoring is not possible for this procedure without compromising the experiment. However, based on our experience over the years, no adverse events occurred during the noise exposure.**

Following noise exposure mice will be immediately returned to home cages. See image below for the noise exposure cage positioned within the noise exposure box and beneath the speaker.



### **Heat shock**

Heat shock will be performed in HSFL, room 643. For the mode of induction of heat shock we would like to follow the following manuscript with minor modifications: Carnemolla, et al, (Human Molecular Genetics, 2014 Jul 15;23(14):3641-56), which uses a 15 minute hyperthermia protocol procedure. Additionally, all of the mice are expected to survive the heat shock protocol. The following manuscript, King, et al, (J Exp Biol. 2002 Jan;205(Pt 2):273-8), demonstrates that a 30 minute whole-body hyperthermia protocol in mice has a survival rate of approximately 100%. Heat shock exposure will not be distressful and/ or painful to the animals as they will be anesthetized during the procedure.

### **Heat Shock Experiment:**

After mice are anesthetized, depth of anesthesia will be ascertained, and an oil-based lubricant (such as Lacrilube or an equivalent clinical product) will be applied to the eyes to prevent corneal injury. **The probe end of a thermometer will be gently inserted into the mouse rectum after applying a lubricant to continually monitor the temperature.**

**Each experimental mouse (the whole body, not including the head) will be wrapped in a Far-infrared warming pad connected to a Temperature Monitoring & Homeothermic Control Module (PhysioSuite from Kent Scientific Corporation) set to 41°C to raise its core body temperature to 3.3°C above the initial temperature (raising the core from temperature from ~37°C to ~41.5°C). Once the mice core temperature is stabilized at the elevated temperature, it will be maintained for 15 minutes and monitored with the rectal thermometer.**

After 15 minutes have elapsed, the mouse will be removed from heat and placed in a recovery box placed over a heating pad maintained at 37°C. The heating pad for the recovery box will be positioned under only half of the cage, so the mice will have the option to move away from the heat if they desire to do so. The mice will be allowed to fully recover from anesthesia before being returned to the animal facility.

For the sham heat shock controls, anesthetized mice are placed in a recovery box on a heating pad, set to 37°C, to maintain the body temperature at the initial core temperature (The heating pad for the recovery box will be positioned under only half of the cage). The mice core temperature will be monitored with a rectal thermometer. They will then be allowed to fully recover from anesthesia before being returned to the animal facility.

Each experimental group will then be exposed to 105dB SPL noise exposure 8-16 kHz for 2 hours 6 hours after the initiation of the heat shock experiment.

### **Justification for Distress Category E:**

When mice are exposed to noise for two hours this elicits a stress response. The mice cannot be anesthetized during this time, and the use of anesthetics during noise exposure is highly controversial for the following reasons: (a) it is accepted that while the prolonged noise exposure does result in some stress it is not a 'highly stressful event', however, the over-handling of animals during administration of anesthetics may cause more stress. Indeed, it has been shown that restraint stress prior to the exposure results in higher changes in the body's endogenous steroid levels, preventing much of the threshold shifts seen with noise exposure. (b) It is possible that the anesthesia will have a protective effect on the hearing - likely skewing the results. (c) The experiments are designed to mimic noise exposures in human, which do not occur with an anesthetic. (d) The standard duration of noise exposure is usually two hours, which would require an inhaled anesthetic for continuous and equal anesthetic throughout the procedure that is not possible in our current setting.

**Exogenous Substances:** (any substance administered to a live animal)

Substance	Dose Range (mg/kg)	Route	pharmaceutical grade* (yes / no)	Chemical Hazard? (No, CL1, CL2)	Purpose (anesthetic, analgesic, paralytic, experimental, etc.)
Tamoxifen	3mg/40g for mice < P21 and 9mg/40g for mice > P21	Intraperitoneal	No	CL2	Experimental
Corn oil	Solvent for tamoxifen	Intraperitoneal	Yes	No	Solvent for tamoxifen
Ketamine	80-150 mg/Kg	Intraperitoneal	Yes	No	anesthetic
Xylazine	10-16 mg/Kg	Intraperitoneal	Yes	No	anesthetic
4% Paraformaldehyde (PFA)	n/a	Transcardial	No	CL1	fixative
Phosphate Buffer Saline (PBS)	n/a	Intraperitoneal	No	No	Perfusion and Diluent for PFA
<p>*Scientifically justify use of non-pharmaceutical grade compounds:  <b>Tamoxifen:</b> We couldn't find tamoxifen with a pharmaceutical grade. The Tamoxifen powder is at &gt;99% purity. This is the commercially available powder that has been used extensively in the literature in mice. We are reconstituting tamoxifen in pharmaceutical grade corn oil as per the guideline of IACUC Guidelines on the use of Non-pharmaceutical Grade Compounds in Animal Use Protocols.  <b>PBS:</b> PBS is used to dilute PFA from 16% to 4% and as a first perfusion step for fixation by transcardial perfusion which is a non-survival procedure. Use of PBS for this procedure is standard protocol and we were previously approved for it.</p>					
<p><input checked="" type="checkbox"/> *I confirm any non-pharmaceutical grade compounds will be reconstituted and stored per the <u>IACUC Guidelines on the use of Non-pharmaceutical Grade Compounds in Animal Use Protocols</u>.</p>					

CL1 – Chemical Level 1; CL2 – Chemical Level 2; Refer to EHS Hazardous Chemical Use in Animal Research website for guidance.

**Identification of Animals:** Please provide details on the method of identification (e.g., ear tagging, tattooing, etc.) used for all animals in the study and the age of animals when procedures are performed.

Mice will be identified using the ear notch numbering system. This will occur when the mice are 10 days old and older. The 2mm in diameter ear punch will be cleaned with 70% Ethanol prior to notching, and after each subsequent use. The ear punch will be placed on the ear pinna in the proper location for identification, then pressed firmly to punch a circular hold through the ear. The punch will be removed carefully, to prevent ripping of the pinna. Alternatively, we will use numbered ear tags as a method of identification for adult animals obtained from the JAX, Charles River. The ear tags and applicator will be cleaned with 70% Ethanol prior to tagging. The ear tag will then be placed in the applicator, and the mouse will be grasped by the scruff and immobilized. The ear will be placed between the point and the hole of the tag, and will be positioned at the lateral base of the ear, approximately 3mm from the edge of the ear pinna. Once the tag is positioned correctly, the applicator will be squeezed firmly to apply the tag. The tag implantation site will be intermittently checked for signs of local infection.

**General Monitoring:** *Please provide details to the general monitoring of animals throughout the course of these experiments. Define parameters to be monitored, frequency of monitoring (at least 3 times a week), and identify the individual(s) responsible for monitoring.*

The animals in the colony are observed at least three times a week by the PI or their research staff designee. The mice are evaluated for general appearance and well-being, whether they are actively in an experiment, pre-experimental, or breeding colony animals. If anything unusual/abnormal about the appearance of the animal is observed, this is reported to the Veterinary Resources so that the animal can be evaluated by a member of the veterinary staff and treated appropriately. Specifically, change in the quality or distribution of the body hair - ruffed hair coat for more than 24 hrs or alopecia of > 25 % of the body hair, self induced trauma, bleeding from any orifice, change in posture or neurological signs will be reported to the animal care facility caregivers to be discussed with the veterinarian and possibly euthanize the animal. Moribund animals will be euthanized.

**Alternative Endpoints:** *Please specify criteria to be used to determine whether early euthanasia (prior to the experimental endpoint) is warranted. Please refer to the Endpoint Guidelines available on the OAWA website and include only those that are applicable to the proposed research.*

Our animals are monitored routinely by our research staff as well as by the animal caregivers in the animal facility. Any change in the animal health suggestive of a deterioration in the animal's well being – specifically change in the quality or distribution of the body hair - ruffed hair coat for more than 24 hrs or alopecia of > 25 % of the body hair, self induced trauma, bleeding from any orifice, change in posture or neurological signs will be reported to the animal care facility caregivers to be discussed with the veterinarian and possibly euthanize the animal. Moribund animals will be euthanized. In addition, the electrode sites and site of IP injection will be inspected for signs of infection which include tenderness, redness or discharge. If these are to be found a veterinary consult will be obtained. As none of the genes we study are oncogenes, we do not anticipate developing tumors in the mutant mice. We also do not anticipate significant weight loss as a result of the mouse genotypes.

**Research Personnel Qualifications, Experience or Training:** Please provide the following information for each person working with live animals under this protocol.  
 List the PI information first, then any Co-PIs, etc.

Name, Email & Phone #	Indicate role in project <u>and</u> list procedures he/she will be performing.	Indicate years' experience working with the <i>species</i> of animals proposed for use in this protocol.	Indicate years' experience performing the <i>proposed procedures in the species</i> utilized in this protocol.	If the individual is not trained in either the procedures or species ( <i>or both</i> ), please indicate how he/she will be trained.
Ronna Hertzano, <a href="mailto:rhertzano@som.umaryland.edu">rhertzano@som.umaryland.edu</a> , 410-328-1892	Principal Investigator; Protocol design, ear tagging and notching, ABR and behavioral studies, tamoxifen and viral injections, general mouse handling and care, fixative perfusion, anesthesia, euthanasia, dissection, tissue harvesting for RNA extraction, immunohistochemistry, Scanning Electron Microscopy, fluorescence activated cell sorting	15 years	15 years	
Beatrice Milon, <a href="mailto:bmilon@som.umaryland.edu">bmilon@som.umaryland.edu</a> , 410-706-2551	Research supervisor; ear tagging and notching, ABR and behavioral studies, tamoxifen injections, general mouse handling and care, anesthesia, euthanasia, dissection, tissue harvesting for RNA extraction, immunohistochemistry, Scanning Electron Microscopy, fluorescence activated cell sorting	5 years	5 years	
Maggie Matern <a href="mailto:MPrescott@umaryland.edu">MPrescott@umaryland.edu</a> 410-706-2551	Graduate student; ear tagging and notching, tamoxifen and viral injections, general mouse handling and care, euthanasia, dissection, tissue harvesting for RNA extraction, immunohistochemistry, Scanning Electron Microscopy, fluorescence activated cell sorting, protein analysis	5 years	5 years	
Mark McMurray <a href="mailto:MMcMurray@som.umaryland.edu">MMcMurray@som.umaryland.edu</a> 410-706-2551	Research Assistant; ear tagging and notching, ABR and behavioral studies, tamoxifen and viral injections, general mouse handling and care, anesthesia, euthanasia, dissection, tissue harvesting for RNA extraction, immunohistochemistry	2 years	2 years	

Benjamin Shuster <a href="mailto:Benjamin.Shuster@som.umaryland.edu">Benjamin.Shuster@som.umaryland.edu</a> 410-706-2551	Research Fellow; ear tagging and notching, noise exposure, ABR and behavioral studies, tamoxifen and estrogen injections, general mouse handling and care, anesthesia, euthanasia, dissection, tissue harvesting for RNA extraction, immunohistochemistry	1 year	1 year	
Kathleen Gwilliam <a href="mailto:kewilliam@umaryland.edu">kewilliam@umaryland.edu</a> 410-706-2551	Graduate student; ear tagging and notching, ABR and behavioral studies, tamoxifen and viral injections, general mouse handling and care, euthanasia, dissection, tissue harvesting for RNA extraction, immunohistochemistry, Scanning Electron Microscopy, fluorescence activated cell sorting, protein analysis	1 year	1 year	
Kevin Rose <a href="mailto:rosekp@umaryland.edu">rosekp@umaryland.edu</a> 410-706-2551	Graduate student; ear tagging and notching, ABR and behavioral studies, tamoxifen and viral injections, general mouse handling and care, euthanasia, dissection, tissue harvesting for RNA extraction, immunohistochemistry, Scanning Electron Microscopy, fluorescence activated cell sorting, protein analysis	4 year	1 year	

*\*\*Please add rows to this table by placing cursor at end of last row and clicking return.*

- As PI, I confirm that no minors will be working with live vertebrate animals per UMB Policy VI-99.01(A).
- As PI, I acknowledge that a COI Exemption must be filed with the UMB Office of Accountability & Compliance should my spouse or a family member work under this animal use protocol per UMB Policy.

**Colony Establishment & Maintenance PI Certification**

- I confirm that these animals are not available from commercial vendors in the numbers or on the schedule required for the proposed research.
- I confirm that all animals brought to UMB from any source will be coordinated through Veterinary Resources to assure that proper health records are obtained, reviewed and approved before animal shipment.
- I confirm that breeding colonies will be monitored at least three times a week (M, W, F) to ensure animal wellbeing and adherence to the VR Policy on Cage Population Densities for Mice.

**1. Colony Identification – Adult Breeders & Offspring Generated**

On the chart below, indicate the number of breeders required, and provide estimates for the numbers of offspring expected and the anticipated disposition of those offspring, by strain, transgene, KO or KI. *Protocols have a life span of 3 years, list numbers anticipated over a 3 year period.*

An excel file named “DOD breeding addendum calculation 2018” is submitted with the protocol for a detailed calculation of the number of animals.

Colony Designation (strain / transgene / KO / KI)	Adult Breeders (strain x strain)	# of male breeders required	# of female breeders required	Expected total # of offspring generated	# Offspring needed for experiments	Approximate # offspring deemed unusable	Approximate # offspring used to replace breeders
				Sum of columns a+b+c	Column A	Column B	Column C
Ribo;PrestinCreER;CBACaJ	CBA/CaJ x Rpl22 <sup>tm1.1Psam/tm1.1Psam</sup> , Prestin <sup>creERT2/creERT2</sup>	27	54	249	248	1	0
Ribo;Sox2CreER;CBACaJ	CBA/CaJ x Rpl22 <sup>tm1.1Psam/tm1.1Psam</sup> , Sox2 <sup>creERT2/creERT2</sup>	27	54	540	288	252	0
Ribo-PrestinCreER	Rpl22 <sup>tm1.1Psam/tm1.1Psam</sup> , Prestin <sup>Cre/Cre</sup> x Rpl22 <sup>tm1.1Psam/tm1.1Psam</sup> , Prestin <sup>Cre/Cre</sup>	1	1	120	0	65	55
Ribo-Sox2CreER	Rpl22 <sup>tm1.1Psam/tm1.1Psam</sup> , Sox2 <sup>Cre/+</sup> x Rpl22 <sup>tm1.1Psam/tm1.1Psam</sup> , Sox2 <sup>+/+</sup>	1	2	240	0	173	67
(Ribo-PrestinCreER)HS	Rpl22 <sup>tm1.1Psam/tm1.1Psam</sup> , Prestin <sup>Cre/Cre</sup> x Rpl22 <sup>tm1.1Psam/tm1.1Psam</sup>	3	6	48	48	0	0
(Ribo-Sox2CreER)HS	Rpl22 <sup>tm1.1Psam/tm1.1Psam</sup> , Sox2 <sup>Cre/+</sup> x Rpl22 <sup>tm1.1Psam/tm1.1Psam</sup>	9	18	216	120	96	0
PrestinCreER;Tomato	Prestin <sup>Cre/Cre</sup> x B6.cg-GT(ROSA) <sup>26Sortm14(CAG-tdTomato)/Hze/J</sup>	1	1	16	16	0	0
Sox2CreER;Tomato	Sox2 <sup>Cre/+</sup> x B6.cg-GT(ROSA) <sup>26Sortm14(CAG-tdTomato)/Hze/J</sup>	1	1	32	16	16	0

\*\*Please add rows to this table by placing cursor at end of last row and clicking return.

2. **Please indicate at what age animals will be weaned. The standard is 21 days. If animals must be weaned at a later point, please specify at what age they will be weaned and provide justification for that request. Please contact Veterinary Resources for assistance as needed.**

Animals will be weaned at 21 to 28 days old. Transgenic mice may be smaller than wild type mice. Therefore, we may need to wait up to P28 for the pups to reach an adequate size/weight for weaning.

3. **If used, please state and describe method(s) of genotyping/phenotyping of the animals.**

Mice will be identified using the ear notch numbering system. This will occur when the mice are 10 days old and older. The 2mm in diameter ear punch will be cleaned with 70% Ethanol prior to notching, and after each subsequent use. The ear punch will be placed on the ear pinna in the proper location for identification, then pressed firmly to punch a circular hold through the ear. The punch will be removed carefully, to prevent ripping of the pinna. **The ear punch will be used for genotyping.**

4. **Discuss whether the generated rodents experience any significant health problems associated with their genetic status, e.g. immunodeficiency, musculoskeletal deficiencies, any problems associated with eating, drinking, metabolism which requires special needs or results in pain or distress. Please discuss the severity of symptoms expected in these animals, if any. What measures will be used to assess the symptoms and relief from pain and/or distress, if necessary. Please assure the IACUC that all moribund animals will be euthanized.**

The animal generated are not expected to experience any significant health problems. The mice have a conditional allele that is activated upon injection of tamoxifen as described in the parent protocol. The conditional allele expressed an HA-tagged ribosomal subunit and does not lead to any health issues.

5. **Please indicate the expected life span for each strain of rodent to be bred.**

All mice in this protocol are expected to have a standard life span similar to the life span of C57BL/6 and CBA/CaJ mice. We expect most mice to live up to 1.5 year old.

6. **Please specify criteria to be used to determine whether early euthanasia of breeder animals is warranted. Please refer to the list of humane experimental endpoints in the Endpoint Guidelines available on the OAWA website.**

Our animals are monitored routinely by our research staff as well as by the animal caregivers in the animal facility. Any change in the animal health suggestive of a deterioration in the animal's well-being – specifically change in the quality or distribution of the body hair - ruffed hair coat for more than 24 hrs or alopecia of > 25 % of the body hair, self induced trauma, bleeding from any orifice, change in posture or neurological signs will be reported to the animal care facility caregivers to be discussed with the veterinarian and possibly euthanize the animal. Moribund animals and mice with 20% weight loss will be euthanized. In addition, the electrode sites and site of IP injection will be inspected for signs of infection which include tenderness, redness or discharge. If these are to be found a veterinary consult will be obtained. As none of the genes we study are oncogenes, we do not anticipate developing tumors in the mutant mice. We also do not anticipate significant weight loss as a result of the mouse genotypes.

7. **Please indicate fate of retire breeders.**     Euthanized     Used experimentally     Other (*describe*):

8. **Please indicate fate of unusable offspring.**     Euthanized     Other (*describe*):

9. **The NIH Guidelines for Research Involving Recombinant DNA Molecules requires that the Institutional Biosafety Committee review and approve experiments involving the generation of rodents in which the animal's genome has been altered by stable introduction of recombinant DNA, or DNA derived**

therefrom, into the germ-line (transgenic animal).

Are two transgenic (or knockout) rodent strains being bred to create a new rodent strain?

YES\*\*  NO

Is a transgenic (or knockout) rodent strain being bred to a new background strain?

YES\*\*  NO

**\*\*If yes, the following questions must be answered:**

1. Does either parental rodent contains the following genetic modifications:

a. Incorporation of more than one-half of the genome of an exogenous eukaryotic virus from a single family of viruses?

YES\*\*\*  NO

b. Incorporation of a transgene that is under the control of a gammaretroviral long terminal repeat (LTR)?

YES\*\*\*  NO

2. Is the transgenic rodent resulting from this breeding expected to contain more than one-half of an exogenous viral genome from a single family of viruses?

YES\*\*\*  NO

**\*\*\*If yes to either 1 or 2 above, the following questions must be answered:**

i. Describe the unique characteristics of the transgenic founder(s).

Click here to enter text.

ii. Describe the expected unique characteristics of viable offspring.

Click here to enter text.

iii. Indicate the type of confinement used to house these animals

ABSL1  ABSL2  ABSL3

iv. Describe the precautions that will be taken (or procedures used) to minimize the possibility that animals could escape confinement.

Click here to enter text.

v. Assume that progeny of the breeding pairs were to escape and mate with wild-type animals. Describe the potential consequences of this event upon the wild population of animals.

Click here to enter text.

Breeding	Breeders	# of breeders daily census	# of breeding refreshment per year	Total breeders for 1 year	Offspring for 1 year	Total breeders for 2 years	Offspring for 2 years	Total breeders for 3 years	Offspring for 3 years	Additional breeders needed for other colonies
Ribo;PrestinCreER	Male	Rpl22 <sup>tm1.1Pcam</sup> /m1.1Pcam;Prestin <sup>CreERT2</sup> /CreERT2	1	4	4	8	80	12	120	27 for Ribo;PrestinCreER;CBA/Cal, 6 for (Ribo;PrestinCreER)HS
	Female	Rpl22 <sup>tm1.1Pcam</sup> /m1.1Pcam;Prestin <sup>CreERT2</sup> /CreERT2	1	4	4	8	80	12	120	
Ribo;PrestinCreER;CBA/Cal	Male	Rpl22 <sup>tm1.1Pcam</sup> /m1.1Pcam;Prestin <sup>CreERT2</sup> /CreERT2	6	18	83	36	166	27	249	n/a
	Female	CBA/Cal	3	9	9	18	166	54	249	
(Ribo;PrestinCreER)HS	Male	Rpl22 <sup>tm1.1Pcam</sup> /m1.1Pcam;Prestin <sup>CreERT2</sup> /CreERT2 or Rpl22 <sup>tm1.1Pcam</sup> /m1.1Pcam	1	3	3	3	48	3	48	n/a
	Female	Rpl22 <sup>tm1.1Pcam</sup> /m1.1Pcam;Prestin <sup>CreERT2</sup> /CreERT2 or Rpl22 <sup>tm1.1Pcam</sup> /m1.1Pcam	2	3	6	6	48	6	48	
	Male	Rpl22 <sup>tm1.1Pcam</sup> /m1.1Pcam;Sox2 <sup>CreERT2/+</sup> or Rpl22 <sup>tm1.1Pcam</sup> /m1.1Pcam;Sox2 <sup>+/+</sup>	1	4	4	8	80	12	240	27 for Ribo;Sox2CreER;CBA/Cal, 18 for (Ribo;Sox2CreER)HS
	Female	Rpl22 <sup>tm1.1Pcam</sup> /m1.1Pcam;Sox2 <sup>CreERT2/+</sup> or Rpl22 <sup>tm1.1Pcam</sup> /m1.1Pcam;Sox2 <sup>+/+</sup>	2	4	8	16	80	24	240	
Ribo;Sox2CreER;CBA/Cal	Male	Rpl22 <sup>tm1.1Pcam</sup> /m1.1Pcam;Sox2 <sup>CreERT2/+</sup>	3	3	9	18	360	27	540	n/a
	Female	CBA/Cal	6	18	18	36	360	54	540	
(Ribo;Sox2CreER)HS	Male	Rpl22 <sup>tm1.1Pcam</sup> /m1.1Pcam;Sox2 <sup>CreERT2/+</sup> or Rpl22 <sup>tm1.1Pcam</sup> /m1.1Pcam	1	3	3	6	144	9	216	n/a
	Female	Rpl22 <sup>tm1.1Pcam</sup> /m1.1Pcam;Sox2 <sup>CreERT2/+</sup> or Rpl22 <sup>tm1.1Pcam</sup> /m1.1Pcam	2	3	6	12	144	18	216	
PrestinCreER;Tomato	Male	B6.cg-GT(ROSA) <sup>26Sor</sup> tm4(CAG-tdTomato)/Hze /J	1	n/a	1	16	16	1	16	n/a
	Female	Prestin <sup>CreERT2</sup> /CreERT2	1	1	1	1	16	1	16	
Sox2CreER;Tomato	Male	B6.cg-GT(ROSA) <sup>26Sor</sup> tm4(CAG-tdTomato)/Hze /J	1	n/a	1	32	32	1	32	n/a
	Female	Sox2 <sup>CreERT2/+</sup>	1	1	1	1	32	1	32	

RECEIVED

Animal Use Protocol – Hazardous Agent Addendum: Chemical Level 1 (Chemicals / Toxins / Hazardous Drugs)  
IACUC # \_\_\_\_\_ TBD \_\_\_\_\_ 0818004 1/4

1. List the chemicals / toxins / hazardous drugs classified as **CHEMICAL LEVEL 1 (CL1)** that will be administered to live animals:

Paraformaldehyde 4% (PFA) in phosphate buffered saline (PBS)

2. Describe the predicted effects of the chemicals / toxins / hazardous drugs on the animal, *i.e.* toxicity to animal.

The animal will be anesthetized during perfusion, which will lead to the death of the mouse.

3. Chemical / toxin preparation prior to administration:

Will any preparation of the chemical/toxin be required prior to administration (e.g. mixing, dilution, or dissolving of powders)?  Yes  No

*If yes, the following questions must be addressed:*

- Describe the preparation process here: A vial containing a solution of 16% PFA will be diluted to 4% in PBS
- Location where preparation will take place: The preparation will take place in the fume hood located in the BioPark I, room 405.
- Preparation of CL1 chemicals must take place in a fume hood or exhaust connected biosafety cabinet.
  - CONFIRM** that a fume hood or exhaust-connected biosafety cabinet will be used.
  - REQUEST EXCEPTION**, please specify: Click here to enter text.
- The minimum personal protective equipment to be used in preparation of CL1 chemicals are a lab coat and gloves.
  - CONFIRM** that the minimum PPE (lab coat and gloves) will be worn during preparation.
  - ADDITIONAL PPE**
    - Dust mask
    - Face Shield
    - Protective laboratory eyewear
    - Shoe Covers
    - Other, please specify: Click here to enter text.

4. Safety procedures and personnel protective equipment *research staff* will use while administering these agents and while handling animals and animal bedding.

- Describe the administration process here: Perfusion will be performed in a fume hood as paraformaldehyde (PFA) is used as the fixative. The mouse to be perfused will be anesthetized with Ketamine/ Xylazine (Ketamine 100-120 mg/kg, Xylazine 10-12 mg/kg, IP, 26G needle). Once deep anesthesia is verified by toe pinch, dissection will begin. Dissection through abdominal tissue and the ribcage will expose the heart. The left ventricle will be identified and punctured with a butterfly needle attached to a 50mL syringe filled with PBS. The right atrium is then cut to allow complete flow through the body. PBS will then be passed through the bloodstream to completely remove the blood from the body, during which time the mouse will die. Sufficient perfusion is verified by observing liver color change from deep red to pale (blanching). A second perfusion with 4% PFA will fix tissue throughout the mouse. The mouse will then be decapitated and the inner ears will be harvested for immunohistological analysis. The remaining carcass will then be properly disposed of in a carcass freezer freezer and the excess perfusate will be collected and scheduled to be disposed by EHS.
- Location where administration will take place: The administration will take place in the fume hood located in the BioPark I, room 405
- Administration of CL1 chemicals must take place in a fume hood or exhaust connected biosafety cabinet.
  - CONFIRM** that a fume hood or exhaust connected biosafety cabinet will be used.
  - REQUEST EXCEPTION**, please specify: Click here to enter text.

- d. The minimum personal protective equipment to be used in administration of CL1 chemicals are a lab coat and gloves.
- CONFIRM** that the minimum PPE (lab coat and gloves) will be worn during administration.
  - ADDITIONAL PPE**
    - Dust mask
    - Face Shield
    - Protective laboratory eyewear
    - Shoe Covers
    - Other, please specify: Click here to enter text.
5. Discuss the length of time the animals will be kept following exposure to the chemicals / toxins / hazardous drugs.
- The animals will be dissected right after the perfusion and will not be kept.
6. Animal housing:
- a. In general, bedding from animals who have been treated with CL1 are NOT considered hazardous to personnel and veterinary resources staff.
    - CONFIRM** that you have understood and read the above.
    - REQUEST EXCEPTION**, explain your answer. Click here to enter text.
  - b. Identify location(s) of animal housing post-exposure: Perfusion of PFA will lead to the death of the animal.
7. Will animals be returned to / housed in the animal facility following exposure?  Yes  No  
*If no, go to item 8. If yes, answer questions a & b below.*
- a. Consult the Veterinary Resources Facilities Manager ([dhull@som.umaryland.edu](mailto:dhull@som.umaryland.edu) or 410-960-2723) or the Deputy Director ([edallen@som.umaryland.edu](mailto:edallen@som.umaryland.edu) or 443-677-9030) to review this form, answer item b (below) and discuss proper cage level documentation and cage handling procedures.  
Date of consult: Click or tap to enter a date.
  - b. Please list precautions and safety procedures *Veterinary Resources staff* should follow when handling the animals and animal bedding. Specifically, identify which category of personal protective equipment (PPE) will be required for handling the animals and animal bedding:
    - Standard PPE [*facility scrubs or lab coat over street clothes, facility issued shoes, gloves (only when handling animals or cages) & particle mask (optional)*]
    - ABSL2 PPE [*facility scrubs, facility issued shoes, lab coat, shoe covers, gloves & particle mask*]
    - Additional PPE, please specify: Click here to enter text.
8. If a toxin, is it classified as a select agent, but permissible below certain amounts (see list: <http://www.selectagents.gov/PermissibleToxinAmounts.html>)?
- Yes  No
  - a. If yes above, have you registered this toxin through the University's due diligence program (<https://afcf.umaryland.edu/ehs/sec/duediligence/>)?
    - Yes  No

RECEIVED

02/18/17 10:04 AM

1. List the chemicals / toxins / hazardous drugs classified as **CHEMICAL LEVEL 2 (CL2)** that will be administered to live animals:

Tamoxifen

2. Describe the predicted effects of the chemicals / toxins / hazardous drugs on the animal, *i.e.* toxicity to animal.

There are no predicted effects of Tamoxifen on the injected animals at the dosage we are using.

3. Chemical / toxin preparation prior to administration:

Will any preparation of the chemical/toxin be required prior to administration (e.g. mixing, dilution, or dissolving of powders)?  Yes  No

*If yes, the following questions must be addressed:*

- a. Describe the preparation process here: Tamoxifen powder (Sigma, St. Louis, MO) is dissolved in corn oil (Sigma) at 56°C (approximately 2 hr). Tamoxifen solution is filter sterilized through a 0.22um filter and stored at 4°C in the dark for up to 7 days.
- b. Location where preparation will take place: The preparation will take place in BioPark I, room 404/405 using a fume hood.
- c. Preparation of CL2 chemicals must take place in a fume hood or exhaust connected biosafety cabinet.
  - CONFIRM** that a fume hood or exhaust-connected biosafety cabinet will be used.
  - REQUEST EXCEPTION**, please specify:
- d. The minimum personal protective equipment to be used in preparation of CL2 chemicals are a lab coat and gloves.
  - CONFIRM** that the minimum PPE (lab coat and gloves) will be worn during preparation.
  - ADDITIONAL PPE**
    - Dust mask
    - Face Shield
    - Protective laboratory eyewear
    - Shoe Covers
    - Other, please specify: Click here to enter text.

4. Safety procedures and personnel protective equipment *research staff* will use while administering these agents and while handling animals and animal bedding.

- a. Describe the administration process here: Mice are intraperitoneally (IP) injected with a 30G1/2 ultrafine needle insulin syringe (Becton Dickinson). We will perform injections at 3mg/ 40g body weight in mice younger than 21 days old, or at 9mg/ 40g body weight in mice 21 days old and older. The concentration used varies from 10 mg/mL to 20mg/mL in order to keep the volume injected below 50 µL in young mice and below 300 µL in adult.
- b. Location where administration will take place: Tamoxifen will be administered in HSF1 room 643A in Class II Biosafety Cabinet.
- c. Administration of CL2 chemicals must take place in a fume hood or exhaust connected biosafety cabinet.
  - CONFIRM** that a fume hood or exhaust connected biosafety cabinet will be used.
  - REQUEST EXCEPTION**, please specify: The Class II BSC in HSF I 643 will be used to parenterally administer Tamoxifen via needle and syringe intraperitoneally. By delivering via this route, it is highly unlikely any aerosols will be created that would warrant the use of a fume hood. Furthermore, the use of a fume hood (personnel protection only) does not afford protection of murine pathogen free mice from exogenous microbial contamination that could alter interpretation of research results. The BSC work surfaces will be cleaned with a chemical disinfectant (chlorine dioxide solution), rinsed with water and wiped dry with paper towels as is required by Veterinary Resources.

Soiled filter top cages will be released to Veterinary Resources staff for further processing after the 48 to 72 hour period as advised.

- d. The minimum personal protective equipment to be used in administration of CL2 chemicals are a lab coat and gloves. *Note that animals treated with CL2 chemicals may require separate housing, which would increase the required PPE. Complete this section after discussion with EHS and/or Veterinary Resources as below.*
- CONFIRM** that the minimum PPE (lab coat and gloves) will be worn during administration.
  - ADDITIONAL PPE**
    - Dust mask
    - Face Shield
    - Protective laboratory eyewear
    - Shoe Covers
    - Other, please specify: Click here to enter text.
5. **Discuss the length of time the animals will be kept following exposure to the chemicals / toxins / hazardous drugs.**  
Mice are injected around P15 and are euthanized between 9-11 weeks of age.
6. **Animal housing:**
- a. In general, bedding from animals who have been treated with CL2 chemicals can be considered hazardous for 48-72 hours past the last administration. Cages must be marked with *Orange Health Hazard cage cards*, noting chemical used, dosage, and date of administration. Veterinary Resources must be notified prior to use of the CL2 chemical in order to arrange for proper housing and waste handling.
- CONFIRM** that you have understood and read the above.
  - REQUEST EXCEPTION**, explain your answer. Click here to enter text.
- b. Identify location(s) of animal housing post-exposure: The animals will be housed in HSFI, room 643A.
7. **Will animals be returned to / housed in the animal facility following exposure?**  Yes  No  
*If no, go to item 8. If yes, answer questions a & b below.*
- a. **Consult the Veterinary Resources Facilities Manager ([dhull@som.umaryland.edu](mailto:dhull@som.umaryland.edu) or 410-960-2723) or the Deputy Director ([edallen@som.umaryland.edu](mailto:edallen@som.umaryland.edu) or 443-677-9030) to review this form, answer item b (below) and discuss proper cage level documentation and cage handling procedures.**  
Date of consult: 7/19/2018
- b. **Please list precautions and safety procedures *Veterinary Resources staff* should follow when handling the animals and animal bedding. Specifically, identify which category of personal protective equipment (PPE) will be required for handling the animals and animal bedding:**
- Standard PPE** [*facility scrubs or lab coat over street clothes, facility issued shoes, gloves (only when handling animals or cages) & particle mask (optional)*]
  - ABSL2 PPE** [*facility scrubs, facility issued shoes, lab coat, shoe covers, gloves & particle mask*]
  - Additional PPE, please specify:** Click here to enter text.
8. **If a toxin, is it classified as a select agent, but permissible below certain amounts (see list: <http://www.selectagents.gov/PermissibleToxinAmounts.html>)?**

Animal Use Protocol – Hazardous Agent Addendum: Chemical Level 2 (*Chemicals / Toxins / Hazardous Drugs*)  
IACUC # TBD 0818004/59

Yes     No

a. If yes above, have you registered this toxin through the University's due diligence program (<https://afcf.umaryland.edu/ehs/sec/duediligence/>)?

Yes     No

**\*\* All Species (except NHP) Enrichment / Socialization Plans \*\***  
**IACUC Animal Use Protocol Addendum**

**PI Name:** Dr Ronna Hertzano

**IACUC #:** TBD 0818004 PW

**AUP Title:** Understanding the molecular basis of acquired hearing loss

**Species:** Mouse

**Environment Enrichment**

Task Completed

1. I confirm that I have reviewed the UMSOM animal care and use program document entitled, "*The Environmental Enrichment Plan for Species Other than Nonhuman primates*".

2. Does the proposed research require an exemption from environmental enrichment as described in the above plan? If YES, please describe and justify below.

Yes    No  
   

Environmental Enrichment Exemption(s):

Click here to enter text.

**Socialization Plan**

Task Completed

3. I confirm that I have reviewed the UMSOM animal care and use program document entitled, "*Socialization Plan for Species Other than Nonhuman Primates*".

4. Does the proposed research require animals to be singly housed? Please note social housing (*housing with at least one other animal in the same cage*) is the standard method of housing unless single housing is scientifically justified. If you will need to house some animals in this protocol *by themselves*, please explain those reasons in the box below.

Yes    No  
   

Examples of Scientific Justification for single housing include (but are not limited to):

- Surgical implants used which are delicate and could be damaged by a cagemate (like cranial implants)
- Implanted access lines (like venous catheters) which could cause illness or death if removed by a cagemate
- Surgical manipulation (like bony manipulation) or immune suppression (as in transplant studies) which causes the animal to be at substantial risk from minor trauma that might commonly occur from cagemates
- Need to collect metabolic products (urine, feces, etc...) from a single animal
- Need to quantitate food and/or water consumption in experimental animals

Scientific Justification for Social Housing Exemption(s):

Click here to enter text.

Ronna Hertzano

Principal Investigator Signature

8/27/2018  
Date

# Towards a molecular understanding of noise induced hearing loss

Log number: MR130240



PI: Ronna Hertzano

Org: University of Maryland School of Medicine

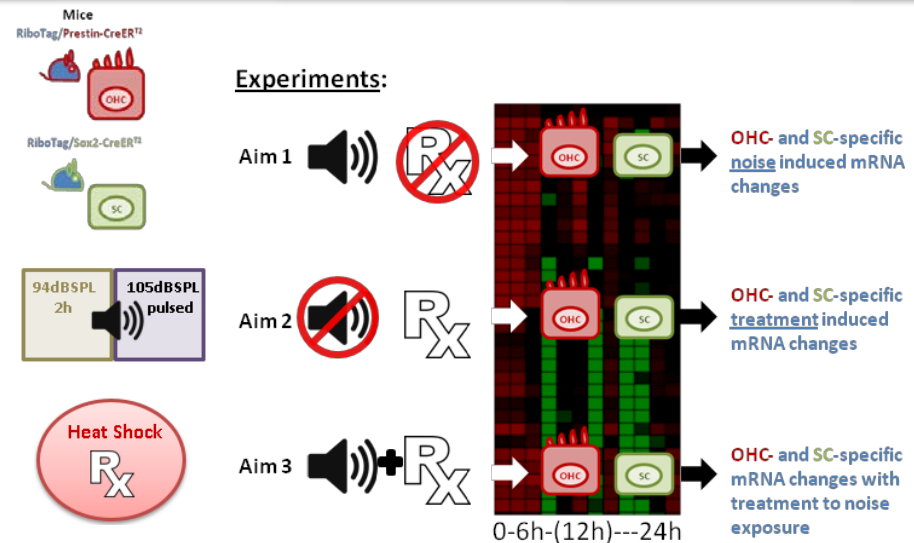
Award Amount: \$1,500,000

## Study/Product Aim(s)

- Characterization of the translomes of adult outer hair cells (OHC) and supporting cells (SC) at baseline.
- Identification, characterization and validation of the cell type-specific translational changes secondary to noise trauma that induces a permanent in comparison to a temporary hearing loss.
- Identification of the cell type-specific signaling cascades activated during successful treatment of noise induced hearing loss in mice (e.g. Heat Shock).
- Define at least two key signaling cascades that could be targeted to develop new therapeutic interventions to prevent and treat noise induced hearing loss.
- Determine the sex-specific differences in the molecular response to noise exposure.

## Approach

We established animal models that allow cell type-specific RNA extraction from adult mouse inner ears, to determine the cell type-specific translational changes at different time points following noise exposure with and without treatment, compared with the baseline translomes prior to exposure. Identified key regulatory pathways will be validated using real time RT-PCR.



## Timeline and Cost

Activities	CY	14-15	15-16	16-17	17-19
To establish the OHC- and SC-specific translome of adult mouse inner ears		█	█	█	█
To determine the OHC- and SC-specific transcriptional and signaling cascades activated in response to PTS-inducing noise injury			█	█	█
To determine the OHC- and SC-specific signaling cascades activated in vivo in response to otoprotective interventions			█	█	█
To evaluate the OHC- and SC-specific signaling cascades affected in vivo in mice, in male s and females separately, to PTS and TTS noise, as well as Heat Shock, and PTS noise and Heat Shock combined					█
<b>Estimated Budget (\$K)</b>		\$400	\$400	\$400	\$300

## Goals/Milestones

### CY14-16 Goal – OHC- and SC- translomes at baseline

- Identification and characterization of the OHC and SC-specific translomes

### CY15-16 Goal – Defining the inner ear translome in response to noise trauma

- Identification of the key signaling cascades initiated by noise trauma
- Identification of differences in the response of male and female mice to noise

### CY16-17 Goal – In vivo dissection of cell type-specific changes in response to treatment and pre-treated noise exposure

- Comparison of the cell type-specific molecular changes in response to PTS- and TTS-inducing noise exposure
- Improved approaches for Ribotag seq using fewer mice per experiment

### CY17-19 Goal – Defining the inner ear translome in response to noise trauma

- Identification of at least two new pathways for generating new interventions to prevent and treat noise induced hearing loss
- Comparison of the cell type-specific molecular responses to PTS-inducing noise with and without protective interventions.
- Identify some of the sex-specific molecular changes in response to noise.

### Budget Expenditure to Date

Projected Expenditure: 1,500,000

Actual Expenditure: 1,372,513

Updated: (October 26, 2018)